A N N U A L R E P O R T

1962

U. S. WATER CONSERVATION LABORATORY
Southwest Branch
Soil and Water Conservation Research Division
Agricultural Research Service
United States Department of Agriculture
Tempe, Arizona

ADMINISTRATIVELY CONFIDENTIAL

This report contains unpublished and confidential information concerning work in progress. The contents of this report may not be published or reproduced in any form without the prior consent of the research workers involved.

LABORATORY STAFF

Professional:

Dr. H. Bouwer, Research Hydraulic Engineer
Mr. K. J. Brust, Agricultural Engineer
Dr. W. L. Ehrler, Research Plant Physiologist
Mr. L. J. Erie, Research Agricultural Engineer
Mr. G. W. Frasier, Agricultural Engineer
Dr. L. J. Fritschen, Research Meteorologist
Dr. R. D. Jackson, Research Physicist
Mr. C. L. Jenson, Agricultural Engineer
Mr. L. E. Myers, Research Hydraulic Engineer
Dr. F. S. Nakayama, Research Chemist
Mr. W. E. Reeves, Physicist
Mr. R. J. Reginato, Research Soil Scientist
Mr. R. C. Rice, Agricultural Engineer
Dr. C. H. M. van Bavel, Research Physicist

Technicians:

R. M. Bula, Engineering Technician
E. J. Durban, Electrical Engineering Aid
E. D. Escarcega, Engineering Draftsman
O. F. French, Hydraulic Engineering Technician
J. R. Griggs, Physical Science Technician
L. E. Lisonbee, Physical Science Aid
J. L. MacIntyre, Physical Science Technician
J. B. Miller, Physical Science Technician
S. T. Mitchell, Physical Science Technician
K. G. Mullins, Physical Science Technician
B. A. Rasnick, Physical Science Technician
A. F. Sandecki, Physical Science Aid
B. W. Tilden, Soils Research Helper

Administrative, Clerical & Maintenance

O. J. Abeyta, Laborer
E. D. Bell, General Machinist
E. E. DeLaRosa, Janitor
A. V. Figueroa, Laborer
B. E. Fisher, Library Assistant
D. S. Fry, Clerk-Stenographer
C. E. Hansen, Clerk-Stenographer
J. M. Hernandez, Laborer
C. G. Hiesel, General Machinist
N. A. Johnson, Administrative Assistant

Administrative, Clerical & Maintenance (Cont'd):

R. C. Klapper, Refrigeration & Air Conditioning Mechanic
J. M. R. Martinez, Laborer
R. S. Miller, Clerk-Stenographer
A. H. Morse, Clerk-Dictating Machine Transcriber
M. E. Olson, Clerk-Stenographer
M. A. Seiler, Clerk-Stenographer
M. M. Zamora, Laborer

TABLE OF CONTENTS

	Page
Changes in Personnel	3
Head Environment of Seepage Meters in Flowing Water	4
Field Application of Falling-Head Technique for Seepage Meters and of Double-Tube Method for Hydraulic Conductivity Measurement	5
Theoretical Effect of Soil, Water Table, and Canal Conditions on Seepage From Canals	34
Measuring Horizontal and Vertical Hydraulic Conductivity of Soil With the Double-Tube Method	52
Soil Treatment to Reduce Seepage Losses from Canals and Ponds	68
Construction and Calibration of a Miniature Net Radiometer	81
Surface Energy Balance and Evapotranspiration of Irrigated Alfalfa	86
Components of the Radiation Balance of Field Crops Under Irrigated Management	137
Instrumentation for Micrometeorological Research	145
Evaporation from the Soil Surface and Soil Moisture Movement	155
Evaluation of Plastic Mulches for Growing Cotton	161
Evapotranspiration from Crops as Related to Management	167
Measurement of Evapotranspiration	175
Application of Hexadecanol - Octodecanol Monofilms to Small Ponds	182
Soil Treatment to Reduce Infiltration and Increase Precipitation Runoff	185
Analyzing Ground Water Mound Formation by Resistance Network	199

Page

The Use of Salty Well Water for the Pre-Planting Irrigation on Silty Clay Soils 210

Measurement and Calculation of Unsaturated Conductivity and Soil-Water Diffusivity 214

Development and Use of Gamma Transmission Equipment for the Measurement of Soil Density and Moisture Content . 266

Dynamic Similarity in Elbow Flow Meters 273

Quantitative Measurement of Water Flow with Chemical Tracers 280

Utilization of Limited Water Supplies for the Greatest Economic Return in the Irrigation of Cotton. 286

Simplified Prediction Method for the Fall of the Water Table in Drained Land 298

Soil Moisture Potentials and Water Uptake by Roots . . . 303

Nondestructive Beta Ray Transmission Method for Measuring Water Content in Plants 315

Water Loss from Plants as Related to Stomatal Diffusive Resistance 329

Water Absorption, Transpiration, and Internal Water Balance of Cotton Plants as Affected by Changes in Evaporative Demands 335

Consumptive Use of Water by Crops in Arizona 347

Analytical Laboratory 370

Radioisotope Storage Facility 371

Papers Prepared or Published During 1962 375

CHANGES IN PERSONNEL

The Laboratory staff has been strengthened during 1962 by the addition of three new members. They are as follows:

A. H. Morse, Clerk-Dictating Machine Transcriber
B. E. Fisher, Library Assistant
S. T. Mitchell, Physical Science Technician

Also during 1962 there were four resignations. They are as follows:

G. L. Jefferies, Physical Science Aid
W. C. McDonnell, Agricultural Aid
W. E. Reeves, Physicist
M. M. Phillips, Library Assistant

The Laboratory staff is now essentially at full strength with one or two exceptions.

TITLE: HEAD ENVIRONMENT OF SEEPAGE METERS IN FLOWING WATER

LINE PROJECT: SWC 4-gG1 CODE NO.: Ariz.-WCL-4

This project, which also includes a study of the direct effect of velocity on seepage, was reported in Annual Report 1961. The study was published in the Proceedings of the American Society of Civil Engineers (57). Pending formal discussion of the paper and preparation of closing remarks, the project will be terminated.

PERSONNEL: Herman Bouwer, L. E. Myers, R. C. Rice.

TITLE: FIELD APPLICATION OF FALLING-HEAD TECHNIQUE FOR SEEPAGE METERS AND OF DOUBLE-TUBE METHOD FOR HYDRAULIC CONDUCTIVITY MEASUREMENT

LINE PROJECT: SWC 4-gG1 CODE NO.: Ariz.-WCL-14

PART I. FALLING-HEAD TECHNIQUE FOR SEEPAGE METERS

INTRODUCTION:

The theory and application of the falling-head seepage meter technique for measuring seepage and hydraulic conductivity of bottom material (see Annual Report 1961 and (17)) were initially based on the assumption that seepage was not affected by pressure head at the bottom of the canal and that the bottom material was of uniform hydraulic conductivity. The theory has now been extended to conditions of seepage affected by head and to stratified bottom materials. The condition of non-uniformity of bottom materials was simplified into the case of (a) bottom material underlain by much more permeable soil, (b) bottom material underlain by much less permeable soil, and (c) thin, slowly permeable layers completely penetrated by the seepage meter. For the latter condition, the conductivity information is obtained in terms of hydraulic impedance and the balanced-flow differential head H_b can be used to evaluate the pressure head immediately below the slowly permeable layer.

Laboratory tests were performed to verify the new principles, and field measurements were made to exemplify the various possibilities for application of the technique. A paper with a complete description of the developments is in press (82).

PROCEDURE:

Seepage and hydraulic conductivity

The extension of the falling-head seepage meter theory to head-affected seepage and stratified bottom materials was done analytically. Since the relationship between seepage and pressure head can be expected to be linear, a linear relationship was employed in the development of the equation for seepage calculation from falling-head measurements.

The principle of the calculation of the hydraulic conductivity K is to substitute I_{s,H_b} and H_b in the flow factor F_f (Annual Report 1961),

since at the balanced-flow level the seepage component and the leakage component are numerically equal. This yields

$$K = \frac{R_c I_{s,H_b}}{F_f H_b} . \qquad (1)$$

In this equation, R_c and H_b are known from the field data and F_f can be determined from one of the graphs presented as Figures 2 and 5 in (22) for the particular value of D or D_p, which refer to the depth of material of much lower or much higher hydraulic conductivity, respectively, below the canal bottom. The seepage component, I_{s,H_b} at the balanced-flow level is not known, however, since the seepage obtained with the seepage meter is the seepage $I_{s,0}$ when $H = 0$. Thus, I_{s,H_b} must be estimated before K of bottom material can be evaluated. This estimation will be done by assuming vertical flow below the canal bottom and applying Darcy's equation to determine I_{s,H_b} from $I_{s,0}$ for the various conditions of non-uniformity or stratification.

For thin, slowly permeable layers that are completely penetrated by the seepage meter, the seepage meter can be considered as a falling-head permeameter and the impedance of the slowly permeable layer, R_s, is derived without aid of the flow factors.

The term H_b is an important indicator of the conditions under which seepage takes place. If seepage occurs in uniform soil with a deep water table, the seepage gradient is not much in excess of one and the seepage is essentially unaffected by pressure head in the canal. For a gradient of one, equation (1) shows that H_b is equal to R_c/F_f. If H_b is smaller than this ratio, the seepage gradient is less than one. This may indicate restricting layers at relatively small distance below the canal bottom or it may indicate presence of relatively high water tables adjacent to the canal. If H_b exceeds R_c/F_f, the material in which the seepage meter is placed is of lower hydraulic conductivity than the underlying material. If H_b approaches the water depth h_w, the bottom layer of lower hydraulic conductivity is rather thin and it is completely penetrated by the seepage cup. If H_b exceeds the water depth, negative pressures exist below the slowly

permeable layer. If H_b exceeds R_c/F_f considerably, but is less than H_w, the slowly permeable bottom layer is not completely penetrated by the seepage meter. Also, a thin layer of moderate hydraulic impedance may be present on otherwise relatively uniform bottom material. The various equations for calculating K and a guide showing what equation to use in relation to H_b is presented in RESULTS AND DISCUSSION.

Laboratory studies

The use of seepage meters to evaluate R_s of thin layers with high hydraulic impedance was tested with a seepage meter in a 55-gallon drum. The drum was filled with sand of 0.5 mm particle size. The sand was covered by a 5-cm layer of 28 μ glass beads to simulate a slowly permeable layer of bottom material. Tensiometers were installed in the sand below the slowly permeable surface layer to verify the pressure head determined with the seepage meter. The test procedure consisted of measuring the outflow from the barrel to calculate the seepage, of reading the tensiometers to determine the pressure head below the slowly permeable layer, and of calculating the impedance R_s of the layer from the seepage rate and the head loss across the layer. The latter was measured as the vertical distance between the water level in the manometer tubes connected to the tensiometers below the slowly permeable layer and the free water above the layer. These quantities are referred to as "seepage tank" and are shown on the abscissa in Figure 1. Falling-head measurements were then carried out with the seepage meter to calculate $I_{s,0}$. After this, the valve between the seepage meter and the falling-level reservoir was closed and H_b was measured for evaluation of the pressure head below the slowly permeable surface layer. These quantities are referred to as "seepage meter" in Figure 1. By manipulating the tail-water level of the seepage tank, positive pressures and negative pressures could be created below the slowly permeable layer. The drum was equipped with air entry vents so that unsaturated conditions below the slowly permeable layer could be established if the pressure were lowered sufficiently for drainage of pore water to occur.

Field studies

The equipment used in the field studies is similar to that reported in the Annual Report 1961. A valve was placed between the falling-level reservoir and the seepage meter. Upon closure of this valve, which is normally open, the balanced-flow level will be rapidly established inside the seepage meter. A mercury manometer was used for measurement of relatively large H_b values.

One of the field studies was carried out in a golf course lagoon west of Phoenix. The object of the study was to determine the depth of the restricting layer as formed by an artificial soil sealant that was applied to the lagoon for reducing seepage. The seepage meters were installed at different depths. As the slowly permeable material was penetrated by the seepage meter, a sharp increase in H_b would be observed. This increase would cease after the meter had completely penetrated the layer. The other field test was performed in an experimental ground water recharge pit northwest of Phoenix. The object of this study was to determine whether a decline in recharge was caused by soil clogging at the bottom of the pit or by a perched ground water mound.

RESULTS AND DISCUSSION:

Seepage and hydraulic conductivity

The inclusion of head-affected seepage in the development of the falling-head seepage meter equation can be described by the equations

$$Q_{s,H} = Q_{s,0} - AH$$

and

$$Q_{L,H} = CH,$$

where A and C are arbitrary constants, $Q_{s,H}$ is the seepage component and $Q_{L,H}$ is the leakage component. At the balanced-flow condition, the two components are numerically equal and opposite, so that the two expressions can be combined to yield

$$Q_{s,0} = (A + C)\ H_b.$$

At any other value of H, we can write for the net flow $Q_{m,H}$ leaving the seepage meter, calling $n = H/H_b$,

$$Q_{m,H} = C_n H_b - Q_{s,0} + AnH_b$$
$$= (A + C)nH_b - Q_{s,0}.$$

Substitution of the expression for $Q_{s,0}$ in this equation gives

$$Q_{m,H} = (n - 1)\ Q_{s,0},$$

which is the same as equation (6) in (17), so that the resulting formula for seepage calculation in the case of head-affected seepage is the same as the equation for the condition of constant seepage, namely,

$$I_{s,0} = \frac{2.3\ H_b\ R_v^2}{tR_c^2} \log \frac{H_b - H_0}{H_b - H_t},$$

where $I_{s,0}$ is the seepage rate at $H = 0$, R_c and R_v are the radii of seepage bell and reservoir, and H_0 and H_t refer to H at time 0 and at time t. Thus, the equation originally presented for seepage unaffected by pressure head on the canal bottom appears to be also applicable to the condition where there is a linear relation between seepage and pressure head.

The following equations were developed for estimating the hydraulic conductivity K of the bottom material for non-uniform conductivity conditions.

$$K = \frac{R_c\ I_{s,0}}{F_f\ H_b} \tag{2}$$

$$K = \frac{R_c\ I_{s,0}}{H_b\ (F_f + \frac{R_c}{D_p})} \tag{3}$$

$$K = \frac{R_c\ I_{s,0}\ (h_w - p - H_b)}{F_f H_b\ (h_w - p - \frac{R_c}{F_f})} \tag{4}$$

$$R_s = \frac{H_b}{I_{s,0}}. \tag{5}$$

The selection of the particular equation depends on H_b. The following values of H_b and the associated procedure for K-calculation are offered here as a guide.

$H_b < 0.2h_w$	Use equation (2). The term D or D_p for evaluating F_f may be derived from the description of the bottom material on the data sheet. For instance, 5 inches of coarse sand on loam would indicate a D of 5 inches. In the absence of knowledge regarding the bottom material, uniform soil conditions may have to be assumed, that is, D or D_p in excess of 2 R_c.
$0.2h_w < H_b < \frac{R_c}{F_f}$	Use procedure as for $H_b < 0.2h_w$.
$\frac{R_c}{F_f} < H_b < 0.8h_w$	Use equation (3) if D_p is known, in which case the pressure head p below the slowly permeable material can also be computed. If D_p is not known, use equation (4) with an assumed value for p, for instance, $p = 0$. D_p can also be estimated in this case.
$H_b > 0.8h_w$	Use equation (5) to obtain hydraulic impedance of the slowly permeable layer.

Laboratory studies

The results of the laboratory study on determining impedance of thin, slowly permeable bottom layers with seepage meters are shown in Figure 1. The agreement between the data obtained from the seepage tank and from the seepage meter appears to be quite good. Although the tests were only made for glass beads and sandy loam as slowly permeable layers, more than two different impedances are shown in Figure 1 because the impedance of a single layer had a tendency to increase during a test because of the formation of a "skin" at the surface of the layer.

Field studies

The results of the seepage meter studies in the golf course lagoon are shown in figure 2, where H_b is plotted as a function of the depth of penetration d of the seepage meter. The heavy line, which indicates the approximate mean of the three seepage meters, shows

that at approximately 3 cm a sharp increase in H_b occurs. The curve then becomes again more vertical at a d-value of approximately 7 cm. This indicates that the slowly permeable layer as formed by the artificial sealant extends from a depth of 3 cm to approximately 7 cm below the canal bottom. At two occasions, negative pressures of the order of 10 cm water were observed below the artificial seal.

The results of the seepage meter tests in the recharge pit indicated the presence of a slowly permeable layer at the bottom of the pit. This was evidenced by the values of H_b, which in most cases approximated and in a few cases even exceeded the water depth h_w. Thus, for increasing the recharge, cleaning of the recharge pit seemed all that was necessary.

SUMMARY AND CONCLUSIONS:

Principles of a falling-head seepage meter technique for evaluating seepage and hydraulic conductivity of bottom materials were extended to conditions of seepage affected by pressure head in the canal and to non-uniform conductivity of bottom material. The principles were reduced to simple procedures for routine application of the method in the field. The equipment includes a vacuum, inverted U-tube manometer for convenient, on the canal bank, measurement of the falling head inside the seepage meter.

Hydraulic conductivity of bottom material is evaluated via the balanced-flow differential head which is measured as the pressure difference between the water inside and outside the seepage meter after closing the meter at the top. Procedures for conductivity calculation are presented which apply to uniform bottom materials and to soils underlain by much less permeable, or by much more permeable, materials. For the case of bottom materials overlying much more permeable soil, the slowly permeable top layer may be partially or completely penetrated by the seepage meter. In the latter case, conductivity information is obtained in terms of hydraulic impedance.

The theory of the falling-head technique was tested in various laboratory models, where good agreement was obtained between seepage

meter results and measured or calculated values of seepage, hydraulic conductivity, impedance, and pressure below slowly permeable layers.

Seepage meters can be used in seepage investigations, in evaluations of the field performance of artificial soil sealants for reducing seepage, and in investigations of recharge installations. Examples are presented to illustrate the various applications of seepage meters and the type information that can be obtained with the falling-head technique.

PERSONNEL: Herman Bouwer and R. C. Rice.

Table 1. Results of seepage meter tests in recharge pit, July 27, 1962.

Seepage meter	h_w inches	d inches	H_b inches	$I_{s,0}$ inches/hr	R_s 1/ hrs
1	53	0.8	46	0.81	57
2	49	0.8	11	1.05	
3	46	1.2	40	11.4	4
4	44	0.4	37	2.0	18
		1.4 2/	41		
5	47	0.4	46	3.0	15
		0.6 2/	50		
6	45	1.6	33	0.60	55

1/ Only calculated where H_b was approximately equal to h_w.

2/ Deeper penetration of seepage bell for H_b measurement only.

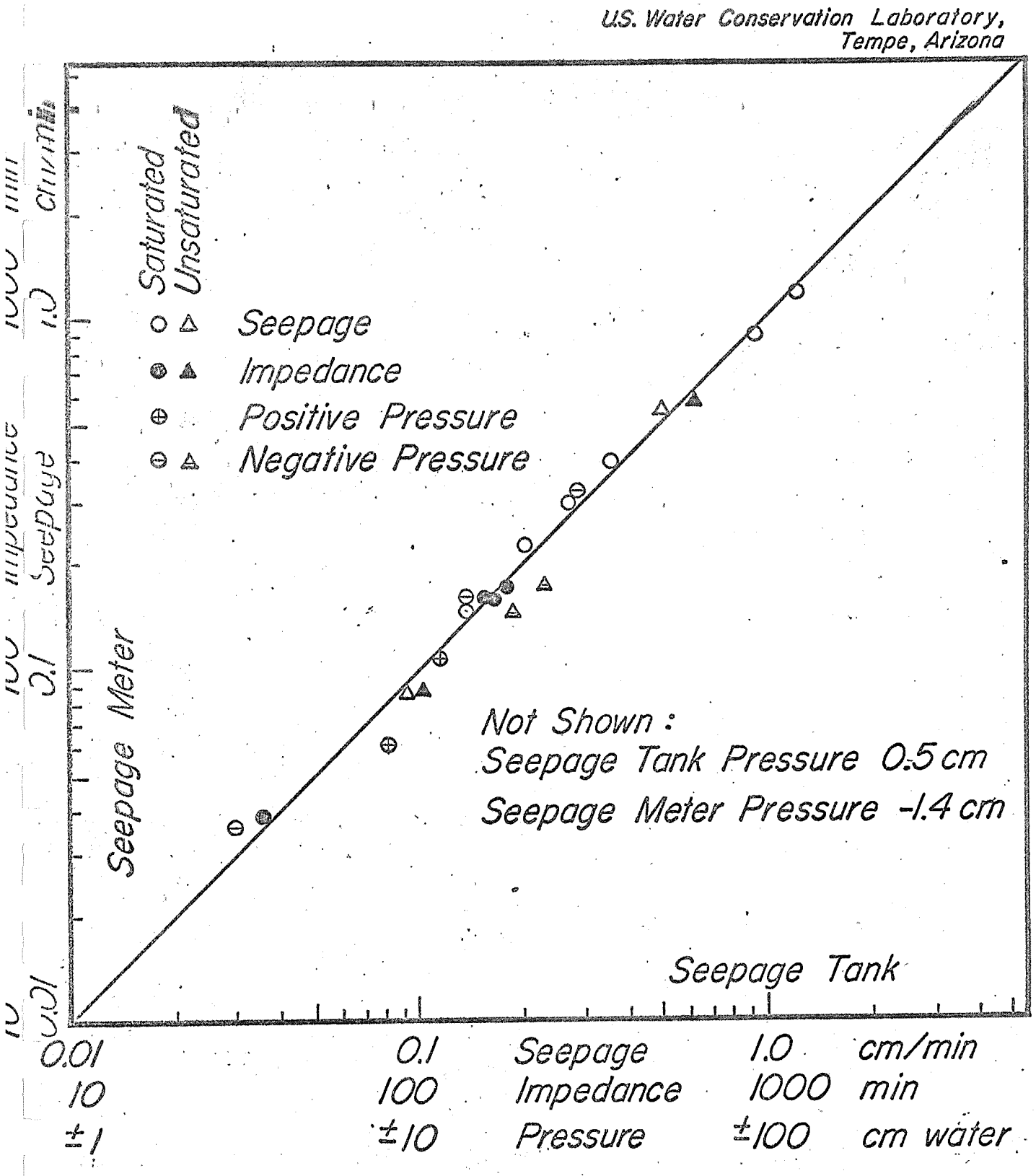

Figure 1. Results of tests with seepage meter in tank.

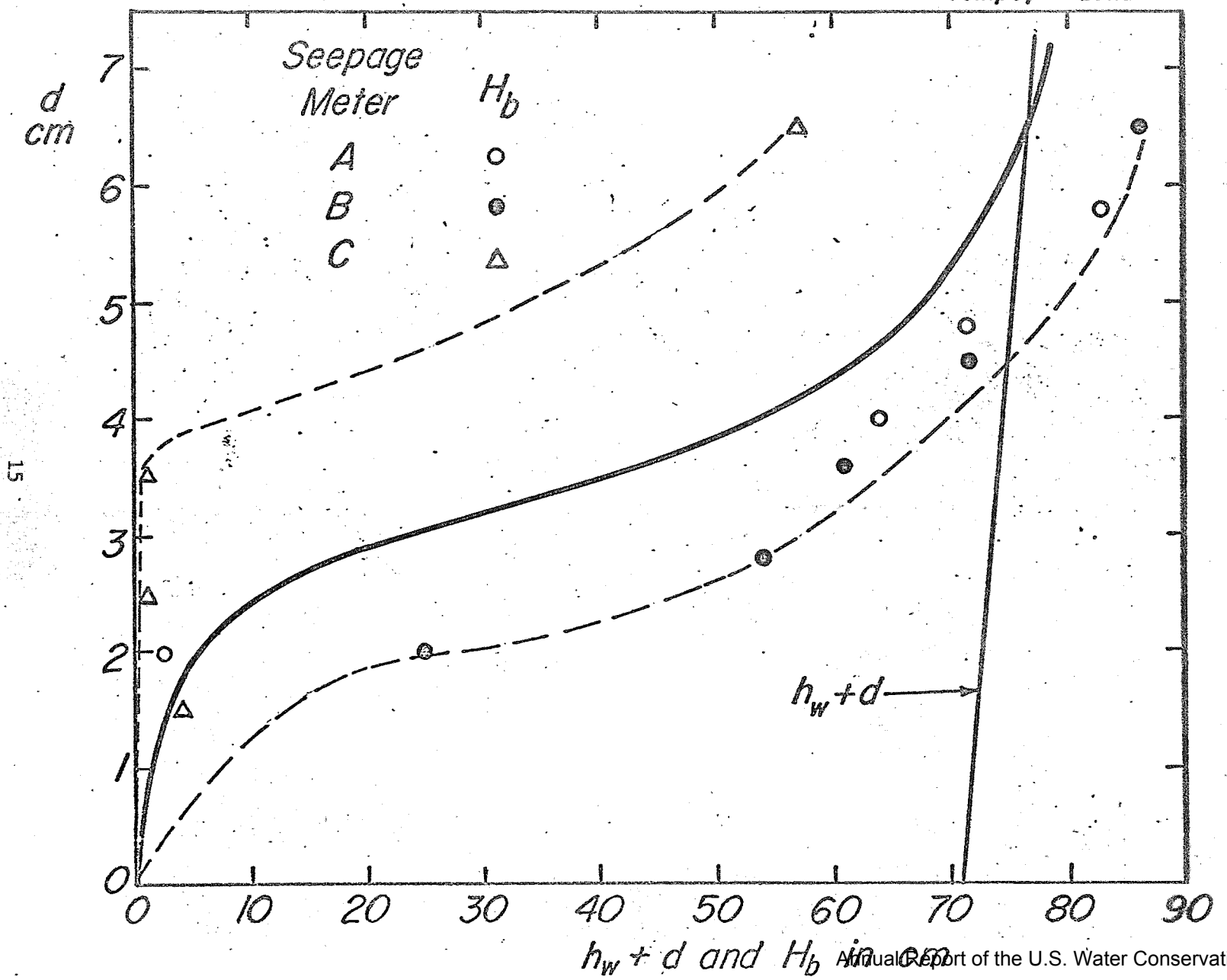
Seepage Meter
H_b
A
B
C
d cm
0
1
2
3
4
5
6
7
0
10
20
30
40
50
60
70
80
90
$h_w + d$
$h_w + d$ and H_b in cm

TITLE: FIELD APPLICATION OF FALLING-HEAD TECHNIQUE FOR SEEPAGE METERS AND OF DOUBLE-TUBE METHOD FOR HYDRAULIC CONDUCTIVITY MEASUREMENT

LINE PROJECT: SWC 4-gG1 CODE NO. Ariz.-WCL-14

PART II. APPLICATION OF DOUBLE-TUBE METHOD

INTRODUCTION:

Although the double-tube method has given good results and shown promise as a suitable field method for measuring hydraulic conductivity in the absence of a water table, it was considered desirable to extend the field testing to develop and test equipment and procedures for routine application. Another point of interest was to determine how the hydraulic conductivity as measured with the double-tube method would vary if the test were carried out for an extended period of time well beyond the minimum time required for sufficient artificial saturation. Finally, a simplified procedure was developed for processing the data to obtain hydraulic conductivity. This procedure, which consisted of an arithmetic integration rather than the graphical integration in the original equation for K, was tested for a rather large number of cases to determine its validity.

PROCEDURE:

Field tests

The field tests were carried out on the Bermuda lawn southeast of the main laboratory building, near the east fence. The soil is Adelanto loam. Three double-tube installations were tested simultaneously and a total of nine locations was tested. The depth of the auger holes ranged from 76 to 186 cm. The duration of the total test periods ranged from 2 to 7 days with K-measurements taken several times daily. In addition, a record was kept of the infiltration rate at the bottom of the hole with both standpipes full, and of the temperature of the water.

The location of the holes, which are identified by number, is shown in Figure 1. Pertinent data for the holes is shown in Table 1.

Simplified procedure

The simplified arithmetic procedure for K-calculation consisted of replacing the graphically determined ratio $\Delta H_t / \int H dt$ by the ratio

$2\Delta t/t^2_{eq.l.}$, which can be directly computed from the equal-level and constant-level H and t measurements (41, 85). The ratio $2\Delta t/t^2_{eq.l.}$ was then used in the equation for calculation of K. The equality of the two ratios appears from Figure 2, where the equal-level and constant-OTS curves are replaced by straight lines.

RESULTS AND DISCUSSION:

Field tests

The variation of hydraulic conductivity, infiltration rate, H_b, and temperature with time is shown for each test in Figures 3 through 11. In general, consistent K-values were obtained after four hours had elapsed. After sufficient saturation was attained, the difference between the maximum and the minimum K-value for any given day did not exceed 50% of the maximum value. The variation from day to day was somewhat greater with the maximum being two to three times the minimum value. In most cases, the trend in the K-values from day to day paralleled that of the infiltration, although daily fluctuations in K did not always follow this trend.

The changes in temperature were not sufficient to explain the variation in K with time. However, temperature may have affected K indirectly, for instance, through formation of air pockets in the soil and subsequent solution of the air in the water due to temperature fluctuations.

Structural decline or microbiological action may cause reductions in K under prolonged inundation. On the other hand, K increases may be caused by repeated "leakage" flow due to falling-level measurements in the inner tube standpipe. This could result in "flushing" or enlarging the macro pores in the soil accounting for the leakage flow. Thus it is possible that K increases or decreases during the period of testing, depending on which action has a predominant effect. In general, however, the variations for extended periods of tests were not prohibitive and "levels" of hydraulic conductivity could be assessed in most instances.

The average K-values or "levels" of hydraulic conductivity for group of holes 2 through 9 ranged from 0.06 cm/min to 0.12 cm/min with

an average of 0.09 cm/min. A graph showing the observed K-values in relation to the depth of the auger hole does not show a clear relation between K and depth (Figure 12). The "outlying" hole No. 1 was close to a structure and the soil may have been affected by excavation.

Simplified procedure

From the falling-level measurements, values of $\Delta H_t/\int Hdt$ and $2\Delta t/t^2_{eq.1.}$ were determined graphically and arithmetically, respectively, and extrapolated to H or t equal to 0 (85). The results (Figure 13) show that 80% of the values of $2\Delta t/t^2_{eq.1.}$ was within plus or minus 20% of the $\Delta H_t/\int Hdt$-values. Most of the values that were not within the 20% limits were calculated from hole No. 1, where ΔH_t was very small and could therefore not be accurately determined from the graph with the equal-level and outer-level constant curves. Since the graphical determination of $\Delta H_t/\int Hdt$ is to some degree subject to the manner in which the curves are drawn through the H and t points, it is concluded that $2\Delta t/t^2_{eq.1.}$ can be used as a convenient and accurate substitute of the ratio $\Delta H_t/\int Hdt$.

SUMMARY AND CONCLUSIONS:

Nine double-tube installations were run for a period of two to seven days in Bermuda-covered Adelanto loam southeast of the laboratory building. Fairly consistent values were obtained within four hours after water application was started. The fluctuation in the K-values did not exceed fifty percent of the maximum value during any one day. The trend in K paralleled that in the infiltration rate at the bottom of the hole. Direct effect of temperature could not be detected. Structural decline, formation of air pockets and subsequent solution of air in the soil water, opening up of pores due to successive leakage flow patterns, and microbiological action can be cited as reasons why hydraulic conductivity may increase, decrease, or fluctuate, during extended test periods. Of the nine holes, eight were located relatively close together. The K-values of these holes ranged from 0.06 to 0.12 cm/min.

Comparison between the arithmetically determined ratio $2\Delta t/t^2_{eq.1.}$ for substitution of the graphically determined ratio $\Delta H_t/\int Hdt$ in the

equation for calculation of K shows that a simplifying assumption is valid and that the former can be used as an accurate substitute of the latter.

PERSONNEL: Herman Bouwer and R. C. Rice.

Table 1. Pertinent Data for Double-Tube Field Tests [a]

Hole No.	d cm	h_w cm	Hole Depth cm
1	1.7	183	76
2	1.3	216	100
3	1.3	342	186
4	1.6	342	181
5	1.6	277	134
6	1.3	216	108
7	1.4	342	178
8	1.5	277	141
9	1.8	216	105

a/ 5" - 8" tubes and 1" standpipes used

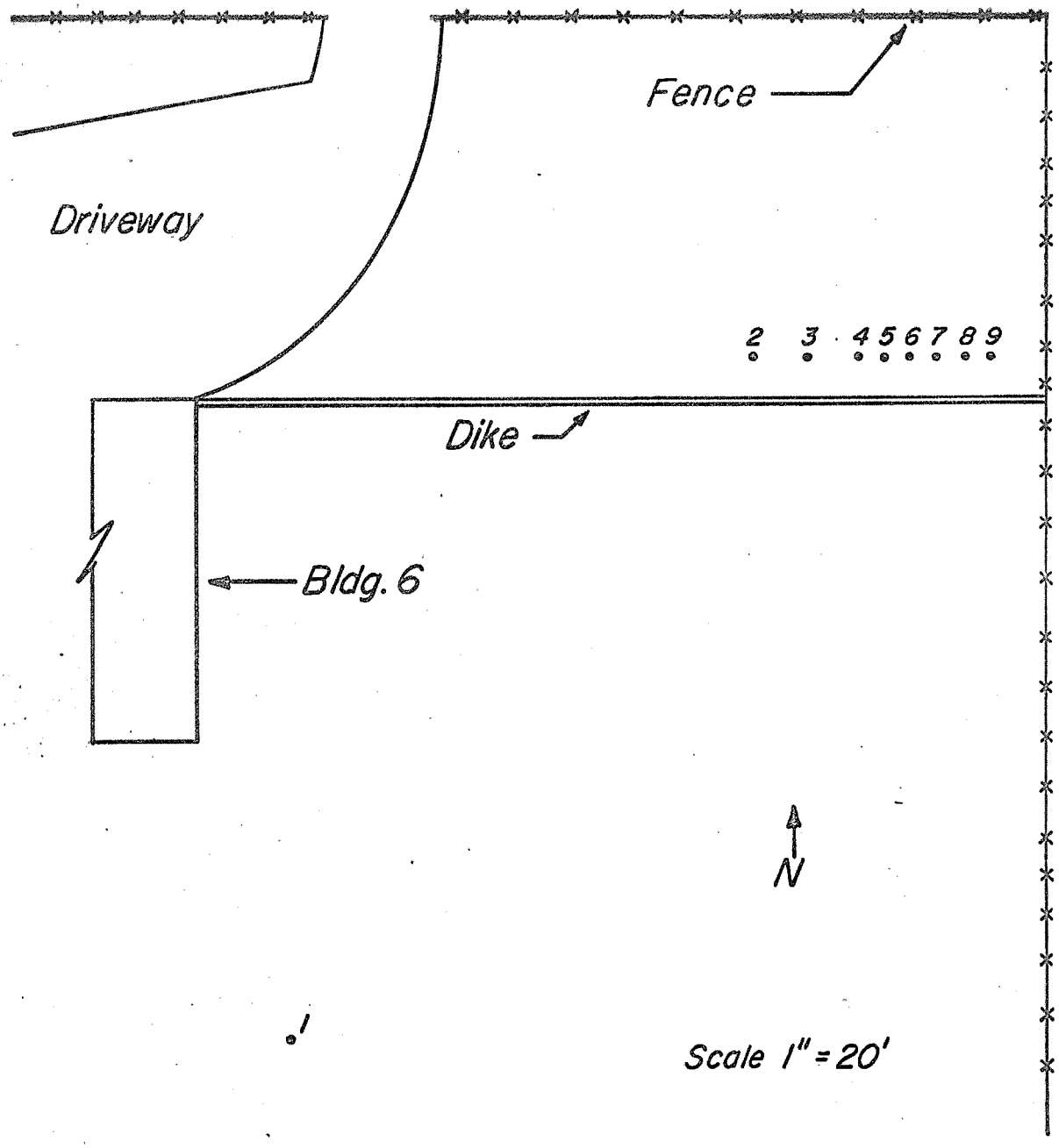

Figure 1. Location of holes for double-tube tests.

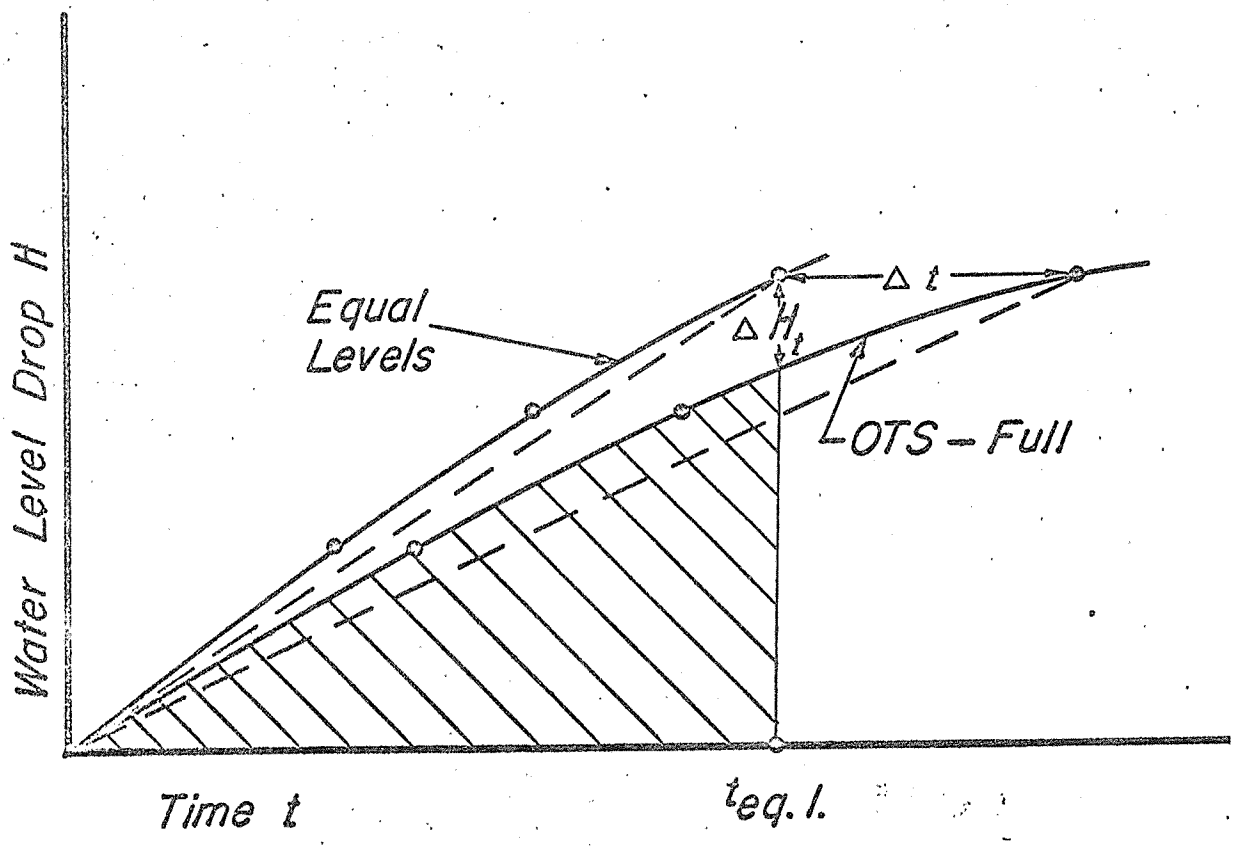

Figure 2. Schematic plot of equal-levels and OTS-full curves showing approximation of $\Delta Ht/\int Hdt$ by $2\Delta t/t^2_{eq.l.}$.

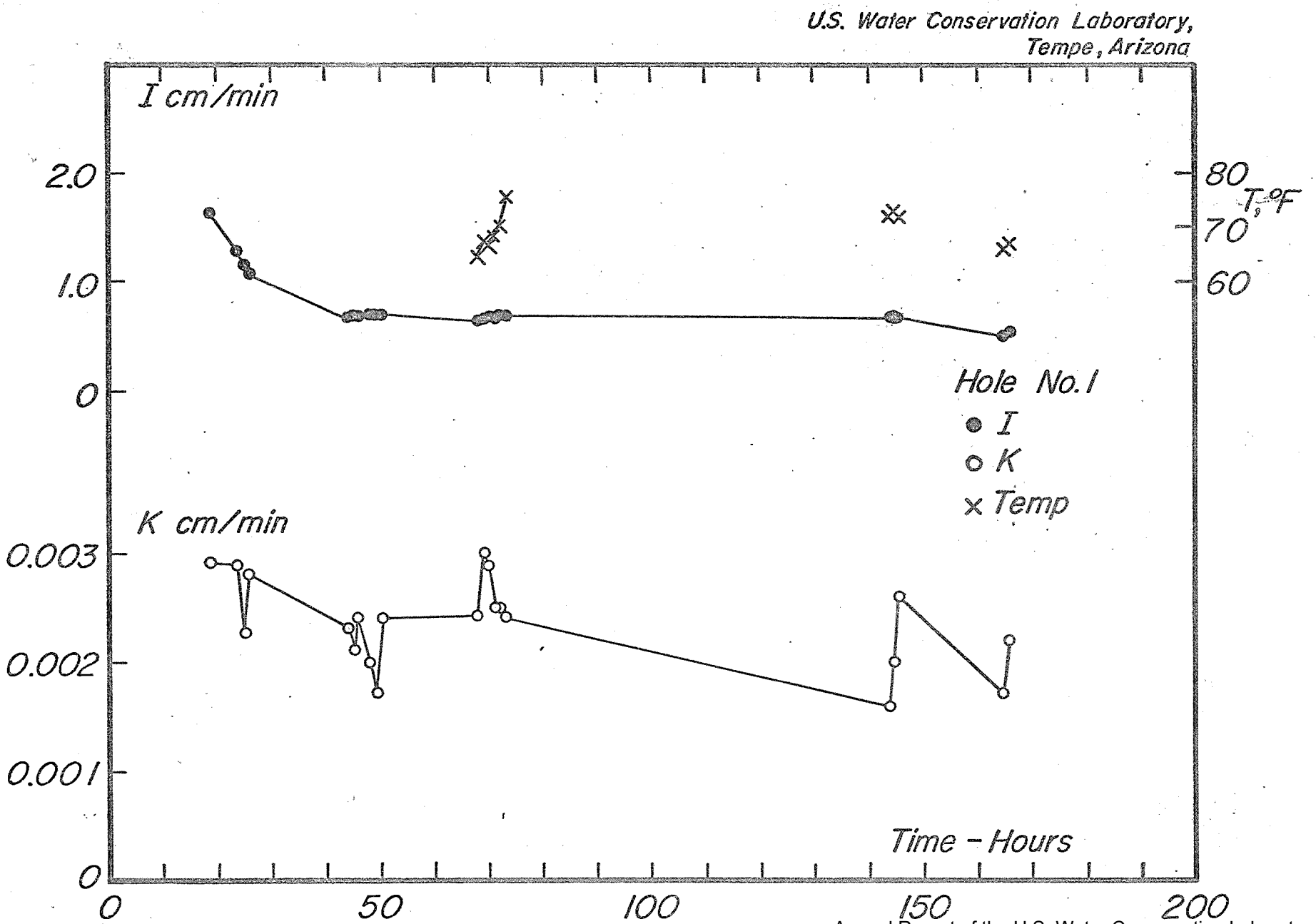

Figure 3. Result of double-tube test at hole No. 1

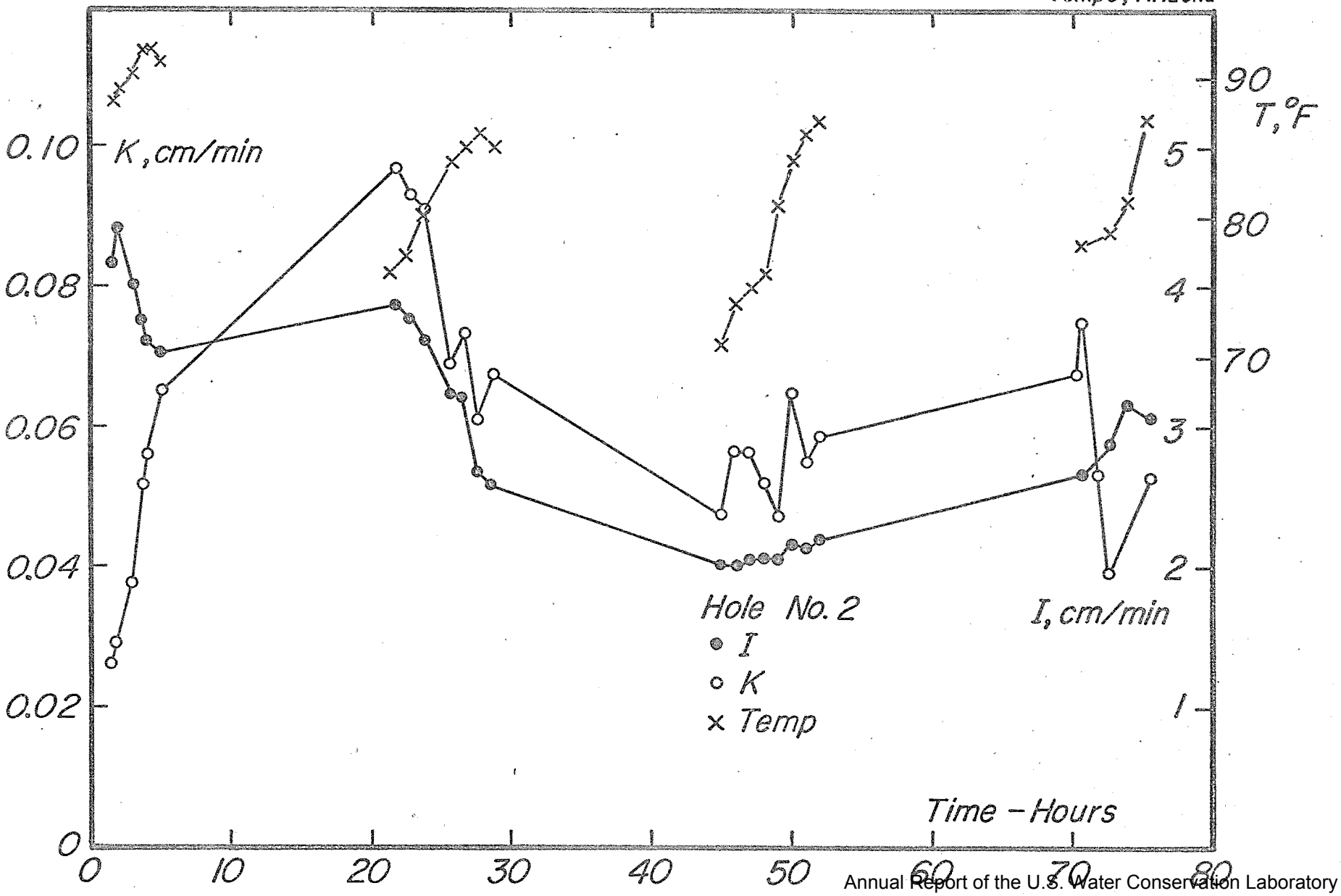

Figure 4. Result of double-tube test at hole No. 2.

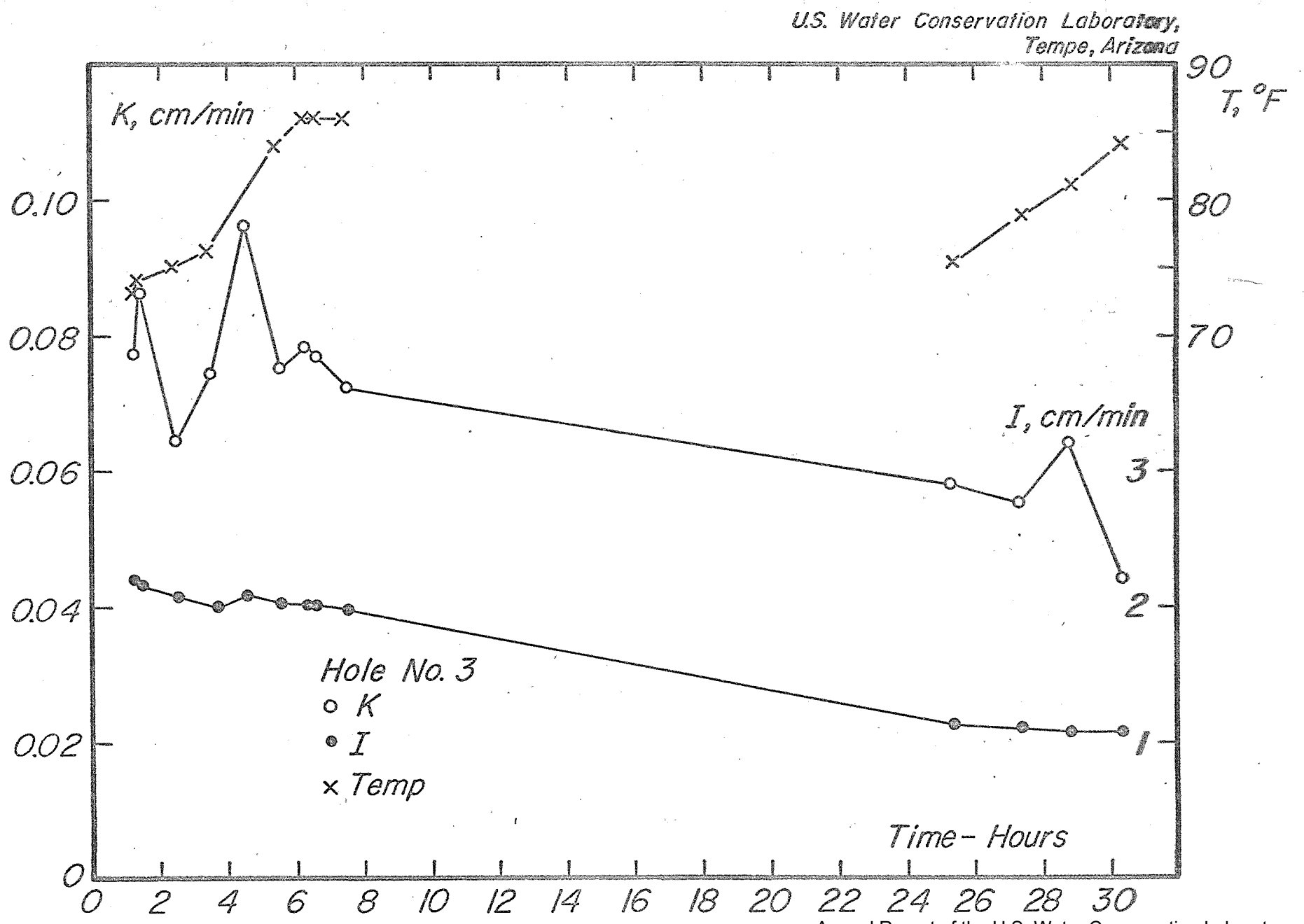

Figure 5. Result of double-tube test at hole No. 3.

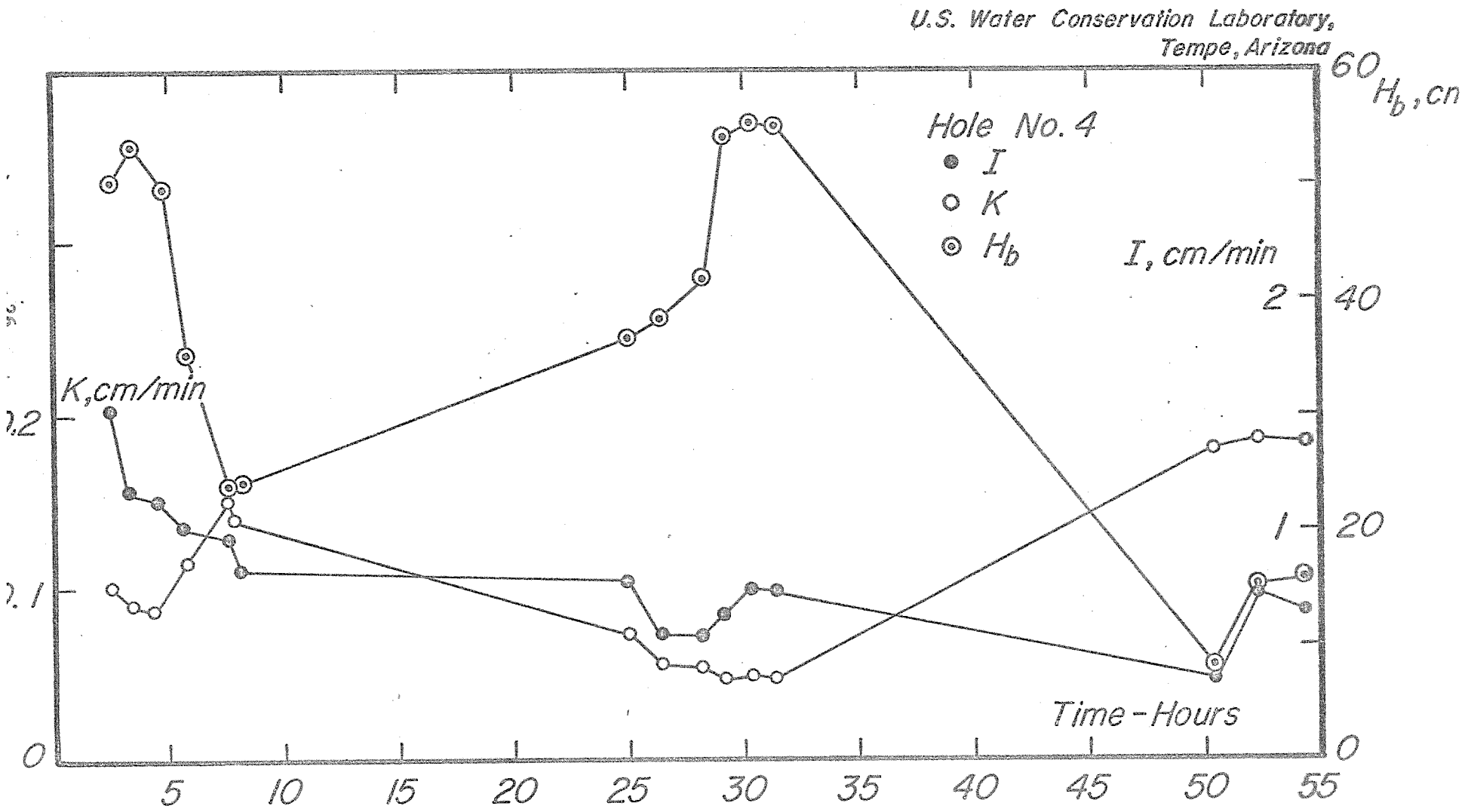

Figure 6. Result of double-tube test at hole No. 4.

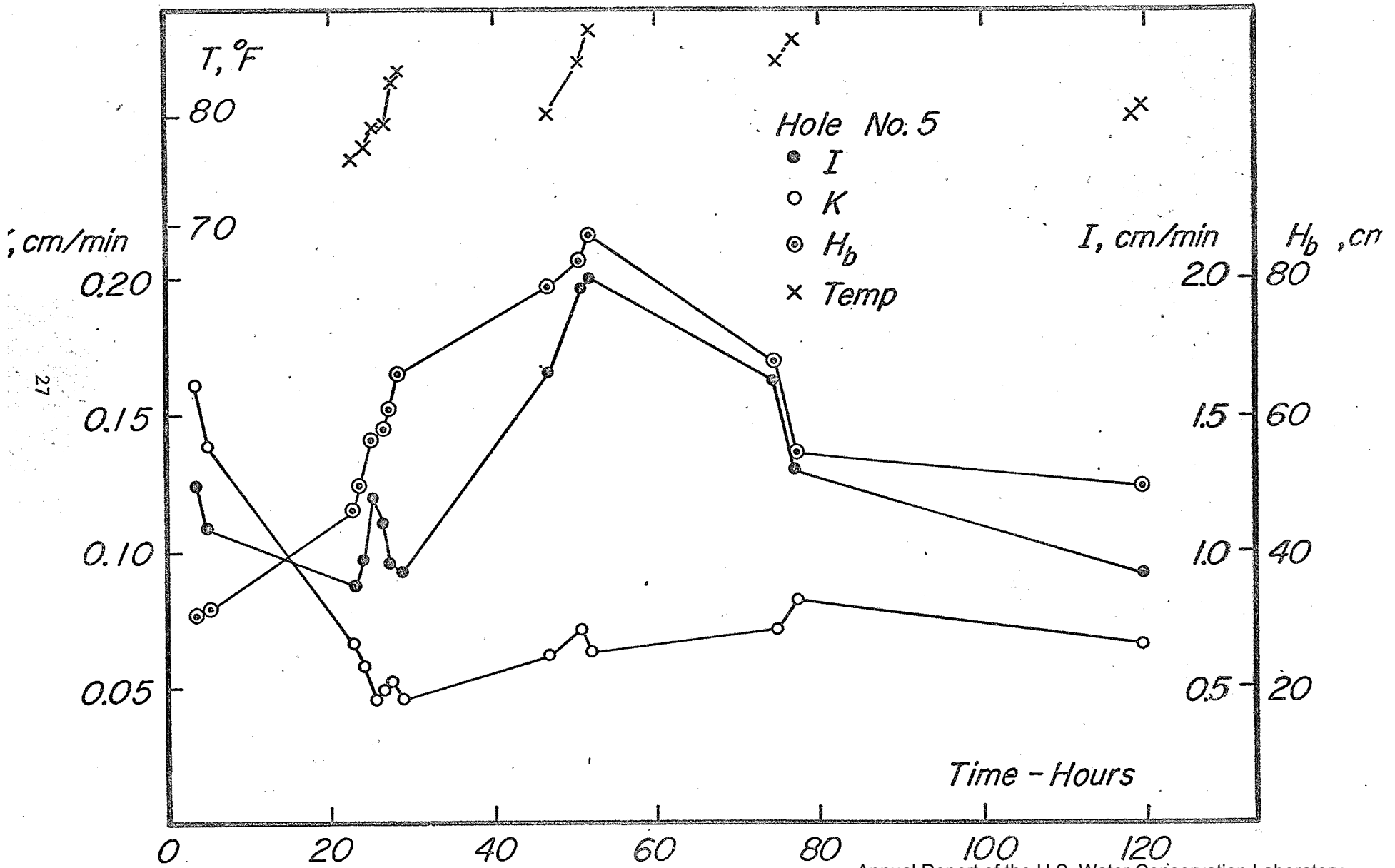

Figure 7. Result of double-tube test at hole No. 5.

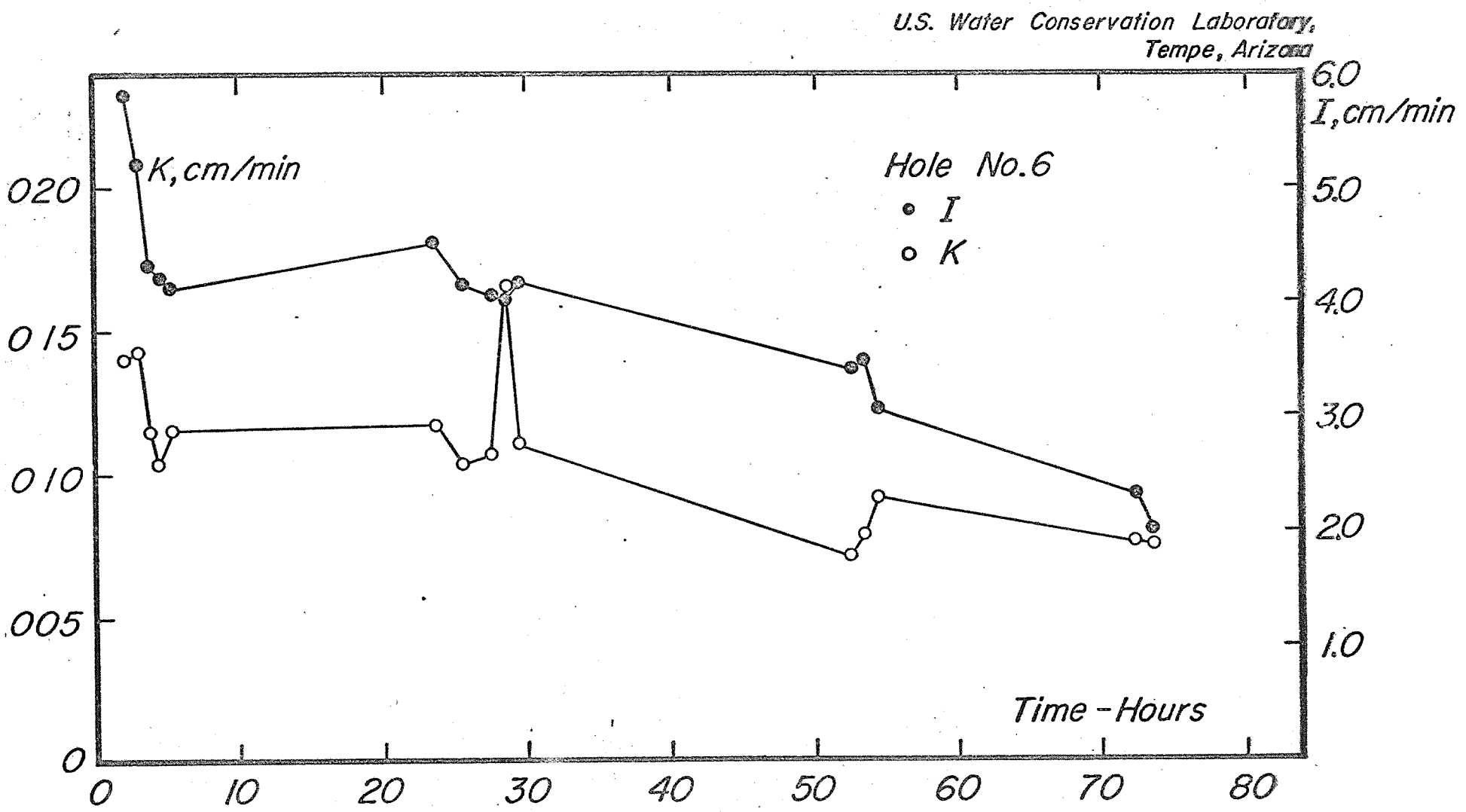

Figure 8. Result of double-tube test at hole No. 6.

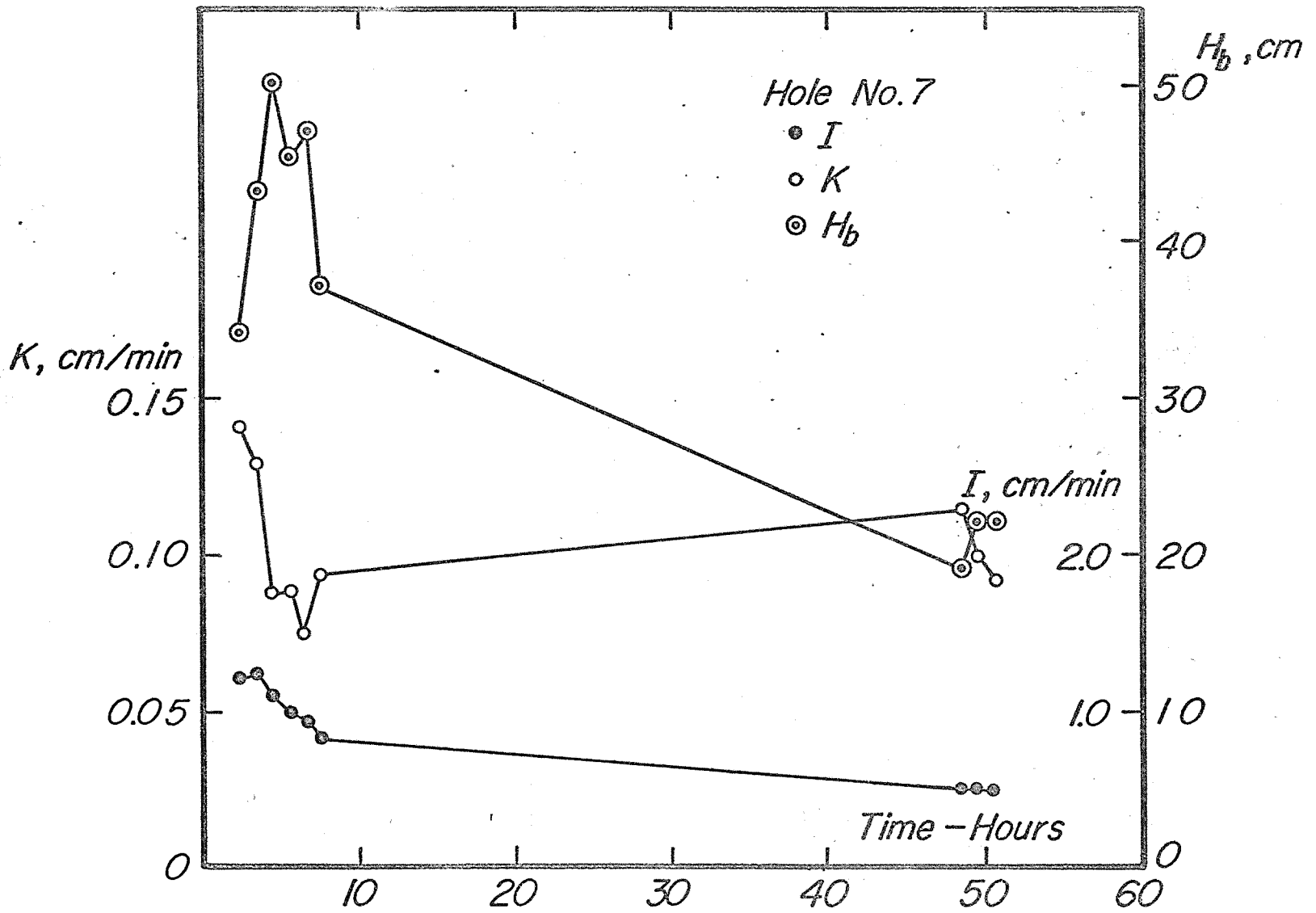

Figure 9. Result of double-tube test at hole No. 7.

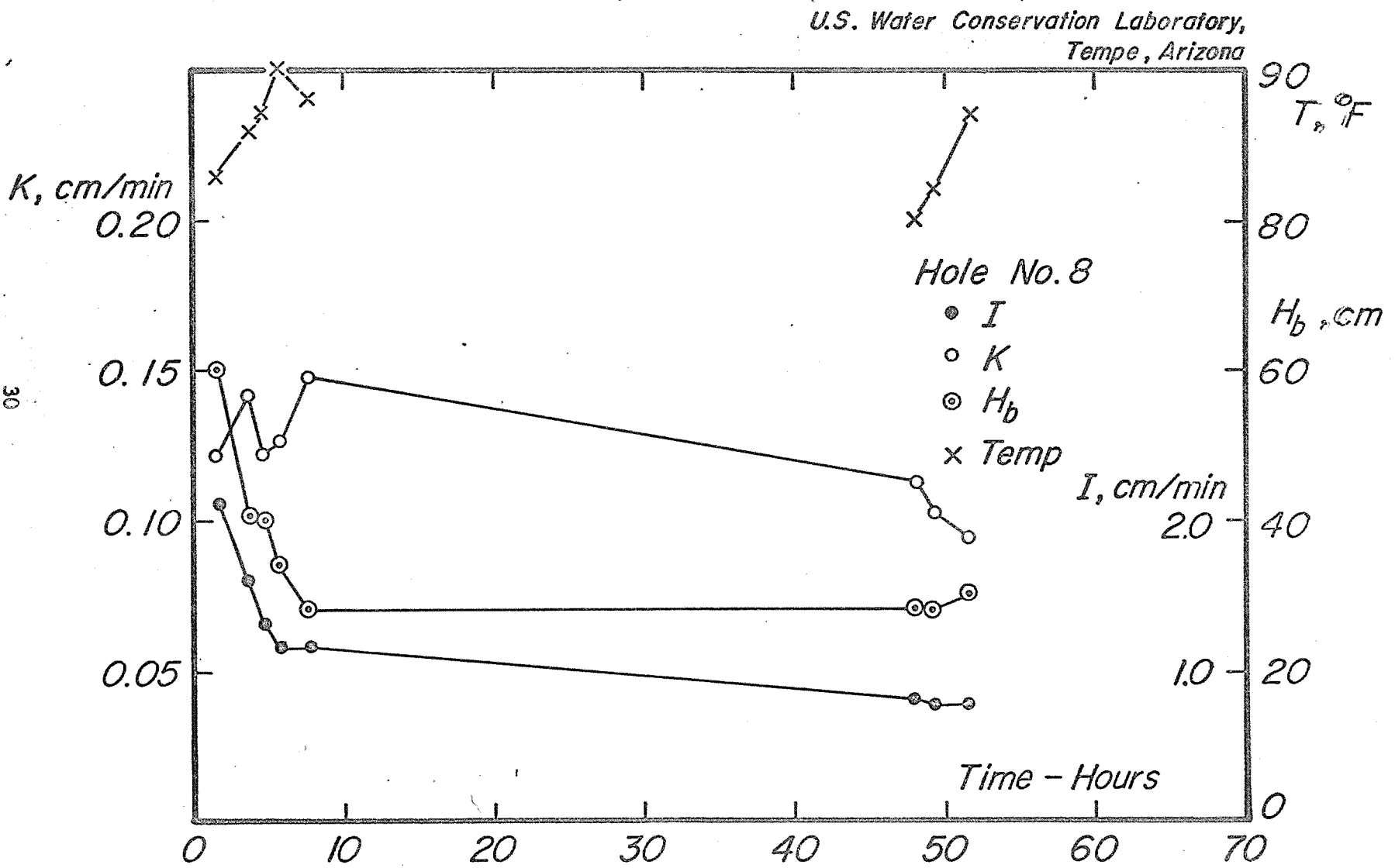

Figure 10. Result of double-tube test at hole No. 8.

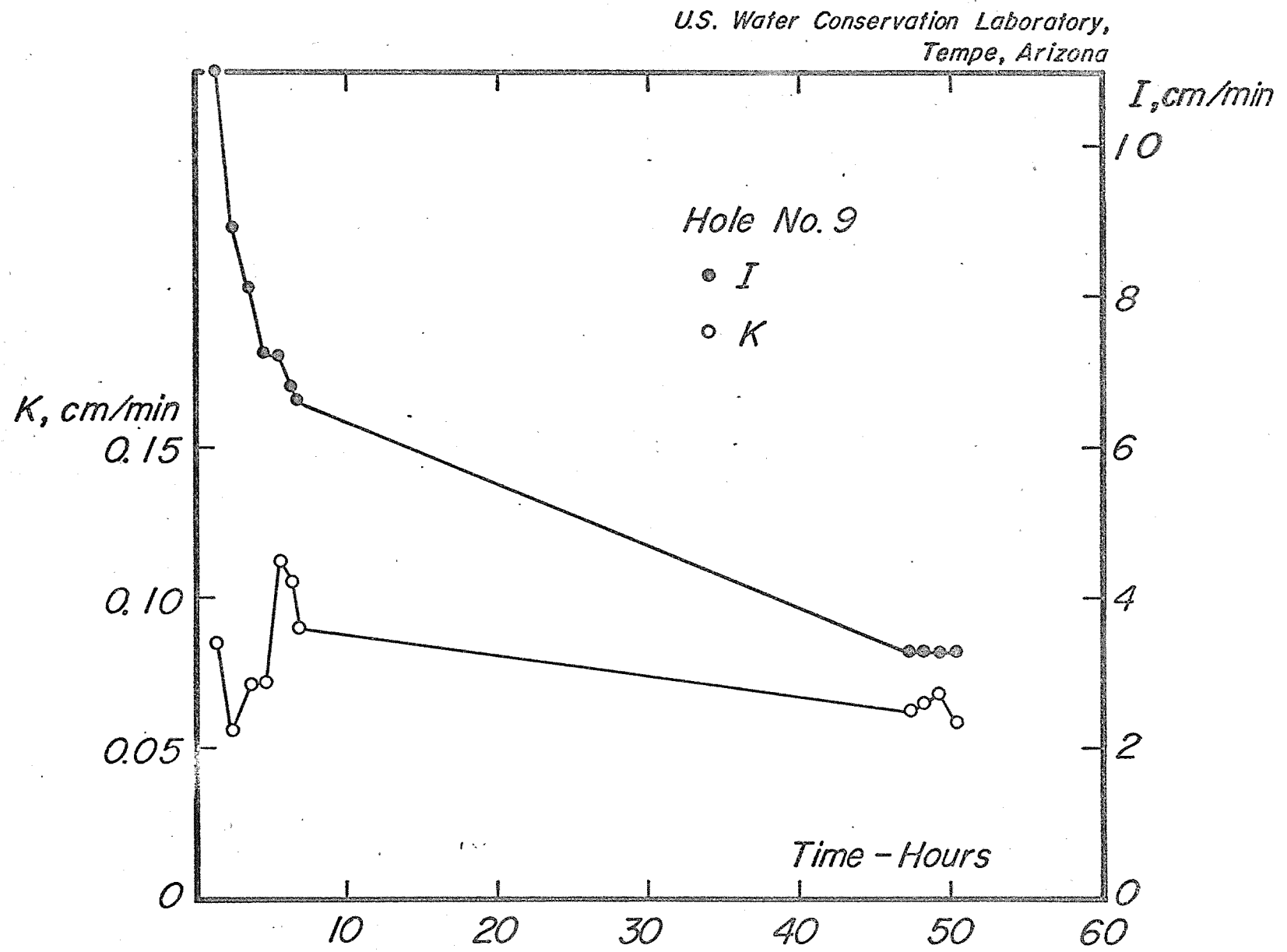

Figure 11. Result of double-tube test at hole No. 9.

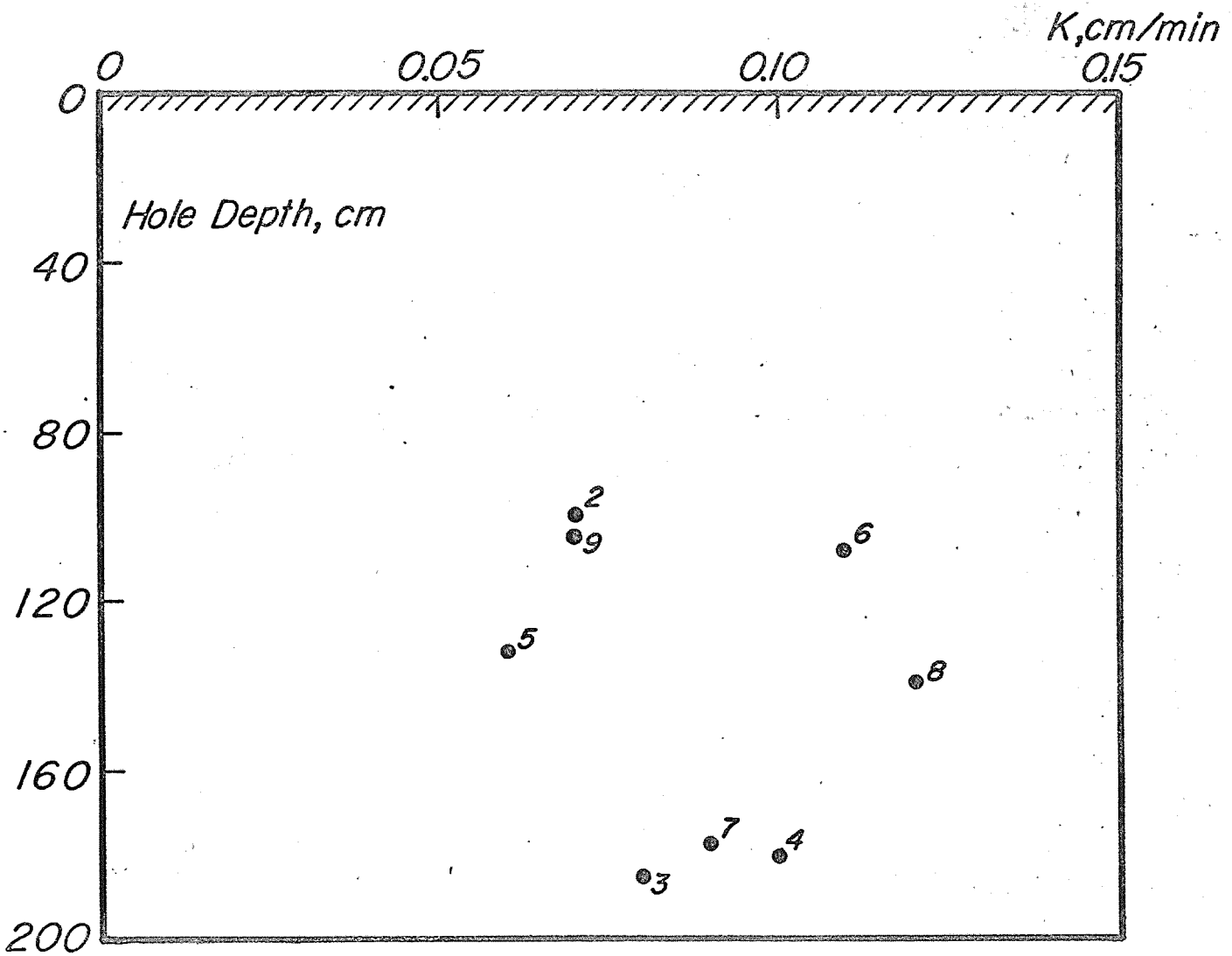

Figure 12. Hydraulic conductivity in relation to depth of hole.

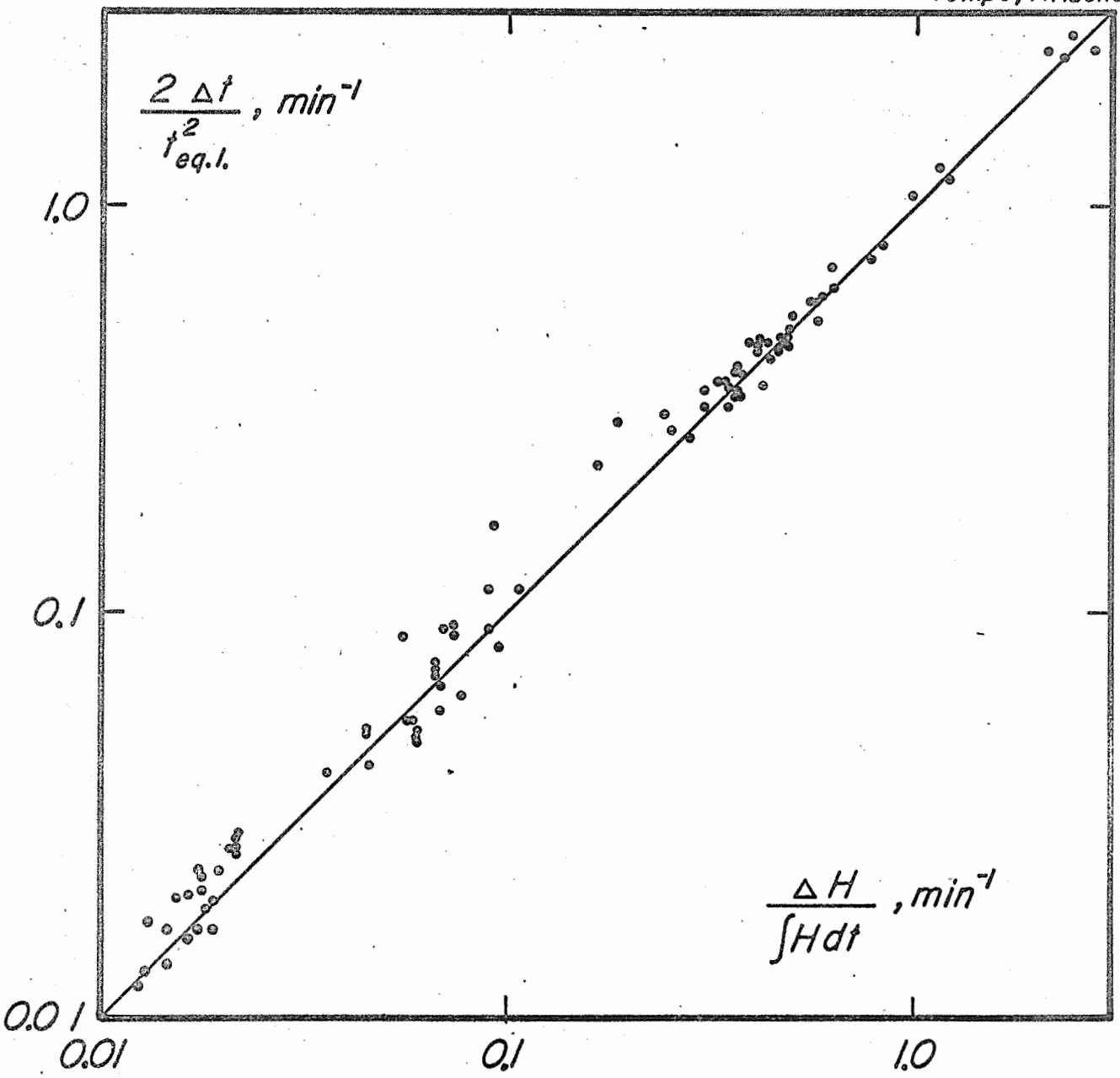

Figure 13. Comparison of $2\Delta t/t^2_{eq.l.}$ and $\Delta H/\int Hdt$.

TITLE: THEORETICAL EFFECT OF SOIL, WATER TABLE AND CANAL CONDITIONS ON SEEPAGE FROM CANALS.

LINE PROJECT: SWC 4-gG1 CODE NO.: Ariz.-WCL-24

INTRODUCTION:

For decision making in water management problems involving canal seepage, a general knowledge as to how seepage is in principle affected by conditions of canal, soil, and water table is desirable. Although for a few conditions analytical or approximate solutions are available, such solutions were not at hand for a number of problems. Since various rather complicated problems were considered to be included in this study, an electrical resistance network was used to obtain solutions. By taking this approach, additional information such as flow nets, water table shapes, capillary fringes, etc., could also be obtained. The experiment is still in progress, and only preliminary data and conclusions will be presented here.

PROCEDURE:

Seepage conditions

The many different conditions under which seepage from canals may take place were simplified into the following three basic conditions:

A. The soil below the canal is considered to be of uniform hydraulic conductivity K and underlain at a depth D_p below the canal bottom by much more permeable material. The water table slopes away from the canal and approaches asymptotically a horizontal water table. The vertical distance of this horizontal water table below the water level in the canal is designated $D_{w,\infty}$. The water table position at an arbitrarily selected distance of five times the bottom width of the canal from the center of the canal is designated $D_{w,5}$.

B. The soil below the canal is underlain at depth D_i by material that is impermeable or of much lower hydraulic conductivity than K. In other respects, this condition is similar to condition A.

C. The canal is surrounded along its wetted perimeter by a thin, slowly permeable layer which restricts the seepage flow. The soil below the slowly permeable layer is unsaturated and the flow in the percolation zone below the canal is essentially downward at unit gradient.

The three conditions are illustrated in Figure 1, which also shows the symbols used. The seepage for conditions A and B was analyzed by means of the resistance network analog, condition C could be treated analytically.

Analog analyses

Variables included in the analyses were the water depth in the canal, the cross section of the canal, the depth of the water table at infinity, the depth of the permeable material (for condition A), the depth of the impermeable material (for condition B), the hydraulic conductivity of the canal bottom material, the hydraulic conductivity of the subsoil, and the unsaturated conductivity characteristics of the medium. For generalization of the results, the data are expressed in dimensionless parameters.

The resistance network for solving conditions A and B was designed so that the grid pattern was densest in the vicinity of the canal and became more extensive with increasing horizontal and vertical distance from the canal. The shape of the water table between the canal and the termination zone of the analog representing infinity conditions were found by trial and error, starting with assumed shapes and making adjustments until the pressure at the water table was measured as atmospheric. The horizontal water table, which in theory is reached at infinity, was simulated on the analog at a distance of 10 W_b from the canal center.

The seepage rates, measured as electrical current, were converted to the volume rate q_s of seepage per unit length of canal, per unit width of the water surface, and per unit hydraulic conductivity of the soil, or $\bar{I}_s = q_s/W_sK$. The dimensionless parameter thus obtained is essentially an expression of the seepage in terms of an average vertical gradient in a hypothetical flow zone extending vertically downward from the water surface of the canal. The parameter can also be considered as the rate of fall of the water surface due to seepage in a ponded canal, expressed per unit hydraulic conductivity of the soil. The geometries of the seepage flow systems were characterized by ratios of characteristic lengths.

Although canals of rectangular and triangular cross sections are also to be included in the study, the results presented here are for a canal of trapezoidal cross section with 1:1 side slopes.

Unsaturated conductivity

The effect of the unsaturated conductivity characteristics of the subsoil was included by the introduction of a critical pressure (head) as it reflects the ability of a soil to transmit water at negative pressures. The critical pressure selected in the analyses was $-W_b/12$. For a canal with a bottom width of 12 ft, for instance, this would mean a critical pressure of 1-ft of water. Conversely, at a critical pressure range of -0.5 to -1.5 ft of water, the selected value of $-W_b/12$ for critical pressure would cover a range in bottom widths of 6 to 18 ft. Since seepage tends to be most severe in coarse soils, which tend to have higher critical pressures, the critical pressure of $-W_b/12$ and the analyses with a critical pressure of 0 can be considered as end points of a range which is likely to cover most cases in practice.

Seepage distribution

To determine the relative magnitudes of seepage from the canal banks and the canal bottom, seepage distribution patterns across the canal wetted perimeter were evaluated for a number of cases. Also, the effect of making the bottom impermeable on seepage was determined to evaluate the feasibility of sealing bottom material only for reducing seepage. Information regarding this effect would be valuable, for instance, in designing minimum cost treatments with water-borne chemical sealants for seepage reduction.

RESULTS AND DISCUSSION:

Conditions A and B

A typical example of the results of the analyses for conditions A and B is shown in figure 2, which applies to a trapezoidal canal with 1:1 side slopes, a water depth of 0.75 W_b, and a critical pressure of 0. Figure 2 shows that low $\bar{I}_s/K$-values occur for shallow water tables and impermeable layers (condition B). The seepage increases as the depth of the impermeable material and that of the water table is increased until a maximum is reached for D_i at infinity. The curves

for condition A are above this curve, starting with deep permeable layers (large values of D_p). As the depth of the permeable layer decreases, the seepage increases. The curves for condition A terminate at the point where $D_p = D_{w,\infty} - H_w$, where the water table coincides with the top of the permeable layer. This seepage condition is essentially one of seepage to a permeable substratum which has sufficient internal drainage to dispose of the seepage without formation of a ground-water table extending above the permeable substratum. Thus, the permeable bed can be just saturated or it can be unsaturated with atmospheric pressure conditions. In any case, the lower boundary of the seepage flow system in this case is a horizontal plane of atmospheric pressure. For further reference, this condition will be designated condition A'.

Figure 2 shows that if $D_p > 4W_b$ and if $D_i > 15W_b$, the seepage approximates that for the curve where D_p or D_i is infinity. Thus, as long as the permeable material is more than 4 bottom widths below the canal, or the impermeable material is more than 15 bottom widths below the canal, the medium can be considered to be uniform for essentially infinite depths. The effect of lowering the water table, that is, increasing $D_{w,\infty}$, is greatest at low values of $D_{w,\infty}$. When $D_{w,\infty}$ has reached a value of approximately 5 W_b, the effect of further lowering the water table on seepage is very small and the system can be considered as that of seepage to an infinitely deep water table or permeable stratum. The very high values of the curve for condition A' at low values of $D_{w,\infty}/W_b$ shows the high seepage rates, or rather gradients, that can occur if canals are underlain by permeable substrata at shallow depths.

Graphs similar to the one in Figure 2 will be prepared for other depths of water in the canal. Average curves for the seepage under condition B, which give the seepage for a depth range of 0.25 W_b to 0.75 W_b with less than 10% error, are shown in Figure 3.

The seepage for conditions A' and B has also been solved mathematically (see, for instance, The Flow of Homogeneous Fluids Through Porous Media by M. Muskat). For the case of seepage to a theoretically infinitely deep permeable bed or water table, the theoretical solution

by Vedernikov gives $\bar{\bar{I}}_s/K$-values of 1.53, 1.67, and 1.78 for H_w/W_b of 0.25, 0.50, and 0.75, respectively. The corresponding values obtained by analog are 1.57, 1.70, and 1.81. Hence a very good agreement.

The seepage of condition B has been treated analytically for relatively shallow water tables and impermeable layers. This theory, which is due to Dachler and is discussed by Muskat, consists of dividing the flow system into two parts, one part with predominantly horizontal flow, and one part with plane-source flow. Using Dachler's procedure, the seepage rate, $\bar{\bar{I}}_s/K$ was calculated for several positions of water table and impermeable layer. The results, indicated as dots in Figure 3, show good agreement even though the theory is approximate and semi-empirical.

Unsaturated conductivity

The main effect of introducing a critical pressure less than 0 is that an extra flow path is provided. For horizontal or mildly sloping water tables (small $D_{w,\infty}$) this extra path is commonly referred to as the capillary fringe. The contribution of the capillary fringe to the seepage flow in this case is approximately proportional to the height of the capillary fringe with respect to the average distance between the water table and the impermeable layer. Thus, the effect of critical pressure on $\bar{\bar{I}}_s$ for condition B can be ignored, except under conditions of shallow impermeable layers. For very deep water tables (large $D_{w,\infty}$), where the seepage flow is mainly downward, the introduction of a critical pressure less than 0 causes an increased divergence of the streamline below the canal, and consequently, a greater width of the flow zone at unit vertical gradient at some distance below the canal.

The effect of critical pressure on seepage for condition A' is illustrated by Figure 4. The greatest effect of the critical pressure appears to occur at relatively large $D_{w,\infty}$-values, where the opportunity for flow divergence is greater than for small $D_{w,\infty}$-values. The increase in seepage, however, is rather small, and insignificant for practical considerations.

Condition C

The seepage for condition C is analyzed from a standpoint of hydraulic impedance, symbol R_s, of the slowly permeable layer, and the unsaturated conductivity characteristics of the underlying soil material as reflected by the critical pressure p_c. Taking the pressure in the unsaturated material below the slowly permeable material as the critical pressure, the seepage at any point can be expressed as $I = \frac{h_w - P_c}{R_s}$. In this equation, it is assumed that the thickness of the slowly permeable layer is insignificantly small compared to the water depth. Applying the above equation to the entire wetted perimeter of the canal gives the following expression for $\bar{\bar{I}}_s$ for the seepage under condition C.

$$\bar{\bar{I}}_s = \frac{H_w - P_c}{W_s R_s} \left(\frac{H_w}{\sin \alpha} + W_b\right). \qquad (I)$$

Seepage distribution

Typical distribution patterns for the seepage inside the canal are shown in Figures 5 and 6 which apply to flow systems of relatively large extent (large $D_{w,\infty}$ for condition A' and large D_i for condition B). The point of highest seepage is at the toe of the canal bank and the local seepage gradients in the bottom are slightly greater than those at the bank. A marked increase in bottom seepage occurs when, for condition A', the atmospheric pressure contour becomes closer to the canal bottom (Figure 7). Although a decrease in $D_{w,\infty}$ causes both bank and bottom seepage to increase, the greatest increases are for the bottom seepage. A decrease in bottom seepage can be observed when, for condition B, the impermeable layer is at relatively shallow depth (figure 8). In the extreme case of $D_i = 0$, no seepage at all occurs at the bottom for condition B. The seepage distribution patterns for condition A can be expected to lie between those for condition A' and B.

The seepage distribution for condition C can be calculated with equation (1). Assuming constant R_s and P_c, the seepage at the bottom

is uniform and equal to $(H_w - P_c)/R_s$. The seepage at the bank varies linearly from $-P_c/R_s$ at the water level to $(H_w - P_c)/R_s$ at the toe of the bank.

The seepage distribution patterns presented here apply to uniform soil or, for condition C, to a uniform, slowly permeable layer underlain by permeable soil. In heterogeneous soils, entirely different distribution patterns may exist.

The effect on seepage of rendering the bottom material impermeable while leaving the permeability of the banks unchanged, is shown in Figure 9 for a few selected values of $D_{w,\infty}$ and D_i for conditions A' and B. The general picture indicated by the curves is that sealing canal bottoms only does not give satisfactory seepage reduction, except for very shallow canals or canals underlain by very shallow permeable substrata.

SUMMARY AND CONCLUSIONS:

Resistance network analyses were made to determine quantitative effects of canal and subsurface conditions on seepage. Variables included were the water depth in the canal, the shape of the canal, the position of the water table at great distance from the canal, and the saturated and unsaturated hydraulic conductivity of the soil. Distinction was made between two subsurface soil conditions. For the first condition (condition A), the soil was considered to be underlain by very permeable material with virtually unrestricted internal drainage. For the second condition (condition B), the soil was considered to be underlain by impermeable material. The depth of the permeable or impermeable material was taken as a variable in the analyses. A third condition (condition C), consisting of a canal surrounded along its wetted perimeter by a thin, slowly permeable layer, was analyzed mathematically. The study is still in progress and only preliminary results applying to a trapezoidal canal with 1:1 side slopes and a water depth of 3/4 the bottom width are presented in the following paragraphs.

The results were expressed in dimensionless terms, showing in graphical form the seepage per unit length of canal, per unit water-

surface width, and per unit soil hydraulic conductivity versus ratios of pertinent system dimensions. For condition A, the seepage increases as the depth of the permeable substratum decreases. For a given water table elevation, a maximum seepage is reached when the top of the permeable material coincides with the water table, in which case the seepage is one of flow to an unsaturated, or just saturated, permeable stratum. This condition can also be handled analytically and for the case of a deep permeable bed the analytical treatment yielded seepage rates that agreed within 3% with those obtained by the analog. Reduced seepage rates occur in the presence of shallow impermeable layers. If the permeable material is at a distance of more than 5 bottom widths of the canal below the canal bottom, its effect on seepage can be ignored and the soil can be taken as uniform to great (infinite) depth. For condition B, this distance for the impermeable layer is 15 bottom widths.

Lowering the water table at great distance from the canal has its largest effect on seepage when the water table elevation is not much below that of the water surface in the canal. The effect on seepage of lowering the water table has ceased when the position of the water table at great distance from the canal is more than 5 canal-bottom widths below that of the water surface in the canal. The seepage can then be considered as one to an infinitely deep water table.

Measurements of the seepage distribution along the canal cross section showed that for seepage into deep uniform soils, the point of highest seepage is at the toe of the bank and that the bottom seepage rates are slightly higher than those for the bank. If, for condition A, however, the permeable layer is brought relatively close to the canal bottom, the bottom seepage rates sharply increase and exceed those of the bank. The reverse is true when an impermeable layer is at relatively small distance below the canal bottom. In that case, the rates at the bank exceed those at the bottom.

Natural or artificial sealing of canal bottoms while leaving the permeability of the canal bank unchanged, gives only substantial

seepage reductions if the canal is very shallow or if the canal is underlain by permeable substrata at shallow depths.

The effect of unsaturated hydraulic conductivity, as evaluated by the introduction of a critical pressure less than 0, is due to a capillary fringe in case of shallow water tables and due to an increase in divergence of streamlines in case of seepage to deep water tables or permeable strata. Excepting conditions of very small ditches or very shallow impermeable layers, the effect of unsaturated conductivity on seepage can be ignored for most practical purposes.

The seepage for condition C was expressed analytically, taking the pressure below the clogged layer as equal to the critical pressure of the underlying soil. Local seepage was then calculated as the total head loss (water depth minus critical pressure) divided by the hydraulic impedance of the restricting layer, and integrated for the wetted perimeter to obtain the total seepage per unit length of canal.

PERSONNEL: Herman Bouwer.

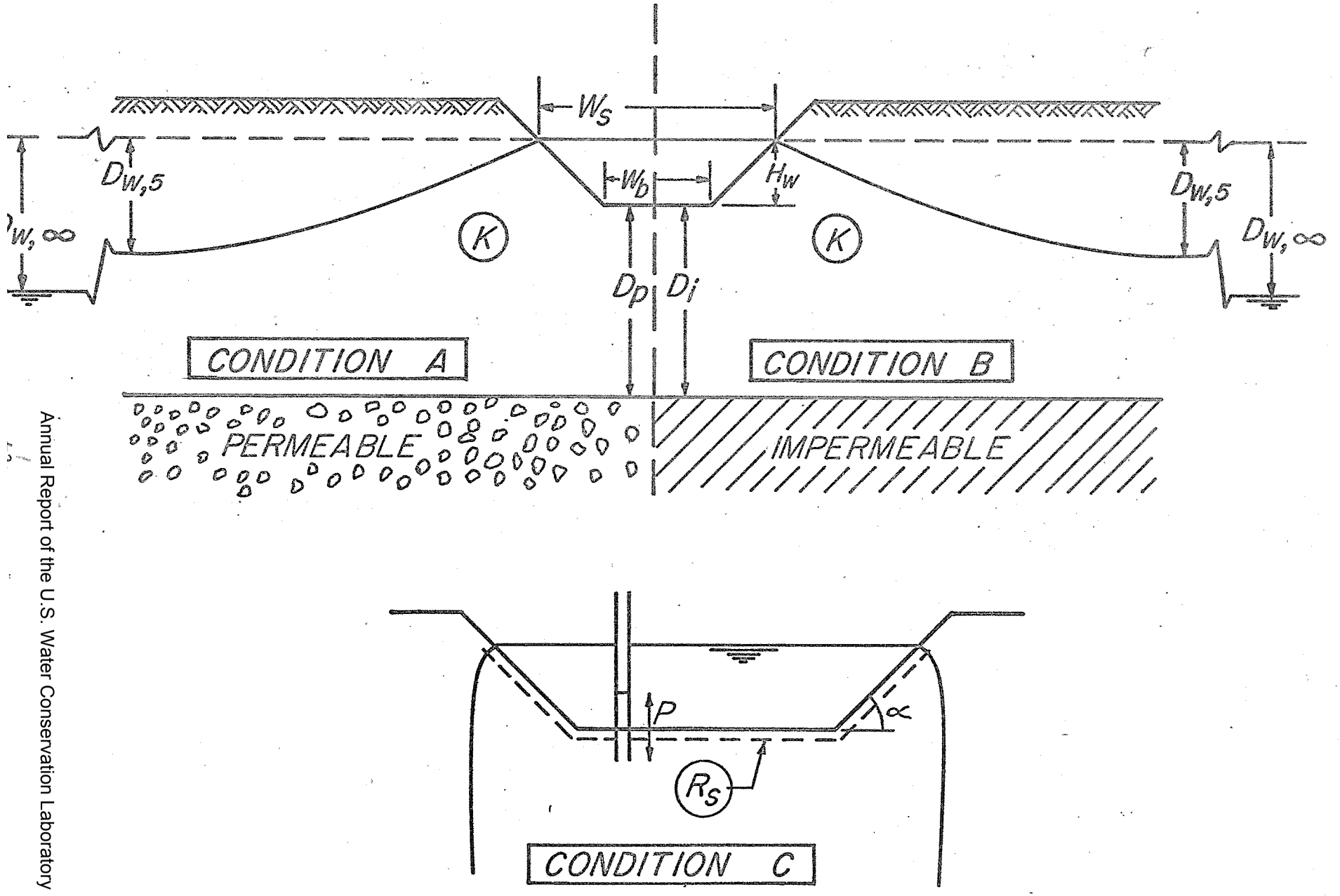

Figure 1. Geometry and symbols of seepage conditions A, B, and C.

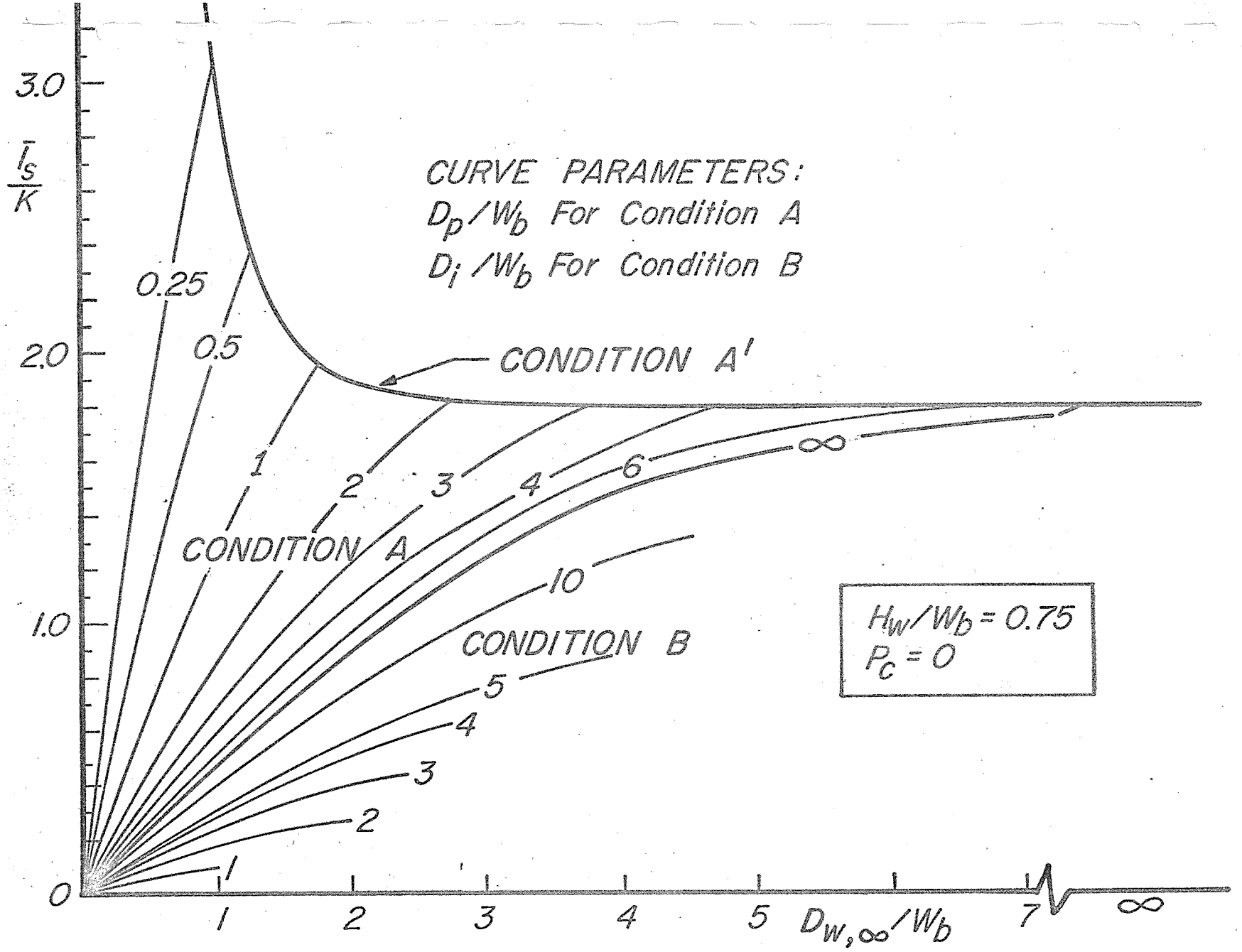

Figure 2. Results of seepage analyses for trapezoidal canal with $H_w = 0.75\ W_b$.

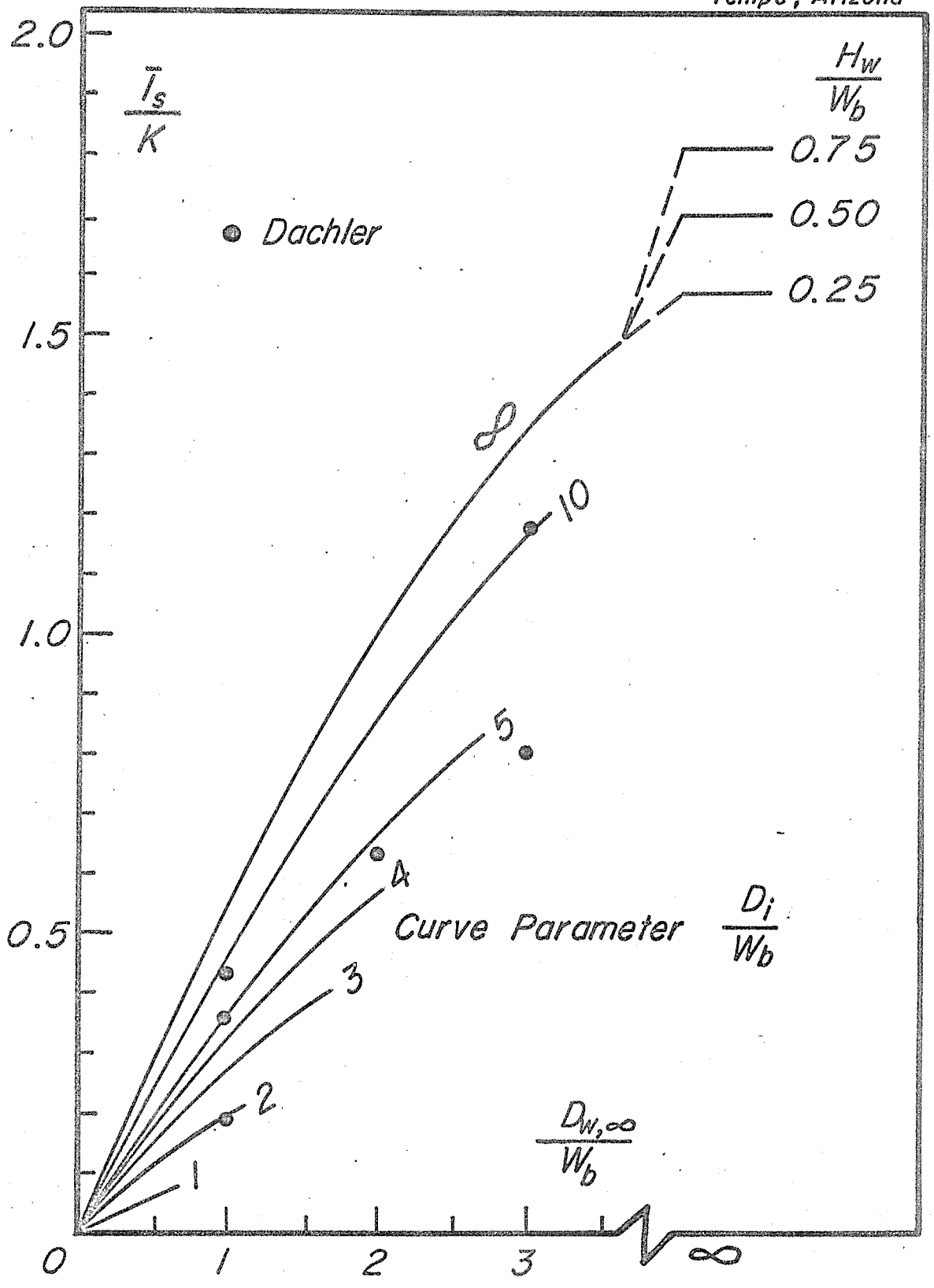

Figure 3. Average seepage curves for three water depths under condition B.

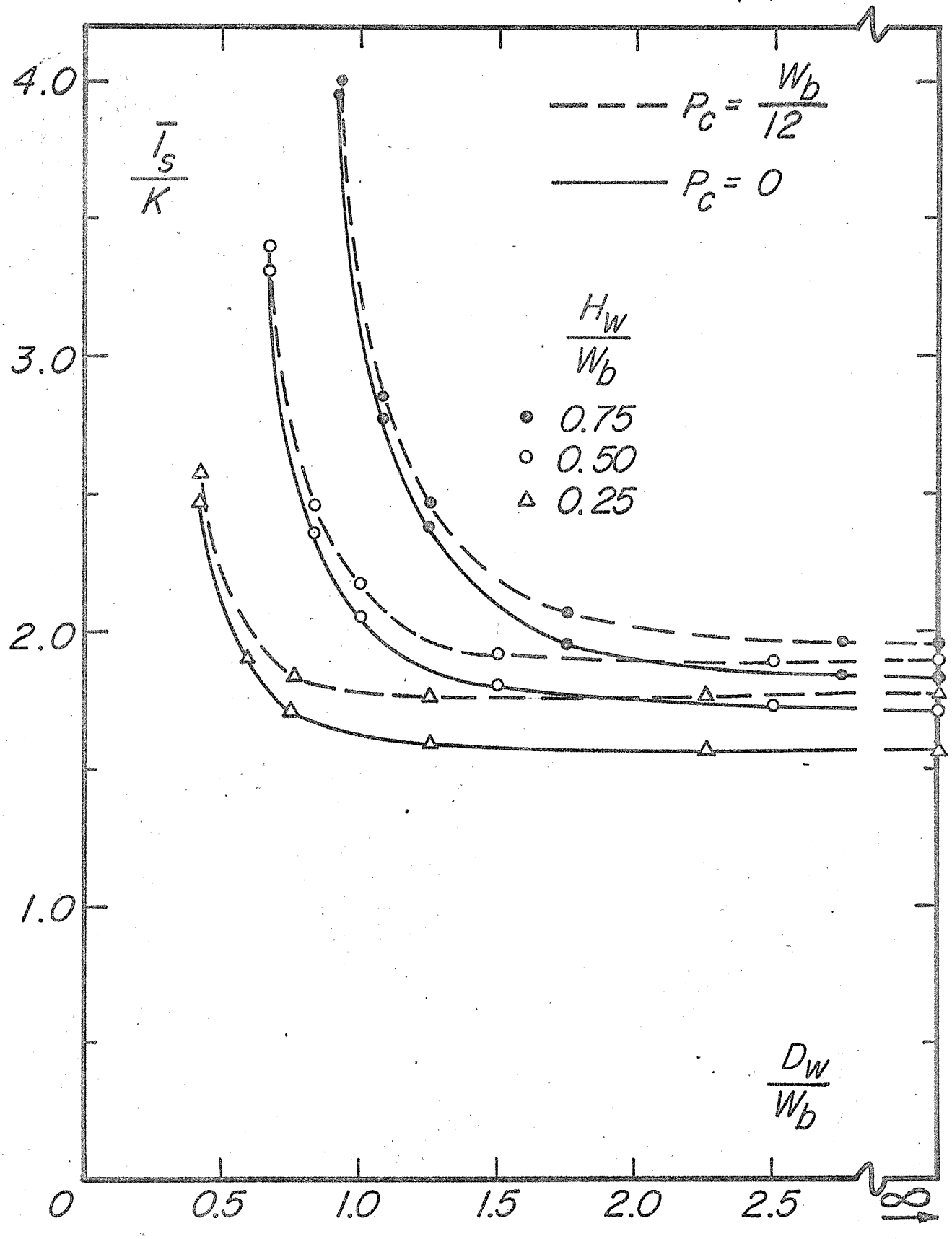

Figure 4. Results of seepage analyses for trapezoidal canal under condition A'.

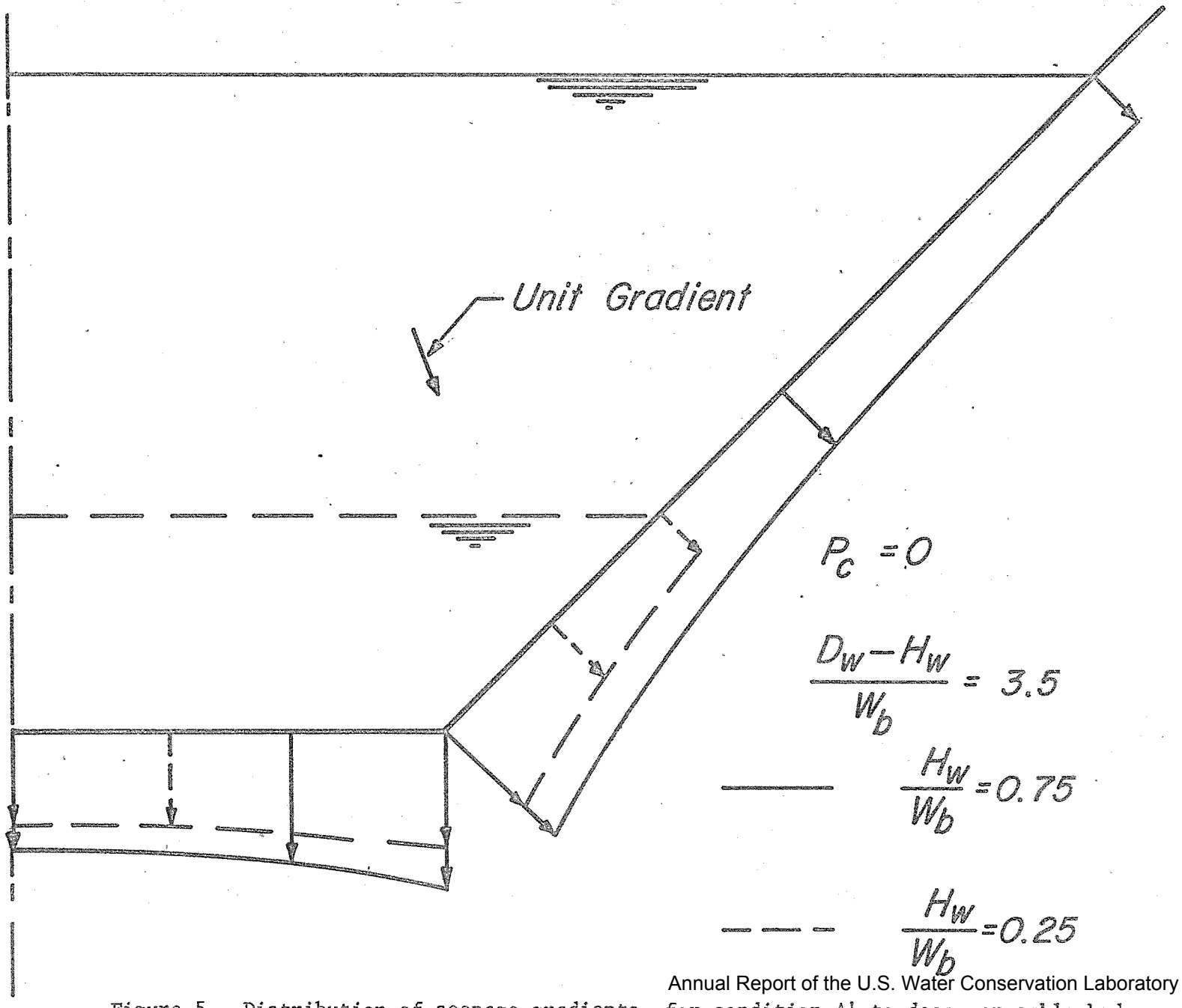

Figure 5. Distribution of seepage gradients, for condition A' to deep permeable bed.

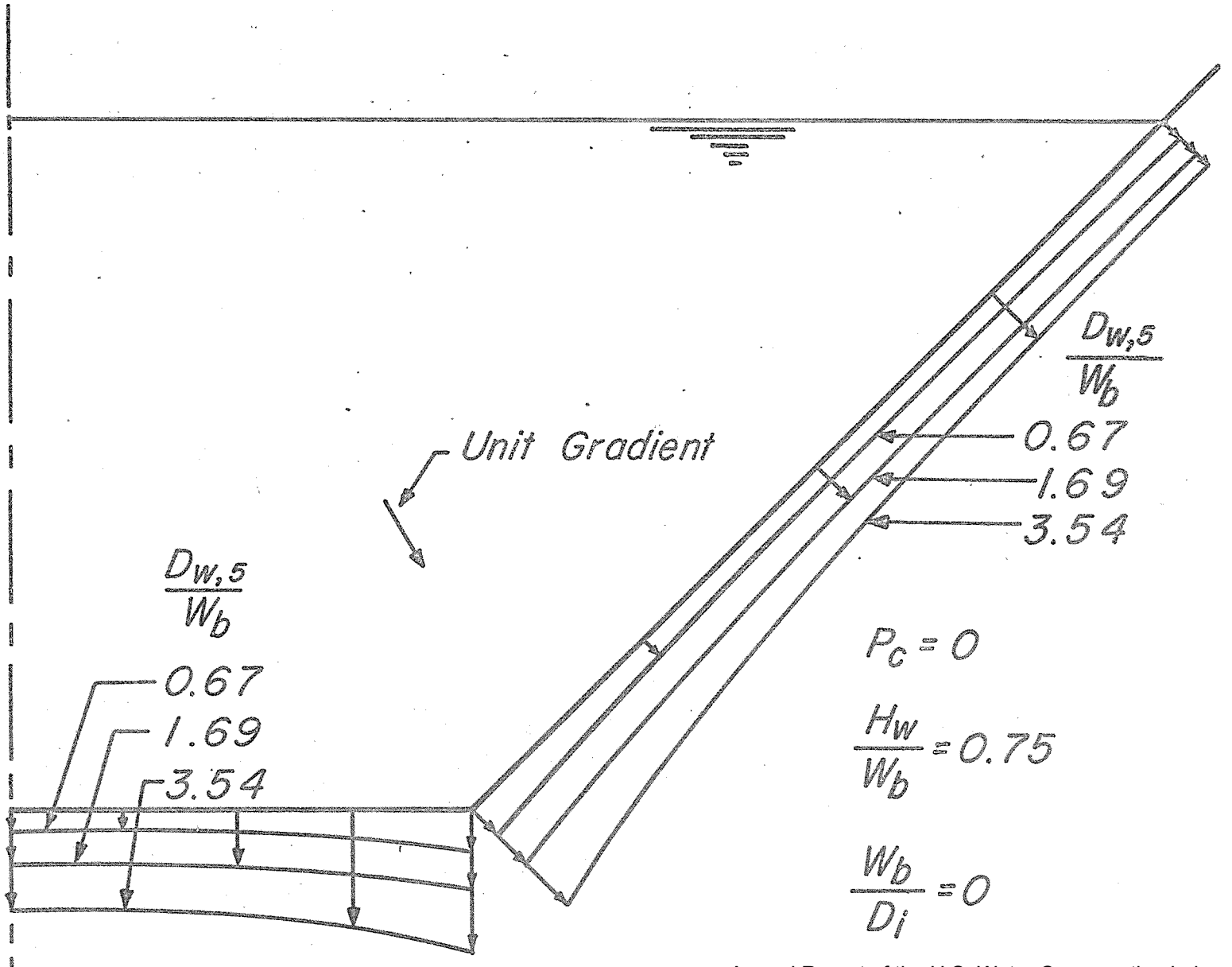

Figure 6. Distribution of seepage gradients for condition B with deep impermeable layer.

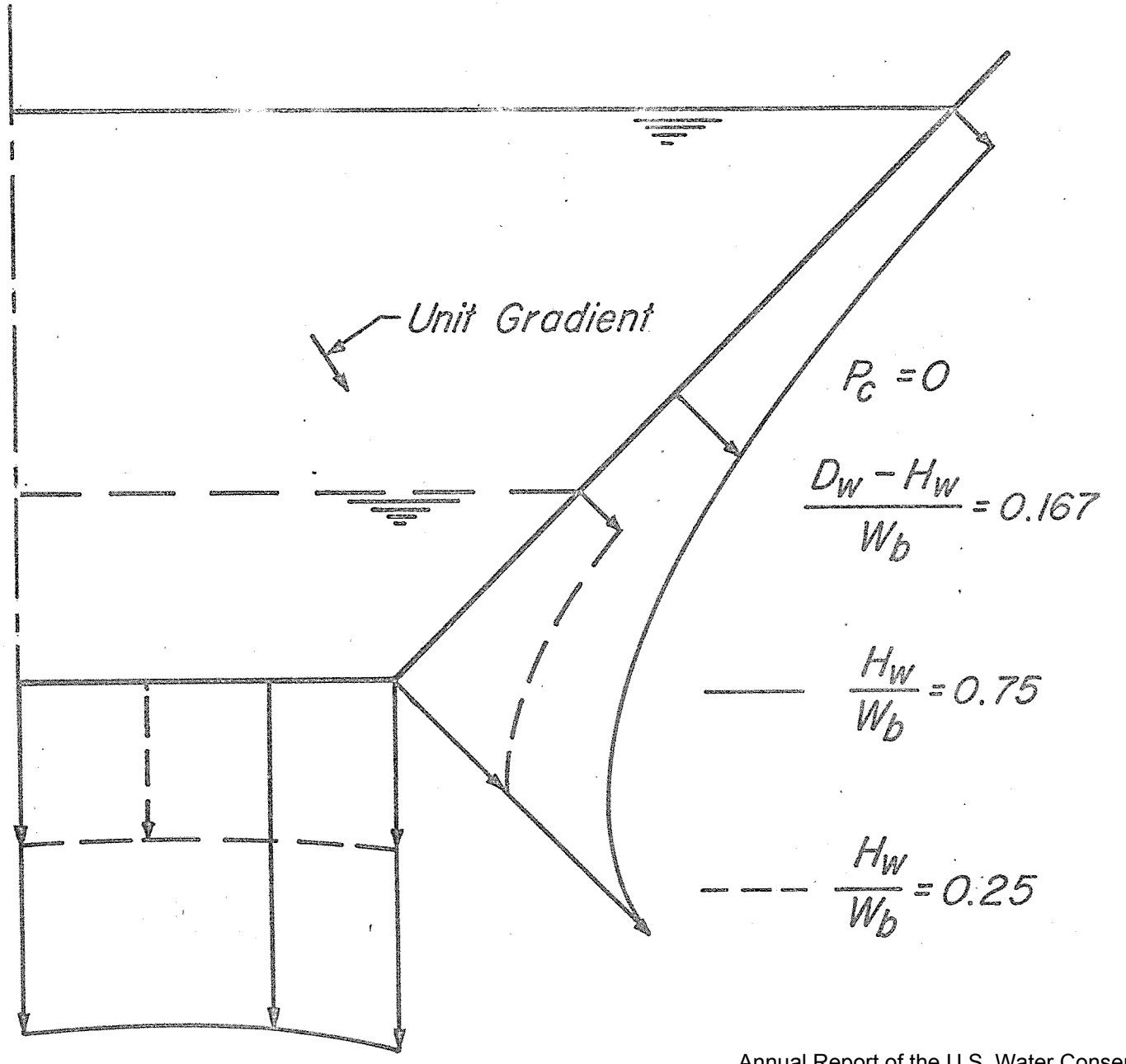

Figure 7. As Figure 5, but shallow permeable bed.

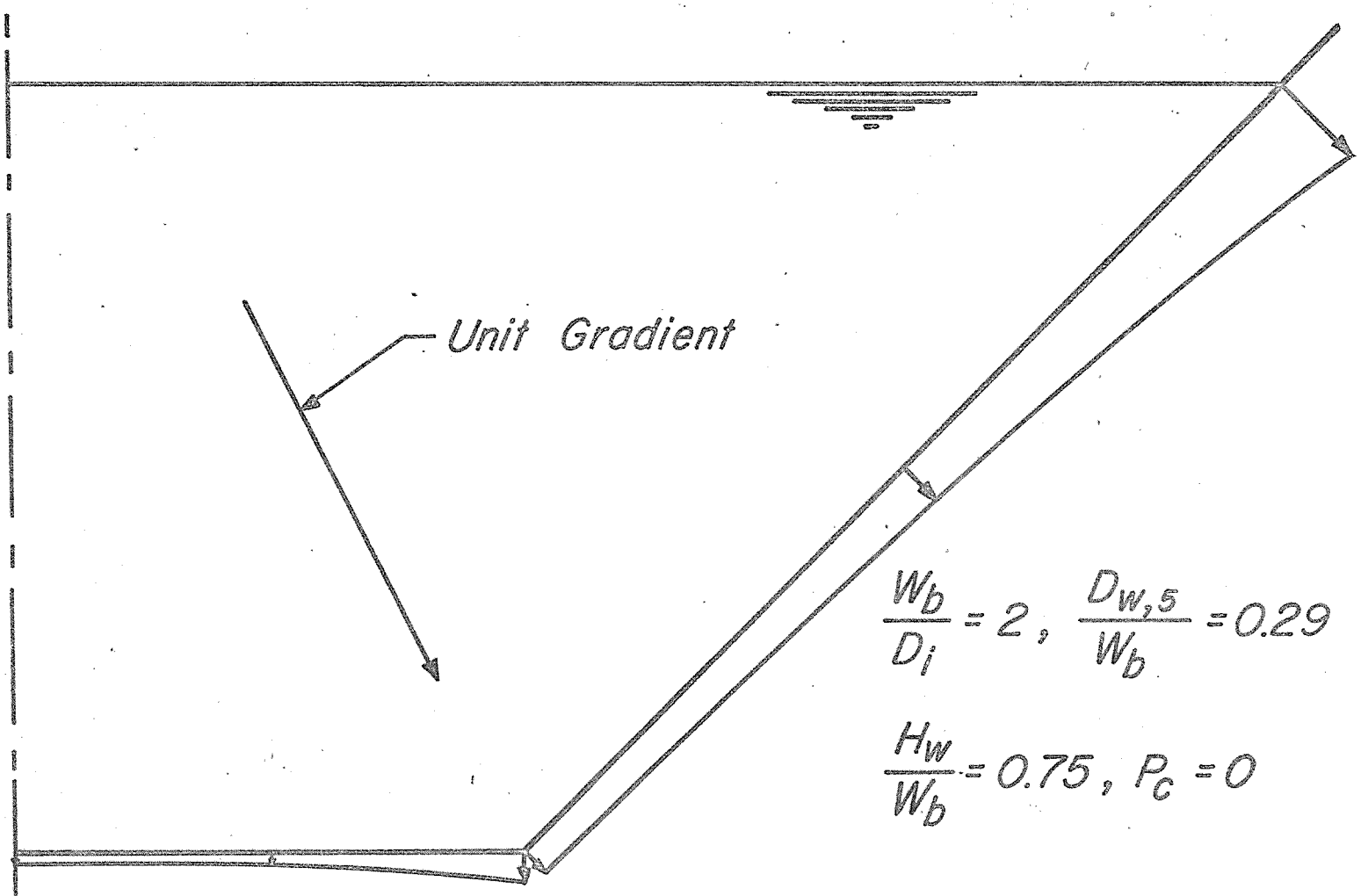

Figure 8. As Figure 6, but shallow impermeable bed.

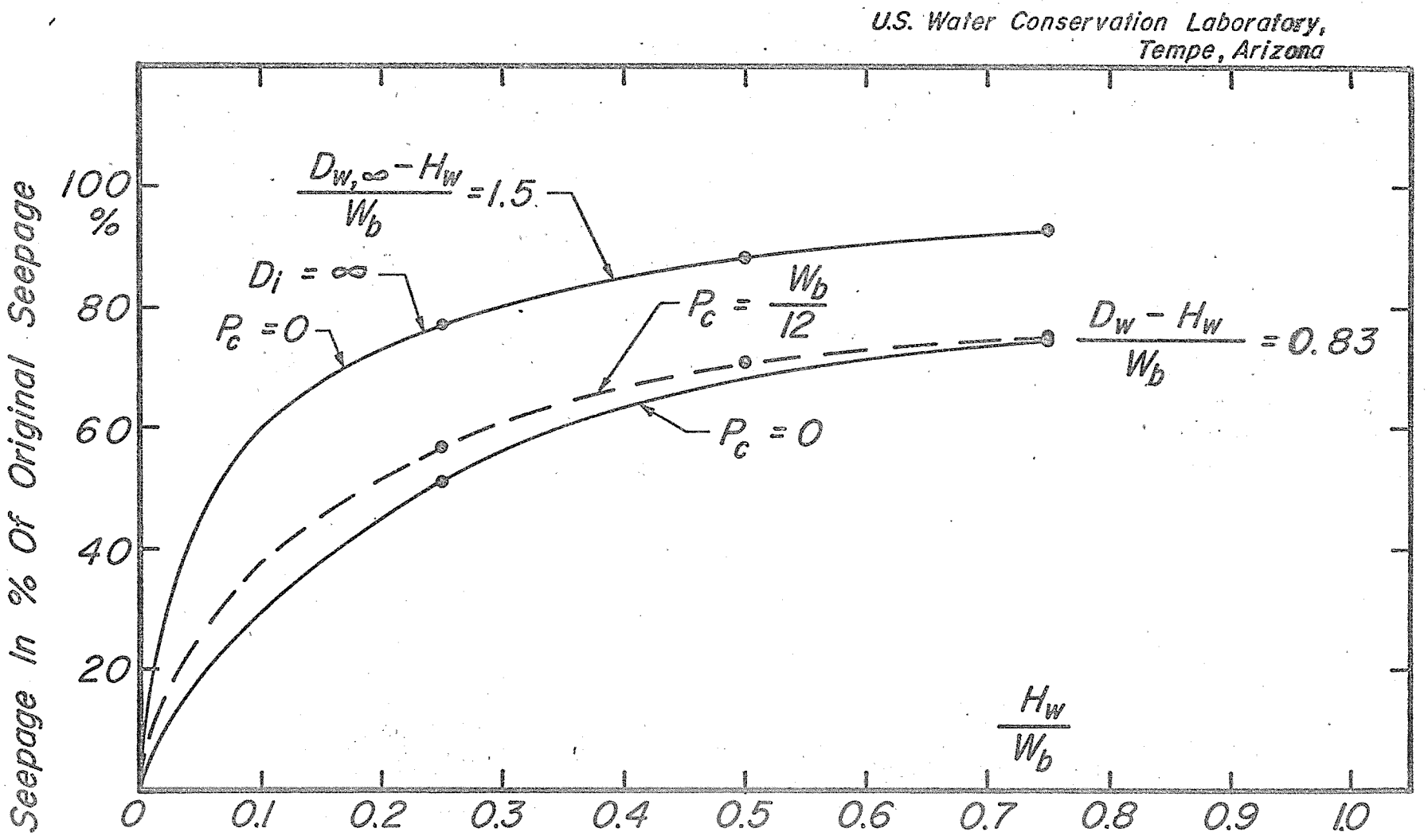

Figure 9. Effect of sealing canal bottom only on seepage.

TITLE: MEASURING HORIZONTAL AND VERTICAL HYDRAULIC CONDUCTIVITY OF SOIL WITH THE DOUBLE-TUBE METHOD.

LINE PROJECT: SWC 4-gG1 CODE NO.: Ariz.-WCL-25

INTRODUCTION:

The double-tube method for measuring in-place hydraulic conductivity in the absence of a water table (22, 41, 85) is based on the assumption that the soil "sampled" for hydraulic conductivity is homogeneous and isotropic. In reality, however, soils may be anisotropic. If it can be assumed that the principal directions of anisotropy coincide with the horizontal and vertical directions, and that there is no anisotropy in the horizontal plane, we have only a horizontal and vertical hydraulic conductivity, symbols K_h and K_v, respectively, to consider. In this report, it will be discussed how the double-tube method can be used to determine K_h and K_v.

PROCEDURE:

Theoretical principles

For a description of the double-tube method, symbols, equations, flow factors, etc., reference is made to previous publications (22,41).

From the theory of Darcian flow in anisotropic media, the double-tube system for an anisotropic soil can be transformed into that for an equivalent isotropic soil by the following transformation.

	Actual Anisotropic System	Equivalent Isotropic System
Radius of inner tube	R_c	$\bar{R}_c = R_c$
Penetration of inner tube	d	$\bar{d} = d\sqrt{K_h/K_v}$
Depth of impermeable soil	D	$\bar{D} = D\sqrt{K_h/K_v}$
Depth of permeable soil	D_p	$\bar{D}_p = D_p\sqrt{K_h/K_v}$
Hydraulic conductivity	K_h and K_v	$\bar{K} = \sqrt{K_h K_v}$
Flow factor	F_f (for d/R_c and assumed isotropy)	$\bar{F}_f$ (for $\bar{d}/\bar{R}_c$ and isotropic $\bar{K}$)

Thus, by multiplying the actual depth of penetration of the inner tube by $\sqrt{K_h/K_v}$, the double-tube system can be considered as that in an

isotropic soil with hydraulic conductivity $\sqrt{K_h K_v}$. This hydraulic conductivity $\bar{\bar{K}}$ could be calculated with one of the two double-tube equations if the flow factor in these equations could be evaluated for $\bar{\bar{d}}/\bar{\bar{R}}_c$, which is equal to $(d/R_c)\sqrt{K_h/K_v}$. The term K_h/K_v is not known initially, so that the flow factor for $\bar{\bar{d}}/\bar{\bar{R}}_c$, symbol $\bar{\bar{F}}_f$, can not be determined.

The apparent hydraulic conductivity calculated with one of the double-tube equations with assumed isotropy will be designated K_{dt}. Thus, K_{dt} is the conductivity obtained when F_f is evaluated for the actual d/R_c of the system. Since R_c, R_v, H and t are not affected by the transformation into the equivalent isotropic system, it follows from the double-tube equations (22, 41), for example,

$$K = \frac{R_v^2}{F_f R_c} \frac{\Delta H_t}{\int_v^t H dt} \tag{1}$$

that the relationship between K_{dt} and $\bar{\bar{K}}$ is

$$\frac{K_{dt}}{\bar{\bar{K}}} = \frac{\bar{\bar{F}}_f}{F_f} . \tag{2}$$

After substitution of $\sqrt{K_h K_v}$ for $\bar{\bar{K}}$ and rearrangement of terms, equation (2) gives

$$\frac{K_{dt}}{K_v} = \frac{\bar{\bar{F}}_f}{F_f} \sqrt{\frac{K_h}{K_v}} . \tag{3}$$

A graph relating K_h/K_v and K_{dt}/K_v for different values of d/R_c is shown in figure 1. This graph was constructed by taking a certain value of d/R_c and calculating $\bar{\bar{d}}/\bar{\bar{R}}_c$ for a number of values of K_h/K_v. The flow factors for d/R_c and $\bar{\bar{d}}/\bar{\bar{R}}_c$ were evaluated from the F_f-graph (figure 2 or 5 in 22) for infinite D or D_p (D or D_p larger than $2R_c$), after which K_{dt}/K_v was calculated with equation (3). This process was then repeated for other values of d/R_c so as to yield the five curves in figure 1.

The principle of evaluating the conductivity in horizontal and vertical direction with the double-tube method consists of obtaining, in addition to K_{dt}, a measurement of K_v. From the ratio K_{dt}/K_v, K_h/K_v is determined from Figure 1 for d/R_c in question. Since K_v is known,

K_h can be computed. Procedures for obtaining K_v with the double-tube installation are discussed later.

In addition to calculating K_h from K_{dt} and K_v as discussed in the previous paragraph, it is possible to calculate K_v from K_{dt} and K_h, if K_h could somehow be measured. For this calculation, equation (3) is multiplied by K_v/K_h, yielding

$$\frac{K_{dt}}{K_h} = \frac{\bar{F}_f}{F_f} \frac{1}{\sqrt{\frac{K_h}{\bar{K}_v}}}. \tag{4}$$

From this equation, a graph as Figure 1 but with K_{dt}/K_h on the abscissa, can be constructed. Still another possibility for evaluating K_h and K_v would be by supplementing the K_{dt}-measurement with a measurement of $\bar{K}$. For calculation of K_h and K_v in this case, a graph similar to Figure 1 could be constructed on the basis of equation (2). Such a graph would have K_h/K_v on the ordinate, $K_{dt}/\bar{K}$ on the abscissa, and a set of curves for different values of d/R_c. For a certain $K_{dt}/\bar{K}$, the ratio K_h/K_v would then be read from that graph and since $\bar{K} = \sqrt{K_h K_v}$ is known, K_h and K_v can be computed.

Thus, it is possible to calculate K_v or K_h if in addition to K_{dt}, a measurement is made of K_h or K_v, respectively. It is also possible to calculate both K_v and K_h, if, in addition to K_{dt}, $\bar{K}$ is known. The reason for only presenting Figure 1 and the corresponding calculation of K_h from K_{dt} and K_v in this paper is that the prospects for the additional measurements of K_h, K_v or $\bar{K}$ with the double-tube installation are much better for K_v than for K_h or $\bar{K}$.

Measurement of K_v

If the water levels in the standpipes on the inner and outer tube are equal, the double-tube installation is similar to that of a buffered cylinder infiltrometer. Consequently, the flow in the soil below the inner tube can be expected to be vertically downward for some distance under these conditions. Thus, K_v in the soil region below the inner tube can be determined from measurement of intake rate and hydraulic

gradient. This vertical gradient, symbol dh/dz, can be determined with piezometers which penetrate the auger hole bottom inside the inner tube (Figure 2). The intake rate can be determined graphically from the slope of an equal-level curve at H = 0. Calling this slope $\left(\frac{dH}{dt}\right)_{H=0}$, K_v is calculated as

$$K_v = \frac{R_v^2}{R_c^2} \left(\frac{dH}{dt}\right)_{H=0} \left(\frac{dh}{dz}\right)^{-1} . \qquad (5)$$

The three piezometers used in the evaluation of K_h of an artificial anisotropic soil (see next section) had a length of 12 cm. The piezometers were tapered from a diameter of 6 mm at the top to 3 mm at the Porvic band. Details of the construction of the piezometers are shown in Figure 2. The piezometers were mounted symmetrically on a 1/4-inch brass plate, which was fastened inside a guide sleeve consisting of a short section of pipe that fitted just inside the inner tube. The position of the plate with the piezometers was controlled by means of a rod, which extended through the top-plate (Figure 1). The piezometers were connected with flexible tubing to manometer tubes above the surface of the ground. To obtain fast measurement of the piezometric levels, small bore tubing was used for the manometers and the manometers could be raised or lowered for rapid detection of the equilibrium level.

Taking piezometric measurements at various depths, the vertical gradient dh/dz can be determined. Since the flow lines below the inner tube tend to diverge at increasing depth, this gradient can only be evaluated for relatively small values of z. The intake rate at the bottom of the auger hole may vary during the course of the piezometric measurements at various depths. Therefore, a record of intake rate should be maintained so that the piezometric measurements can be corrected to a common intake rate.

Laboratory tests.

The principles and procedures for evaluating conductivity components in anisotropic soils were tested in the laboratory. Anisotropic soils were obtained by placing alternating layers of medium sand and loamy sand in a 55 gal. drum. The thickness of the individual

sand layers was 0.5 cm. Anisotropic media were also prepared from loamy sand and Pine clay loam. The vertical and horizontal conductivity of the medium was calculated from permeameter data on the individual soils and also from the vertical hydraulic conductivity of the medium in the drum by operating the drum as a large cylinder permeameter. Next, double-tube equipment similar to that in Figure 2 was installed and K_v and K_{dt} were measured, after which K_h could be calculated. Thus, comparisons could be made between K_h and K_v and the K_h and K_v determined with the double-tube method. In addition, the double-tube method was used to determine K_h and K_v in sand of round, uniform particles, that could be expected to be essentially isotropic.

The tube diameters were 8 and 5 inches. In one instance (test 3), a seepage meter with a radius of 12.7 cm was used as inner tube and the barrel itself was considered the outer tube.

RESULTS AND DISCUSSION:

The first three tests (Table 1) were conducted to determine the general validity of the theoretical principles and also to check if the 0.5 cm layers were thin enough to yield an essentially continuous anisotropic medium. This was important since the depth of penetration of the inner tube was only a few cm, or only a few layers of the materials. Test 1 and test 2 were done with the 5-inch-8-inch double-tube combination, test 3 was done with the seepage meter as inner tube. The general procedure was to determine $\bar{K}$ with the double-tube method, using the known ratio K_h/K_v for determining $\bar{d}$ from d and, subsequently, $\bar{F}_f$. This value of $\bar{K}$ was then compared with the $\bar{K}$ calculated from the known K_h and K_v. The loamy sand for the three tests was not obtained from the same source. Thus, K-values for this material were determined each time in permeameters using samples from the particular "mix" that was used in the test. The same applies to the Pine soil, which, for test 2, was ground finer than for test 3. The results in Table 1 show that good agreement was obtained, which demonstrated the validity of the theory and the use of alternating 0.5 cm layers of two soils as a suitable anisotropic medium.

The next test consisted of determining K_h and K_v from K_{dt} and piezometer measurements with the double-tube installation. The values for K_h and K_v thus obtained were compared with K_h and K_v determined prior to installation of the double tube from measurements in permeameters and in the tank itself. The soil materials were medium sand and loamy sand and K_v was measured in the tank as 0.11 cm/min. The conductivity of the medium sand being 1.68 cm/min, the conductivity of the loamy sand could be calculated as 0.056 cm/min. This yielded a horizontal conductivity of the anisotropic medium of 0.87 cm/min. Double-tube equipment similar to that in Figure 2 was installed. The outer tube penetrated the hole bottom approximately 6 cm and the inner tube 4.2 cm. Thus, R_c/d was 1.51, for which F_f was evaluated as 0.81 from the lower curve in Figure 3 (see third paragraph from here). From double-tube measurements, K_{dt} was calculated as 0.195 cm/min. The piezometers inside the inner tube were now forced into the hole bottom 2 cm at a time. A record of the intake flow was maintained. From the measurement of vertical gradient and intake rate, K_v was calculated with equation (5) as 0.133 cm/min. This gave a value of 1.47 for K_{dt}/K_v, which for $d/R_c = 0.66$, yielded $K_h/K_v = 6.5$ from Figure 1. Since $K_v = 0.133$ cm/min, K_h could be calculated as 0.86 cm/min. These values agreed very well with the known K_v and K_h of 0.11 and 0.87 cm/min.

The test with the double-tube installation in uniform sand of relatively round particles yielded a K_{dt} of 3.94 cm/min and a K_v of 4.06 cm/min as measured with the piezometers inside the inner tube (h versus z for this test is shown in Figure 3). The closeness of these two values indicates that the sand was essentially isotropic.

Figure 1 shows that K_{dt}/K_v varies only from approximately 0.5 to 2.7 for a thousandfold change in K_h/K_v. Thus, small changes in K_{dt}/K_v have a considerable effect on the value of K_h/K_v as evaluated from Figure 1. It is, therefore, important that K_{dt} and K_v be determined as accurately as possible and replicate tests should be performed for measurements in the field. This is particularly true if K_{dt} and K_v are relatively close together.

The F_f-factors in (22) are in theory for an outer tube of infinite radius. It was shown by analog that these values could be used with less than 10% error as long as the outer tube radius was at least 1.67 R_c. In view of the importance of a 10% change in K_{dt} for determining K_h/K_v with Figure 1, F_f-values are presented in Figure 4, which are applicable to tube-size ratios of 1.67, as approached by the five-eight inch combination used in this example. The lower curve should be used particularly if the outer tube is driven in somewhat deeper than the inner tube to extend the zone of vertical flow below the inner tube for measurement of K_v with piezometers.

Since K_{dt} is already closer to K_v than to K_h (Table 1 and Figure 1), the measurement of soil anisotropy would be considerably more accurate if, instead of K_v, a measurement could be obtained of K_h, after which K_v can be determined from K_h and K_{dt} by means of a graph constructed from equation (4) as discussed under PROCEDURE. However, obtaining a measurement of K_h seemed to be much more difficult than that of K_v.

In addition to measuring directional conductivity components by equipping the double-tube installation with piezometers for K_v measurement, three other approaches were considered. Although these approaches had certain advantages, they also had inherent weaknesses that did not favor their application. For the sake of completeness, these three approaches will be briefly discussed.

One possibility investigated was that of determining K_{dt} for different penetration depths of the inner tube and evaluating K_v and K_h from the variation of K_{dt} with d/R_c. The curves in Figure 1 show, however, that for a certain K_h/K_v, the variation in K_{dt}/K_v, and thus in K_{dt}, due to different d/R_c, is quite small. Therefore, it would be difficult to conclude whether, for instance, a reduction in K_{dt} after increasing d is due to anisotropy with K_h larger than K_v, or due to soil compaction as the inner tube is pushed further into the hole bottom, or due to a change in the soil region "sampled" for K_{dt}.

A second approach consisted of considering the advancing saturation front below the auger hole as a sharp interface between soil of saturated conductivity and soil of much lower unsaturated conductivity. In

that case, the depth to the saturation front in the equivalent isotropic system could be represented by $\bar{D}$. Figure 2 in (22) shows that as $\bar{D}$ increases, F_f reaches an essentially constant value and the value of $\bar{D}$ whereby F_f becomes essentially constant can be determined from that graph. If K_{dt} determinations are made at regular intervals after the beginning of the water application, the moment that K_{dt} becomes essentially constant can be detected. From the intake rate,

$$I = \frac{R_v^2}{R_c^2} \left(\frac{dH}{dt}\right)_{H=0}$$

at that moment, $\bar{K}$ can be calculated as

$$\bar{K} = \frac{\bar{D}}{h_w} I, \tag{6}$$

where h_w is the distance between the top of the standpipes and the bottom of the auger hole (22). In this equation, the pressure head at the saturation front is assumed to be negligibly small compared to h_w. Since $\bar{D}$ in equation (6) can not be evaluated from Figure 2 in (22), unless $\bar{d}/\bar{R}_c$ is known, a trial-and-error procedure would be required. A certain ratio K_h/K_v would be assumed and $\bar{d}/\bar{R}_c$ would be calculated. From Figure 2 in (22), $\bar{D}$ whereby F_f becomes essentially constant could then be evaluated. If $\bar{d}$ becomes large, $\bar{D}$ where F_f becomes constant approaches $\bar{d}$. The equivalent isotropic conductivity $\bar{K}$ can now be computed with equation (6). Knowing K_{dt} and $\bar{K}$, K_h/K_v can then be calculated. This K_h/K_v should be equal to the initially assumed ratio. If not, the procedure is repeated until the assumed and calculated values of K_h/K_v are the same. Since $\bar{K} = \sqrt{K_v K_h}$, the individual components K_v and K_h can then be computed. Although this approach has shown promise in laboratory studies, its major disadvantage is that the exact moment where K_{dt} becomes essentially constant is difficult to assess. Since this moment may occur rather shortly after the start of the water application to the double-tube installation, the intake rate may still be decreasing rapidly, so that small errors in determining the moment that K_{dt} becomes essentially constant can cause a rather large error in I, and consequently in $\bar{K}$.

The third alternative considered was based on deriving K_v from the relationship between the intake rate inside the inner tube and the total water depth for successive equal-levels measurements (41). For a particular equal-levels measurement, this relationship can be written as

$$I = K_v \frac{h_w - H - p + D}{D}, \qquad (7)$$

if it is assumed that vertical flow exists between the auger-hole bottom and the saturation front at depth D, and that the measurements are carried out sufficiently fast for D to be essentially constant during the test. The term p denotes the pressure head at this front. From successive equal-levels tests, a number of equations (7) are obtained from which K_v can be determined. The solution utilizes graphs showing I as a function of $h_w - H$. For proper construction of these graphs, it is necessary that the equal-level tests be performed for the highest H-values obtainable. Although this calculation of K_v showed promise in preliminary studies on laboratory columns, the assumptions of vertical flow and constant D can not very well be met concurrently. The assumption of vertical flow tends to be valid at the beginning of the test when D is still small. However, at the beginning of the test D is also increasing rather rapidly and the assumption of D constant during a particular test may not be valid. An essentially constant D during an equal-levels test may occur after water application has been going on for some time, but then D may be too large for the assumption of vertical flow between the auger hole and the saturation from below the inner tube to be valid.

Despite the fact that all three approaches discussed would permit evaluation of K_h and K_v with the double-tube installation as such without need for additional equipment, inherent weaknesses and disadvantages did not favor adoption of any of these three possibilities. Therefore, the measurement of K_v with piezometers was selected here for use of anisotropy evaluation with the double-tube method, despite the disadvantage of the added equipment.

SUMMARY AND CONCLUSIONS:

The double-tube method was used to determine horizontal and vertical hydraulic conductivity in anisotropic soils. If it is assumed that the principal directions of anisotropy in the soil are in the horizontal and vertical direction and if it is further assumed that there is no anisotropy in the horizontal plane, the conductivity components to be considered are the horizontal conductivity K_h and the vertical conductivity K_v.

The basic principle of evaluating these components with the double-tube method consists of manipulating flow direction in the soil region below the inner tube. If the water levels in the standpipes are equal, the double-tube system acts as a buffered infiltrometer and the flow below the inner tube is initially in vertically downward direction. With piezometers for measuring the vertical gradient and knowing the intake rate, K_v may be obtained. If the water levels in the standpipes are different, the streamlines in the resulting flow system between the two concentric tubes have both vertical and horizontal portions. The conductivity measured from this flow system is the conductivity K_{dt} yielded by the double-tube method on the basis of assumed isotropy.

The magnitude of K_{dt} is affected by both K_h and K_v, with K_v having a stronger influence on K_{dt} than K_h. From the theory of flow in anisotropic media, the relationship between K_{dt}/K_v and K_h/K_v can be determined. A graph has been prepared showing this relationship for different depths of penetration of the inner tube. Thus, if K_{dt} and K_v are measured with the double-tube system equipped with piezometers inside the inner tube, K_h/K_v can be determined from that graph, and since K_v is known, K_h can be computed.

Laboratory studies were performed in a 55-gallon drum with artificial anisotropic soil consisting of alternating 0.5 cm layers of relatively coarse and relatively fine soil. The conductivity of each soil was determined separately in cylinder permeameters, so that K_v and K_h of the layered medium could be calculated. Also, since the layers were placed horizontally in the drum, K_v could be determined in-place by using the drum as permeameter. The resulting values were $K_v = 0.11$ cm/min and $K_h = 0.87$ cm/min. Next, double-tube equipment was installed

and K_{dt} was measured according to the double-tube principle from falling-level measurements in the standpipes. After this, the piezometers inside the inner tube were pushed into the soil and the vertical gradient was measured. Knowing the intake rate, K_v could be computed. The ratio K_{dt}/K_v was then calculated, from which K_h was determined by means of the graph relating K_h/K_v and K_{dt}/K_v. The resulting values, i. e., K_v = 0.13 cm/min and K_h = 0.86 cm/min agreed with the previously determined values of 0.11 and 0.87 cm/min, respectively.

Other laboratory studies with layered soil were performed to verify the theoretical principles and to determine whether 0.5 cm layers were thin enough so that the medium could be considered an anisotropic continuum. A study with the double-tube system in uniform sand yielded K_{dt} = 3.94 cm/min and K_v = 4.06 cm/min, which indicated that the sand was essentially isotropic.

PERSONNEL: Herman Bouwer and R. C. Rice.

Table 1. Results of double-tube tests in tank (all length dimensions in cm, K dimensions in cm/min).

		Test 1	Test 2	Test 3
Tank and permeameters	Rel. coarse soil	medium sand	loamy sand	loamy sand
	Rel. fine soil	loamy sand	Pine si. cl. loam	Pine si. cl. loam
	K of rel. coarse soil	1.3	0.050	0.060
	K of rel. fine soil	0.080	0.00092	0.0017
	K_v	0.15	0.0018 3/	0.0033 3/
	K_h	0.69	0.025	0.031
	$\bar{K}$	0.32	0.0067	0.010
Double-tube	d	2.2	3.3	5
	$\bar{d} = d\sqrt{K_h/K_v}$	4.7	12.3	15.3
	R_c/d	2.88	1.92	2.54
	F_f	1.26	1.03	1.19
	K_{dt}	0.24 1/ 0.21 2/	0.0030 1/	0.0071 1/
	$R_c/\bar{d}$	1.35	0.52	0.82
	$\bar{F}_f$	0.84	0.49	0.64
	$\bar{K}$	0.36 1/ 0.31 2/	0.0063 1/	0.013 1/

1/ from equal-level and OTS-full measurements

2/ from balanced-flow equation

3/ measured in tank

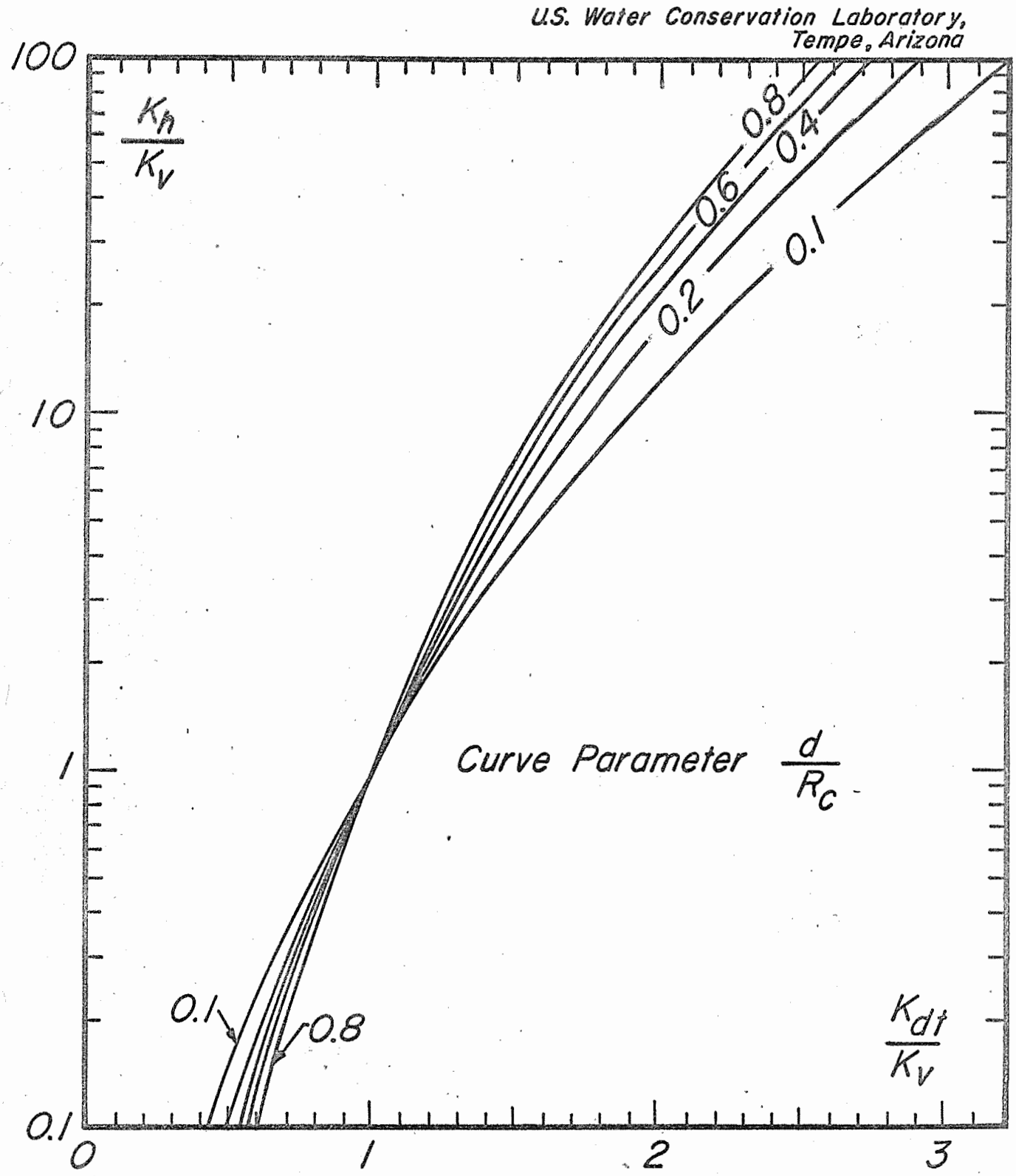

Figure 1. Graph showing K_h/K_v as a function of K_{dt}/K_v for different values of d/R_c (on the curves).

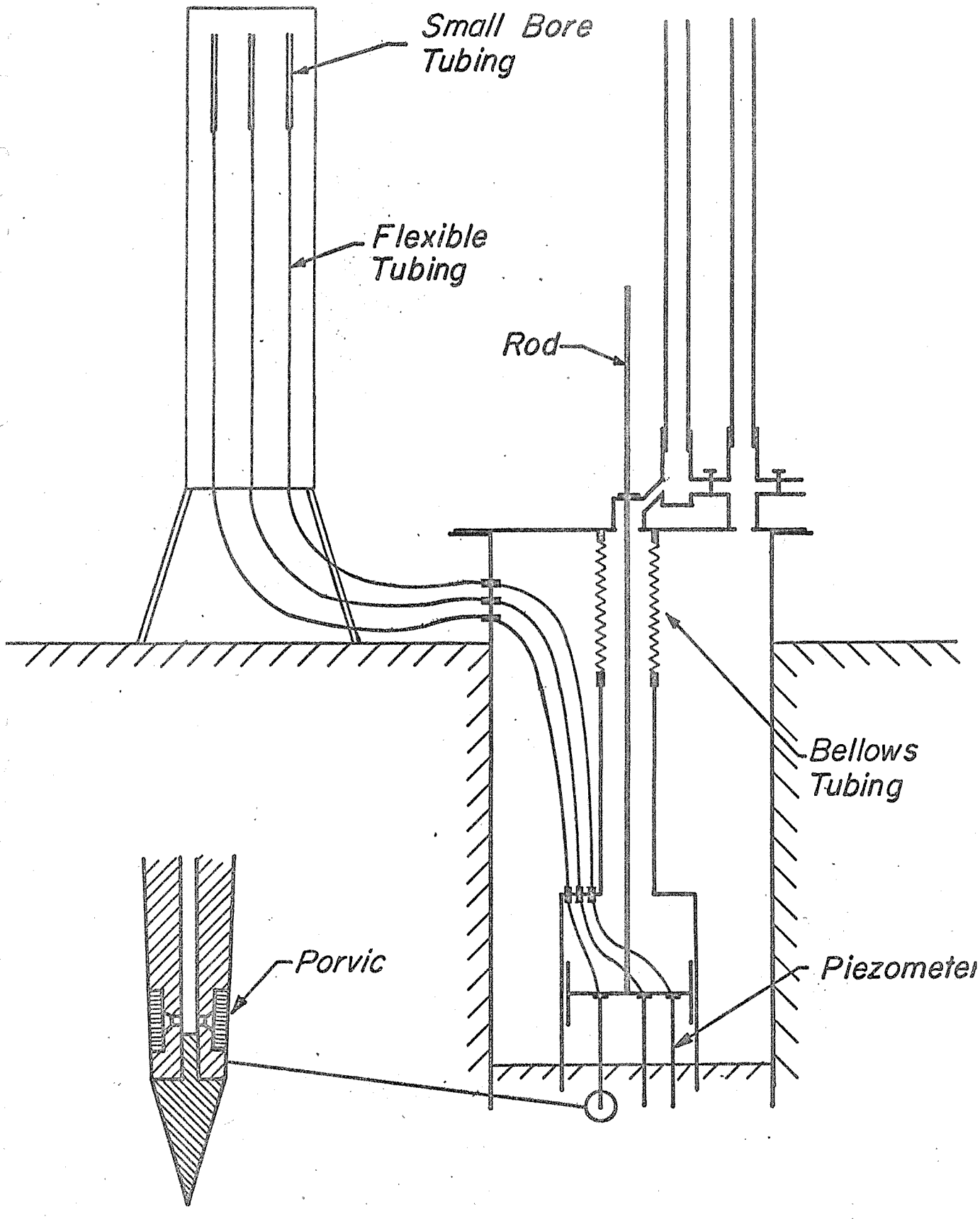

Figure 2. Sketch of double-tube system with piezometers for measurement of K_v.

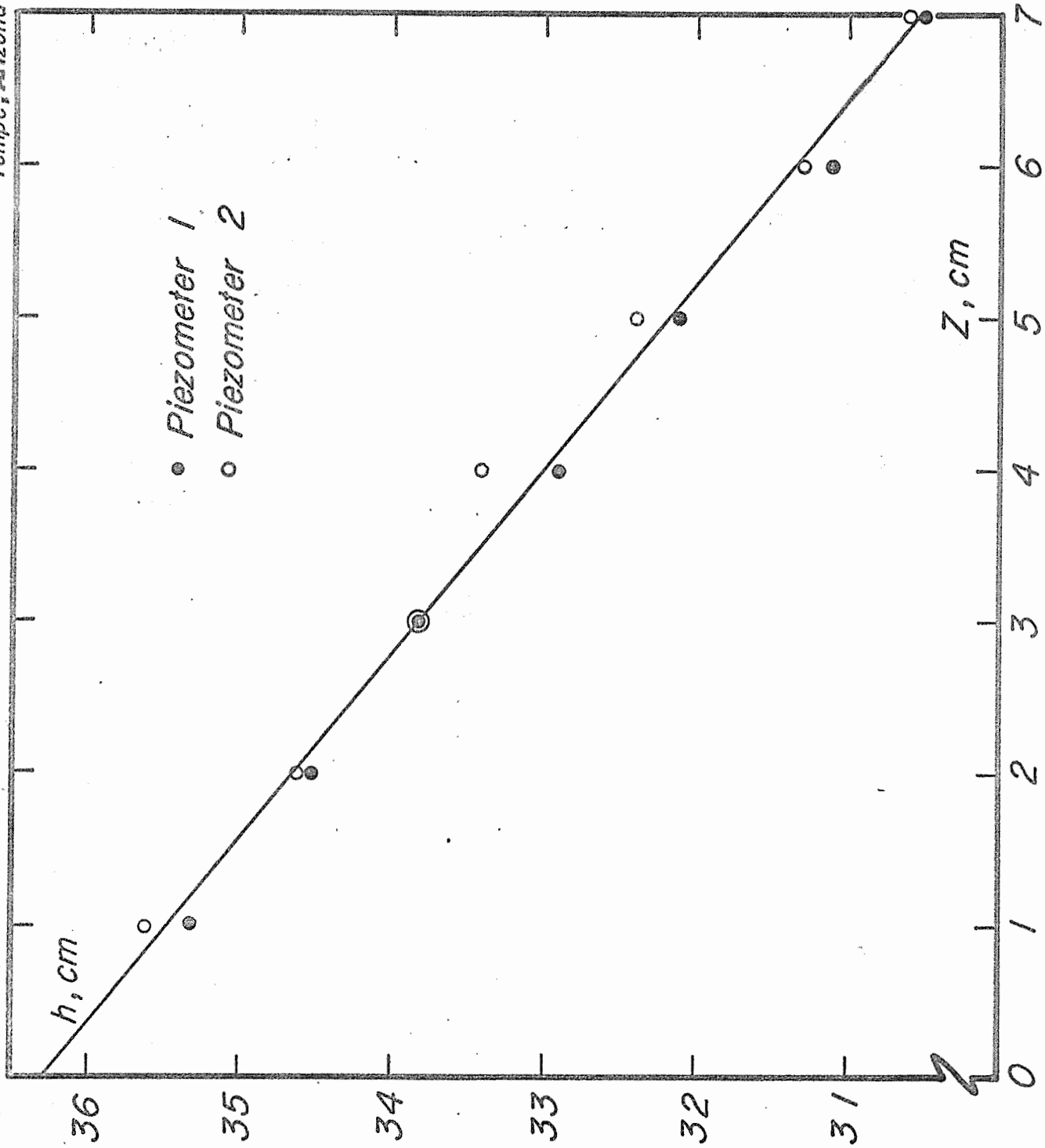

Figure 3. Graph of h versus z for double-tube test in uniform sand (d = 4.5 cm).

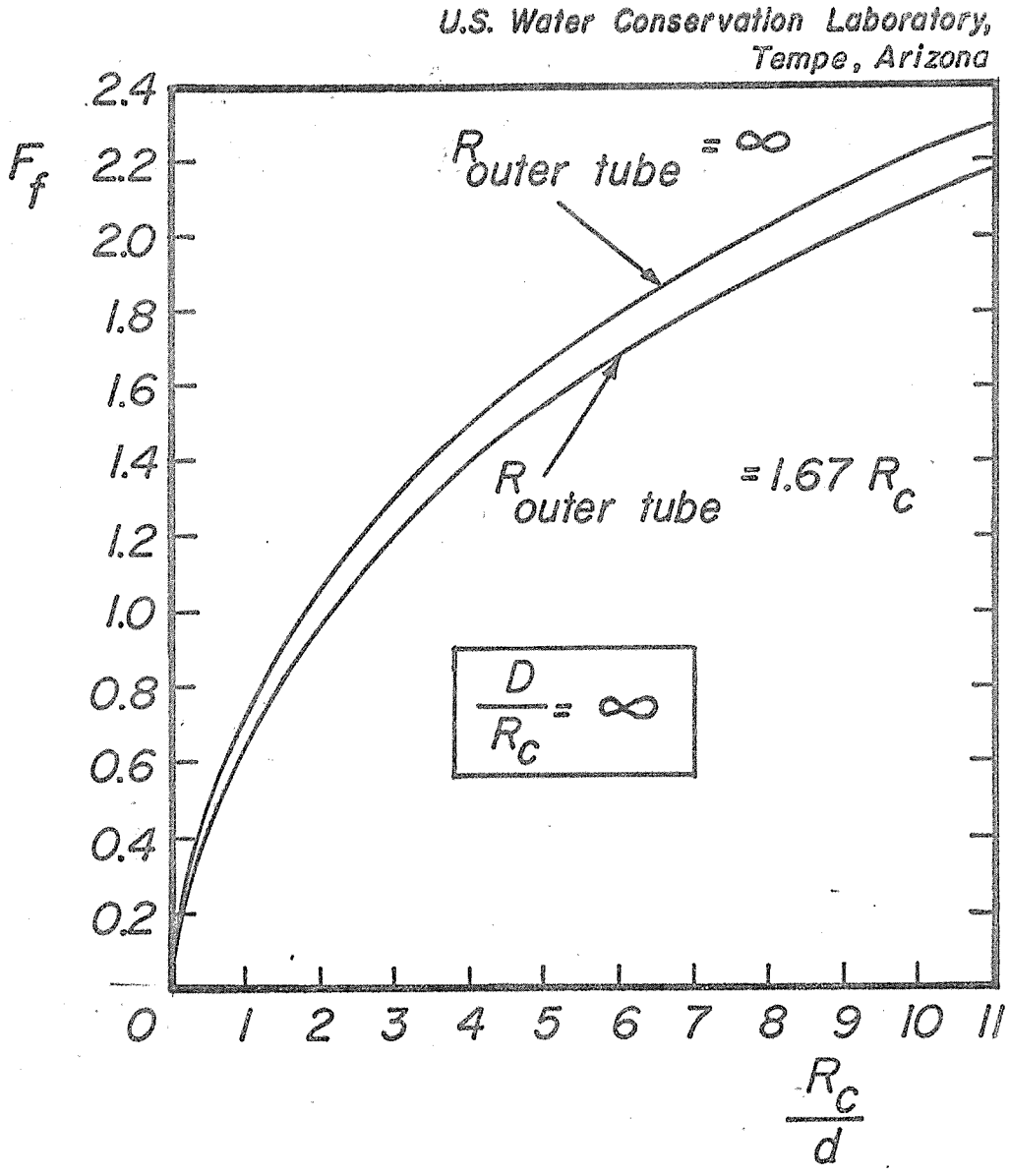

Figure 4. Graph showing F_f as a function of R_c/d for two outer-tube sizes.

TITLE: SOIL TREATMENT TO REDUCE SEEPAGE LOSSES FROM CANALS AND PONDS

LINE PROJECT: SWC 4-gG1 CODE NO.: Ariz.-WCL-8

INTRODUCTION:

Observation of the John Randall pond, sprayed with a soil dispersant to reduce seepage as described in the 1961 Annual Report, indicated that the treatment failed because the resulting dispersion was primarily in the surface soil which rapdily eroded. Accordingly, laboratory and field studies were initiated to see if treatments could be designed to provide a controlled degree of deflocculation or to deflocculate the soil at some depth beneath the soil surface.

Previous work in 1961 showed that ponding or spray applications of cationic asphalt emulsions reduced seepage but were destroyed by erosion. Studies were initiated at the Lakin test site to evaluate ditch linings which include reinforcing materials in addition to asphalt.

Seepage from concrete canal and ditch linings has become an increasingly serious problem which has not been solved. Limited work was initiated to explore possibilities for sealing concrete ditch linings.

PROCEDURE:

Same as reported in the Annual Report for 1960 except for analysis of soil samples. Standard methods described in USDA Handbook 60 were used to determine concentration, ESP, and chemical composition of soil and leaching solutions. Percent dispersed clay was determined by the standard hydrometer method except that soil samples were not treated with additional dispersant and were not dispersed in a mechanical mixer.

RESULTS AND DISCUSSION:

Soil dispersants - Pine ponds. Spray application of sodium hexametaphosphate on pond 1 failed as reported for 1961 because the deflocculated surface soil washed away. An attempt was made in 1962 to reduce seepage by mixing NaCl with the top three inches of soil. Laboratory studies showed that NaCl mixed with the

surface three inches of soil could reduce seepage through the Pine soil without any mechanical compaction. Ponds 1 and 2 were disked to a depth of three inches, extra coarse NaCl was spread uniformly at rates of 4,000 pounds per acre on pond 1 and 6,000 on pond 2, and the ponds were disked again. Considerable difficulty was encountered in disking the steep banks.

The treatments reduced seepage as shown in Table 1. Seepage reduction increased with decreasing water depth, indicating that the treatment was least effective on the upper slopes of the pond banks. Stair-step erosion occurred on the banks. The seepage reduction is not considered satisfactory. Uniform mixing of NaCl in the soil was not adequately accomplished by the type of disking operation used. The treatment cannot be successful unless adequate mixing of salt and soil is obtained.

Soil dispersants - Dick Mason pond. A field study site was obtained near Flagstaff, Arizona, in the Dick Mason pond, about 1/7 acre in area and 5 feet deep, owned by Mr. Kel Fox. Water is obtained from snowmelt in the spring and rain during the late summer. The initial seepage rate was measured by Mr. Fox at about 5 inches per day.

The soil is a well flocculated clay loam: 40 percent clay, 33 percent silt, and 27 percent sand. Chemical analysis in meq/100 grams soil was: CEC - 64.4, Na - 0.26, Ca - 20.9, Mg - 24.0, and K - 0.79. Surface area in square meters per gram was: external - 53, internal - 195, total - 248. pH was 5.2.

The laboratory study of seepage control with dispersants on Dick Mason soil showed no advantage costwise for either NaCl, sodium hexametaphosphate, or tetrasodium pyrophosphate. However, tetrasodium pyrophosphate supplied more Na^+ per unit weight than sodium hexametaphosphate. The polyphosphates also form insoluble compounds with calcium and magnesium and this is thought to be beneficial in clay dispersion. For these reasons, anhydrous tetrasodium pyrophosphate was selected for use in treating the

Dick Mason pond on August 31, 1962. One thousand pounds were spread in the pond after disking the soil 2 - 4 inches deep. The soil was then disked twice to hopefully mix the salt thoroughly with the soil. A small area of porous rock in the pond bottom was sealed with asphalt and covered with soil before treating the pond. Part of the pond sideslopes were too steep to cultivate easily with the tractor. These steep sideslopes may be eroded by wave action when the surface soil is dispersed and may cause the sideslopes to leak. There has not been sufficient rainfall to fill the pond since it was treated. However, water has remained in the pond bottom from September to December. The treatment will be evaluated after the pond fills next spring.

Soil dispersants - Laboratory studies. The relationship between ESP and seepage rates for Pine soil was investigated by using 5,000 ppm solutions of NaCl and $CaCl_2$ to equilibrate triplicated 5-inch soil columns to ESP of 7.5, 14.1 and 21.2. ESP of the untreated soil was 1.4. After equilibration, the solution was replaced with distilled water and seepage rates with an 18-inch head were: ESP 1.4 - 0.27, ESP 7.5 - 0.16, ESP 14.1 - 0.10, and ESP 21.2 - 0.0037 inches per hour. The effect of equilibrating solution concentration was checked by making similar triplicated runs using solutions with SAR of 12.0 (ESP 14.1) and concentrations of 500, 1,000, 2,000, and 10,000 ppm. Post-treatment average seepage rates with distilled water ranged from 0.004 to 0.007 inch per hour. These data indicated that concentration of the treating solution had relatively little effect and that there was a convenient relationship between ESP and the seepage rate with distilled water.

Clay dispersion associated with ESP was investigated by treating columns of Dick Mason soil with various amounts of NaCl, leaching with distilled water, slicing the columns into 1-inch layers, and analyzing each layer for ESP, percent dispersed clay, and soil solution concentration. The collected data are enclosed within the three-dimensional surface plotted in Figure 1 which

shows the general relationship of dispersed clay to ESP and soil solution concentration. These data show quite clearly that ESP alone cannot be used to predict dispersion when the soil solution concentration exceeds 2,000 ppm. The distribution of dissolved salt following treatment must also be considered.

Seepage can be expected to decline with increasing clay dispersion up to a point where increased dispersion permits the clay to wash out of the soil. This breaking point appears to be about 26 percent dispersed clay, on the basis of total soil, for Dick Mason soil as shown in Figure 2. Dick Mason soil is 40 percent clay. Mixing NaCl in the top 5 inches and leaching with distilled water until the seepage rate stabilized, resulted in maximum dispersion in the 1 to 2 and 3 to 4 inch soil layers. The average percent dispersed clay in these layers is plotted against seepage rate in Figure 2.

The relationship between ESP and clay dispersion is influenced by the type of sodium salt used for treatment as well as by soil solution concentration. Figure 3 shows ESP versus percent dispersed clay for Dick Mason soil when NaCl and tetrasodium pyrophosphate TSPP were used for treatment. Soil solution concentrations were below 2,000 ppm, ranging from 676 to 1,400 ppm for NaCl and 772 to 1305 ppm for TSPP, and should not have materially influenced the results. These data indicate that for a given ESP the deflocculation is generally higher for TSPP than for NaCl. The reasons for this reaction have been speculated upon by several eminent soil chemists but the actual mechanisms involved are not known.

A simple means of avoiding deflocculation of the surface soil was tested by comparing the deflocculation obtained with NaCl in finely powdered versus coarse crystal form. The salt was mixed with the top 5 inches of Dick Mason soil at a rate of 2,280 pounds per acre, the columns were leached with distilled water until the seepage rate stabilized, and the columns were then sectioned and analyzed for dispersed clay. Distribution of the deflocculated clay is shown in Figure 4. As expected, the

widely scattered salt crystals did not deflocculate the surface soil as did the powdered salt.

Low-cost ditch linings. Various types of low cost ditch linings were applied to sections of an operational head ditch at the Lakin test site. The ditch had been filled in and reshaped but the Bermuda grass sod remained in the ditch bank soil. Treatments and results were as follows.

Three sections were treated by adding different modifications of an asphalt emulsion to water ponded in the sections. All treatments were destroyed by erosion the first time water was turned in to the ditch.

Two sections were treated with surface sprays of cationic asphalt emulsion. These were tougher coatings than the ponded applications but were gradually destroyed by erosion during the summer irrigation season.

One section was sprayed on March 7, 1962, with cationic asphalt emulsion modified to obtain penetration into soil. Penetration was about 0.25 inch. Bermuda grass readily grew through the coating despite heavy pretreatment applications of polyborchlorate. The lining did not erode but was destroyed by cattle during October and November.

Black 10 mil polyethylene sheeting was bonded to the ditch bed with cationic asphalt emulsion in two 50 foot long sections on March 5, 1962. One section received a top spray of emulsion and the other was left uncovered. The top sprayed lining became coated with soil which should have provided some protection against weathering. Bonding to the ditch bed was not continuous because of surface irregularities but was sufficient to prevent wind and water from moving the sheet. Cost of materials was about 30 cents per square yard, including soil sterilant. The linings were in good condition until destroyed by cattle about eight months after application.

A section of jute-asphalt lining as developed by C. W. Lauritzen was installed. The jute had not been properly rot-proofed and the

lining failed because the jute decomposed within 6 months.

Fifteen mil butyl sheeting was used to line one test section on March 5, 1962. The sheet was bonded to the soil with cationic emulsion and was not covered. Total cost of materials was about $1.10 per square yard, including soil sterilant. The lining is in excellent condition except for two punctures made by cattle which have jumped onto the lining on numerous occasions. Soil under the lining is firm.

Chopped fiberglass mat, one ounce per square foot, and asphalt emulsion were used to line one 260 foot long section on May 16. The ditch was sprayed with emulsion, the mat was laid down, and the mat was saturated with emulsion. Total materials cost, including soil sterilant, was about 70 cents per square yard. Some damage occurred by unexpected flow of water over the lining immediately after installation before the emulsion had completely broken. The damage was easily repaired. Growth of Bermuda grass through the lining has been negligible. Cattle have damaged the lower end of the lining where underlying soil is muddy because of an above grade structure. Strength of the lining has increased with time from May to December and cattle have not damaged the lining where the underlying soil is reasonably firm.

Sealing concrete ditch linings. Previous attempts to seal concrete ditch linings with asphaltic materials have been hampered by difficulties in obtaining a good bond between the sealing material and concrete covered with a thin film of silt and algae. Cationic asphalt emulsion has excellent bonding properties and may solve some of the concrete sealing problems when used as a tack coat, slurry, or sand mix. Preliminary testing was done on a slip-form concrete farm ditch.

The tack coat problem was readily solved by a simple modification of the cationic asphalt emulsion. Although the modified emulsion penetrated silt up to 1/2 inch thick, the asphalt impregnated silt is not a tough and durable material. Elaborate cleaning is not required but the concrete should be swept reasonably clean. The

emulsion readily penetrates a thin layer of silt and algae to make an intimate bond with the concrete.

Procedures were developed to mix cationic asphalt with sand to make soupy slurries and stiff sand mixes. The slurries are applied to the concrete with a squeegee to fill small cracks, and the sand mixes are used to fill larger cracks and holes. Both slurries and sand mixes had limited plasticity after curing. Expansion and contraction of cracks in the concrete test lining resulted in cracking of the asphalt-sand mixtures. Modifications to improve plasticity are under investigation.

SUMMARY AND CONCLUSIONS:

Laboratory studies showed that clay soils can be deflocculated to a controlled degree to reduce seepage without creating an erosion problem because of excessive dispersion. Previous use of dispersants to reduce seepage from ponds where compacting equipment could not be used had resulted in failure because the dispersed surface soil washed away. Proper analysis of the soil, combined with adequate knowledge of soil chemical-physical processes, will permit selecting the type, quantity, and placement of salt to partially, but not completely, break down the soil structure. Limited studies determined the following general relationships for a highly permeable, acid clay soil: (1) seepage rates versus percent deflocculated clay, (2) percent deflocculated clay versus exchangeable sodium percentage versus soil solution concentration, (3) percent deflocculated clay versus exchangeable sodium percentage versus salt type, and (4) percent deflocculated clay versus soil depth versus size of salt crystals. Although the relationships appear confusing, because many interrelated factors are involved, these studies indicate that nomographs and three-dimensional graphs can be developed to clarify the relationships and permit the rational design of deflocculating treatments for seepage reduction.

Lack of suitable equipment for properly mixing salt with soil was found to be a major problem in field trials of soil deflocculation for seepage reduction. Stock ponds are often in remote areas and

application equipment must be light-weight and easily portable in a small truck. It must also be capable of thoroughly mixing salt in the surface six inches of soil while operating on steep side slopes. Such equipment can be developed but is not presently available.

Several types of low-cost ditch linings were installed in an operating irrigation ditch. Linings consisting of ponding applications of asphalt emulsions were rapidly destroyed by erosion. Spray applications of asphalt emulsions produced a tough lining which resisted erosion but was readily penetrated by Bermuda grass. Black polyethylene, bonded to the ditch with asphalt emulsion, resisted erosion and weed growth but was destroyed by cattle. Fifteen mil butyl sheeting, bonded to the soil with asphalt, resisted all damage except for two minor punctures by cattle but costs $1.10 per square yard for materials alone. Slip-form concrete linings cost about $1.00 per square yard installed. Fiberglass mat bonded to the soil and sealed with cationic asphalt emulsion resisted all damage where the sub-grade was firm. A small area was damaged by cattle where the sub-grade was saturated next to a faulty seal on an above grade structure which kept water ponded in the ditch. Installed cost of this lining will be 80 to 90 cents per square yard. The fiberglass lining may have some promise for use where slip-form concrete lining is not feasible. Additional installations and improved formulations are being developed.

A modified cationic asphalt emulsion has been developed which bonds very well to concrete ditch linings which have a surface coating of silt and algae. Repair of cracked concrete linings has been very difficult in the past because sealing materials would not bond to the concrete unless it was thoroughly cleaned. Cationic asphalt slurries appear promising as crack fillers but improved elasticity is required. Formulations with increased elasticity are being developed.

PERSONNEL: L. E. Myers and C. L. Jenson.

Table 1. Reduction in seepage from Pine test ponds by treatment with NaCl.

Water Depth	Seepage Rates					
	Pond 1 - 4,000 lb. NaCl per acre			Pond 2 - 6,000 lb. NaCl per acre		
	Untreated 1960	Post-Treatment 1962	Reduction	Untreated 1960	Post-Treatment 1962	Reduction
feet	inches/day	inches/day	percent	inches/day	inches/day	percent
6				9.1	5.1	44
5	9.9			7.4	4.1	45
4	9.4			5.7	2.4	58
3	8.1	2.6	68	3.9	1.0	75
2	5.7	2.1	63	1.3	0.5	62

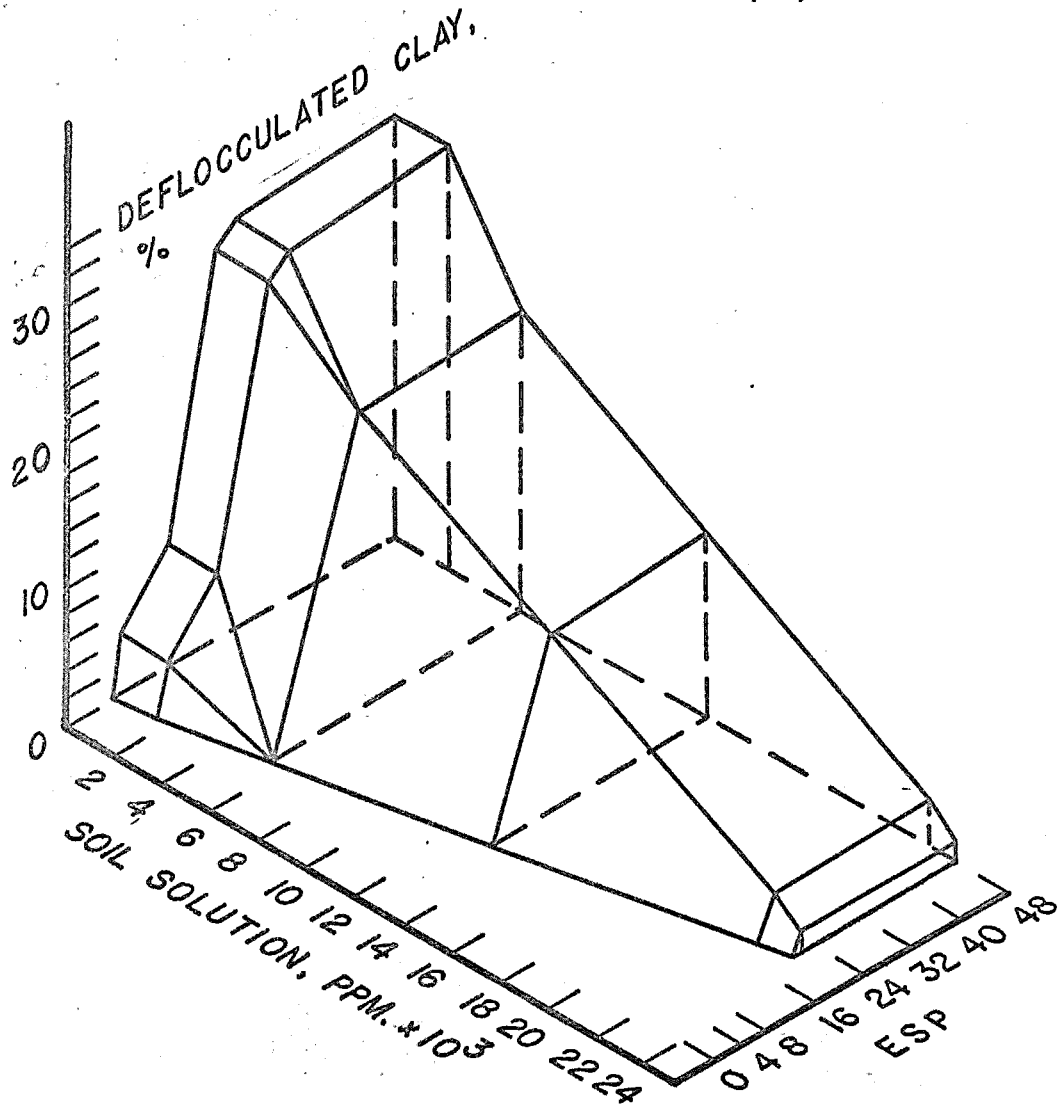

Figure 1. Percent deflocculated clay vs ESP and soil solution concentration for Dick Mason soil treated with sodium chloride.

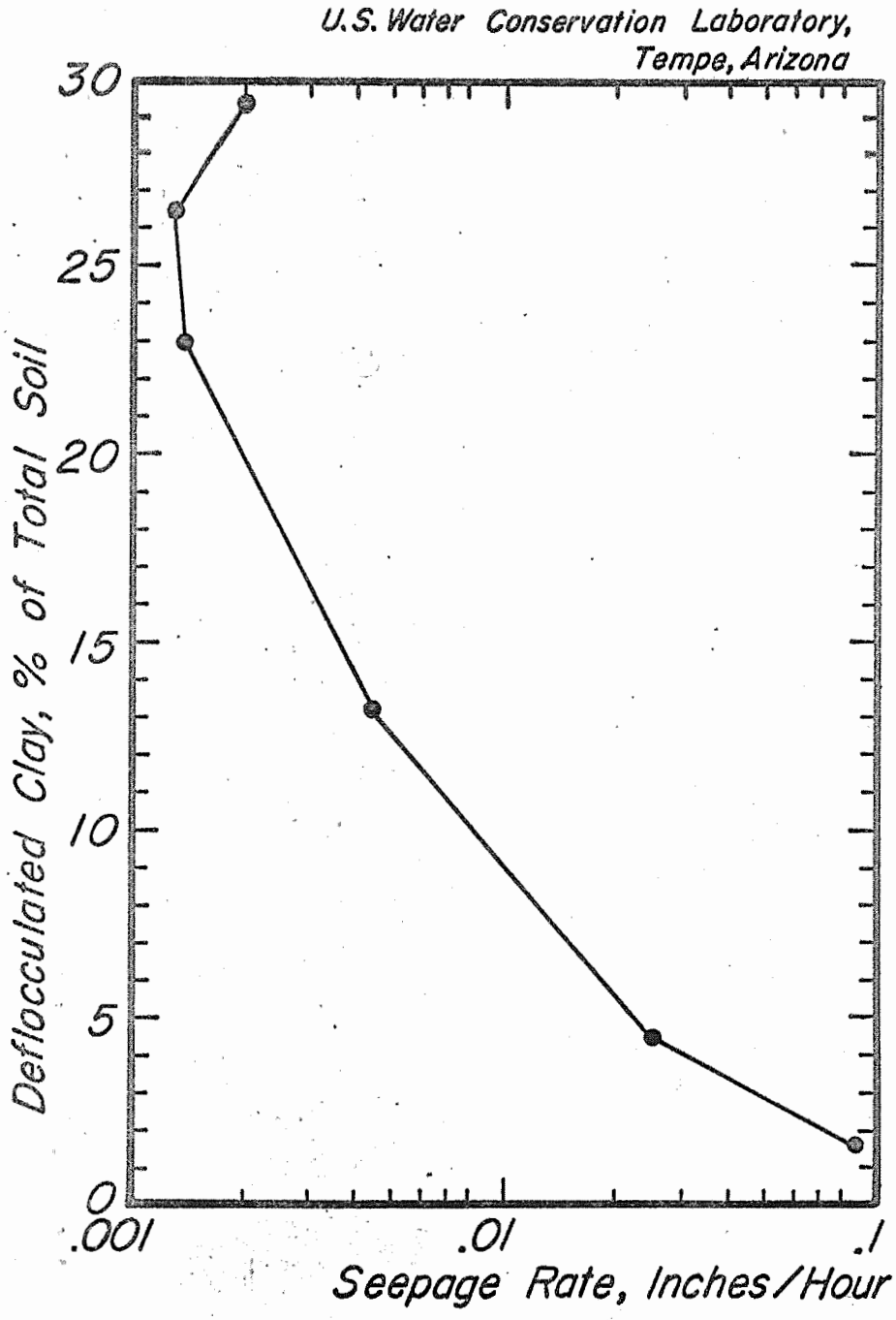

Figure 2. Relationship between seepage rate and percent deflocculated clay for Dick Mason soil treated with sodium chloride.

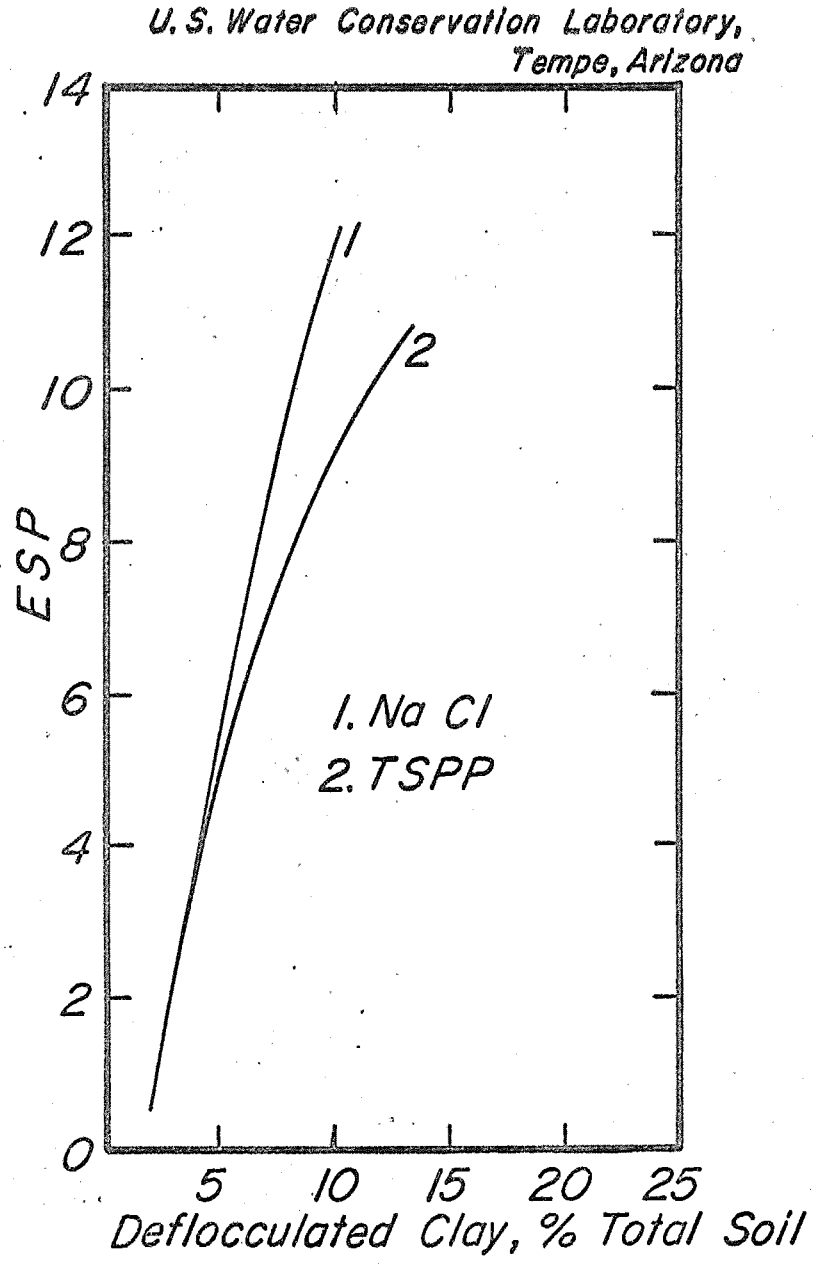

Figure 3. Relationship between ESP and percent deflocculated clay for Dick Mason soil treated with sodium chloride and tetra-sodium pyrophosphate.

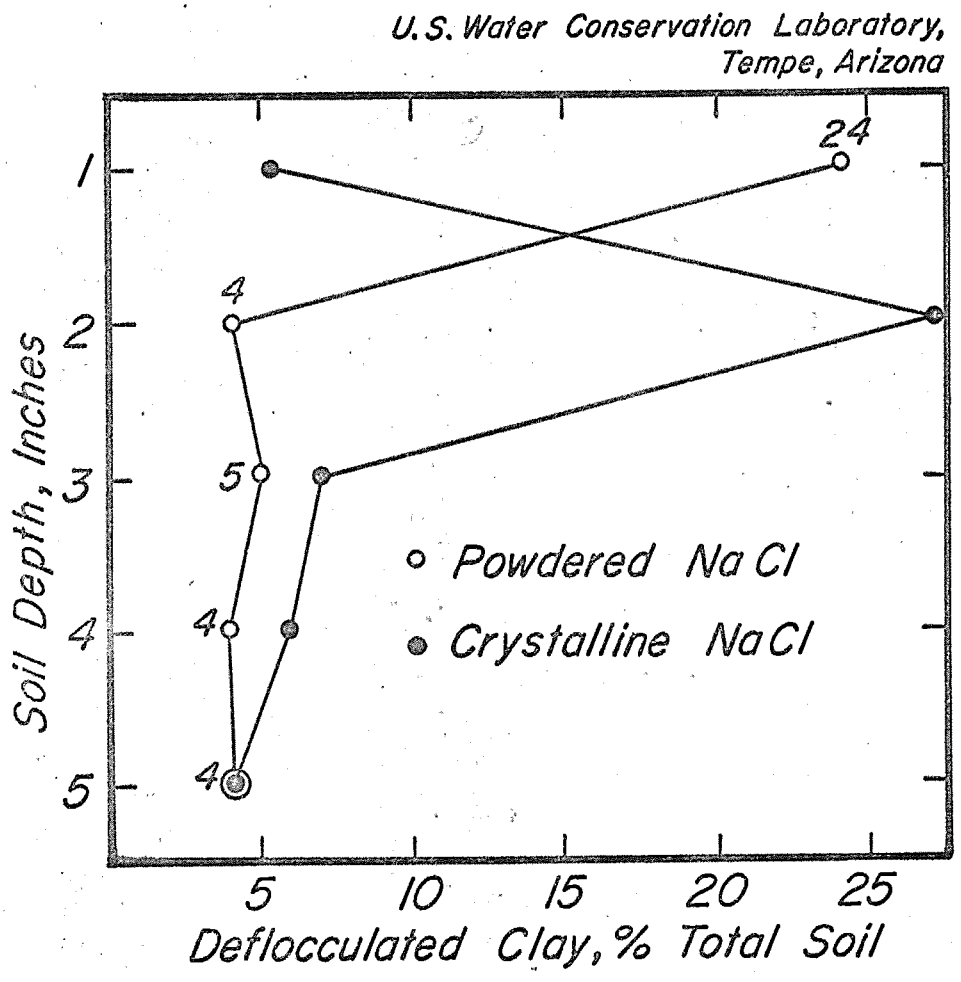

Figure 4. Vertical distribution of deflocculated clay treated with powdered and crystalline sodium chloride.

TITLE: CONSTRUCTION AND CALIBRATION OF A MINIATURE NET RADIOMETER

LINE PROJECT: SWC 4-gG2 CODE NO.: Ariz. WCL-6

INTRODUCTION:

The energy budget method, by which the flux of water vapor and sensible heat may be estimated, requires measurement of net radiation. Instruments for measuring net radiation, in addition to having good instrument qualities, must be economical so that they can be replicated sufficiently. Such an instrument and methods of calibration were described in the 1960 Annual Report. Recent emphases have been on increasing the output of the miniature net radiometer, simplifying its construction, and modifying the instrument so that it can be used to measure total hemispherical radiation.

PROCEDURES:

To increase the output of the miniature net radiometer and maintain its desirable features, new transducers were constructed. The construction entails winding 4-mil constantan wire on 1/16- by 3/8- by 3/4-inch glass plates. Half of the coil is overplated with copper so the copper-constantan junctions are on the 3/8- by 3/4-inch surfaces. Two coils are then connected in series and cast in epoxy, forming the transducer.

Previously, the transducer was supported between two sheets of plastic film. This method of assembly required a spacing ring and a jig to stretch the plastic. The new transducers need not be supported by the plastic film, thus reducing the components of the net radiometer to the transducer, two hemispherical-shaped radiation windows, and two clamping rings.

Modification of the miniature net radiometer to measure total hemispherical radiation was accomplished by attaching a hemispherically shaped dome on one side (either top or bottom) of the net radiometer. By knowing the temperature of the dome, the output of the transducer, and assuming that the dome and the surface are in radiation equilibrium, total hemispherical radiation can be calculated.

A calibration coefficient was determined for each dome in the calibration chamber using long-wave radiation, the coefficient being dependent upon the proximity of the thermocouples to the concave surface of the dome and the number of coats of paint on that surface.

RESULTS AND DISCUSSION:

The calibration factors of the miniature net radiometers are about 10 times greater when the new transducers are used, the average calibration factor being 1.5 mv ly^{-1} min. The miniature net radiometer, with the new transducer, appears to have all the desirable features of the previous model plus the larger output. The transducer has a temperature coefficient at 1 ly min^{-1} net radiation of 0.07 percent $^{o}C^{-1}$ deviation from ambient temperature of $20^{o}C$. When the ambient temperature is $40^{o}C$ and net radiation is 1 ly min^{-1}, the temperature coefficient is equivalent to 1.4 percent or 0.14 ly min^{-1}.

During September 1962, three miniature net radiometers (two with hemispherical domes) and two solarimeters were placed in the experimental field 1 meter above the Sudangrass. One of the total hemispherical radiometers (net radiometer with dome) and one of the solarimeters were inverted. With this combination of instruments, all of the components of net radiation could be measured or obtained with the use

of the following relations:

$$R_t \downarrow = R_l \downarrow + R_s \downarrow \qquad [1]$$

$$R_t \uparrow = R_l \uparrow + R_s \uparrow \qquad [2]$$

$$R_n = R_t \downarrow - R_t \uparrow \qquad [3]$$

$R_t \downarrow$ and $R_t \uparrow$ were measured with the total hemispherical radiometers; $R_s \downarrow$ and $R_s \uparrow$ were measured with the solarimeters, and R_n was measured with a net radiometer.

The results obtained from 0000 to 0600, 17 September 1962, indicated that $R_t \downarrow$ averaged 0.545 ly min^{-1}, while $R_t \uparrow$ averaged 0.574 ly min^{-1} giving a calculated R_n [3] of -0.03 ly min^{-1}. The average R_n, measured over the lysimeters about 30 meters away, for the same period was -0.03 ly min^{-1}. During darkness, $R_t \downarrow = R_l \downarrow$ and $R_t \uparrow = R_l \uparrow$.

The total upward long-wave radiation from a surface with emissivity, ϵ, may be written as

$$R_l \uparrow = \epsilon \sigma T_o^{\,4} + (1 - \epsilon) R_l \downarrow$$
$$= \sigma T_o^{\,*4} \qquad [4]$$

where T_o is the true temperature and T_o^* is the apparent temperature, assuming $\epsilon = 1$. The average T_o measured at the surface of the

Sudangrass was 20.6°C, while T_o^* computed from the radiometer data was 16.5°C, indicating an emissivity, ϵ, of 0.94. Values of ϵ found in the literature range from 0.98 for vegetation to 0.9 for bare soil. Since the Sudangrass did not form a complete canopy, 0.94 seems to be a good estimate of the emissivity.

The results obtained during the daylight hours (0615 to 1400, 17 September 1962) were not as good. $R_t \downarrow$ averaged 1.250 ly min^{-1} and $R_t \uparrow$ averaged 0.778, resulting in a calculated R_n 0.64, as compared to a measured R_n of 0.53. $R_s \downarrow$ and $R_s \uparrow$ averaged 0.731 and 0.167 ly min^{-1}, respectively. Thus $R_l \downarrow$ and $R_l \uparrow$ from [1] and [2] were 0.519 and 0.611 ly min^{-1}. The $R_l \downarrow$ was 0.026 ly min^{-1} less and $R_l \uparrow$ was only 0.038 ly min^{-1} greater during daylight period than the nighttime period. The average apparent temperature (T_o^*) was 21.0°C, while the temperature measured at the top of the Sudangrass (T_o) was 31.3°C, indicating an emissivity of 0.86.

The poor daytime results appear to be due to internal reflection of short-wave radiation, which will be eliminated when the new transducers are used. Therefore, this study will be continued in the future.

SUMMARY AND CONCLUSIONS:

The output of the miniature net radiometers was increased to approximately 1.5 mv ly^{-1} min by using transducers made in the Laboratory. The use of the new transducer also simplifies the assembly by reducing the number of components to five, while maintaining the desirable characteristics of the previous transducer.

The miniature net radiometer was modified to measure total hemispherical radiation by the addition of a hemispherical dome. Preliminary tests yielded good results during periods of darkness. Internal reflection of short-wave radiation causes erroneous daytime values. During the night, the downward flux of radiation was 0.545 ly min^{-1}, while the upward flux was 0.574 ly min^{-1}. An emissivity of 0.94 was computed for a Sudangrass cover, which compared favorably with emissivities found in the literature (0.98 for vegetation and 0.9 for bare soil).

Symbols and dimensions:

R_n = net radiation [ly min^{-1}]

R_t = total hemispherical radiation [ly min^{-1}]

R_l = long-wave radiation [ly min^{-1}]

R_s = short-wave radiation [ly min^{-1}]

$\downarrow$ or $\uparrow$ indicate the direction of the radiant flux

PERSONNEL: Leo J. Fritschen

TITLE: SURFACE ENERGY BALANCE AND EVAPOTRANSPIRATION OF IRRIGATED ALFALFA.

LINE PROJECT: SWC 4-gG2 CODE NO.: Ariz.-WCL-17

INTRODUCTION:

Measurements or estimations of evaporation from various surfaces in an arid, warm climate are generally not available. This is especially true for short periods. The data which are available generally have not been augmented with sufficient atmospheric measurements for estimation of evaporation by micrometeorological models. In order to better understand the mechanisms of latent and sensible heat transfer and to test models and equipment for estimating these fluxes, detailed studies need to be conducted that fully describe the pertinent, physical variables of the atmospheric and soil environments. Some of the objectives of these studies are:

(1) to measure the energy balance components of various crops from seeding to maturity;

(2) to test various models for estimating evaporative rates; and

(3) to estimate the evaporative rate of various surfaces throughout the growing season.

SUMMARY OF ACTIVITIES:

The following is a summary of the activities of the past year, including analysis of data collected during the previous year. Unfortunately, all of the data collected has not been analyzed due to a delay in writing the generalized linear computer program to process the data. The program is described under "Instrumentation for micrometeorological research."

November - December 1961. Alfalfa was seeded in the experimental field during November 1961. Measurements were made to determine how the emerging seedings affect the energy balance components. However, since the crop failed, the measurements made during that period are over bare soil. Net radiation was measured at 10 cm over each of the three lysimeters. Soil heat flow was measured at 5-cm depth in each of the three lysimeters. Incoming and reflected solar radiation and

wind direction were also measured. These micrometeorological parameters were sampled hourly. The data were combined with those from the lysimeter to solve the energy balance equation for the sensible heat flux. Soil temperatures were not measured, so it was not possible to compute the change in the energy storage of the soil layer above the heat-flow transducer.

February - March 1962. Measurements of soil temperature and soil heat flux inside and outside of the lysimeters were made to determine if there was any difference in the temperatures between the lysimeter and the surrounding field. In addition, data was collected to determine the energy balance components over bare soil during periods of low radiation intensity. Net radiation was measured at 10 cm over each of the three lysimeters. Soil heat flow was measured at 5 cm in each of the three lysimeters. Soil temperatures were measured at the "surface" and at 5-cm depth to determine the change in energy storage of the layer above the heat-flow transducer. Incoming and reflected solar radiation, wind speed at 1 meter, and wind direction were also measured. All the micrometeorological parameters were recorded at 15-minute intervals.

March - April 1962. Alfalfa was again seeded in the experimental field during March 1962. Measurements were again made to determine the effect of the emerging crop upon the components of the energy balance. A satisfactory stand was not obtained; therefore, the alfalfa was removed and Sudangrass was planted. Net radiation was measured at 10 cm over each of the three lysimeters. Soil heat flow, "surface" soil temperature, and the temperature at 5 cm were measured in each of the lysimeters. Incoming and reflected solar radiation, wind speed at 1 meter, and wind direction were also measured. These parameters were recorded at 30-minute intervals.

May 1962. The emerging Sudangrass was approximately 5-cm high. Data were collected to determine the components of the energy balance equation and to calculate the flux of the sensible heat by aerodynamic techniques. Net radiation was measured at 10 cm above each of the lysimeters. Soil heat flux was measured at a depth of 5 cm.

"Surface" soil temperature and the temperature at 5 cm were measured in each lysimeter. Incoming and reflected solar radiation, wind speed and wind direction were also measured.

Three air-temperature masts containing two-junction thermopiles between 5 and 10, 10 and 20, 20 and 40, and 40 and 80 cm, and a thermocouple located at 80 cm, were placed in the experimental field, as shown in Figure 1. At location two, the air-temperature differentials between 5 and 10 and 10 and 20 cm were recorded continuously on two strip-chart recorders. All other temperature differentials were recorded with the data-handling system at 5-minute intervals. Anemometers were placed near location two at 5, 10, 20, 40, and 80 cm above the soil surface. The wind speeds at the various elevations were integrated for 5-minute intervals and then recorded along with the wind direction and other micrometeorological parameters.

June - July 1962. Data were obtained to determine the components of the energy balance over growing Sudangrass. Net radiation, soil heat flow, "surface" soil temperatures, and the 5-cm soil temperature were measured over and in one lysimeter. Incoming and reflected solar radiation and wind speed were also measured. These parameters were recorded at 30-minute intervals.

12 - 14 and 20 - 23 July 1962. Measurements were made to determine the effect of crop height and maturity upon the components of the energy balance. The Sudangrass on checks 5, 6, and 7 was allowed to grow. Checks 1 through 4 were mowed at approximately 20-cm height. Then two weeks prior to the experiment, check 4 was allowed to grow, while checks 1, 2, and 3 were mowed at 20-cm height. Thus at the experimental time, checks 1, 2, and 3 were approximately 20 cm; check 4 was 75 cm; and checks 5, 6, and 7 were 140 cm. At this time the Sudangrass in checks 5, 6, and 7 was headed out, while the Sudangrass in the other checks was not. Data collected for two days, 12 and 13 July, consisted of measurements of net radiation 1 meter above the crop and 5 cm above the soil surface in each of the three lysimeters. Soil heat flow was measured in each of the three lysimeters at the 5-cm depth. "Surface" soil and 5-cm temperatures

were also measured. Incoming and reflected solar radiation, wind direction and wind speed 1 meter above the crop in check 4 were also measured.

After 13 July, checks 5, 6, and 7 were mowed and checks 1 through 4 were allowed to grow. By the time the second set of data were collected, 20 - 23 July, checks 1, 2, and 3 were approximately 40-cm tall, while check 4 was 100-cm tall, Sudangrass beginning to head out. Checks 5, 6, and 7 had not recovered from the mowing, the stubble being 8-cm tall. Data collected during this period consisted of net radiation measured 1 meter above the crop in checks 2 and 4, 1 meter above the stubble in check 6, and 5 cm above the soil surface within the crop canopy on checks 2 and 4. Heat flow at 5 cm, "surface" soil, and 5-cm soil temperatures were also measured. Incoming solar radiation, wind direction and wind speed 1 meter above the crop were measured. Reflected solar radiation was measured over checks 4 and 6. All micrometeorological parameters were printed out at 15-minute intervals.

July - August 1962. During the latter part of July and the first part of August, routine measurements were made over the growing Sudangrass crop. These measurements consisted of net radiation measured 1 meter above the crop, soil heat flow and soil temperature at 5 cm, "surface" soil temperature, incoming and reflected solar radiation, and wind direction. These micrometeorological parameters were printed out at 30-minute intervals.

14 - 16 August 1962. During 14 to 16 August, the effect of periodic radiation upon evaporation was investigated. The results are reported under "Evaporation and periodic irradiation."

August - September 1962. Measurements made during this period were similar to those made during latter July and first part of August.

12 - 18 September 1962. Detailed information was collected to determine the energy balance over each lysimeter and to calculate the flux of sensible heat by the aerodynamic gradient technique. These measurements consisted of net radiation measured 1 meter above the crop in each of the three lysimeters, soil heat flow, "surface" and

5-cm soil temperature, incoming and reflected solar radiation, and wind direction. Wind speed was measured at 10, 20, 40, and 80 cm at locations within the experimental field. These parameters were printed out on one system at 15-minute intervals. On the second data-handling system, the following temperatures were printed out at 1-minute intervals: the temperature difference between 5 and 10 cm, 10 and 20 cm, 20 and 40 cm, 40 and 80 cm; the temperature at 80 cm, and at the grass surface. These temperature measurements were replicated at three locations in the experimental field. In addition, the 5- and 10- and 10- and 20-cm temperature differentials at location two were recorded on two drag pen recorders.

RESULTS AND DISCUSSION:

November - December 1961. Hourly components of the energy balance equation plus solar radiation and wind direction for two selected clear days are presented in Figures 2 and 3. These days--19 and 28 November--occurred 3 and 12 days after the field was irrigated, respectively; therefore, they represent the case of moist and dry soils at this time of the year. During this period solar radiation intensity was dropping rather rapidly. The components of the energy balance equation appeared to be about twice as large on 19 November as on 28 November. Part of this is due to the lower radiation intensity from the sun and part is due to the fact that the soil surface was drier on the latter day.

February - March 1962. The hourly components of the energy balance equation, solar radiation, wind speed and wind direction for two selected clear days--17 February and 1 March--are shown in Figures 4 and 5. The lysimeter field was irrigated on 15 February; therefore, these two selected days represent the 2nd and 14th day after irrigation. In the interim between these two days, 17 mm of precipitation occurred, the last of which fell on 25 and 26 February. The two days selected can be considered representative of wet and relatively dry soil; however, no direct comparison can be made since solar radiation intensity increased considerably during the intervening period. Net radiation on both days was the same. Evaporative

flux was approximately one-half as much on 1 March as on 17 February. The greatest difference appeared in the sensible heat flux to the air, which was almost twice as large on 1 March as on 17 February. The lower evaporative flux and the higher sensible heat flux to the air can be attributed directly to the drier soil surface.

March - April 1962. Data from March and April 1962 have not been analyzed as of this date. They will be reported later.

May 1962. The hourly components of the energy balance equation plus solar radiation, wind speed and wind direction for 29 May are shown in Figure 6. At this time the emerging Sudangrass was approximately 5-cm high. These data then cannot be directly compared to any of the previous work dealing with evaporation from bare soil. However, if one wishes to compare these data against some of the data from Big Mud 1, 30 April 1961, it appears that for similar solar radiation and intensity, net radiation is higher, evaporative flux is lower, and the sensible heat flux to the air is larger. These facts are attributed to the presence of the emerging Sudangrass, which could reduce the wind movement and consequently, the evaporation from the soil surface.

Comparisons of integrated versus sampled temperatures were made on the data collected 29 May 1962. The charts upon which the air-temperature differentials were recorded were analyzed using a planimeter to obtain half-hourly averages of the temperature differential. The half-hourly averages of the 5-minute samples of temperature differentials were also obtained. Thus forty-eight 30-minute averages were recorded during the day for each of the heights. Regression analysis was used to compute the sample standard deviation of the 5-minute samples on the integrated averages. The results indicated that the average of the 5-minute samples could be used to estimate the integrated averages within $\pm 0.068^{\circ}C$ at the 5- and 10-cm height, and $\pm 0.094^{\circ}C$ at the 10- to 20-cm height. The difference between these two values was due to the fact that the air-temperature differential at the higher elevation varied more than it did at the lower elevation. Thus 5-minute samples can be

used to estimate the true temperatures if one is willing to accept an error within $\pm 0.09^{\circ}C$. Further studies should be conducted to determine how much 1-minute samples would decrease this error of estimation.

The 80-cm temperatures at location one, two, and three were analyzed to determine if there was a horizontal temperature gradient across the field due to local advection. The data obtained indicated that there was no appreciable temperature difference between any of the three locations for the period 0000 to 0800 and 1700 to 2400. A temperature difference of the order of magnitude of 1 degree or less was noted between 0800 and 1700. During this period the wind was primarily from the east or southeast. At 1600, the wind direction became southwesterly; the temperature at the 80-cm height on location two was approximately $0.5^{\circ}C$ higher than that at location three and $1^{\circ}C$ higher than that of location one. If horizontal advection existed, then one would expect a temperature gradient to exist from location three through one when the wind was from the east, and location one through three when the wind was from the southwest. The opposite of this appeared to be true in that the temperature in the middle of the field was warmer than the temperatures toward the edge of the field. This is contrary to what would be expected when considering that the lysimeter field was irrigated the day previous and surrounding area was relatively dry. If a horizontal temperature gradient does exist, it must be closer to the edge of the field and possibly at a greater elevation, the lower temperatures of each of the three profiles being relatively similar.

The two-hourly plots of the air-temperature profiles averaged over a 30-minute period are shown in Figure 7. The absence of any appreciable temperature gradient between 40 and 80 cm is the predominant feature of this graph. Below 40 cm, temperature gradients do occur. However, these gradients appear to be in the opposite direction of the gradient of the soil "surface" to the 5-cm height. This would indicate that if air temperature gradients were used to calculate the flux of sensible heat, the answer in many cases would be qualitatively wrong.

Before the start of the experiment, it was doubted whether wind-speed profiles could be obtained by placing the anemometers so close to the surface of the soil, and it was questionable what the wind speeds so recorded actually mean. The surprising thing was that during most of the day the anemometers continued to rotate; however, the wind speeds between 0000 and 0530, and after 1930, were too low to be measured accurately. The 5-minute wind speeds were averaged for 30 minutes and the plot on two-hourly intervals are shown in Figure 8. If one can assume that the measurements at the lower levels, 5 and 10 cm, are true measurements of the wind speed, then it appears that the wind-speed profiles below 20 cm obey the logarithmic law throughout the daylight hours, and that the wind speeds above 20-cm level do not appear to obey the logarithmic law. The anemometers used in this study were calibrated before and after the study and the wind speeds for each anemometer were corrected for the calibration constant.

Previous results obtained in 1961 using aerodynamic calculations to determine sensible heat flux indicated that the values obtained were qualitatively of the opposite sign of those obtained from the solution of the energy balance equation. The air temperature differences used in these studies appeared to have the wrong sign compared to the temperature differences between the surface and 40 cm. Accordingly, the studies on 29 May were conducted with the temperature profile below 80 cm. As could be expected from examining the gradients of the temperature profiles, aerodynamic calculations of the sensible heat for the data obtained on 29 May 1962 are qualitatively in error. The results of these calculations plus the calculations made in 1961 are shown in Figure 9. With further examination of the temperature profiles, it becomes quite obvious that if one is to make calculations of the sensible heat flux at the surface, then the surface temperature should be one of the parameters to be used in each calculation. Further studies will be pointed toward this direction.

June - July 1962. The data collected in June and July 1962 have not been analyzed as of this date and will be reported at a later time.

12 - 14 and 20 - 23 July 1962. By 12 July the Sudangrass had attained the average height of 25 cm on the first three checks, 75 cm on the 2nd check, and 140 cm on the 5th, 6th, and 7th checks. The 140-cm Sudangrass had developed seedheads. Unfortunately, the stand near lysimeter I in check 3 was not continuous enough to validity the results obtained from lysimeter I. Therefore, it will be disregarded in this discussion.

The results from the 75-cm and the 140-cm crops are shown in Figures 10 and 11. Evapotranspiration from the 75-cm crop was 243 ly day^{-1} greater than that from the 140-cm crop. A similar difference was not reflected in the measurements of net radiation and soil heat flow. The evapotranspiration rate of the 75-cm crop exceeded net radiation plus soil heat flow. The source of the extra energy to sustain this large evapotranspiration rate must be the sensible heat from the air, whereas the evapotranspiration from the 140-cm crop did not exceed net radiation; therefore, energy was given off in the form of sensible heat. One notable fact is the absence of a midday depression even with this high evapotranspiration rate.

By the 20th of July, the Sudangrass in check 4 had reached a height of 100 cm (intermediate to the heights on 12 and 13 July) and had started to develop some seedheads. Data collected on 20 July are shown in Figure 12. Even though solar-radiation intensity was lower and the average dewpoint was higher, the components of the energy balance equation were similar to those in Figure 11; consequently, the 100-cm Sudangrass can be said to be similar to the 75-cm Sudangrass with respect to these components. The difference that existed between the 75-cm and 140-cm Sudangrass also existed between the 100- and 140-cm Sudangrass. This was not due to physiological maturity because the evapotranspiration from the 140-cm crop increased to 10.05 mm day^{-1} compared to 9.01 mm day^{-1} when the grass around the lysimeter was cut, permitting energy to reach the transpiring surfaces. The reason for the difference appears to be due to the presence of seedheads. The seedheads, not able to transpire,

absorb a portion of the energy and convert it into sensible heat, and also provide an aerodynamic barrier for the transfer of sensible heat to the transpiring surfaces.

A comparison of the effect of wind speed upon evapotranspiration may be made by comparing Figures 10 and 13. On 13 July, the average wind speed was 139 cm sec^{-1} as compared to 247 cm sec^{-1} on 12 July. The evapotranspiration curve of the shorter crop prior to 1000 is very similar after 1000. A marked difference appeared in that the evapotranspiration rate on 12 July increased with increasing wind speed and remained greater than that of 13 July throughout the remainder of the day. The differences in the evapotranspiration rate are then reflected in the sensible heat flux term, net radiation plus soil heat flow being essentially the same. On both days, sensible heat was derived from the air to maintain the evapotranspiration rate of the shorter crop, the amount being 70 cm larger on 12 July. Energy in the form of sensible heat was given off from the taller crop, with 30 ly more being given off on 13 July.

July - August, August - September 1962; 12 - 18 September 1962.

The data obtained during these periods have not been analyzed as of this date due to a revision of the computer program. These data will be reported at a later time.

SUMMARY AND CONCLUSIONS:

Surface energy balance and evaporation or evapotranspiration was measured over bare soil and Sudangrass due to a failure to establish a stand of alfalfa. All of the data have not been completely analyzed because of a delay in writing a generalized linear computer program to process the data. Of the data that was collected, the following conclusions can be drawn:

(1) Measurements made over wet and dry bare soil November 1961, and February and March 1962, indicated that in all cases, the evaporative flux was less than net radiation, energy was derived from the underlying soil, and energy was utilized in heating the air. The fact that net radiation always exceeded the evaporative flux may be characteristic of the winter season, which has low-radiation intensity and cooler temperatures.

(2) Measurements made over emerging Sudangrass indicate that for similar solar-radiation intensity, net radiation is higher, evaporative flux is lower, and the sensible heat flux to the air is larger than over wet, bare soil. These facts are attributed to the presence of the emerging Sudangrass, which could reduce the wind movement and consequently, the evaporation from the soil surface.

(3) Comparisons of integrated versus sampled air-temperature differentials indicate that 5-minute samples can be used to estimate integrated values within $\pm 0.094^{\circ}C$.

(4) Air-temperature profiles measured at three locations across the experimental field did not indicate any appreciable horizontal temperature gradient at 80 cm, even though the experimental field was wet, while the surrounding area was relatively dry. If a horizontal temperature gradient does exist, then it must be closer to the edge of the field and possibly, at greater elevations than those measured.

(5) Wind-speed measurements made at 5, 10, 20, 40, and 80 cm indicate that the wind-speed profiles below 20 cm obey the logarithmic law throughout the daylight hours, and that the wind speeds above 20 cm do not appear to obey this law.

(6) Aerodynamic calculations of the sensible heat flux indicate that the flux is often of the opposite sign to that determined by the energy balance equation, and that the temperature of the surface should be one of the parameters used in these calculations.

(7) Measurement of the energy balance components over Sudangrass of 75-, 100-, and 140-cm height indicated that the net radiation was similar, while evapotranspiration was much less and the sensible heat flux was considerably larger over the 140-cm crop. This difference was not explained by physiological maturity because the Sudangrass was able to increase its transpiration rate to that of the 100-cm crop when the surrounding area was cut allowing energy to reach the transpiring surfaces, but was attributed to the presence of the seedheads. The seedheads, not being able to transpire, absorbed a portion of the radiant energy and converted it into sensible heat; also, provided

an effective aerodynamic barrier against the transport of sensible heat to the transpiring surfaces.

(8) When evapotranspiration rates were determined during periods of maximum insolation and large vapor-pressure deficits, no midday depressions were observed. These measurements were made under high soil-moisture conditions, and may not be characteristic of any other crop but Sudangrass.

PERSONNEL: Leo J. Fritschen, C. H. M. van Bavel, W. Reeves.

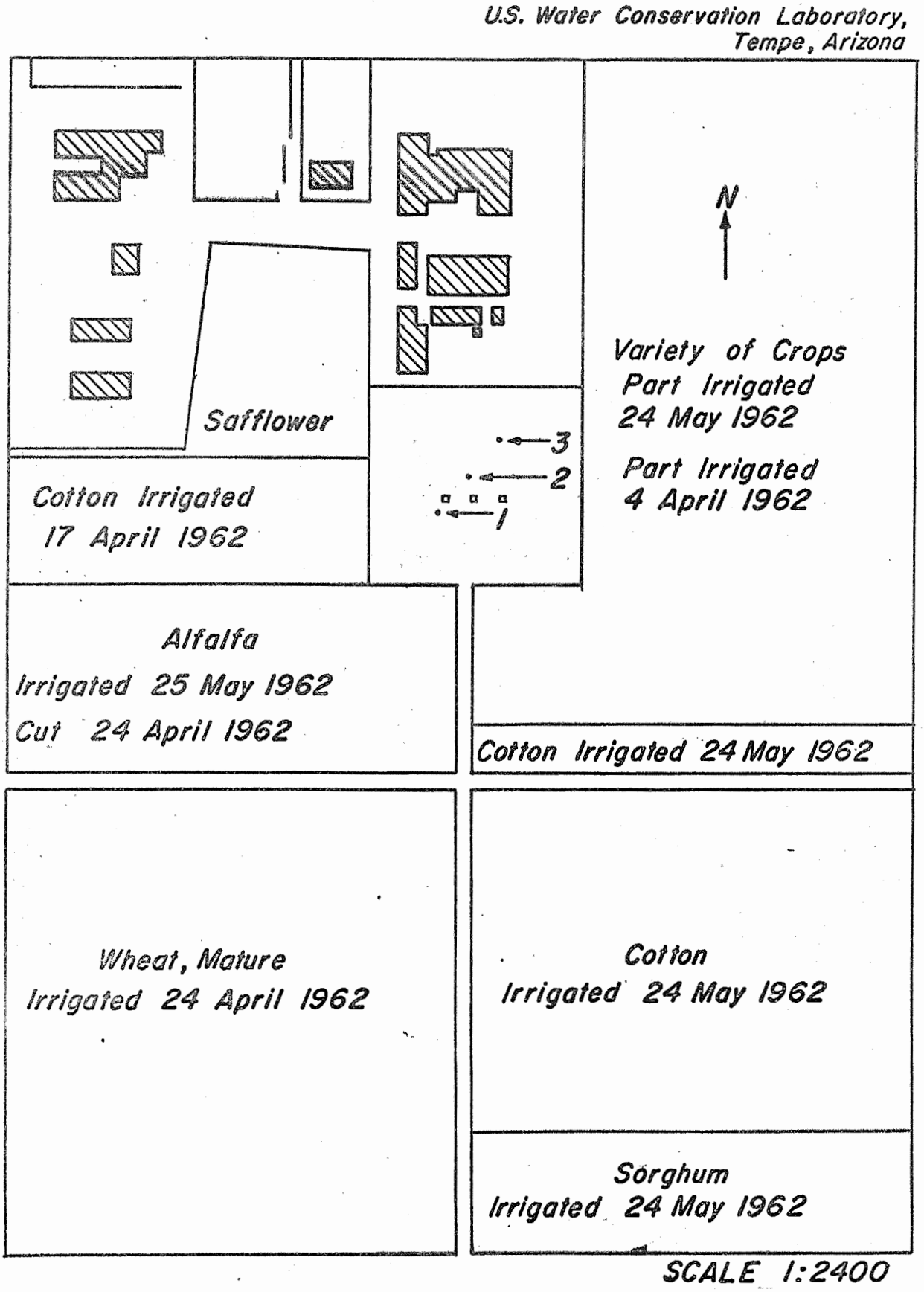

Figure 1. Observation field and location of air-temperature and wind-speed recording equipment

Annual Report of the U.S. Water Conservation Laboratory

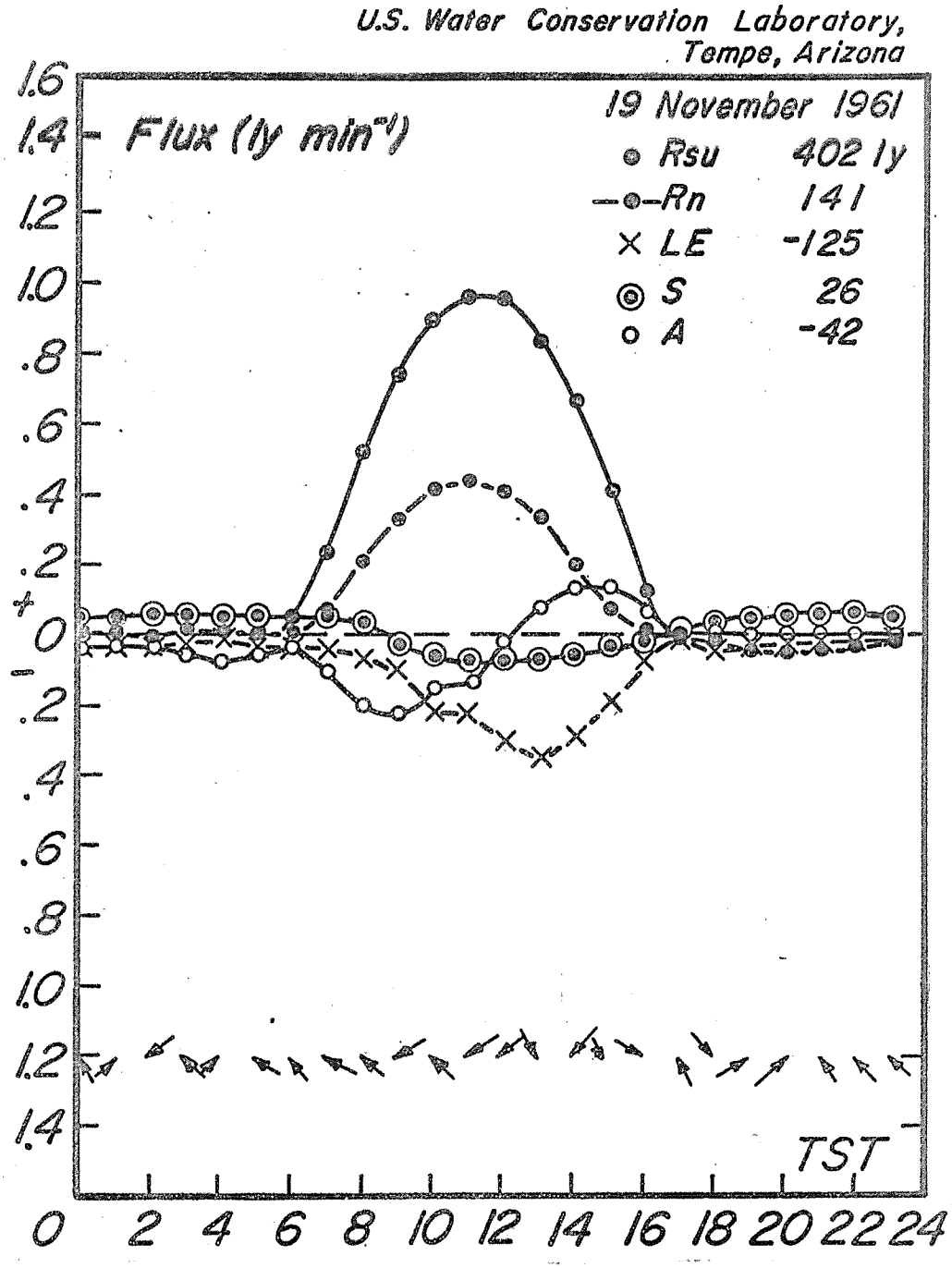

Figure 2. Hourly energy balance and wind direction over a bare, wet surface on 19 November 1961.

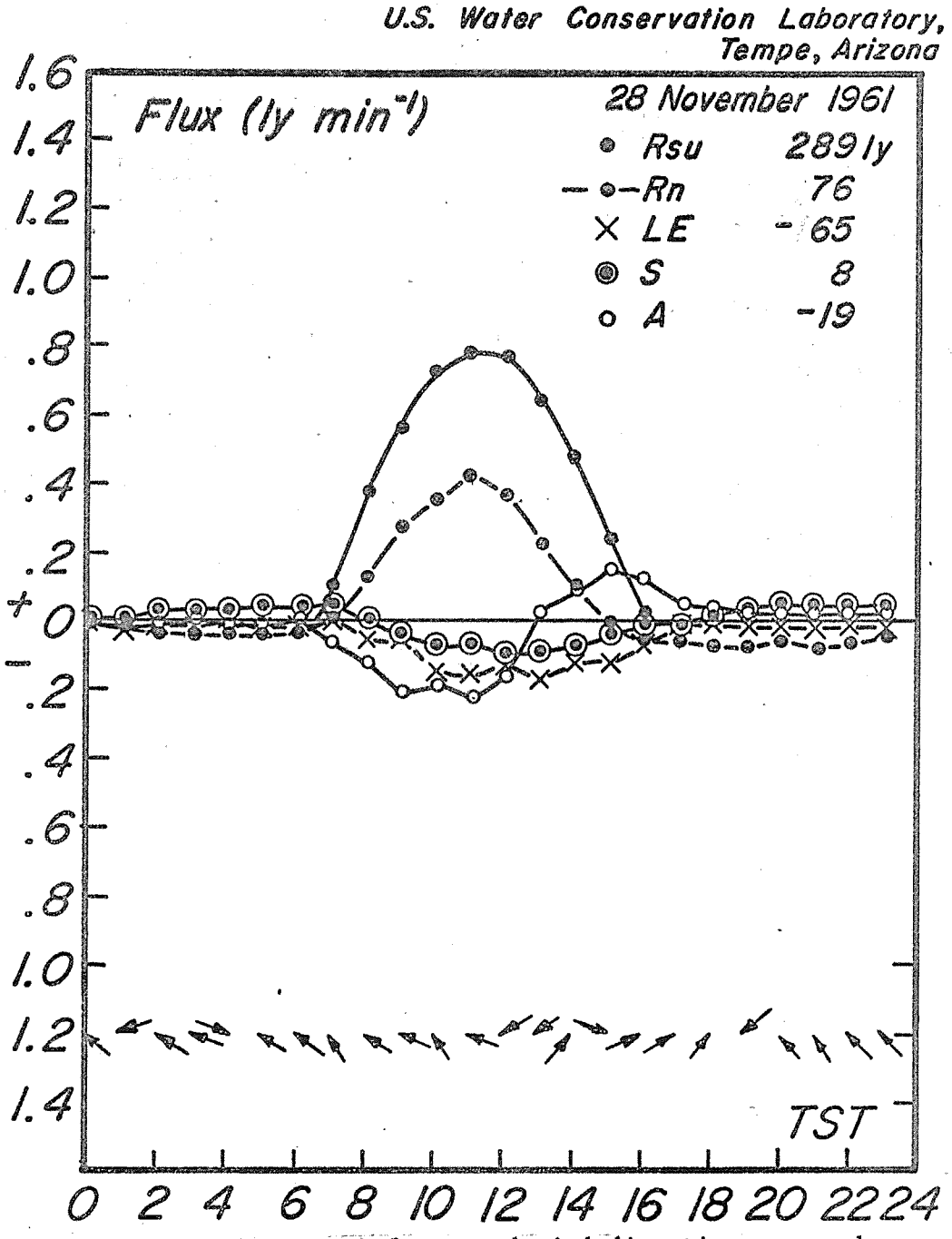

Figure 3. Hourly energy balance and wind direction over a bare, dry surface on 28 November 1961.

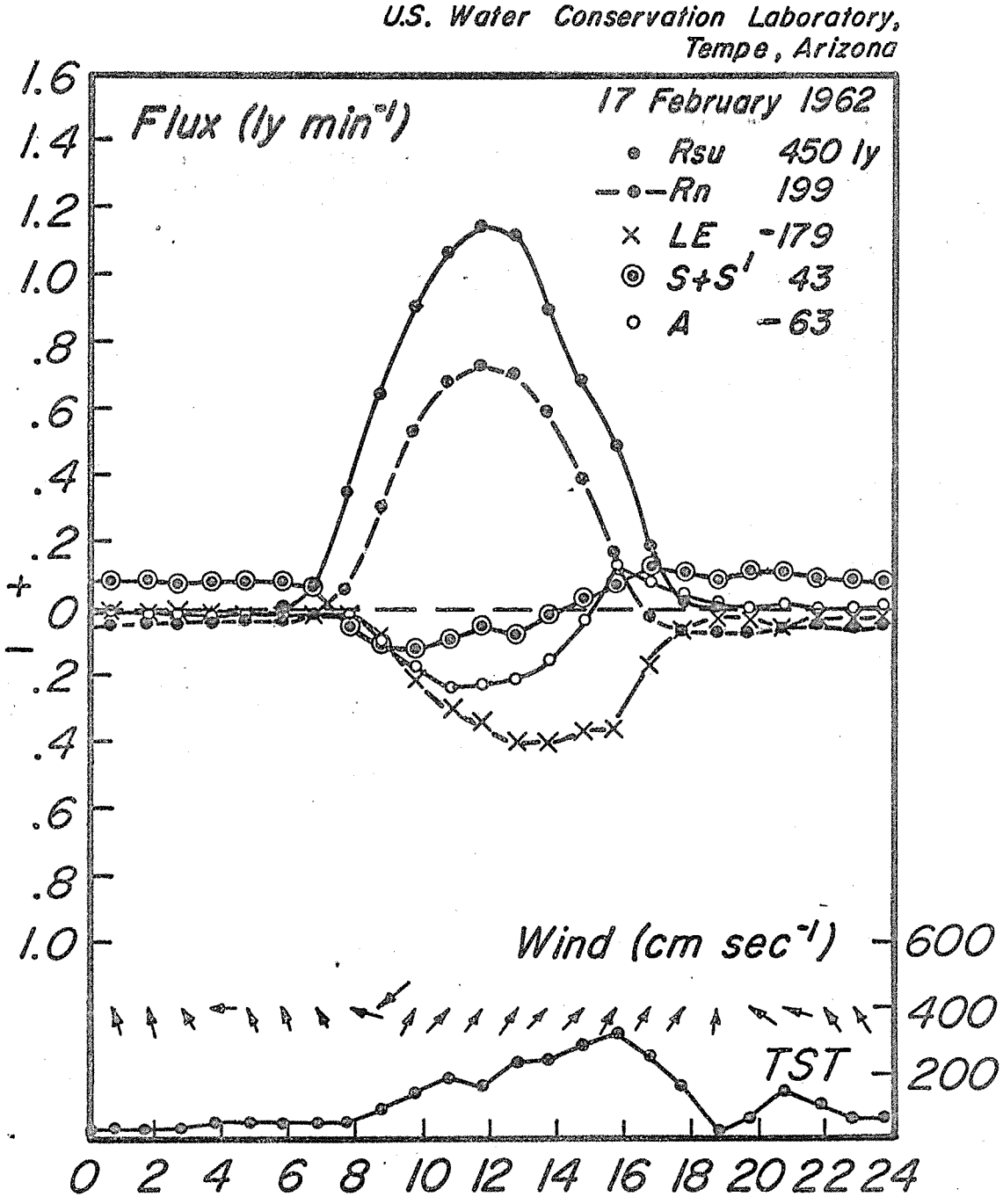

Figure 4. Hourly energy balance and wind movement over a bare, wet surface on 17 February 1962.

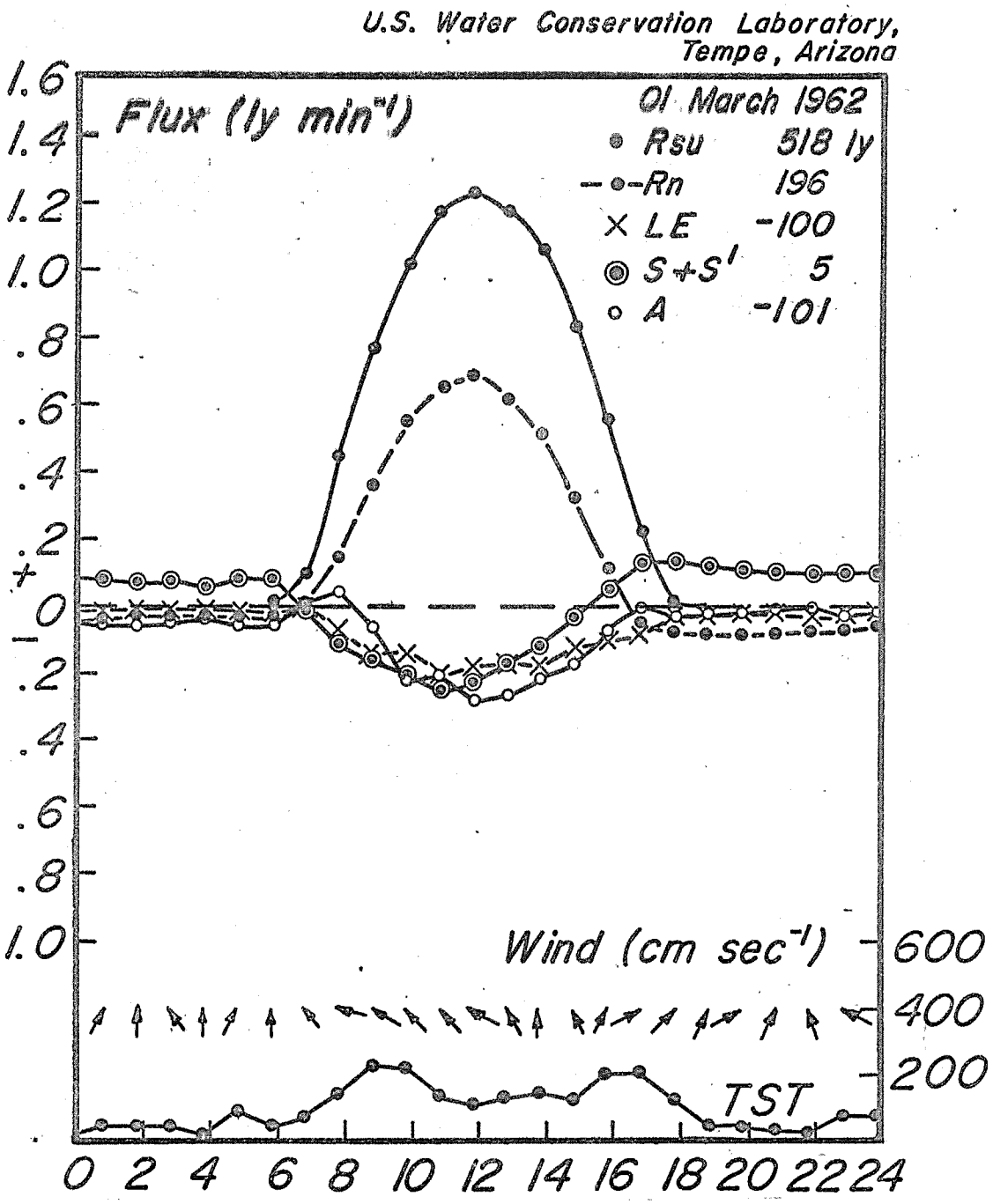

Figure 5. Hourly energy balance and wind movement over a bare, dry surface on 1 March 1962.

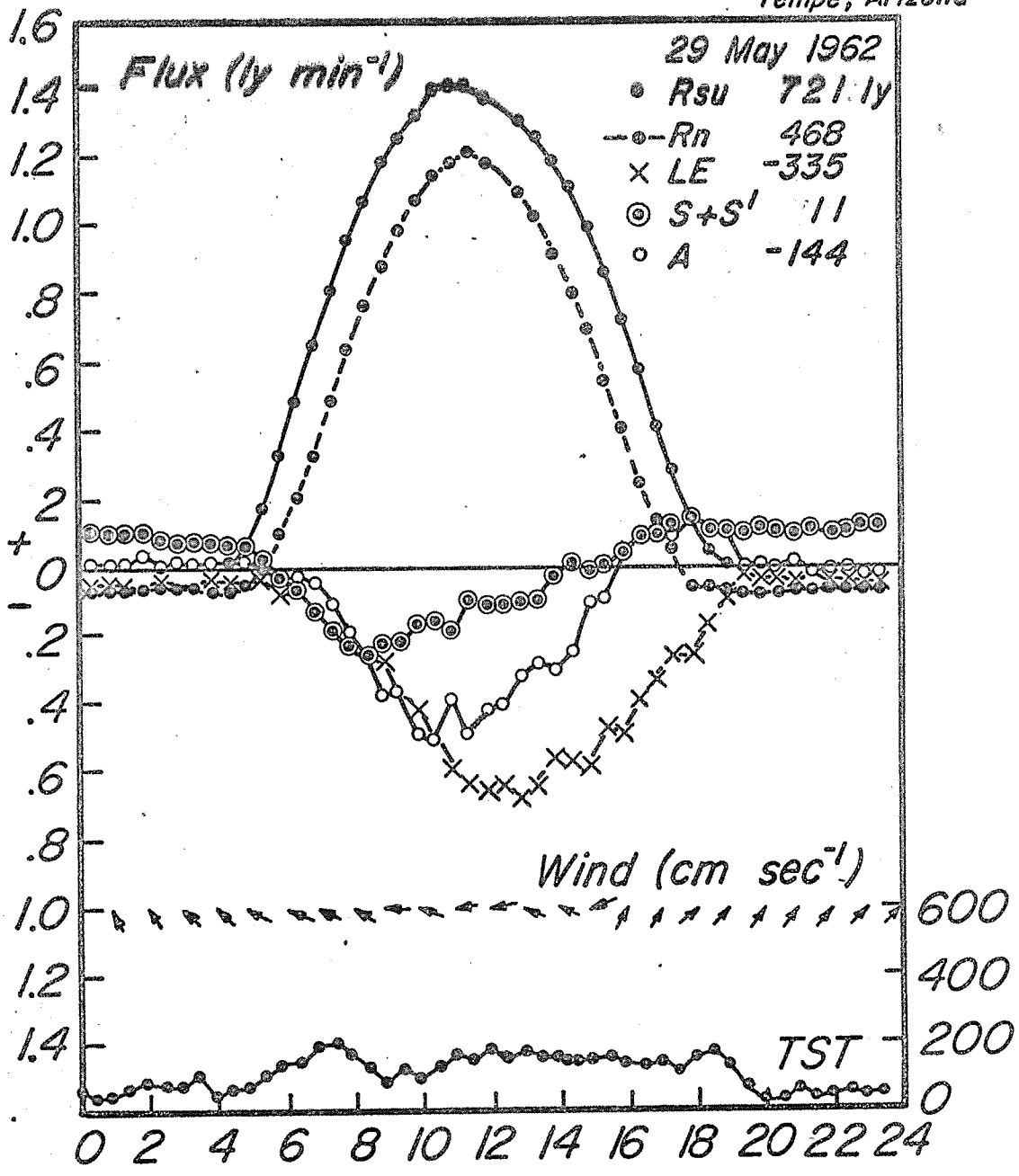

Figure 6. Hourly energy balance and wind movement over a wet surface with 5-cm high emerging Sudangrass on 29 May 1962.

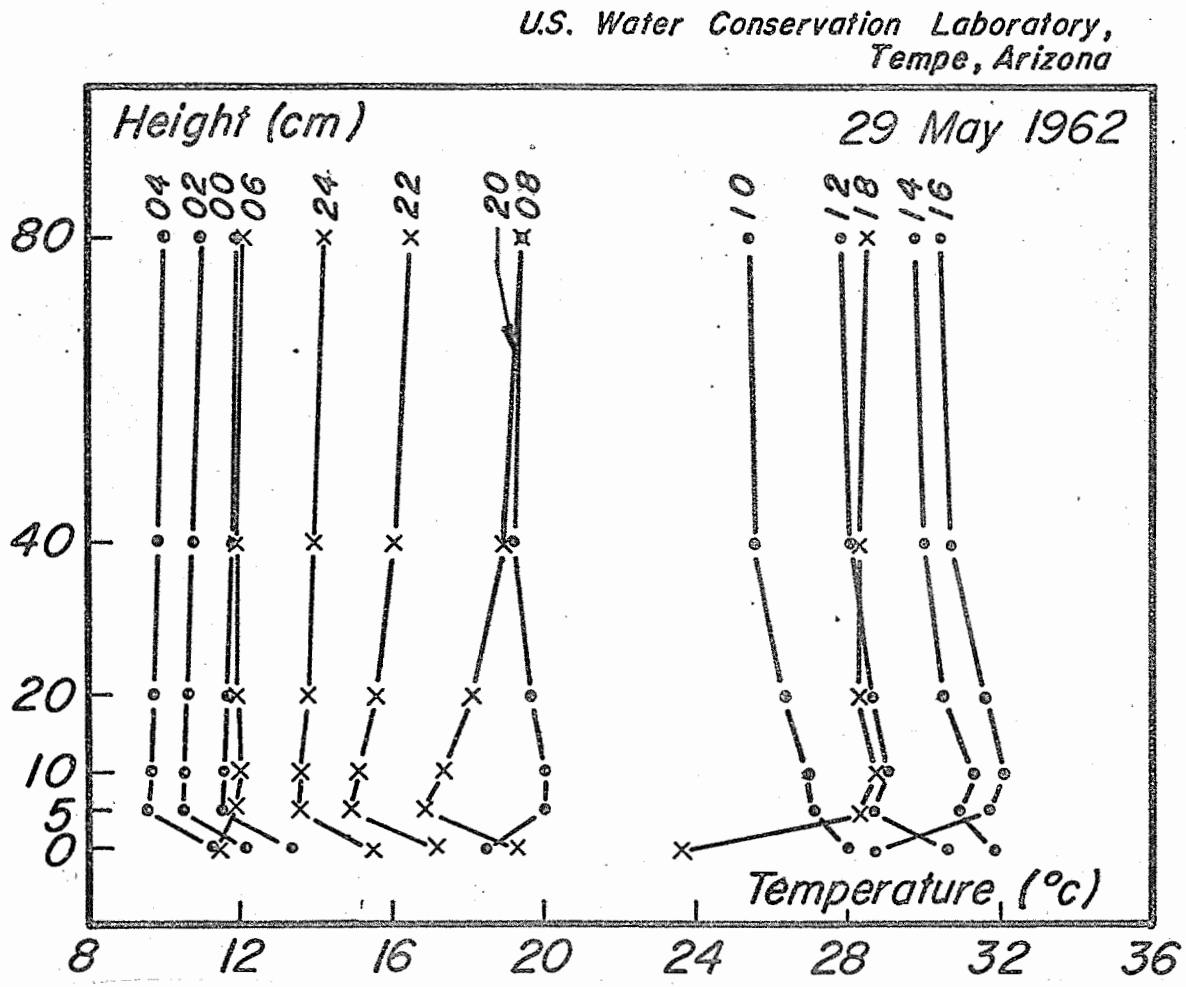

Figure 7. Temperature profiles over a wet surface on 29 May 1962.

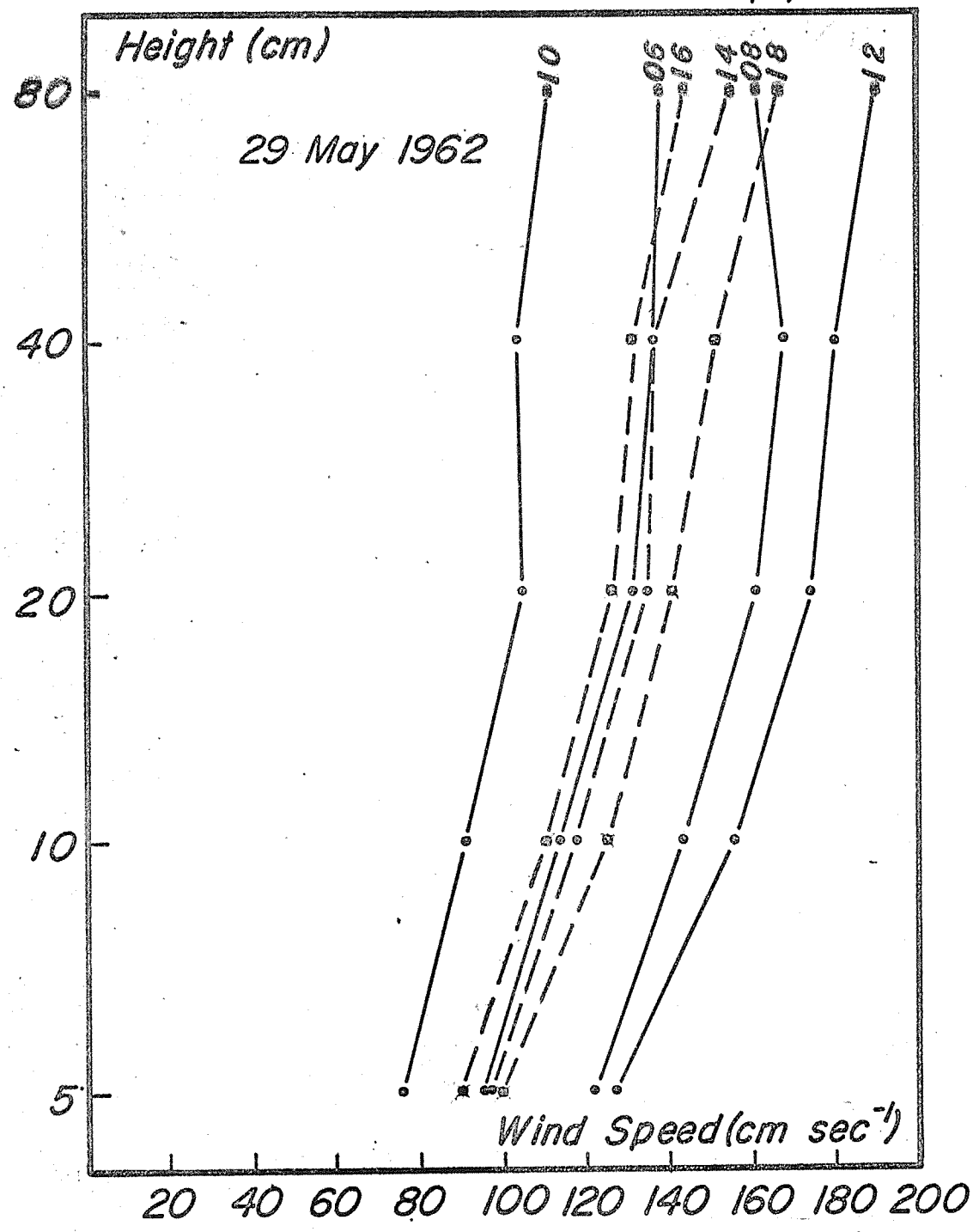

Figure 8. Wind profiles obtained on 29 May 1962.

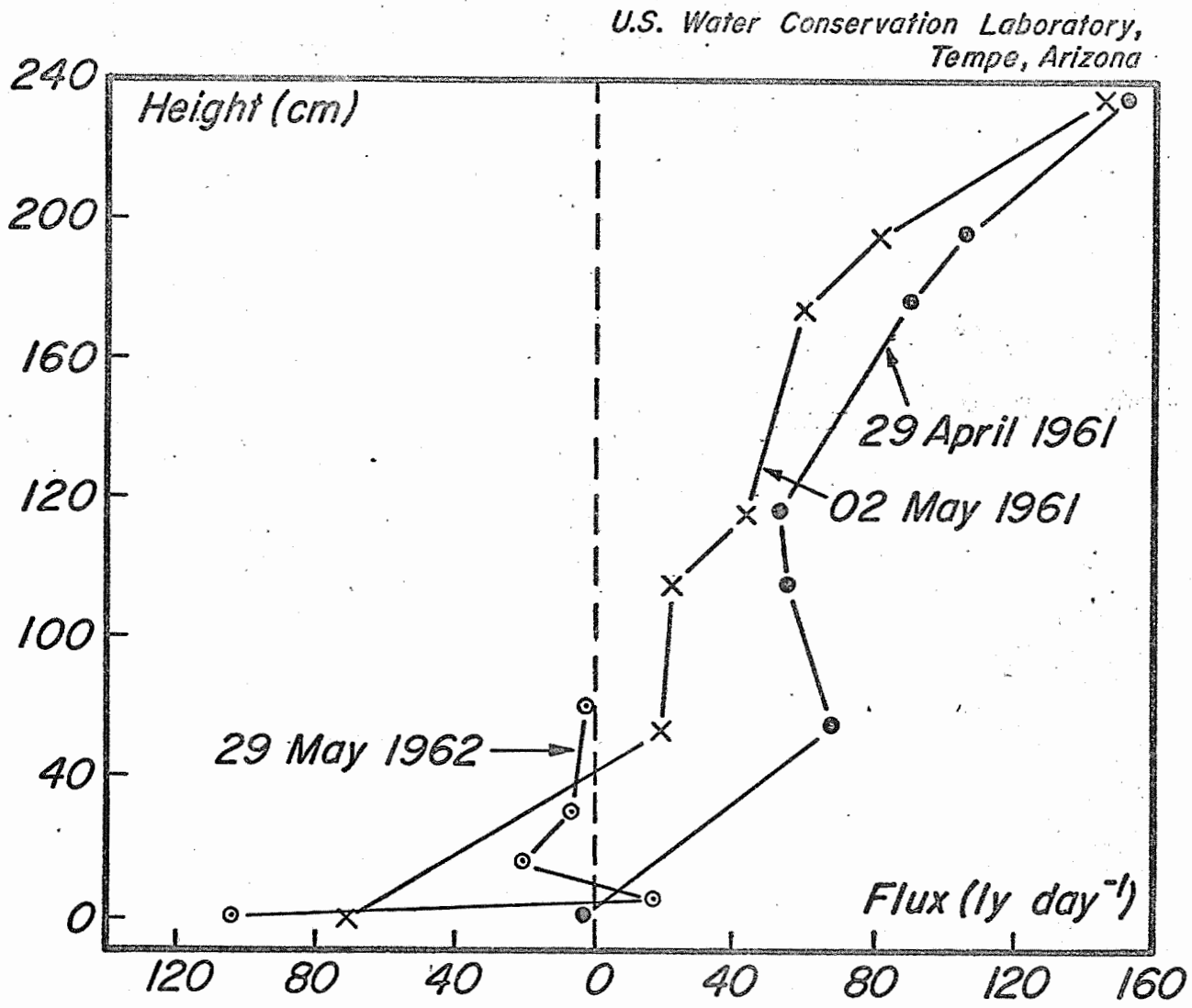

Figure 9. Sensible heat flux as measured and calculated at different elevations on 29 April 1961 and 29 May 1962.

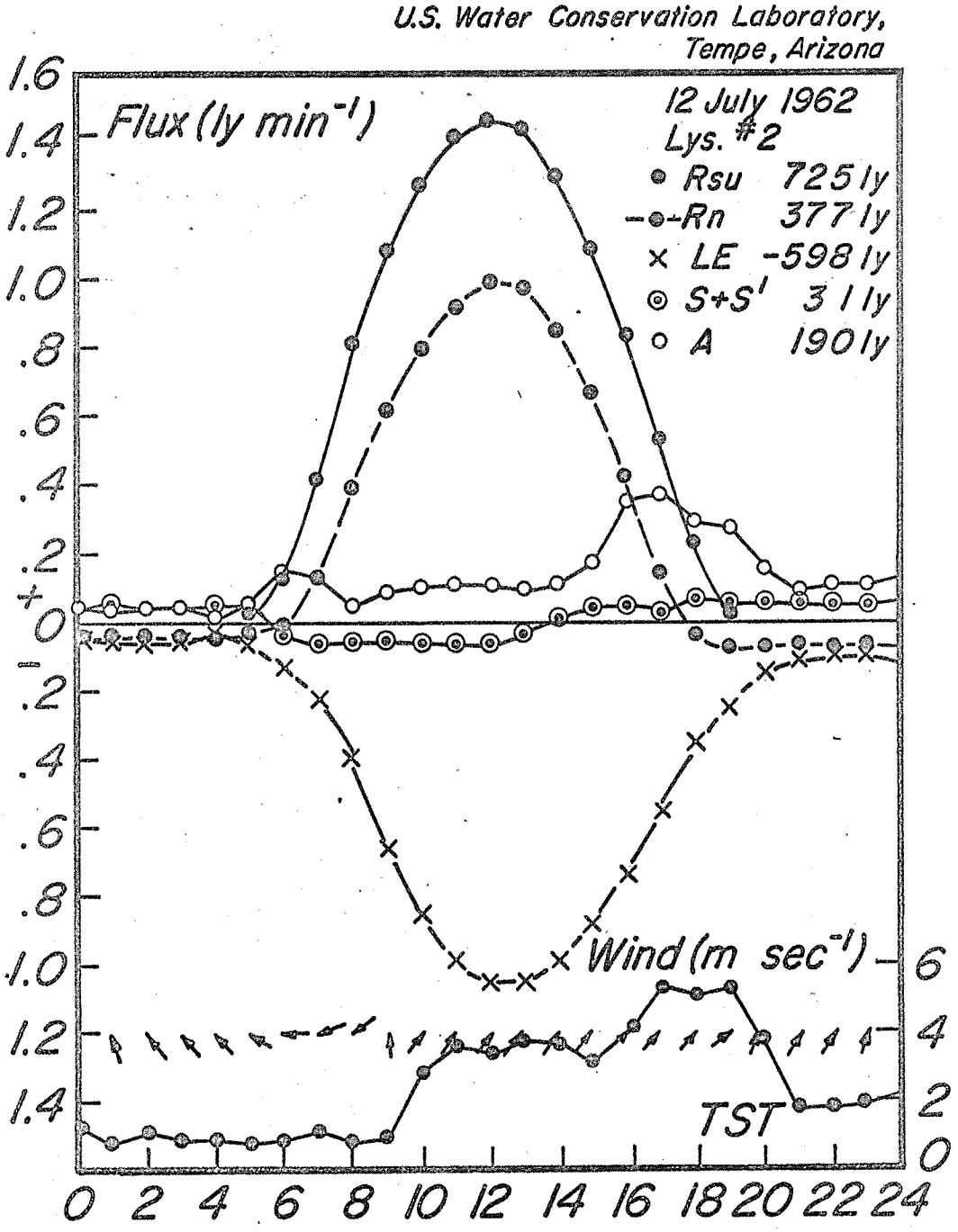

Figure 10. Hourly values of the components of the energy balance equation, solar radiation, wind speed and direction measured over Sudangrass 75 cm tall.

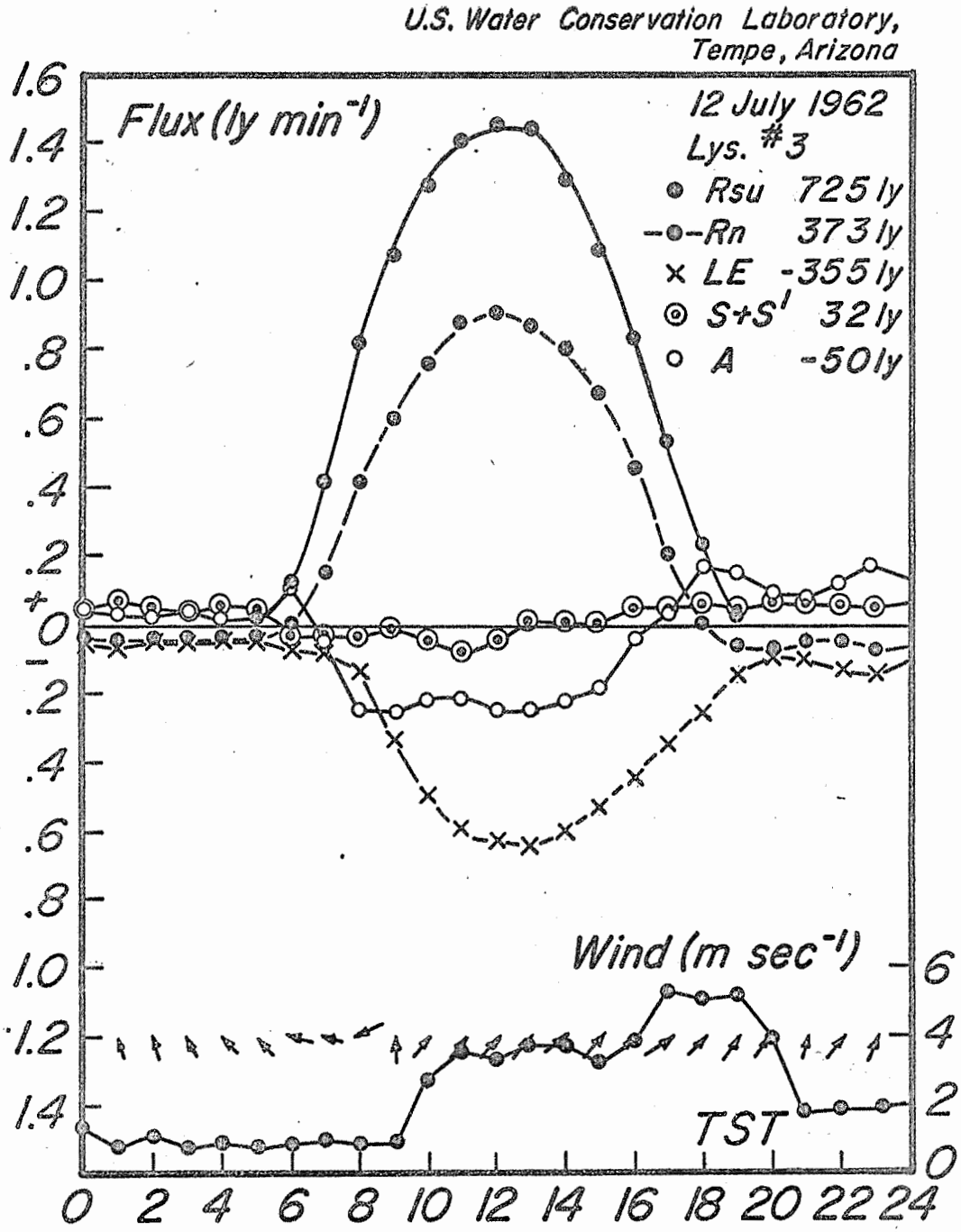

Figure 11. Hourly values of energy balance components, solar radiation, wind speed and direction measured over Sudangrass 140 cm tall.

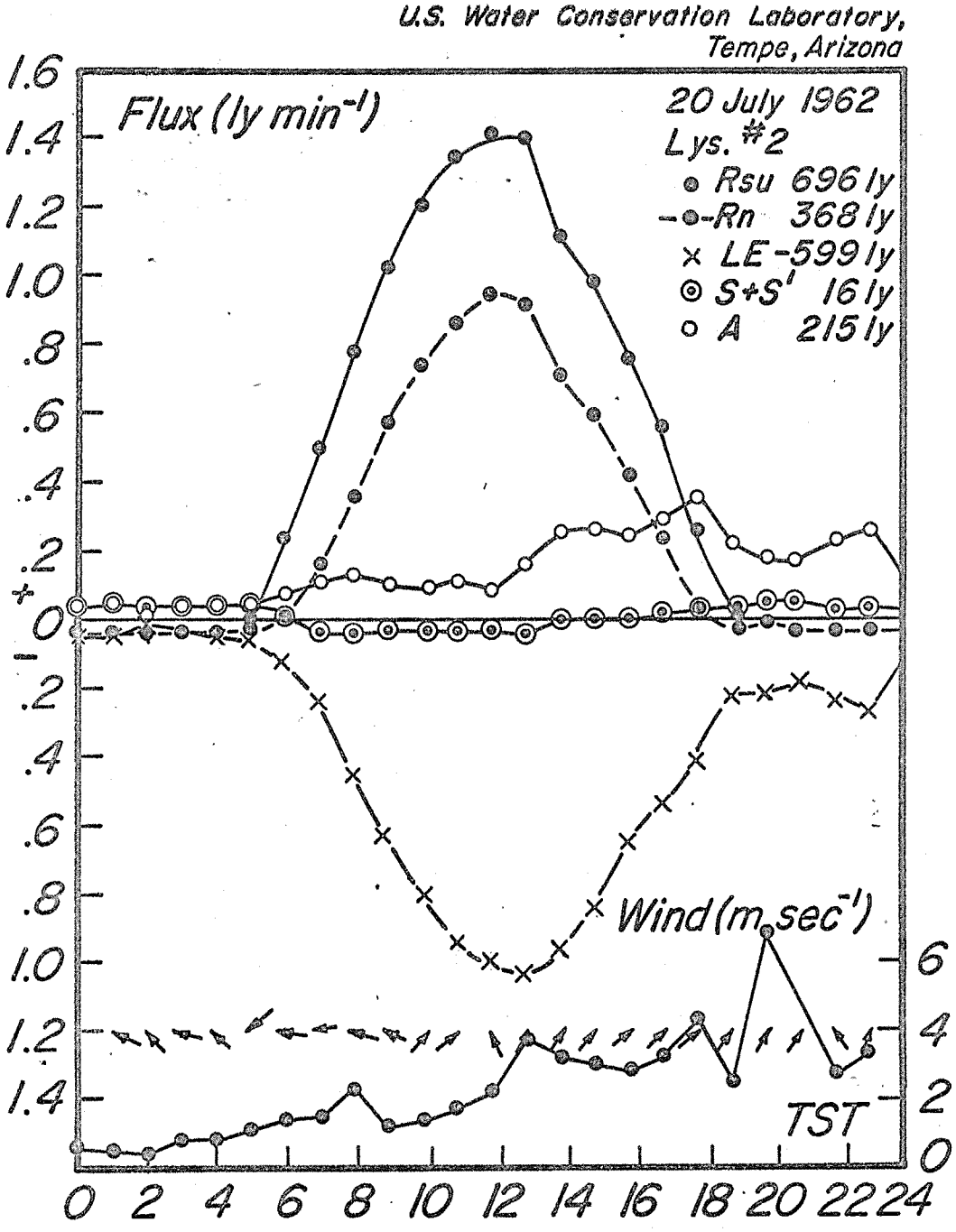

Figure 12. Hourly components of the energy balance, solar radiation, wind speed and direction measured over Sudangrass 100 cm tall.

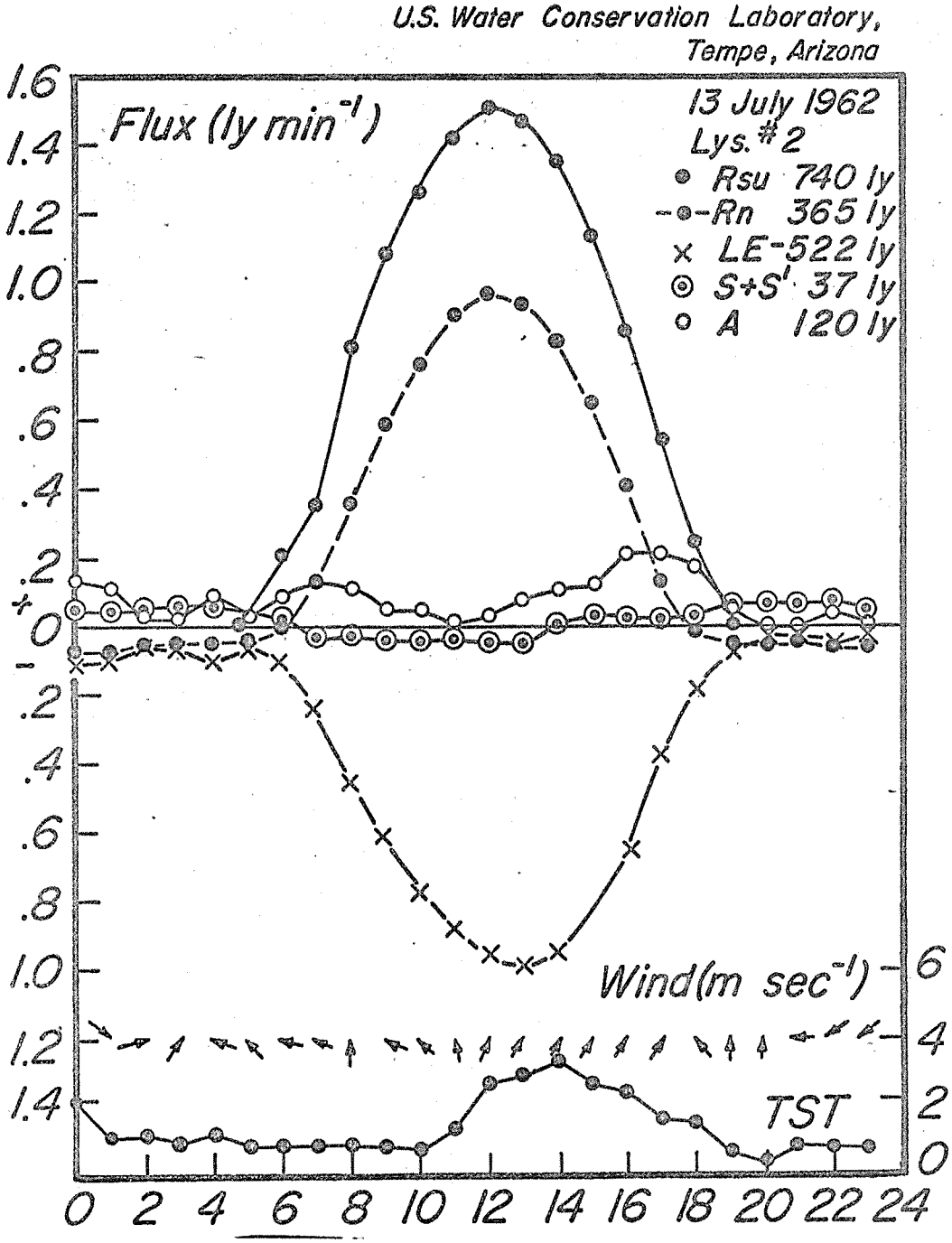

Figure 13. Hourly components of the energy balance, solar radiation, wind speed and direction measured over Sudangrass 75 cm tall.

SUPPLEMENT: A. EVAPORATION AND PERIODIC IRRADIATION

INTRODUCTION:

Energy for evaporation is supplied by radiative, convective, and conductive transfer. Each of these components has its own typical rapidity, the first being instantaneous, the second with transfer coefficients of the order of decimeters squared per second, and the latter on the order of a fraction of a centimeter squared per second.

The relative significance of each transfer process, and quantitatively, the transfer coefficients, can be studied by periodically turning one of the sources of energy off and on. In the case of the earth's surface, this can be done conveniently during the daytime and clear weather by shading.

PROCEDURES:

A preliminary experiment was carried out in Tempe, Arizona, on 14 and 16 August 1962, on a field of irrigated Sudangrass that had a height of about 50 cm. The field was approximately 100 by 100 meters, and three precision lysimeters were available to measure evaporation. The lysimeters were 1 m^2 in size, and a shade was constructed of sheet metal about 1.3 by 1.3 meters, suspended above one lysimeter at a height of about 4 meters. Two lysimeters had a reasonably good stand of grass, one (#2) was selected to be shaded, the other (#3) was used as a control. The shade would, between 1000 and 1500, cover the entire lysimeter plus a border of about 10 cm. The shade could be quickly pulled over the lysimeter and was adjusted by a rope to keep pace with the moving sun, the operator being sufficiently removed from the shaded site.

Evaporation was measured by recording the lysimeter weight to the nearest 0.01 mm every five minutes in triplicate. Smoothing and interpolation of the weight-loss curves gave reasonably accurate figures for the evaporation rate over 5-minute periods. The error is estimated at 0.04 mm hr^{-1}, or 5 percent of prevailing rates (0.8 mm hr^{-1}).

Net radiation was measured with miniature instruments over each lysimeter to the nearest 0.02 ly min^{-1}, as was soil heat flux immediately below the surface. Thermocouple thermometers were imbedded in the soil surface and mounted at the crop surface, which was approximately 50-cm high. Radiation shielding of the latter was not required.

Windspeed was measured at 20 and 200 cm over the crop surface with Casella anemometers. Solar radiation was measured with a Kipp solarimeter.

All variables were recorded every minute on punched paper tape during the experiment. On 14 August, the land had been irrigated 6 days earlier, but the crop was still well supplied with water. The experiment was run from 1020 to 1520 under perfect weather conditions, light winds, and temperatures around 40°C. The shade was "on" from 1045 to 1115, 1145 to 1245, and 1345 to 1415. During this period solar radiation varied between 1.0 and 1.3 ly min^{-1}. True noon occurred at 1228.

On 15 August, the field was irrigated with about 100 meters of water and the experiment repeated on 16 August during the same time period and with the same "shading" schedule. Some scattered cloudiness occurred until 1110, thus invalidating the first part of the data. For the remainder of the day the weather was the same as on 14 August.

On the control lysimeter (#3), net radiation was the same on both days, varying from 0.65 to 0.95 ly min^{-1} during the measurement period. Evaporation had a maximum value of 0.80 mm hr^{-1} on 14 August and 0.95 mm hr^{-1} on 16 August. Air temperature at crop height had a maximum of 40°C on 14 August and 39°C on 16 August. Surface temperature showed a maximum of 42°C on 14 August and 39°C on 16 August. Soil heat flux was typically about 0.06 ly min^{-1} on both days during the experimental period. Thus we conclude that on 16 August conditions resulting from the recent irrigation with 100 mm of water would tend to promote greater downward energy flow as sensible heat from the air during the latter part of the day.

RESULTS AND DISCUSSION:

Figure 1 and 2 summarize, by 5-minute periods, the effects of shading on the energy balance components R_n, S, LE, and A on 14 August. Also portrayed are windspeed at 2 meters above the crop and the temperature difference of the air above the shaded and unshaded lysimeter, both quantities having a bearing on advection of sensible heat to the shaded lysimeter. The latter information is shown for 16 August in Figure 2.

Results on both days were quite similar except that A was greater on 16 August than on 14 August (see A_3 in both figures). Since 14 August was a more complete series of measurements, reference is made primarily to Figure 1 giving the data for 14 August.

Response to shading of net radiation is immediate, a balanced value of R_n in the shade occurring after about 5 minutes. Response to eliminating the shade takes place in 1 minute. The temperature of the air at the crop surface and the temperature differential between shaded and unshaded areas were also established with a lag of no more than 5 minutes. The temperature record is more variable and conclusions less certain.

The soil surface temperature reacts more slowly, requiring about 15 minutes to become near-stationary. Also, evaporation responds more slowly to shading, the first 5-minute period evidencing no effect and the final value established only after 15 to 20 minutes, as clearly shown in the second shading period. Since soil heat flow shows also a fast response with less than a 5-minute lag, A_2 reflects changes in E. From a "normal" value of about -0.15 ly min^{-1}, A_2 reverses in sign to be first as high as +0.5 ly min^{-1}, and then settles to a value of about +0.2 ly min^{-1}. After 1400, all values of A become more positive, but the effects are the same.

Windspeed was low for most of the day, between 1 and 1.5 m sec^{-1}.

DISCUSSION:

The data clearly indicate the subordinate role of sensible heat exchange in the evaporation process, in spite of the fact that the area studied was only 1 m^2 in size. This is further evidenced from

the occurrence of air temperatures 4° to $5^{o}C$ lower over the shaded lysimeter, as compared to its surroundings.

In view of the rapid response of radiation, air temperature, and soil heat flux, the question arises why evaporation does not respond faster also. This anomaly appears very clearly when A is computed by 5-minute periods (see Figure 1). The sensible heat flow (A) shows--at first--an abnormal value which is not in accord with the air-temperature differential between the shaded area and its environment.

One could suppose that the anomaly in behavior of A is the result of neglecting a storage factor in the energy balance. The weight of the crop is--very roughly--estimated at 1 kg m^{-2} and its change in temperature, at $4^{o}C$, representing an energy storage change of 0.4 cal cm^{-2}. The deviation of A from a "normal" pattern, that is extrapolation of the equilibration value to the time of putting on or removing the shade, was estimated at around 3 to 4 cal cm^{-2}. Thus, crop storage of heat is not a sufficient explanation.

An additional and more adequate explanation is in the fact that the heat-flux plates were at the surface, and just at that location no evaporation took place, resulting in an initial underestimate of the soil heat flux when shading, and an initial overestimate when unshading. The nature of the soil surface temperatures supports this view by implying that right after shading, the true soil heat flux becomes rapidly positive and declines close to zero after 15 to 20 minutes, and similarly, right after unshading, becomes rapidly negative and then settles to a larger but still negative value.

The nature of the plant cover and the soil surface was such that as much evaporation could have occurred as transpiration.

Uniformity of cover and proper exposure of instruments left much to be desired in this experiment, and a repetition under more stringent conditions is necessary. Nevertheless, one may draw two conclusions: first, changes in net radiation are rapidly reflected, with a lag of 5 to 10 minutes in the evaporation rate from a vegetated

surface; second, the horizontal advection of heat for evaporation from an environment injecting around 0.2 cal cm^{-2} min^{-1} into the air averaged about 0.25 cal cm^{-2} min^{-1} over a shaded surface of 1 m^2. This illustrates the relative ineffectiveness at low wind speeds of advection in comparison to radiative transfer.

The entire picture is clouded by the fact that the evaporation, and the radiation to sensible heat transfer took place throughout a 50-cm-deep layer of transpiring leaves and at a moist surface. A more conclusive study could be carried out with a wet and bare soil.

SUMMARY AND CONCLUSIONS:

An experiment was conducted to study the effect of alternately excluding and admitting direct solar radiation around noontime to a 1 m^2 area of Sudangrass, coinciding with one of the weighing lysimeters. The effect of shading on the energy balance and on soil and air temperature was measured.

The experiment was preliminary and inadequate in several regards, but some important effects could be established. First, the response of evaporation to sudden changes in radiation was rather fast, taking about 15 to 20 minutes. The lag is thought to arise from heat storage effects in the soil and--to a lesser degree--in the crop. This conclusion is not adequately supported by data.

Further, the small area extracted heat from its surroundings at a rate of about 0.2 ly min^{-1} with surface temperatures some 4° to $5^{o}C$ less than that of the environment.

The experiment demonstrated the feasibility of measuring 5-minute values of the evaporation rate and the informative value of a shading treatment. The experiment will be repeated under conditions that will produce more definite information.

PERSONNEL: C. H. M. van Bavel, L. J. Fritschen, W. Reeves.

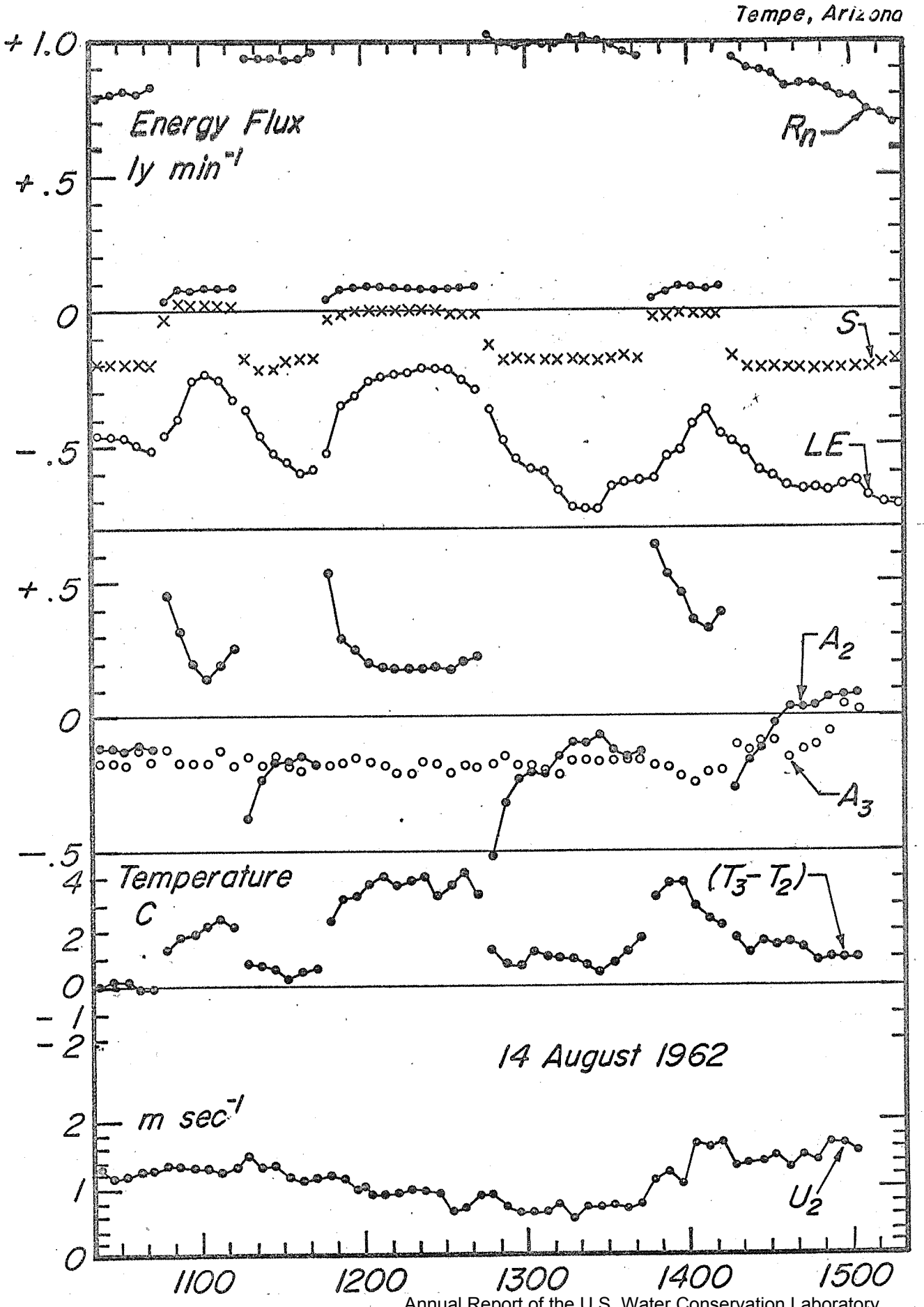

Figure 1. Energy balance, sensible heat flow, air temperature differential and wind movement on shading experiment, 14 August 1962.

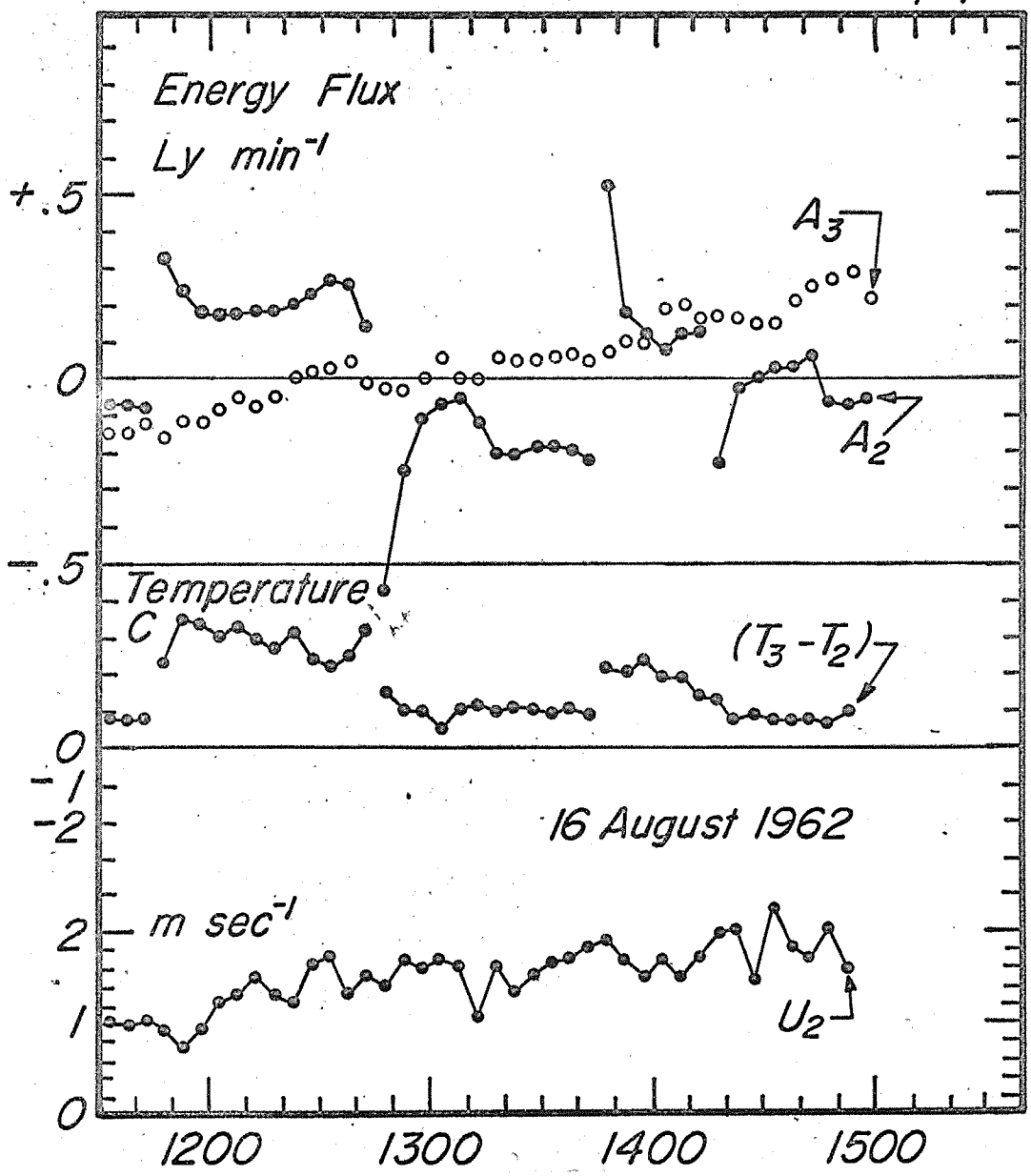

Figure 2. Sensible heat flow, air temperature differential and wind movement on shading experiment, 16 August 1962.

SUPPLEMENT: B. EXPERIMENTAL EVALUATION OF TRANSPORT MODELS OF LATENT AND SENSIBLE HEAT OVER IRRIGATED SURFACES.

List of symbols and dimensions.

A = sensible heat flux in air [cal cm^{-2} min^{-1}]

D = diffusivity of water vapor in air [= 0.249 cm^2 sec^{-1} at 25°C, 1000 mb]

E = evaporative flux [g cm^{-2} min^{-1}]

K_h = eddy diffusivity for sensible heat [cm^2 min^{-1}]

K_m = eddy diffusivity for horizontal momentum [cm^2 min^{-1}]

L = latent heat of vaporization [cal g^{-1}]

P = air pressure [mb]

R_n = net radiation [cal cm^{-2} min^{-1}]

S = soil heat flow [cal cm^{-2} min^{-1}]

S' or W = change in heat storage of the layer of soil or water, respectively, above the heat-flow transducer [cal cm^{-2} min^{-1}]

T = temperature [°C]

U = wind speed [cm sec^{-1}]

U_* = friction velocity [cm sec^{-1}]

Z = height [cm]

Z_0 = aerodynamic surface roughness [cm]

c_p = specific heat at constant pressure [cal g^{-1} $°C^{-1}$]

e = vapor pressure [mb]

k = von Karman's constant

β = Bowen ratio

δ = thickness of the laminar layer [cm]

κ = molecular diffusivity for heat [0.208 cm^2 sec^{-1} at 25°C, 1000 mb]

ρ = density of air [g cm^3]

Subscripts.

w = water

a = air

INTRODUCTION:

Agricultural use of water in arid lands is scrutinized more closely because a limited supply of water must be shared with an increasing population and industry. Short-period determinations of evaporation, transpiration, and related atmospheric processes are required to obtain a better understanding of complex soil-plant-atmospheric relationship, and, ultimately, to make more efficient use of the water that is available.

Lysimetric measurement of soil-moisture depletion by weighing is undoubtedly the best method to routinely and accurately determine evapotranspiration for short periods (15 minutes or longer). Lysimeters, however, have limited use due to immobility, time required for establishment of an installation, and the size required for certain plants. Micrometeorological methods such as the energy balance or the aerodynamic technique can be used to estimate evapotranspiration from periods of one hour or less (King, 1961). Micrometeorological methods have several distinct advantages: they do not require alteration of the surface, are not limited to a particular crop or surface, can be employed with a great deal of mobility, and can provide information on the fluxes of sensible heat and carbon dioxide. The main limitations are the instrumentation and the basic assumptions of the methods, which may not be met under given conditions.

The most promising research avenue appears to be the verification of instrumentation and basic assumptions of the micrometeorological methods with a lysimeter installation under conditions that exemplify agricultural use of water.

EXPERIMENTS AND METHODS

Research completed to date combining lysimetric and micrometeorological data is limited to evaporation from bare-soil and free-water surfaces. The condition of the field and the lysimeters during the experiments is shown in Table 1.

TABLE 1. Condition of the Experimental Field and the Lysimeters during Experiments

Date	Experimental Field	Lysimeters
1961		
April 25-26	Flooded, 2 to 10 cm of water	Free water*
April 28-30	Wet bare soil	Wet bare soil
May 1-2	Drying bare soil	Drying bare soil

*The lysimeters were covered with two layers of 0.15-mm polyethylene film and about 2 cm of water impounded on top.

During the experiments the evaporative flux (LE) was determined by multiplying the change in weight indicated by each lysimeter and the appropriate heat of vaporization.

Net radiation was measured with a miniature net radiometer located at 8 cm over the center of each lysimeter. At 8-cm height, the lysimeter surface was 96 percent of the bottom-view factor of the net radiometer. Solar radiation was measured for reference with an Eppley pyrheliometer, Model 50.

Soil heat flow was measured in each lysimeter with a Beckman and Whitley heat-flow transducer, Model ST-201-1. The heat-flow transducers were located immediately beneath the plastic film on 25 and 26 April, and 2 cm below the soil surface from 28 April to 2 May.

The change in heat storage of the layer of soil or water above the heat-flow transducer was calculated using the change in water and soil temperatures. The water or "surface" soil temperatures were measured with three parallel thermocouples in each lysimeter, while the temperature at the heat-flow transducers was measured with single thermocouples.

Air vapor pressure was determined at 155 cm (150 cm on 25 and 26 April) from measurements made with an Aminco electrical hygrometer, Model 15-2001. The vapor pressure of the water or soil was determined using the water or "surface" soil temperature.

Errors of estimate of the micrometeorological elements are given in Table 2.

TABLE 2. Errors of Estimate of the Micrometeorological Elements

Element	Error
Evaporative flux	0.02 ly min^{-1}
Net radiation	0.02 ly min^{-1}
Soil heat flow	0.02 ly min^{-1}
Temperature: absolute, recording	0.45°C 0.16°C
Wind speed	15 cm sec^{-1}
Air vapor pressure	0.6 mb

Air temperature and wind speed were measured in the center of the field at 35, 75, 155, 315, and 635 cm. (The heights were 30, 70, 150, 310, and 630 cm on 25 and 26 April due to the water layer.) Air temperatures were measured with 24-gage thermocouples supported in sensors having two radiation shields on top and bottom of the thermocouple. Wind speeds were measured with sensitive anemometers manufactured by Casella & Company.

METHODS OF DATA ANALYSIS:

Calculations of the fluxes of water vapor and sensible heat using micrometeorological models may be evaluated by comparing the results with the evaporative flux obtained from the lysimeters and the sensible heat flux obtined from solution of the energy balance equation.

The energy balance equation at the soil or water surface is given by (1):

$$R_n + S + (S' \text{ or } W) + LE_0 + A_0 = 0 \qquad (1)$$

The air-soil or air-water interface is considered to be the reference plane of zero heat capacity. All heat flows to the reference plane are positive, and all heat flows away from the reference plane are negative. The subscript "0" indicates that

the flux is considered at the surface. Net radiation was measured at 8 cm, but this is not considered to be appreciably different from the net radiative flux at the surface.

Bowen (1926) combined a ratio of sensible and latent heat with the energy balance equation to obtain an equation to estimate the evaporative flux from a water surface. Bowen's equation in our notation is given by

$$LE = -(R_n + S)/(1 + \beta) \tag{2}$$

where

$$\beta = \frac{(929)\rho c_p P(T_w - T_a)}{L\ (e_w - e_a)} \tag{3}$$

Sensible heat flux over a water surface may also be estimated by Bowen's method

$$A = -(R_n + S)/[1 + (1/\beta)] \tag{4}$$

Since vapor pressure was measured at one level, only aerodynamic models for estimating the evaporative flux, requiring one-level observations, could be tested. Sverdrup (1937) developed such an equation, which he later modified in 1946. However, Marciano and Harbeck (1954) obtained better results with Sverdrup's 1937 equation. Therefore, it was chosen to be tested and in our notation is

$$E = \frac{(60)(0.623)\rho k U_* (\bar{e}_Z - \bar{e}_0)}{P\left[\ln \frac{Z_1 + Z_0}{\delta + Z_0} + \frac{k\delta U_*}{D}\right]} \tag{5}$$

Sheppard (1958) proposed an alternate approach to Sverdrup's (1946) development, (equation 6)

$$E = \frac{(60)(0.623)\rho k U_* (\bar{e}_Z - \bar{e}_0)}{P\left[\ln \frac{kU_* Z}{D}\right]} \tag{6}$$

Sufficient air temperature measurements were made to test gradient and one-level models for estimating sensible heat flux. Sheppard's (1958) one-level equation for sensible heat flux, analogous to equation 6, is

$$A = \frac{(60)\rho c_p k U_* (T_Z - T_0)}{\ln \frac{kU_* Z}{K}} \tag{7}$$

Under adiabatic conditions, equation (8), as formulated by Lettau (1957) among others, using gradients of wind speed and air temperature may be used to estimate the flux of sensible heat

$$A = \frac{(60)\rho c_p k^2 (U_2 - U_1)(T_2 - T_1)}{\left[\ln\left(\frac{Z_2}{Z_1}\right)\right]^2} \cdot \frac{K_h}{K_m} \tag{8}$$

RESULTS AND DISCUSSION:

The energy balance equation (1) may be solved for A_0 by inserting measured values of R_n, S, S' or W, and LE. Examples of the diurnal variations of the components of the energy balance

equation averaged for two locations over shallow free-water and wet bare-soil surfaces are shown in Figures 1 and 2. The daily totals of the sensible heay flux indicate that energy was used to heat the air over the water surface on a 24-hour basis, but not over the wet soil surface. The hourly values of A_0 on 25 April are at least qualitatively verified by the air-water temperature differences, as shown in Figure 3, thus supporting the entire energy balance evaluation. According to the convention used, the sensible heat flux should be positive when the air temperature is greater than the water temperature, and vice versa.

Hourly values of the evaporative flux over the water surface calculated by Sverdrup (5), Sheppard (6), and Bowen (2) equations are shown in Figure 4 along with values determined using the lysimeters. The nighttime values of the calculated fluxes agree with the lysimetric values within the margin of error, which is relatively large.

During the daylight period, Sverdrup's equation seriously underestimates the flux. The evaporative flux calculated by Sheppard's and Bowen's equations appears to be out of phase with lysimetric values of the flux; that is, Bowen's equation precedes--and Sheppard's equation lags behind--the direct measurement (0600 to 1400[1/], 25 April 1961). After 1400, the phase relationships are obscured due to an increase in wind speed (Figure 1). The results obtained from Bowen's equation appear to be in phase with net radiation which is the principal term in that equation, and the results from Sheppard's equation appear to be in phase with the vapor-pressure gradient. Similar results were obtained on 26 April 1961.

Calculations of the evaporative flux were also made for the wet bare-soil surface, assuming that the vapor pressure at the surface equaled the saturation vapor pressure at the "surface" soil temperatures. The results obtained for 29 April 1961 are shown in Figure 5. These results are similar to the results obtained over water 25 April 1961,

---

1/ All times are true solar time.

in that Sverdrup's equation tends to underestimate the flux, while Sheppard's and Bowen's equations give reasonable estimates but with the same, more pronounced, phase relationships.

Daily totals of calculated and measured evaporative fluxes, and deviations from lysimetric values for 25, 26, and 29 April 1961, are shown in Table 3.

TABLE 3. Daily Totals of the Evaporative Flux as Measured and Calculated by Equations (2), (5), and (6)

	April 1961					
	25		26		29	
	ly day^{-1}	% D*	ly day^{-1}	% D*	ly day^{-1}	% D*
Lysimeters	-351		-308		-413	
Sverdrup (5)	-197	-44	-183	-36	-262	-37
Sheppard (6)	-334	-2	-305	-1	-406	-1
Bowen (2)	-379	+5	-341	+10	-387	-6

* Percent deviation from the evaporative flux determined with the lysimeters.

Sverdrup's equation underestimates the evaporative flux from 36 to 44 percent. Sheppard (1958) stated that Sverdrup's (1946) equation may give values up to 50 percent from those given by (6). Apparently, this is also true for his 1937 equation. Sheppard's equation estimated the evaporative flux better than Bowen's equation, when daily totals are considered. Hourly values obtained with both methods were in error due to the phase differential.

The most notable fact evident from these data is that wet, bare soil may be treated with the same methods as a free-water surface; that is, the models used estimated the evaporative flux from a bare-soil surface and a free-water surface with the same accuracy. A similar analysis of the data obtained on 1 and 2 May showed that the methods did not apply, as would be expected from the method of determining the vapor pressure. However, these same models could be used over a cropped surface when soil water is not limiting.

Tanner (1960) has successfully used a modification of the Bowen equation over a cropped surface.

The results of hourly calculations of the sensible heat flux in air by the energy balance (1), Sheppard's (7), Bowen's (4), and the aerodynamic (8) equations over water and bare-soil surfaces are shown in Figures 6 and 7, respectively. Over a free-water surface Sheppard's and Bowen's equations gave a fair estimate of sensible heat flux, within 0.1 ly min^{-1}. Over a bare soil, neither model seems applicable. For neither case did the aerodynamic equation show any degree of agreement.

Daily totals of calculated hourly sensible heat flux in air over water and soil surfaces are listed in Table 4, which include the results of 2 May for a dry surface.

TABLE 4. Calculation of the Sensible Heat Flux by Equations (1), (4), (7), and (8)

		April 1961			May 1961
		25	26	29	2
		ly day^{-1}			
Energy balance (1)		-73	-84	1	-69
Bowen (4)		-45	-37	22	--
Sheppard (7)		-34	-27	-44	4
Aerodynamic (8)	1, 2	-3	-2	71	-25
	1, 3	-1	10	57	21
	2, 3	6	19	54	45
	1, 4	18	30	90	60
	2, 4	33	64	106	82
	3, 4	84	133	173	146
	1 = 30 cm, 2 = 70 cm, 3 = 150 cm, 4 = 310 cm				

The results from Bowen's and Sheppard's equations over the water surface (25 and 26 April 1961) were of the same sign as the results from the energy balance equation. This statement cannot be made with

respect to the results from the aerodynamic equation. They were of the opposite sign, and increased in magnitude with height. Similar to the hourly values, no model seemed to fit the situation over bare soil. It is interesting that a combination of Sheppard's estimate of the evaporative flux and the energy balance equation gives better results than Sheppard's direct estimate of sensible heat flux.

The data and results presented should be considered as indicators for future research. The accuracy of the calculations of the fluxes of sensible and latent heat may have been improved if the measurements were made at lower heights and if the variables had been sampled spatially. Pasquill (1949) stated that wind velocity and humidity gradient data should be confined to the first 50 cm above the surface. Bryson (1955) pointed out the need for spatial sampling during periods of light winds when vertical convection cells exist. More frequent sampling or complete integration of the elements would also increase the accuracy. However, any increase in accuracy of measurement would be reflected in all of the equations, consequently would not appreciably change the conclusion that the Bowen and Sheppard equations gave the best estimates.

The nonagreement between the models and the lysimetric evaporative flux or the energy balance sensible heat flux may be due to the basic assumptions used in the models, or in the applicability to the experimental site. Certainly, the fact that Sheppard's equations did not estimate the flux of water vapor and sensible heat with the same accuracy indicates errors in the models or divergence of the fluxes.

SUMMARY AND CONCLUSIONS:

To make more efficient use of the water available to agriculture, knowledge of the short-period evapotranspiration of various crops under different cultural and management practices is required. Micrometeorological methods of estimation of evapotranspiration appear to be the most promising. However, the models and instrumentation should be verified by a lysimeter installation before they can be safely used.

To accomplish this end, three automatic weighing-type lysimeters (sensitive to 0.02 mm of water) were installed at the U. S. Water Conservation Laboratory. A 40-channel data-handling system was also installed to automatically record micrometeorological elements in conjunction with the lysimeters. A second data-handling system was mounted in a self-contained trailer to record the micrometeorological elements in remote areas.

Research completed to date combining lysimetric and sufficient micrometeorological data has been limited to evaporation from bare-soil and free-water surfaces. From this research the following conclusions can be drawn:

(1) The best estimates of the fluxes of water vapor and sensible heat were obtained with Bowen's and Sheppard's equations.

(2) Evaporation from wet bare soil may be estimated with the same models and techniques as evaporation from a water surface.

(3) Calculations of the sensible heat flux with an aerodynamic equation indicate that the flux is not constant with height. Furthermore, the results do not agree with the sensible heat flux at the surface determined by the energy balance equation.

(4) Advection determined by the energy balance equation was usually minor, if occurring at all, even though measurements were made in an area heterogeneous with respect to surface wetness.

REFERENCES:

Bowen, I.S., The ratio of heat losses by conduction and by evaporation from any water surface, Phys. Rev., 27, 779-787, 1926.

Bryson, R. A., Convective heat transfer with light winds, Trans. Am. Geophys. Union, 36, 209,212, 1955.

King, K. M., Evaporation from land surfaces, Proc. Hydrology Symp. No. 2, Evaporation, pp. 55-82, 1961.

Lettau, H. H., Computation of heat budget constituents of the earth/air interface, in: Exploring the Atmosphere's First Mile, 1, pp. 305, Lettau, H. H., and B. Davidson, ed., Pergamon Press, New York, 1957.

Marciano, J. J., and G. Earl Harbeck, Jr., Mass transfer studies. Water-loss investigations: Lake Hefner studies, U. S. Geol. Survey Profess. Paper 269, pp. 46-70, 1954.

Pasquill, P., Some estimates of the amount and diurnal variation of evaporation from a clay land pasture in fair spring weather, Quart. J. Roy. Meteorol. Soc., 75, 249-256, 1949.

Sheppard, P. A., Transfer across the earth's surface and through the air above, J. Roy. Meteorol. Soc., 84, 205-224, 1958.

Sverdrup, H. U., On the evaporation from the oceans, J. Marine Research, 1, 3-14, 1937.

Sverdrup, H. U., The humidity gradient over the sea surface, J. Meteorol., 3, 1-8, 1946.

Tanner, C. B., Energy balance approach to evapotranspiration from crops, Soil Sci. Soc. Proc., 24, 1-9, 1960.

PERSONNEL: Leo J. Fritschen and C. H. M. van Bavel

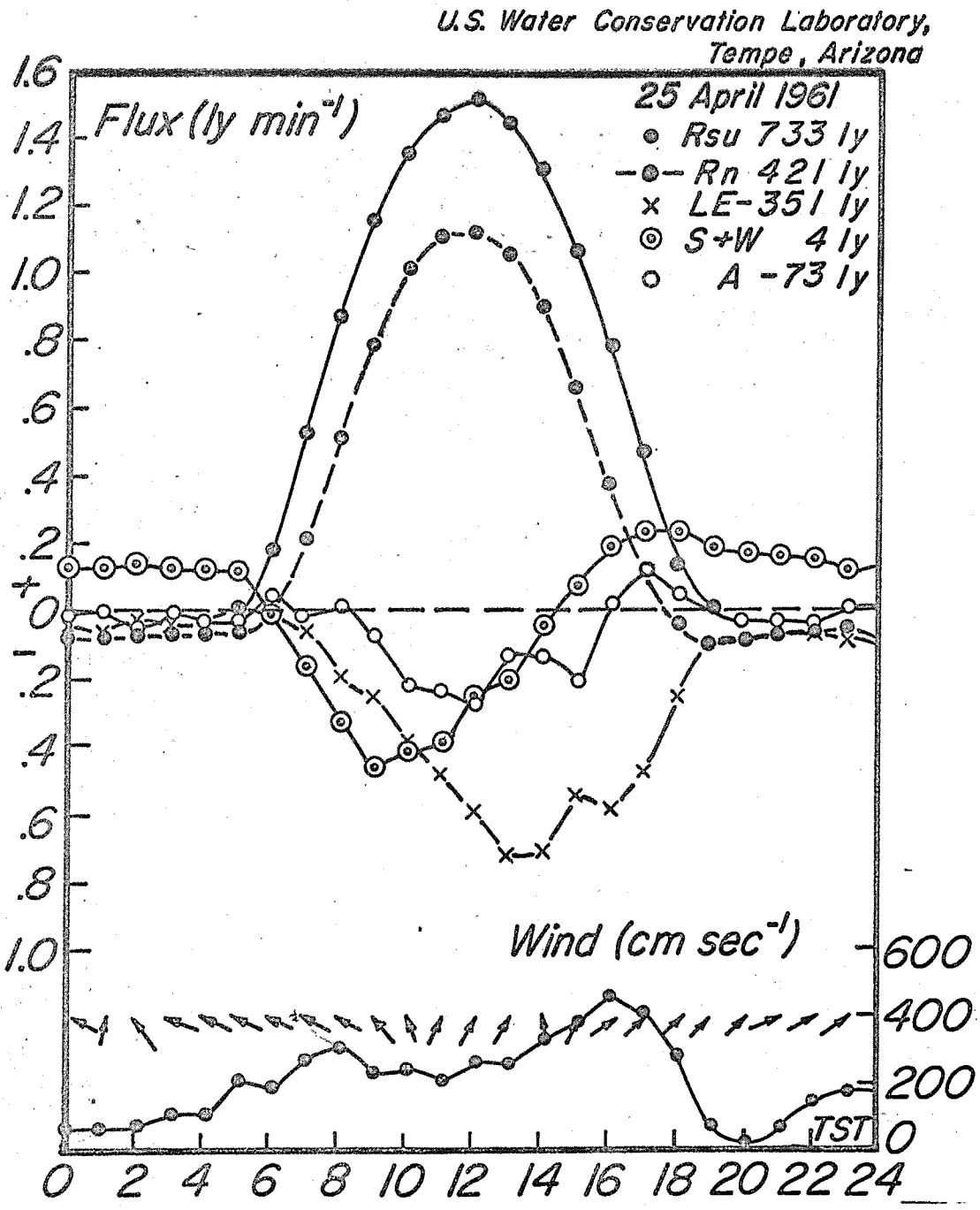

Figure 1. Solar radiation (R_{su}), net radiation (R_n), evaporative flux (LE), soil and water heat flux (S + W), sensible heat flux in air (A), wind speed at 150 cm, and direction, over a shallow free-water surface on 25 April 1961.

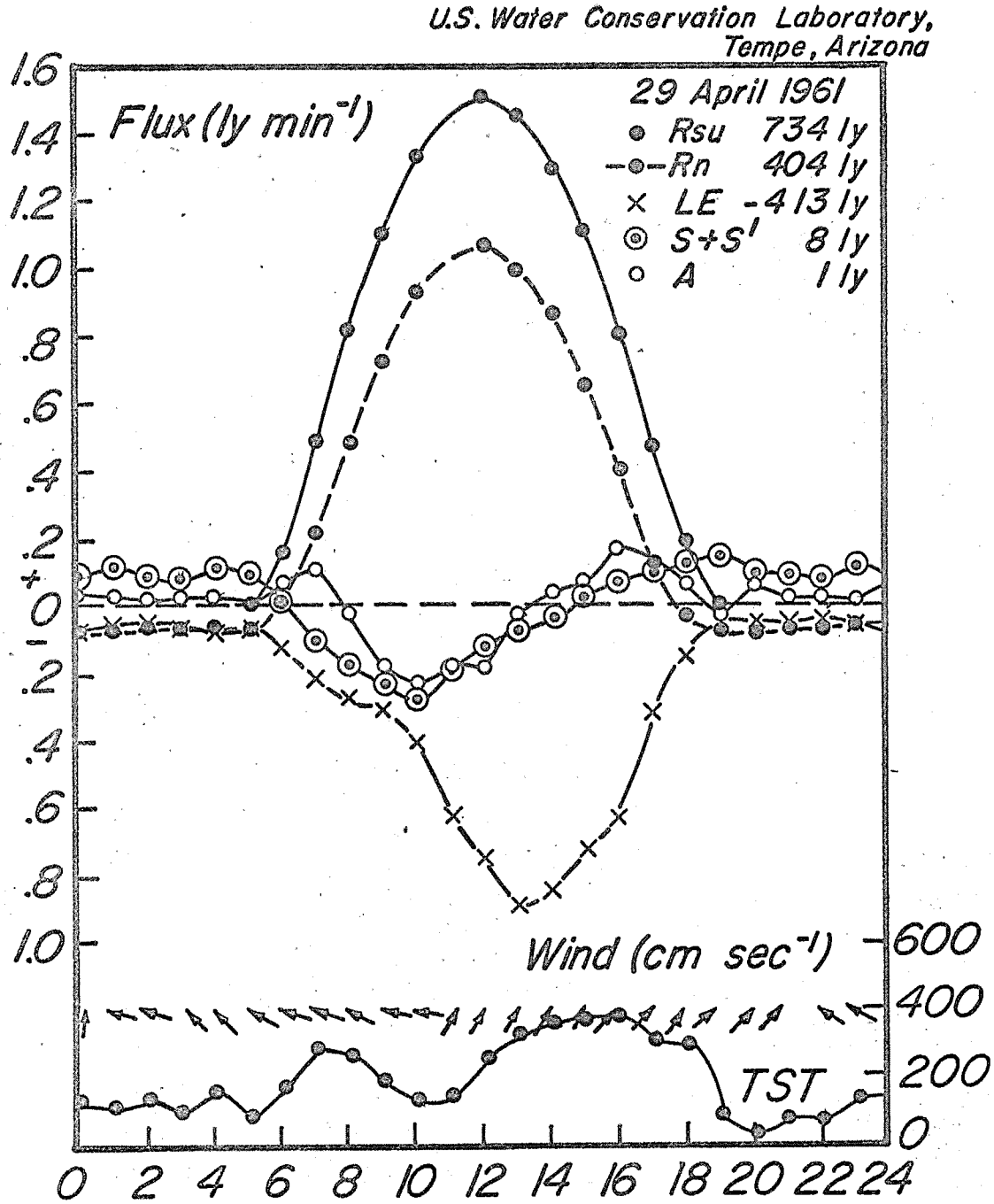

Figure 2. Solar radiation (R_{su}), net radiation (R_n), evaporative flux (LE), soil and water heat flux (S + S'), sensible heat flux in air (A), wind speed at 155 cm, and direction, over a shallow free-water surface on 29 April 1961.

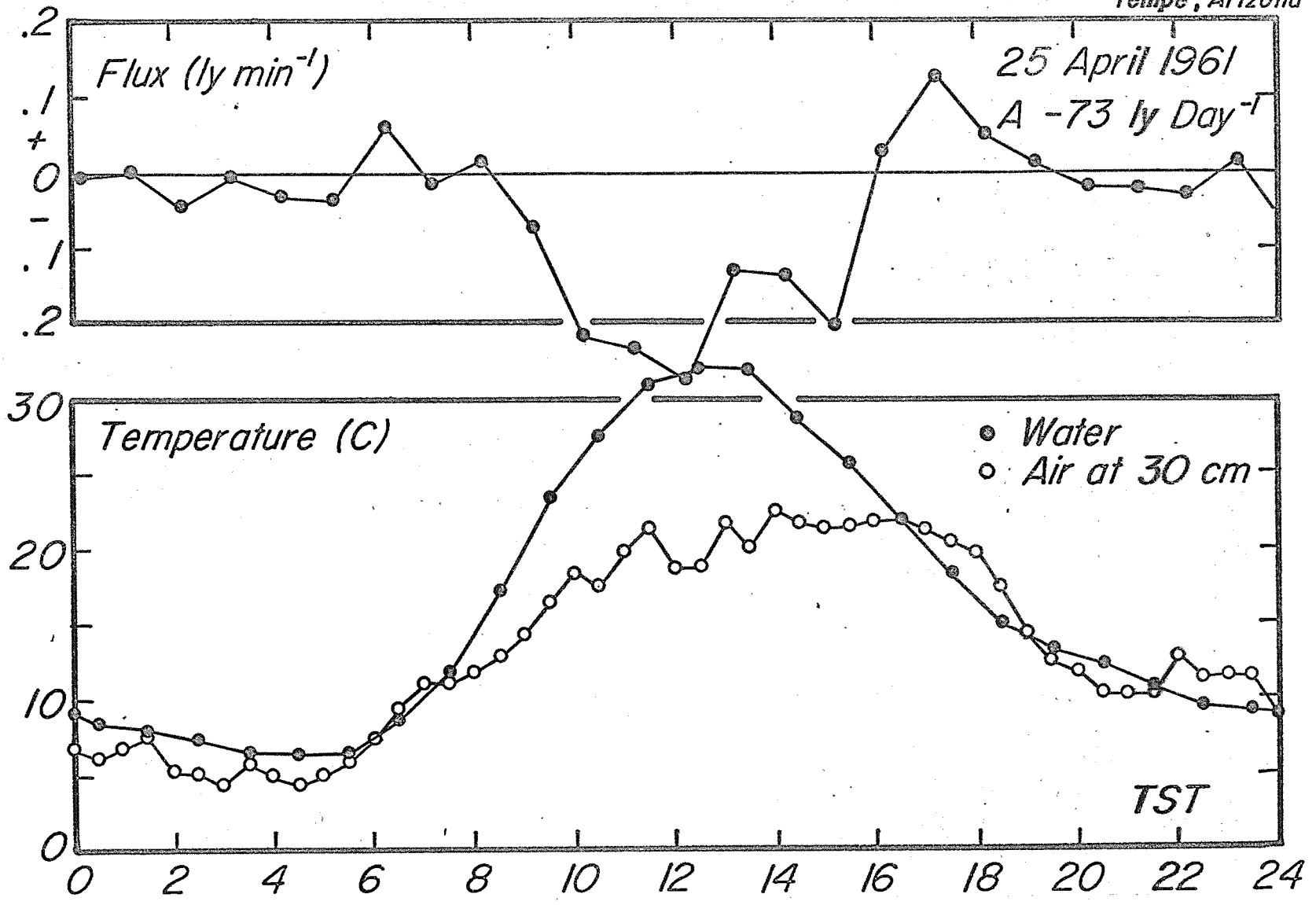

Figure 3. Sensible heat flux in air (A), water temperature, and air temperature at 30 cm on 25 April 1961.

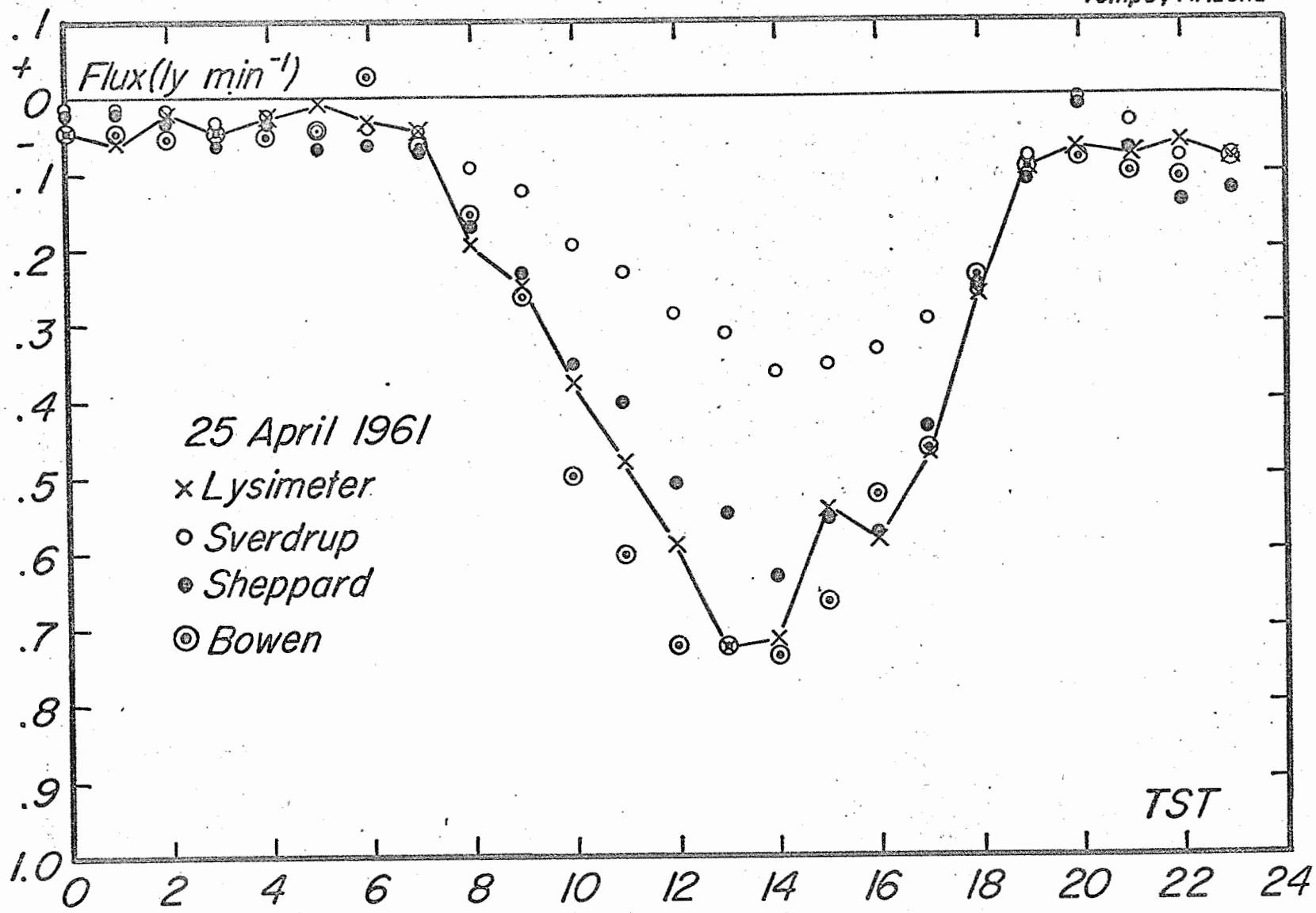

Figure 4. Evaporative flux over a shallow free-water surface as determined with lysimeters and calculated by the Sverdrup (5), Sheppard (6), and Bowen (2) equations, 25 April 1961.

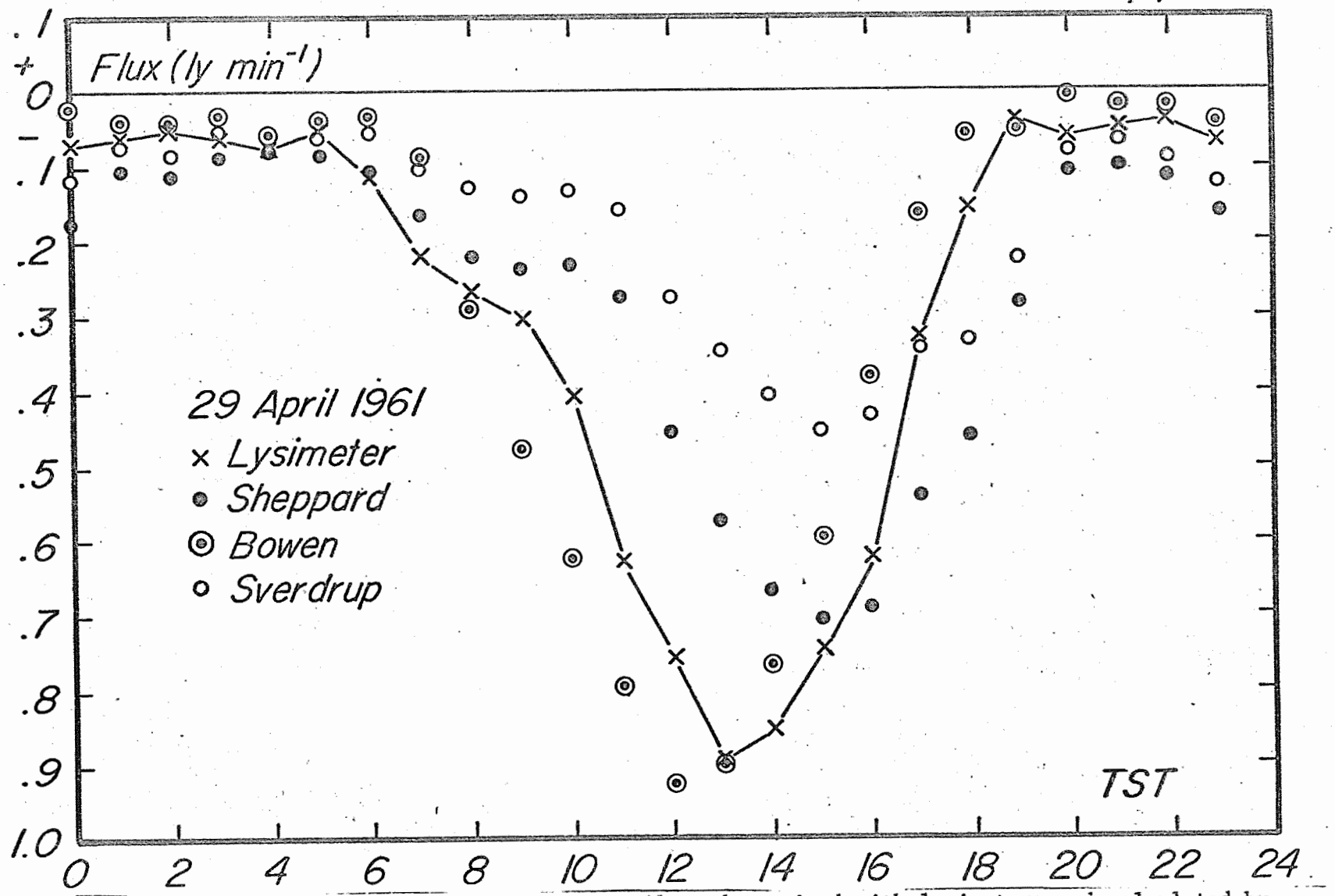

Figure 5. Evaporative flux over bare, wet soil as determined with lysimeters and calculated by the Sverdrup (5), Sheppard (6), and Bowen (2) equations, 29 April 1961.

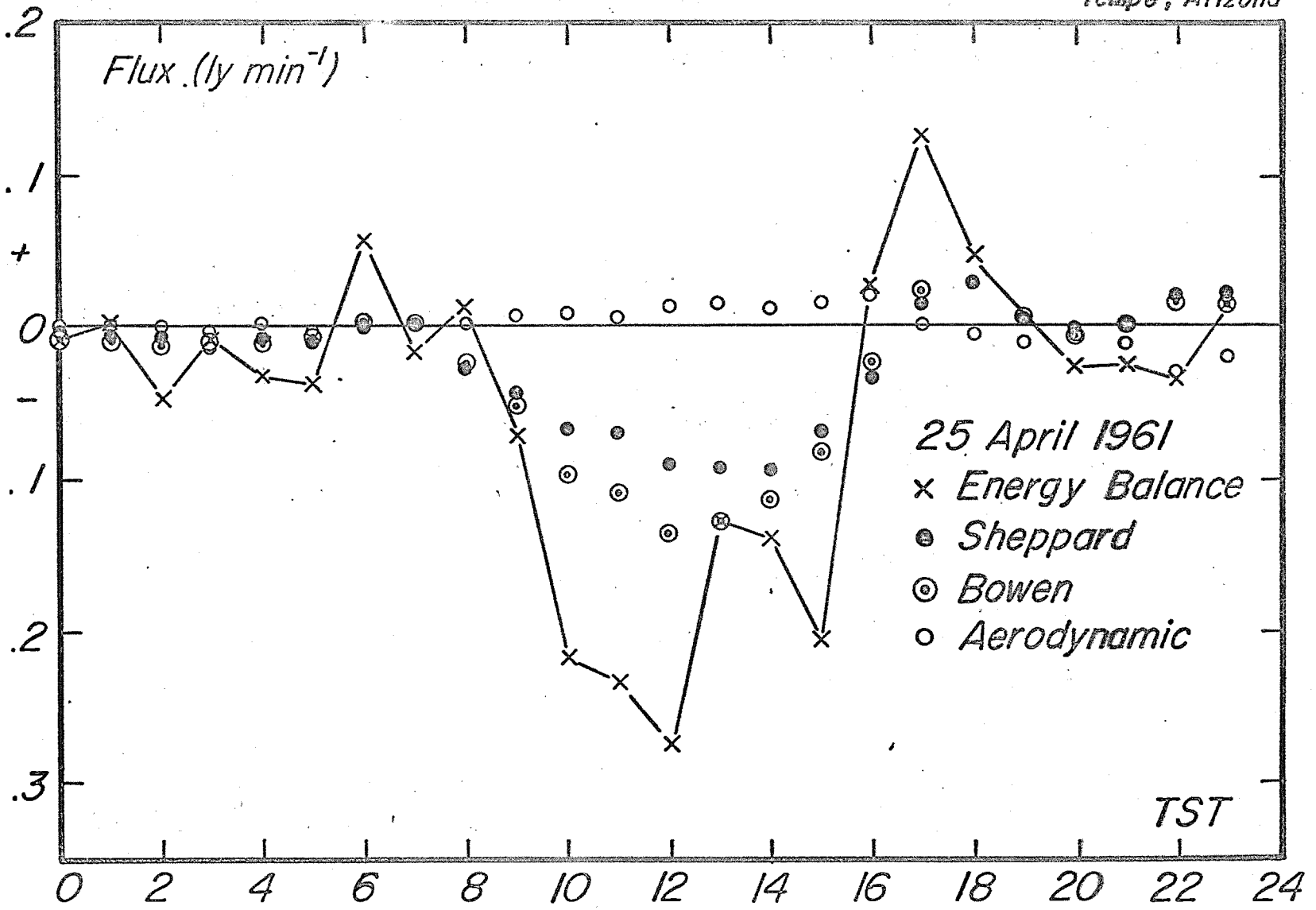

Figure 6. Sensible heat flux in air over a shallow free-water surface calculated by the energy balance (1), Sheppard (7), Bowen (4), and aerodynamic (8) equations, 25 April 1961. Data collected at 30 and 150 cm were used in the aerodynamic equation.

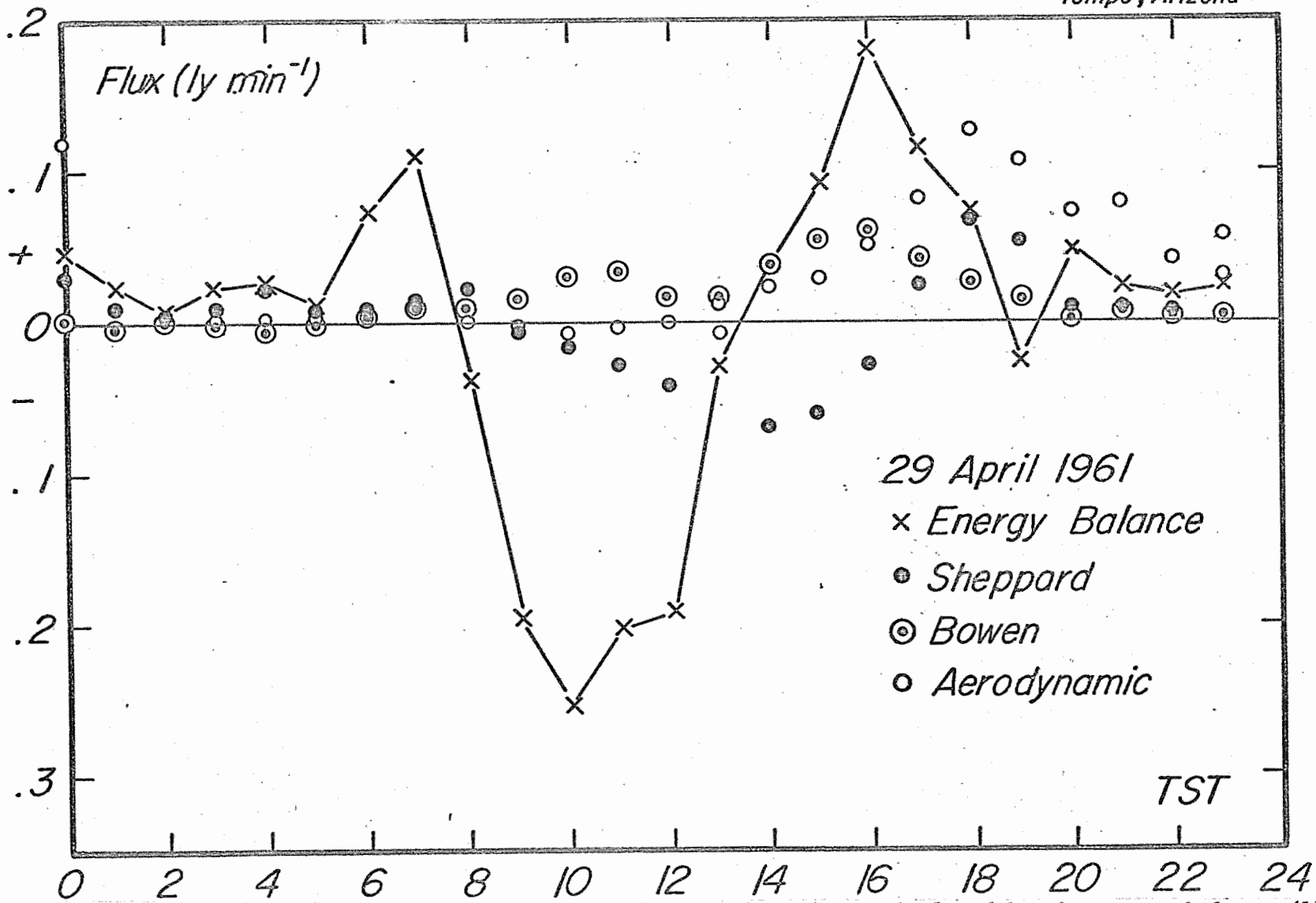

Figure 7. Sensible heat flux in air over a wet bare-soil surface calculated by the energy balance (1), Sheppard (7), Bowen (4), and aerodynamic (8) equations, 29 April 1961. Data collected at 35 and 155 cm were used in the aerodynamic equation.

TITLE: COMPONENTS OF THE RADIATION BALANCE OF FIELD CROPS UNDER IRRIGATED MANAGEMENT

LINE PROJECT: SWC 4-gG2 CODE NO.: Ariz.-WCL-18

INTRODUCTION:

Evaporation and evapotranspiration from fields are more closely approximated by net radiation than any other single parameter. Net radiation under field conditions is a measure of the energy that is available for evaporation, heating the soil, the air, and the crop, and photochemical processes. At any given time the variation of net radiation from field to field is directly related to the different managerial and cultural practices to which the fields are subjected. The study of the effect of the various managerial and cultural practices upon net radiation--particularly, the components of net radiation, terrestrial and reflected radiation--appears feasible. This report contains a summary of the data recorded in the interim of construction of the mobile micrometeorological laboratory (described under "Instrumentation for micrometeorological research").

I. INCOMING AND REFLECTED SOLAR RADIATION OVER BARE SOIL.

Procedures. Incoming and reflected solar radiation are measured with two solarimeters, one being inverted over wet and dry soil.

Results. Listed in Table 1 are incoming and reflected solar radiation measurements over wet and dry soil for various times of the year. The percentage of solar radiation reflected is the highest in the morning and evening hours and lowest at solar noon. The percent reflected for the hour ending 1300 MST decreased from 20 percent on 19 November 1961, to 13 percent on 17 February 1962, and then increased to 23 percent on 1 March 1962. A lower reflection is noted on 29 May 1962, of 13 percent. This lower reflection is probably associated with the presence of emerging Sudangrass.

II. INCOMING AND REFLECTED SOLAR RADIATION AND NET RADIATION OVER SUDANGRASS OF DIFFERENT HEIGHTS.

Procedures. The effect of crop height and maturity upon net radiation and reflected solar radiation was studied for two periods

in July 1962. Previous to the first period, the Sudangrass was mowed in one location and not in the other, so that at the recording time, the Sudangrass was approximately 75-cm tall on one location, and 140-cm tall and completely headed out on the second location. After two days of record were obtained, the Sudangrass on the second location was cut to 8 cm, while the Sudangrass on the first location was allowed to grow. By the time of the second period of measurement, the Sudangrass on the first location was 100-cm tall and just starting to head out, while the Sudangrass on the second location had not completely recovered from the mowing and can be considered as stubble approximately 8-cm high.

During the first period of measurement, incoming and reflected solar radiation was measured over the 140-cm crop, while net radiation was measured 1 m above each surface, at one-half the crop height within the canopy, and 5 cm above the soil within the canopy. During the second period, solar radiation and reflected solar radiation were measured over each surface. Net radiation was measured 1 m above each surface and within the 100-cm canopy at 5, 15, 45, and 75 cm above the soil surface.

The complete experimental field was irrigated immediately prior to each period of recording. Four millimeters of rainfall occurred on 20 July; therefore, the data were collected during a time of year when maximum evapotranspiration could be expected.

Results. The daily totals of the parameters measured during the two periods are listed in Tables 2 and 3. The days of 12 and 13 July were quite comparable with respect to solar radiation; however, the average wind speed was 109 cm sec^{-1} greater on 12 July than on 13 July. Reflected solar radiation appeared to be slightly less on 12 July than on 13 July, but this is in line with the difference in incoming solar radiation. Net radiation measured over the two different crops on those days was comparable; therefore, there did not appear to be any effect of crop height or wind speed upon the measurement of net radiation over the crop surface. The wind speed did seem to have an effect on the net

radiation measured within the canopy. Waving of the leaves appeared to cause more net radiation to be absorbed in the upper portion of the canopy leaving less energy to be transferred to lower portion of the canopy. This is evident in both the 75- and 140-cm canopies on 12 and 13 July.

The data collected during the second period, 20 through 22 July, are not directly comparable to those collected during the first period since solar-radiation intensity was somewhat lower. However, it is interesting to note that the amount of net radiation measured over the 100-cm crop is very similar to that measured over the 75- and 140-cm crop. A greater amount of reflected solar radiation was measured over the crop surface than over the stubble surface, while the opposite is true for net radiation (Table 2). These facts indicate that the proportion of long-wave radiation to short-wave reflection of the outgoing radiation is smaller for a crop surface than a bare soil surface. Again as was noted during the previous recording cycle, a larger portion of the net radiation was absorbed in the upper crop canopy when the average wind speed was the greatest.

A 30-min plot of net radiation, solar and reflected solar radiation, measured over and within the 100-cm crop canopy for the daylight hours is shown in Figure 1. The nighttime values are not shown because the measurements are all similar. Since net radiation at the 15-cm height was similar to that at the 5-cm height, it is not shown. The graph illustrates that the majority of net radiation was absorbed in the upper 25 cm of the canopy. Net radiation at all levels was diminished by temporary cloudiness. Other irregularities in net radiation measured in the crop canopy are due to location variations. This variation, plus the fact that net radiation at 45 cm exceeded that at 75 cm, emphasizes the need for replication of instruments, even within a closed crop canopy such as Sudangrass.

SUMMARY AND CONCLUSION:

Evaporation and evapotranspiration from fields are more closely related to net radiation than any other single parameter. At any given time, the variation of net radiation from field to field is directly related to the different cultural practices. Measurements are being made to determine the effect of different cultural practices upon net radiation, reflected solar and terrestrial radiation. The results indicate that the percentage of solar radiation which is reflected is the greatest during the morning and evening hours; that the percentage of solar radiation reflected at solar noon is the largest when the solar altitude is the smallest; that of the outgoing radiation, the proportion of long-wave radiation to short-wave radiation was smaller for a crop surface than for the stubble surface; that net radiation measured over Sudangrass of different heights was essentially the same, even though the heights were 75, 100, and 140 cm, with the 140-cm crop being completely headed out; and that the amount of radiation absorbed in the upper-half of the plant canopy was proportional to the average wind speed.

PERSONNEL: Leo J. Fritschen

Table 1. Hourly solar and reflected solar radiation.

Hour Ending	19 NOV 61		28 NOV 61		17 FEB 62		01 MAR 62		29 MAY 62	
	R_{su}	fR_{su}	R_{su}	fR_{su}	R_{su}	fR_{su}	R_{su}	fR_{su}	R_{su}	fR_{su}
MST	ly min^{-1}									
05										
06									.12	.02
07									.41	.06
08	.16	.09	.11	.02	.07	.02	.10	.02	.72	.10
09	.44	.12	.38	.08	.34	.06	.44	.08	1.00	.12
10	.69	.16	.56	.07	.64	.09	.77	.15	1.22	.15
11	.86	.18	.72	.13	.90	.12	1.02	.22	1.34	.17
12	.94	.18	.78	.12	1.06	.14	1.17	.26	1.38	.18
13	.94	.19	.77	.12	1.14	.15	1.24	.28	1.36	.18
14	.86	.19	.65	.10	1.11	.15	1.20	.28	1.28	.17
15	.71	.16	.48	.05	.89	.12	1.06	.25	1.14	.15
16	.48	.14	.26	.03	.68	.10	.83	.20	.92	.12
17	.20	.08	.03	.00	.48	.07	.55	.14	.64	.09
18	.05	.04			.18	.04	.23	.07	.36	.05
19							.02	.01	.07	.01

R_{su} : Solar radiation.

fR_{su} : Reflected solar radiation.

Table 2. Incoming and reflected solar radiation, net radiation, and wind speed.

Date	Lysimeter	U	R_{su}	fR_{su}	R_n 1/	R_n 2/	R_n 3/
July		cm sec^{-1}	- - - - - - -	- - - - - - -	ly day^{-1}	- - - - - - -	- - - - - - -
12	2	247	725		377	192	58
	3			149	373	104	43
13	2	139	740		365	226	66
	3			160	373	208	40

1/ measured 1 m above the crop canopy.

2/ measured within the canopy at one-half crop height.

3/ measured within the canopy 5 cm above the soil.

Table 3. Incoming and reflected solar radiation, net radiation, and wind speed.

Date	Lysimeter	U	R_{su}	fR_{su}	R_n 1/	R_n 2/	R_n 3/	R_n 4/	R_n 5/
July		cm sec^{-1}	- - - - - - - - - - - -			ly day^{-1}	- - - - - - - - - - - -		
20	2	232	696	163	368	83	88	26	26
	3			126	342				
21	2	99	527	105	254	189	118	7	-11
	3			91	221				
22	2	158	683	150	377	182	79	6	1
	3			115	361				

1/ measured 1 m above the crop canopy.

2/ measured within the canopy 75 cm above the soil.

3/ measured within the canopy 45 cm above the soil.

4/ measured within the canopy 15 cm above the soil.

5/ measured within the canopy 5 cm above the soil.

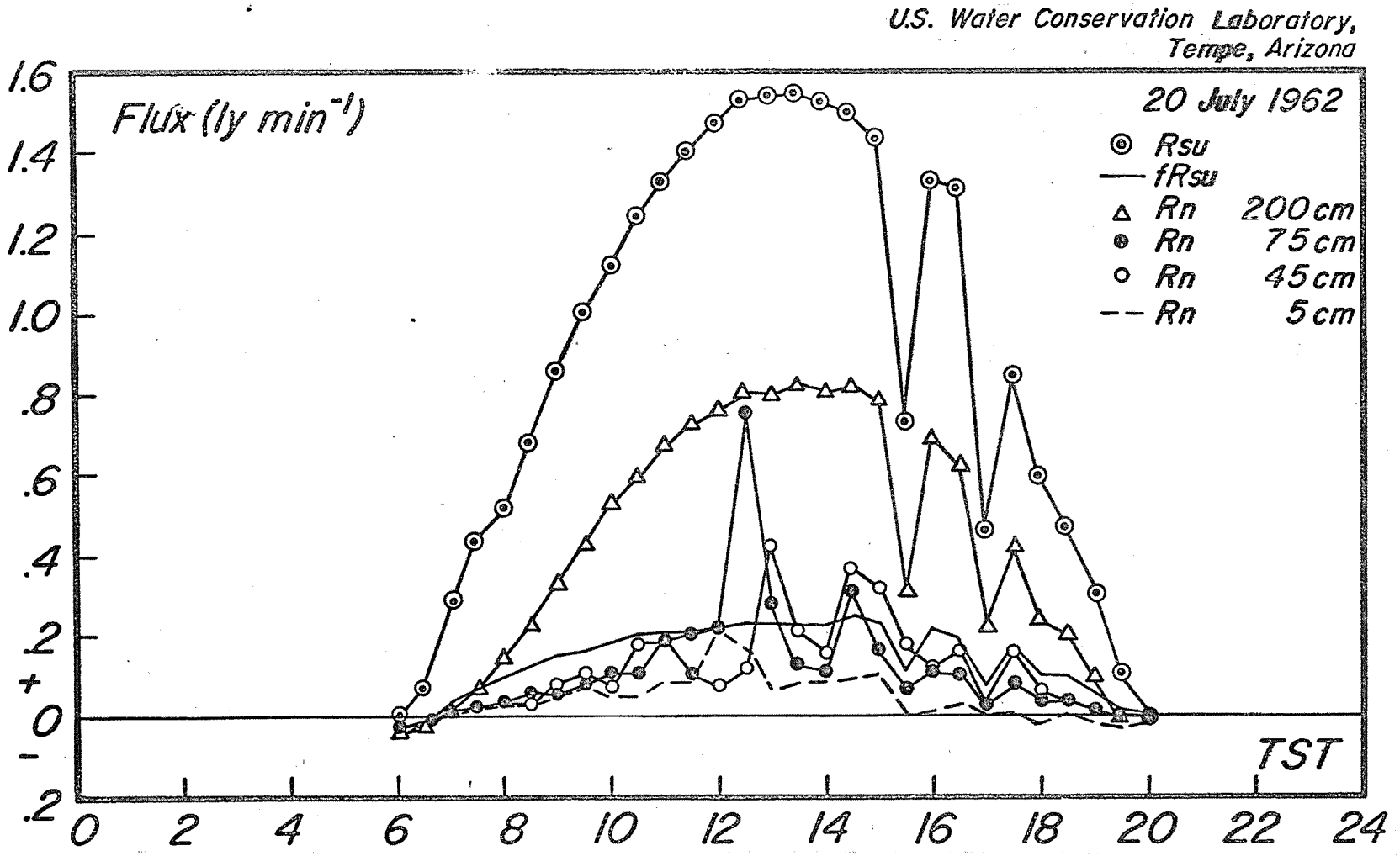

Figure 1. Solar, reflected solar, and net radiation measured over Sudangrass, and net radiation measured at different levels within the Sudangrass canopy.

TITLE: INSTRUMENTATION FOR MICROMETEOROLOGICAL RESEARCH.

LINE PROJECT: SWC 4-gG-2 CODE NO.: None.

I. MOBILE MICROMETEOROLOGICAL LABORATORY.

INTRODUCTION:

Micrometeorological research requires measurement of many different elements under field conditions. The precision required is such that commercially available sensors and equipment cannot be readily used without modification; in some cases, commercial sensors are not available and must be designed, constructed, and tested to meet the local conditions. All sensors, whether of commercial or local manufacture, must be tested to determine if the desired accuracy can be obtained under field conditions. Therefore, this report contains materials relating to the construction, calibration and testing of sensors, and to recording of micrometeorological variables under field conditions.

PROCEDURES:

To rapidly record many micrometeorological elements over a period of time and over different surfaces, a recording system which is not dependent upon line-transmitted current is required. A data-handling system was purchased and mounted in a self-contained trailer, the whole assembly being called the mobile micrometeorological laboratory.

The self-contained trailer, 8 x 7 x 16 feet, was built to specifications supplied by the U. S. Water Conservation Laboratory, and has ample room for the data-handling system and sensors. It contains a marine toilet, 30-gal water supply, 2 cu ft refrigerator, and a gas hotplate. The trailer is cooled and heated by a heat pump.

The current required to operate the data-handling system, heat pump, and other items is supplied by a 110/220 VAC, 5 kw generator, which is mounted on the hitch of the trailer. The generator is self-starting and operates from LP fuel supplied through an automatic crossover regulator by 100-lb bottles. The trailer was built to travel over rough terrain and to give the data-handling system a smooth ride. The frame is rugged, being constructed from 6-inch I-beam, Tandem axles, large wheels, and tires provide surface support and clearance,

which enables the trailer to be towed over soft terrain and through small gullies.

The data-handling system, although not complete, now contains facilities to rapidly and sequentially measure 40 different voltage signals, convert the measurements into digital form, and to record the digital data on punched paper tape or in the form of tabular listings. The system contains a triple-range, self-balancing potentiometer, four 10-channel input scanners, 1000-digit shaft encoder, digital clock, and control chassis. A wind register system is now being built which will be connected to the data-handling system. The wind system will contain eight 4-digit electromechanical counters having electrical readout and reset facilities. The data-handling system was modified by an addition of a pinboard, 15 voltage dividers, and control clock. The pinboard enables rapid programming of the system. The voltage dividers are used to adjust the output voltage of the transducers so that the system's output is in standard physical units, and the control clock is used to turn the system on and off at midnight, thus reducing the operating time on the system since our recording day officially starts and ends at midnight.

The features of the data-handling are:

(1) It is capable of transforming 40 different voltage signals into output of digital form suitable for punched tape recording or listing by typewriters.

(2) The number of inputs to be recorded is limited to groups of 10.

(3) Each input may be programmed to any one of three ranges independently of the other inputs.

(4) The system can accumulate eight channels of electrical pulses for a preset period of time and print the data in digital form.

(5) The inputs are recorded at the rate of 1 sec^{-1}, with the complete printout requiring less than 1 min.

(6) The input voltage may be scaled down with the aid of potentiometers so that the output is in standard physical units.

(7) The output is recorded on an 8-channel punch tape or listed by an electric typewriter.

(8) The typewriter may be used to list a punch tape and to make duplicate tape.

(9) The tape code is such that it can be rapidly converted into punch cards or magnetic tape for machine processing.

(10) The recording cycle may be manually or automatically initiated at selected intervals.

(11) In manual mode, a single channel may be automatically recorded at selected intervals or continuously displayed in the light bank.

(12) The system is very flexible with regard to the number and magnitude of inputs to be recorded.

To facilitate rapid installation of sensors and wiring at a particular recording site, standard cables were constructed, each being 200-ft long and having gold-plated taper pins on one end and standard connectors on the other end. These cables are stored on reels in two boxes mounted under the trailer. A total of 3000 ft of 2-conductor, shielded copper cables and 1000 ft of stranded thermocouple cable is stored under the trailer. Roof antenna mounts were purchased to be used as collapsible tripods for mounting sensors in the field. These tripods, along with the necessary masts, are also stored and transported between the I-beams of the frame.

SUMMARY:

A mobile micrometeorological laboratory was constructed and equipped to enable rapid recording of micrometeorological elements, independent of line-transmitted current, at any location. The laboratory contains a data-handling system that can rapidly transform 40 channels of voltage input and 8 channels of electrical pulses into an output which is placed on an 8-channel punch paper tape or listed by an electric typewriter. The laboratory is an 8 x 16 ft trailer of rugged construction, having tandem axles, 30 gal water supply, marine toilet, 2 cu ft refrigerator, gas plate, heat pump, and a 5 kw generator. The trailer also contains facilities for

storing micrometeorological sensors, conducting cables, and the necessary mounting apparatus.

PERSONNEL: Leo J. Fritschen.

II. INSTRUMENTATION FOR TURBULENT TRANSFER STUDIES.

INTRODUCTION:

The fluxes of sensible and latent heat may be estimated by several meteorological models. Some models require measurements that are difficult to obtain on an operational basis. The aerodynamic gradient model and a model which combines the energy balance equation with the Bowen ratio are the most widely used and require measurements which can be obtained continuously. Previous tests indicate that the latter model appears to be the most promising.

The Bowen equation, in addition to net radiation and soil heat-flow measurements, requires precise measurement of air-temperature and vapor-pressure gradients. These gradients not only must be sampled in time, but also must be sampled in space. To accomplish this, an air-sampling tower has been designed and is currently being constructed.

PROCEDURES:

The sampling tower contains facilities to move the sensors in space and to cancel out systematic sensor errors. To sample in space, the tower has a 10-ft horizontal arm. One end mounts the sensors, and the other end is fastened by a gear train and motor to a vertical support. The gearing and motor speed are such as to cause the horizontal arm to sweep out a 180-degree arc in 10 minutes. The motor torque is then reversed and the arm moves in the opposite direction for 180 degrees.

A sensor is mounted on each end of a 60-inch arm which is attached at right angles to the end of the horizontal arm. The horizontal arm rotates 90 degrees on a command from the data handling system. The 90-degree rotation causes the upper and lower sensors to change position--thus cancelling out any systematic sensor errors.

The sensors, each containing dry- and wet-bulb thermocouples, are being constructed to have 2-minute time constants. If the data are recorded at a 5-minute frequency and the sensor position changed immediately after each recording, then the sensors will have sufficient time to adjust to the new environment prior to the next recording.

The air sampling is designed so that gradient space may be varied from 0 to 40 inches and the height of the lowest sensor above the surface may be varied 0 to 10 feet.

SUMMARY:

The fluxes of sensible and latent heat may be estimated with micrometeorological models. The Bowen equation, one of the most promising models not only requires measurements of net radiation and soil heat flow, but also requires precise measurement of air-temperature and vapor-pressure gradients. To obtain the required precision, the gradients must be sampled in time and space. This requires an air-sampling tower which is capable of continuously moving the sensors in a horizontal plane. The precision of measurement may also be increased by frequently switching the sensors, which cancels out any instrument errors.

An air-sampling tower containing these features is being constructed. Two sensors, each containing a wet- and dry-bulb thermocouple having 2-minute time constants, will be attached to the air-sampling tower to obtain the required gradients.

PERSONNEL: Leo J. Fritschen.

III. METHOD TO CALIBRATE HEAT-FLOW TRANSDUCERS.

INTRODUCTION:

Heat-flow transducers are used in the energy balance equation to measure the heat-flow component in the soil. Even though the soil heat flow is usually a small portion of the total, it cannot be ignored.

Usually heat-flow transducers are purchased with calibration factors. These calibration factors need to be checked periodically when the heat-flow transducer is used in the soil. A precise calorimeter is needed for this purpose.

PROCEDURE:

The calorimeter was constructed similar to the one described by H. Stanford Hatfield and F. J. Wilkins in "A net heat-flow meter," Journal of Scientific Instruments 27:1-3, 1950. The calorimeter consists of three heating elements fastened between copper sheets. One of the heating elements acts as a guard-ring around the second, which is 14 inches square. These two heating elements are located 1 inch above the third element, 18 inches square. The 1-inch space between the elements being filled with vermiculite. Four to eight layers of felt are placed above the first two elements. The complete assembly is placed in an insulated wooden container.

In operation, a heat-flow transducer is placed between two of the layers of felt above the center heating element. A current applied to all of the heating elements is adjusted until the temperature of the elements is the same. The heat flow from the center element then flows vertically through the felt, and is calculated from the voltage and resistance.

RESULTS AND DISCUSSIONS:

When the calorimeter was constructed as described, it had two serious limitations: (1) the maximum output that could be obtained while maintaining the plate temperature below 65C (the critical temperature for the insulation) is 0.15 ly min^{-1}; (2) the heat-flow disc could not be calibrated at a constant temperature or at a desired ambient temperature. To overcome these limitations, a heat-exchanger is being constructed which will be placed on top of the layers of felt. The exchanger will be cooled with water that is temperature controlled. With the exchanger a greater output can be obtained from the calorimeter, while maintaining a lower temperature; thus, it should be possible to not only calibrate a heat-flow transducer, but also to determine its temperature coefficient.

SUMMARY:

A calorimeter was constructed to calibrate heat-flow transducers which are being used to measure the soil heat-flow component of the energy balance equation. The maximum output that could be obtained

while maintaining the temperature below 65C was 0.15 ly min^{-1}. The calorimeter is now being modified to increase the output and to control the temperature so that heat-flow transducers may be calibrated over a greater range and that their temperature coefficients can be determined.

PERSONNEL: Leo J. Fritschen.

IV. COMPUTER PROGRAM CONTAINING A GENERALIZED LINEAR EQUATION.

INTRODUCTION:

Micrometeorological research requires the rapid recording of many variables; thus in a short period of time, a large volume of data is accumulated. Computers are required to efficiently reduce this volume of data so that it may be studied within a short period of time after collection.

Micrometeorological elements to be studied depend upon the particular model used. Consequently, the elements to be recorded are frequently changed. Each change requires a change in computer program which is not only costly but requires time. To eliminate the reprogramming cost and to decrease the time required to process the data, a generalized linear program was written.

PROCEDURES:

The generalized linear program enables the solution of the following linear equation:

Equation I = [(channel A - channel B) × C + Equation J + D] × F

where Equation J represents the solution of any equation previous to Equation I; channels A and B represent data recorded and may range from 1 to 49 channels; C, D, and F represent constants which may be different for each equation. The values of C, D, and F may range from 0.0001 to 999.9999.

A total of 100 Equation I's may be solved during each recording cycle. The recording cycles may occur at a frequency of 1-, 5-, 15-, 30-, or 60-min intervals.

With the generalized linear program, a linear output from any transducer may be rapidly converted to the proper physical units.

The solutions of Equation I are then averaged for each hour and totaled for each day.

SUMMARY:

To efficiently reduce the necessary volume of micrometeorological data to a required form, to eliminate reprogramming costs, and to decrease the time required to process the data, a generalized program was written for the computer. The program will solve any linear equation, and will combine two or more solutions. The solutions are then averaged for each hour and totaled for each day.

With the generalized linear program, the micrometeorological data recorded can be rapidly converted to the proper physical units and summarized in a suitable form for future calculations.

PERSONNEL: Leo J. Fritschen.

V. INTEGRATOR FOR VARIABLE DC SIGNALS

INTRODUCTION:

At times it is necessary, or at least desirable, to know the time-averaged value of certain variables that characteristically vary rapidly. For work related to energy balance studies such variables are, for example, wet and dry bulb temperature, temperature differential in the air, vapor pressure in air, or certain radiation components.

The time over which the average is sought is usually from 5 to 60 minutes, too long for ordinary RC averaging. In addition, a RC circuit has a high output impedance, incompatible with high speed recording. In principle, this problem can be solved with mechanical integrators, but these have a high cost and also are not suitable for direct readout. Therefore, another approach is being investigated, in which the average output is transferred to electromagnetic counters with electric readout that are already available as part of the micrometeorological data logging system.

PROCEDURE:

The general approach consists in measuring the DC signal--usually of the order of a few millivolts--with a sensitive and fast recording potentiometer and to translate the varying signal into a varying

resistance by means of a transmitting slide wire mounted on the shaft of the balancing slide wire. Then, the transmitting slide wire is made part of an oscillator, each discharge of which is recorded as an individual count on the available electromagnetic registers. The registers can be read out and reset at predetermined time intervals and the count thus recorded is a measure of the average value of the variable studied.

The objective is to obtain a system that has a precision of, say, 2% and that is cheap enough so that its use on several channels would not be prohibitive.

For a recorder, we use a Speedomax H-AZAR on the slide wire shaft of which a 0.25% linear single turn slide wire of 50 K total resistance is mounted. With suitable capacitors, this variable resistance forms a tank circuit, the discharge of which is controlled by a unijunction transistor. The discharge pulse is transferred by a silicon controlled rectifier to an intermediate, low power relay, which in turn operates the 6 V DC relays that are part of the windspeed recording registers. The oscillator circuit is powered by a constant voltage 24 V DC supply. A circuit diagram is not given since the design is still being evaluated.

The design is calibrated by imparting known voltage signals to the measuring recorder for known periods of time and computing the relation between counting rate and recording reading. Then, a voltage signal of known variation is applied, and calculated and known average voltage are compared.

RESULTS AND DISCUSSION:

During the summer and fall of 1962 a number of successive design changes were evaluated. It was found that the capacitor in the tank circuit of the oscillator had to be quite large (20 microfarad) and of the dekanol type to give stability.

A final result of calibration was the following equation:

$$r = 17.90 - \frac{1}{2.067 \times 10^{-4} \times (\text{cpm})}$$

in which

r = averaged recorder indication, if recorder range is from 0.00 to 10.00 units.

cpm = counts per minute.

In this case, zero and full scale correspond to 270 and 613 cpm, respectively. The following integrations were then carried out, the variable indicated in units from 0 to 10

Range	Computed Average	Measured Average	Deviation in % of Computed	Deviation in % of Full Scale
0 - 2	1.00	1.11	11.0	1.1
2 - 4	3.00	3.10	3.3	1.0
4 - 6	5.00	5.06	1.2	.6
6 - 8	7.00	7.04	0.6	.4
8 - 10	9.00	8.96	0.4	.4

This result indicates that the accuracy may be acceptable, since many sensors are no more accurate than 2% full scale.

The long-range stability of the circuit is still under investigation and results to date are preliminary.

SUMMARY AND CONCLUSIONS:

An integrating device for small DC signals has been designed and partially tested. It operates from a transmitting slide wire on a sensitive recorder and produces a count rate, related to the input signal by a simple formula. The count over a known period of time can be registered automatically, along with other data and is a measure for the average value of the variable measured.

Preliminary data indicate satisfactory accuracy and stability. Further work is necessary.

PERSONNEL: C. H. M. van Bavel, W. Reeves.

TITLE: EVAPORATION FROM THE SOIL SURFACE AND SOIL MOISTURE MOVEMENT.

LINE PROJECT: SWC 4-gG2 CODE NO.: Ariz.-WCL-19

INTRODUCTION:

In previous studies (see Annual Report 1961) it was found that the evaporation rate from bare soil shows a diurnal fluctuation under all circumstances, including very dry surface soil. A detailed study of hourly changes in soil temperatures and soil moisture contents at shallow depths may show how transport phenomena in the soil are tied to the diurnal energy input fluctuation at the surface. A preliminary set of observations was obtained during the period February 27 through March 7, 1962 to set the stage for later, more definitive studies.

PROCEDURES:

The lysimeters and field were bare and were irrigated on February 16. Following a rainy period, a drying period ensued with mostly sunny weather starting on February 27. Hourly measurements were made of evaporation, half-hourly ones of soil temperature at 1/2, 1, 2, 4, 8, 16, and 32 cm, using thermocouples, and of net radiation and soil heat flux. Daily or twice-daily measurements were made of soil moisture content by direct sampling in 1-cm increments from 0- to 18-cm depths. The most complete set of data was obtained on March 1 and March 2 and these will be discussed as illustrative.

RESULTS AND DISCUSSION:

1. Soil Temperatures. The daily course of soil temperatures on March 1 and 2 is indicated by Figure 1 showing the temperature profile at the time that the daily maximum and minimum occurred on each day at .5 cm depth. Also shown is the air temperature at 30 cm. The two days are nearly identical with regard to soil and air temperature and show an amplitude less than 1°C at 30 cm depth, as compared to a surface amplitude of 30°C. Assuming a homogeneous soil, this indicates a thermal diffusivity of 2.8×10^{-3} cm sec^{-1}. In the layer from 1/2 to 8 cm the temperature gradients are the largest and are reasonably uniform. In Table 1 the average gradient and the evaporation rate are shown for each hour of March 2.

At a depth of 5 cm, the temperature varies by about 20°C during the course of a day. This is insufficient to materially change the soil water pressure potential gradient. However, soil water diffusivity may be 1.3 times greater at the maximum than at the minimum temperature. The vapor pressure gradient in the soil is large because of the large temperature gradient and is directed downward during the day and upward during the night. Thus, the upward liquid flow of water is intensified during the day but opposed by vapor movement. At the same time (see Table 1) the evaporation is intense during the day. At night liquid flow continues, now aided by vapor flow, while evaporation is slight.

2. Soil Moisture Content. Figure 2 gives the moisture profile at 1530, March 1 and 0900 and 1530 on March 2. According to data obtained by Jackson, liquid diffusivity below 3 cm would be about 0.8 cm^2 min^{-1}. Above 3 cm the diffusivity is an order of magnitude less.

Figure 2 shows that the sum total of liquid and vapor movement of water does not match evaporation during the day and the top layer loses water. These losses are regained during the night, as also seen in Figure 2. The data are also indicative of the fact that below 2 cm, moisture movement at least equals evaporation during any time of the day. The question then is why evaporation is not greater during most of the day.

It is suggested that the evaporation cannot be greater than the "minimum" in isothermal diffusivity proposed by Philip and De Vries. For Yolo light clay this was given as about 5×10^{-5} cm^2 sec^{-1}. With a moisture gradient of 0.10 cm^{-1} as found in the upper 2 cm in Figure 2, a moisture movement of 0.18 mm hr^{-1} results, reasonably close to the maximum of Table 1.

Obviously, much more detailed studies of soil moisture content, distribution of the soil constants and of the concepts used must take place before the moisture losses from bare soil are better understood. Such experiments are planned in the near future with the aid of gamma transmission for the detailed description of moisture distribution.

SUMMARY AND CONCLUSIONS:

Following experiments carried out in 1961 on the detailed nature of evaporation from bare soil at different times of the year, a first attempt was made in early 1962 to tie in the course of evaporation with the thermal and hydraulic processes in the soil. Detailed and adequately precise measurement of the temperature of the field could be made, but the description of moisture content and status in the surface layer was inadequate. Future work will require gamma densitometry, now under development, and, also, careful measurements of the moisture characteristic and vapor absorption isotherms, to permit estimates of the moisture transfer coefficients in vapor and liquid form. This work is now in progress.

PERSONNEL: C. H. M. van Bavel, R. D. Jackson, R. J. Reginato.

TABLE 1. Hourly evaporation rates in mm hr^{-1} and soil temperature gradients in C cm^{-1} in the .5- to 8-cm layer.

02 MAR 62					
HOUR	E	ΔT	HOUR	E	ΔT
	mm hr^{-1}	C cm^{-1}		mm hr^{-1}	C cm^{-1}
1	.02	+ .71	13	.15	-1.84
2	.01	+ .72	14	.16	-1.84
3	.02	+ .72	15	.13	-1.66
4	.03	+ .70	16	.12	-1.19
5	.05	+ .70	17	.09	- .73
6	.03	+ .65	18	.04	- .08
7	.01	+ .67	19	.04	+ .44
8	.00	+ .52	20	.02	+ .61
9	.07	- .15	21	.02	+ .64
10	.11	- .77	22	.02	+ .65
11	.13	-1.36	23	.02	+ .68
12	.14	-1.72	24	.01	+ .69

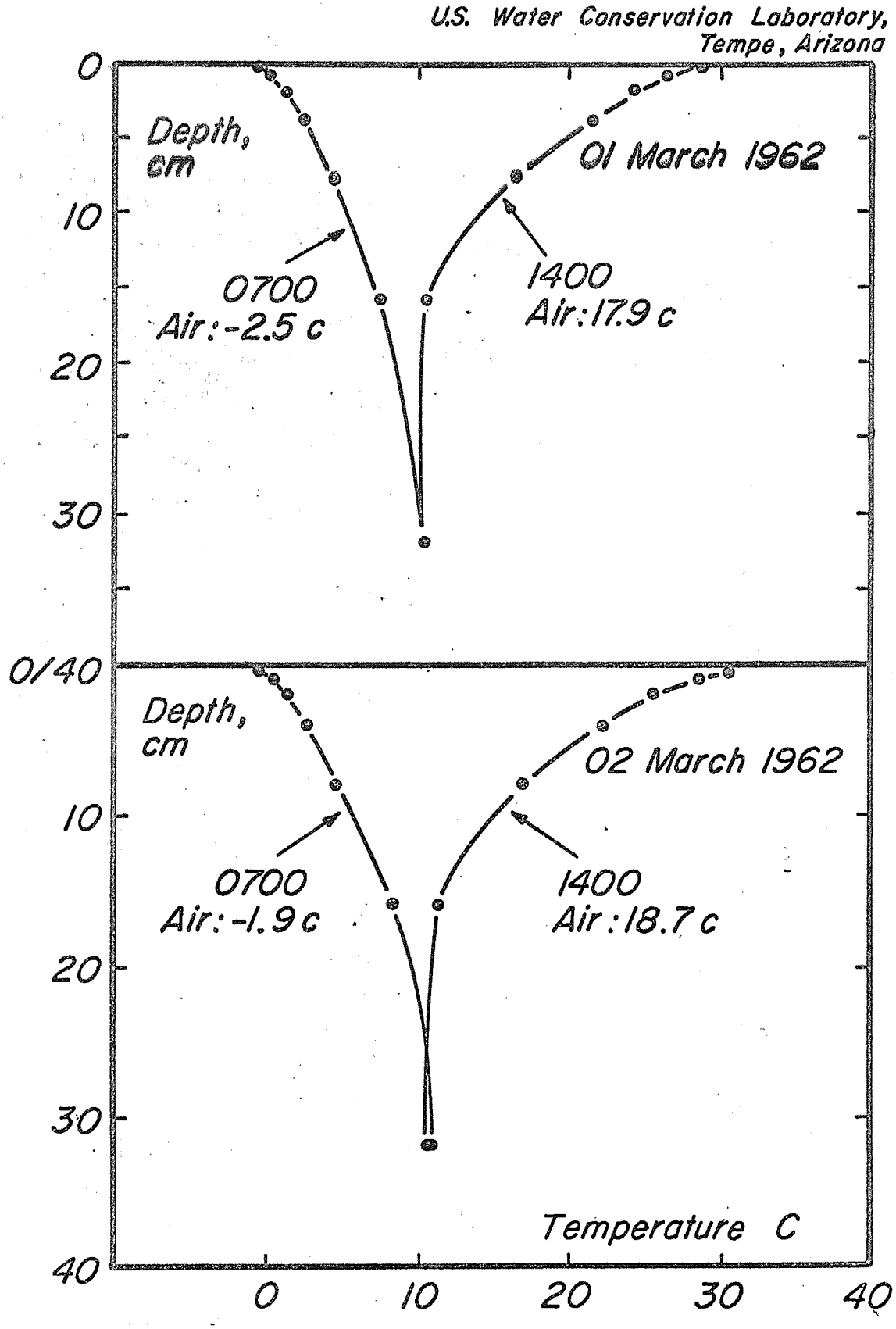

Figure 1. Soil temperature profile at 0700 and 1400 MST under a bare, dry surface on 1 and 2 March 1962.

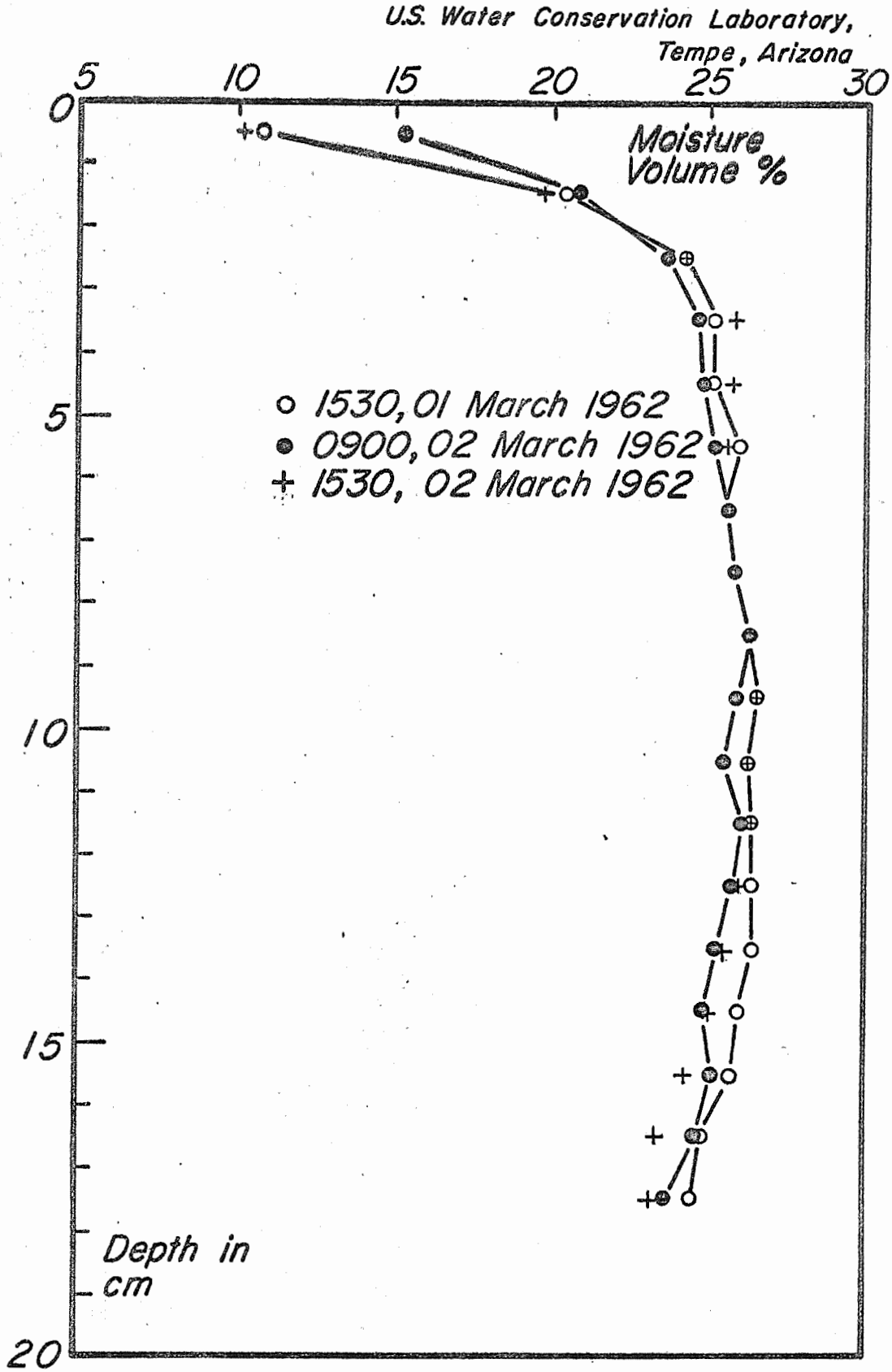

Figure 2. Soil moisture profile under a bare dry surface on 1 and 2 March 1962.

TITLE: EVALUATION OF PLASTIC MULCHES FOR GROWING COTTON.

LINE PROJECT: SWC 4-gG2 CODE NO.: Ariz.-WCL-27

INTRODUCTION:

During 1962 large-scale tests were intitiated by several farmers in the Chandler area to evaluate the effectiveness of black polyethylene mulch on cotton production. The mulching practice consists of laying down a 20-inch wide strip of 1-mil polyethylene over a ridge in which, in the same operation, cotton is planted. The cotton seed emerges through crosscut openings in the plastic made by a special attachment to the seeding and plastic-laying machine. The edges of the plastic are covered up with soil to prevent blowing off. This practice is being carried out on standard 40-inch rows. Approximately 1/3 of the surface actually consists of plastic and is effectively sealed against evaporation.

Any effects of the practice on the growth of cotton may, in part, be explained through the changes that this mulching practice has on the physical environment. Since these tests were carried out on large areas it was decided to make some measurements to find out whether plastic mulching as described would affect such environmental factors as net radiation, soil and air temperature, and soil-moisture content.

PROCEDURE:

The measurements were carried out on a field which is part of the Tschudy Ranches west of Chandler, Arizona. Cooperation was furnished by Mr. Tschudy and his staff. Two 6 1/4-acre fields, 226 feet wide and 1200 feet long with rows running from east to west were situated side by side, one being treated with plastic mulch and the other untreated. Two test areas in each field approximately 40 feet on each side of the dividing line and 200 feet from the edge of the fields were selected and a Leeds and Northrup Speedomax H AZAR recorder was mounted on the dividing line between the two fields. The following variables were measured:

1. Soil Moisture Content. Neutron access tubes were installed, 5 in each test area, and soil moisture content was determined at

6-inch intervals to a total depth of 63 inches once a week, starting 16 April through 23 July, using the neutron method with a Troxler probe and a Tempe rate meter.

2. Soil Temperature. Soil temperatures were measured by means of Palmer maximum-minimum dial thermometers, the sensing elements of which were located at 5 cm depth. Three thermometers were mounted in each test plot with the sensing element running in the direction of the row and on the crest of the ridge. The maximum-minimum soil temperature was recorded for every day starting with 16 April through 19 August.

3. Air temperature. Air temperature was measured with Weston maximum-minimum dial thermometers that were mounted in aluminum shields at 10 cm above the ground. This measurement was also made in triplicate.

4. Net Radiation. Net radiation was measured with miniature net radiometers as designed by Fritschen (low output type). Three net radiometers were located in each plot so as to be always over the crop and so as to represent positions over the ridge, in between the ridge, and halfway between the furrow and ridge in an effort to average the exposure conditions. Another 5 net radiometers were exposed in each plot located at 20 cm height so as to eventually be covered by the developing crop. Radiation was recorded every half-hour for each of the four exposures, the radiometers of like exposure being connected in series. Totalizing the half-hourly measurements resulted in data totals.

5. Water Measurements. An effort was made to ascertain how much water was applied to the soil in each plot with the customary irrigation practices. To this end the supply ditch was provided with three standard cross-sections made out of plywood to accommodate a Pendvane flow meter. The standard cross-sections were located upstream and downstream of each plot, one of these being in common to both. Since the land was not dead level but laid out so that considerable runoff could occur, arrangements were made to measure the tailwater by means of a trapezoidal flume and water stage recorder.

RESULTS AND DISCUSSION:

1. Soil Moisture Content. The maximum moisture content of the profile in the field was about 430 mm (17 inches) and the amount of total available moisture for plant extraction was about 250 mm (10 inches). The frequency of irrigation was such that the moisture content of the soil was never reduced to a figure even approximating the lowest possible moisture content. Both fields were generally irrigated at the same time, the need for irrigation being determined from observations on the rate of elongation of selected nodes of the cotton plant.

   Irrigations took place on 23 April, 30 May, 25 June, 9 July, 18 July, 27 July, 7 August, 16 August, and 24 August. As could be expected from such a frequent irrigation schedule, and a minimum, practical application of some three or four inches, it often exceeded the deficit and the profile was always high in moisture content. Also, no difference between the treatments could be detected in moisture content or in moisture depletion. Only during May was there some indication that moisture extraction took place to a somewhat greater depth on the mulched plots. Also, the moisture depletion from the layer between 9 and 21 inches seemed to be somewhat larger on the mulched versus the unmulched plot indicating a higher rate of evapotranspiration on the mulched plot. Immediately under the mulch, the soil was always more moist than on the untreated surface.

   In view of the large amount of irrigation water so frequently applied and the continued high moisture content of the profile and the seepage resulting therefrom, no conclusions whatsoever could be drawn from the data as to the consumptive use by the crop, let alone to conclude any difference between the two treatments.

2. Soil Temperature at the 5-cm Depth. Soil temperatures were significantly higher during the month of May by 2 to 3 F under the mulch as compared to the bare plot. By the end of May this difference increased to about 6 F following irrigation and decreased again to 2 to 3 F for the remainder of June. During July the

mulched plot was about 4 to 5 F warmer but by the beginning of August the difference had become quite small and seemed no longer significant. This finding is in general accord with that of others showing that black plastic films will result in an increased temperature of the soil, although not as high as will be obtained when using clear plastic.

3. Air Temperature at the 10-cm Height. During April and May the air temperatures tended to be lower in mulched plots compared to the unmulched ones by about 1 F. During June and July this difference persisted, though it was noticeably larger immediately after irrigation up to 3 F. During August the difference disappeared.

   These findings, though only a small difference on the margin of significance, indicate that evapotranspiration on the mulched plots may have been slightly greater during June and July than on the unmulched plots. This conclusion is corroborated by the fact that the plants on the mulched plots were generally somewhat higher, bushier, and had more leaves.

4. Net radiation. There was no difference in the net radiation between treatments either at the top or bottom level through the first week in June. After 10 June the crop began to shade the net radiometers located at a height of 20 cm and the radiation at that level was reduced to effectively zero by 10 July. In this respect no difference could be demonstrated between the two treatments. A malfunction was discovered in one of the net radiometers located over the mulched cotton. Since it was impossible to determine when this malfunction occurred, no comparisons of the net radiation measured over the treatments can be made.

5. Water Measurements. Trying to obtain accurate data on the amount of water applied to each plot proved to be difficult, if not frustrating. On the first irrigation the siphons were set for about 12 hours and a very large net application resulted of about 160 mm (6.5 inches). This being clearly out of line with the moisture deficiency of the profile, recommendations were made to reduce the time of set and in succeeding irrigations the amount of

water applied was generally less and was estimated from the deficiency of soil moisture of the profile. The amount of water applied varied between 75 and 125 mm (3-5 inches).

However, these are mere estimates of the amount of water that actually was applied to the test site or to any particular spot in the field since the field was laid out very unevenly and insufficient control existed over the head in the supply ditch as well as over setting the siphons in individual rows. An estimated total amount of water applied to the field during the growing period is 900 mm (35 inches) which, combined with initial available amount of some 250 mm (10 inches) is well in excess of the maximum possible consumptive use and results in a considerable amount of continuous downward seepage. Under such conditions it is not possible, as pointed out before, to arrive at any worthwhile conclusions with regard to water use. It should be stated that the layout of the field and the nature of the irrigation system was not conducive to the accurate control of water applied, nor to uniform and efficient water application.

6. Cotton Yields. The lint cotton harvested from the untreated plot was 6777 pounds or 1080 lbs/acre, whereas the mulched plot yielded 8372 pounds or 1340 lbs/acre, an increase of 24% over the control. These data are in line with the observations made on the field during the growing season.

On the same farm other comparisons were made, some of which were more favorable, others less favorable. The impression is that the increases due to mulching are greater as the over-all yields are higher. Actually, on the test plots reported the yield level was just fair. A great deal of additional agronomic field work must further elucidate the picture.

SUMMARY AND CONCLUSIONS:

The practice of "half-mulching" cotton with black, thin polyethylene film covering the ridges and allowing seed to germinate through it was examined. Most of the expected benefits were agronomic but effects specifically related to moisture conservation could also occur.

Therefore, the effects of mulching on soil and air temperature, on net radiation and on soil moisture utilization were measured. Before a closed stand was produced, soil temperature under the mulch was a few degrees F higher and air temperature over the mulch slightly lower. The latter effect is attributed to better growth and greater transpiration with the mulch. Net radiation and moisture utilization were not affected by mulching but the data were not very accurate and conclusive.

Yields were 24% higher on the mulched plot (2.7 versus 2.2 bales/acre), indicating a significant increase in water use efficiency. However, the type of data obtained so far do not give an explanation of the yield increase and a different approach is required.

PERSONNEL: C. H. M. van Bavel, L. J. Fritschen, K. J. Brust.

TITLE: EVAPOTRANSPIRATION FROM CROPS AS RELATED TO MANAGEMENT.

LINE PROJECT: SWC 4-gG2 CODE NO.: None

INTRODUCTION:

This experimental outline concerns the measurement of evapotranspiration from various crops as measured with the weighing lysimeters on the observation field south of the Laboratory buildings. These measurements serve many purposes as they are an integral part of energy balance studies, verification of aerodynamic transport models and of certain studies of the effect of soil moisture content and plant physiology on the losses of water to the atmosphere. However, the data, as such, have considerable interest in themselves since detailed data on daily and weekly evapotranspiration losses of field crops under arid conditions are not available. The reason for this fact is that only by means of weighing lysimetry can such measurements be made and suitable installations have heretofore not existed. Obviously, the evapotranspiration of a crop on a daily or weekly basis is not only dependent on the crop itself and its environment, but also the manner in which it is managed. The purpose of this work is to report on the conditions under which measurements were made, and to attempt to relate the data obtained to pertinent aspects of the crop and its management.

MANAGEMENT AND PROCEDURES:

The field was prepared for seeding during the first week of May and planted to sudangrass on 10 May. During the first few weeks the field and lysimeters were irrigated on 11, 15, and 28 May. The lysimeters were irrigated with small amounts in-between times to insure a good stand of sudangrass. Soil crusting created a stand problem. By 28 June a fairly complete and mature stand of sudangrass was obtained over the entire field. On lysimeter No. 1 and the associated checks Nos. 5, 6, and 7, the crop was held at a height between 20 and 40 cm at all times by periodic mowing. Irrigation took place on the entire field frequently enough so as to keep the soil at a high moisture content at all times until 15 August. After that, no irrigation was given until 14 September. The dates of irrigation and mowing for the entire field are indicated in Table 1.

Lysimeter No. 2 and the associated check No. 4, was mowed for the last time on 26 June after which the grass was allowed to grow to a height of approximately 150 cm and the development of some seed heads ensued between 15 and 19 July. On 24 July the surroundings of lysimeter No. 2 were mowed but not the lysimeter itself which remained isolated until 27 July. After this, No. 2 was treated as was No. 1.

Similar treatment was given to lysimeter No. 3 and the checks Nos. 1, 2, and 3. These were mowed for the last time on 12 June and allowed to grow until 16 July. By that time the height of the crop was approximately 2 m and a heavy development of seed heads had taken place. After 16 July the crop was allowed to re-develop and was treated similarly to lysimeter No. 1.

The entire field was plowed on 1 October. No data were obtained for the period 19 September through 30 September, owing to frequent small rains. During the period up until 18 September no rainfall of consequence fell.

The uniformity of the stand in the field left much to be desired at times. The stand in and, particularly, around lysimeter No. 1 was always sparse and spotty and data from this lysimeter probably cannot be considered as typical. The stand and environment of lysimeter No. 2 was relatively good throughout the season. The stand around lysimeter No. 3 was always good but the crop inside the lysimeter at first grew slowly and tended to lag behind its environment. After the first week in July the data from lysimeter No. 3 are considered reliable and at the end of the season the stand and environment of this particular lysimeter were the best of all. The mowing of the sudangrass generally was more or less a trim which left a green transpiring crop behind. However, when the crop was allowed to attain a considerable height as indicated above on lysimeters No. 2 and 3, the subsequent mowing left a stubble without any green leaves and it required some 10 to 14 days before a green cover was re-established on the plot.

Irrigation was supplied somewhat in excess of the measured evapotranspiration and twice during the season the excess moisture

accumulating in the bottom of the lysimeter was drained so as to maintain moisture content and tension approximately equal to that in the surrounding field. This was verified by weekly tensiometer and neutron moisture measurements.

Hourly measurements of evapotranspiration were made throughout the entire season with the exception of two days in June when equipment failure fouled up the data. On several days more intensive measurements were made, usually in connection with detailed studies of the energy balance or for the purpose of measuring the evaporative and sensible heat flux over the field. Hourly measurements were worked out and tabulated by hand; intensive measurements, usually in triplicate on a 15-minute schedule, were handled by the electronic computer.

RESULTS AND DISCUSSION:

In Table 1 the evapotranspiration from the sudangrass as measured on the three lysimeters is summarized by decades from May through September. Also, some of the most pertinent management features are given in this table. A direct comparison of the three lysimeters is not possible since they were not identically treated, as pointed out in the previous section.

However, through the second decade of June the treatment was quite comparable and the table shows that the amounts of evapotranspiration were not materially different between different lysimeters. Much of the water lost during this period must have been direct surface evaporation since, particularly during May, the lysimeters were irrigated quite frequently with small amounts of water. A tendency can be noted of lysimeter No. 1 to lose more water than the others, a feature which persisted throughout the season. This is attributed to the fact that the stand in lysimeter No. 1 was notably better than that of the immediate surroundings of the lysimeter which actually had some bare areas. Thus, sensible heat could easily be transferred from the environment onto the lysimeter and thereby increase the evaporation in comparison with the other two lysimeters which had a more normal environment.

During the third decade of June and also the first two decades of July, it can be seen that lysimeter No. 3, which now had the tall crop with developed flowers and seed heads in it, was appreciably less than that of lysimeter No. 2 which had a vegetative normal cover. The mowing of lysimeter No. 3 during the second decade of July resulted in a low evaporation rate for two or three days after which rapid regrowth resulted in a rate of loss which was actually considerably greater than that taking place when the grass was very tall. Compare, for example, the second and third decade of August with the third decade of June and the first decade of July.

Lysimeter No. 2 was mowed during the third decade of July from a tall crop and was much slower in recovering as evidenced by the data for the first, second, and third decade of August. Beginning with the third decade of August all three lysimeters were again in a comparable condition and comparable amounts of water were lost from all three.

Taking the season as a whole, the conditions on lysimeter No. 2 were considered to be the most representative. A more detailed picture is given in Figure 1 of management operations and the daily loss of water from lysimeter No. 2. In this figure, individual irrigations are shown together with the time of day on which the water was applied (hatched circles). Also shown are the dates of mowing of the grass. The mowing that took place on 16 July only applied to the surroundings and not to the lysimeter proper. On the 19th the lysimeter itself was mowed.

It may be seen from Figure 1 that during the initial stages of development, including the first two decades of June, irrigation during the morning hours generally resulted in an increase of the daily evaporation rate on the same day that irrigation took place as well as on the following day. This is understandable since much of the water losses took place as evaporation from the surface which had become dry immediately prior to irrigation. The irrigation cycle starting with the application of water on 29 June shows an interesting reversal in trend. Immediately following irrigation, the daily rate of loss increases and then shows a tendency to decrease again. However, this

trend does not persist but reverses itself, indicating that now a predominant part of the water loss took place in the form of transpiration. The dip in the evaporation rate is in part caused by a day on which solar radiation was less than normal as shown in the solar radiation graph in Figure 1.

The following two irrigation cycles show very clearly that on the day of irrigation the loss of water is appreciably less than one would normally expect and also that the evapotranspiration is not notably increased on the days following irrigation. To a lesser extent, this can also be noted from the irrigations that took place on 8 August and 16 August.

The mowing of the surroundings of lysimeter No. 2 on 25 July resulted in a very large increase in evapotranspiration from the lysimeter as a result of its being exposed to an area evaporating at a low rate and also to radiation and wind movement in a manner entirely opposed to that of a closed stand. Evaporation rose to 16 and 15 mm per day on the 25th and 26th. A detailed study of the hourly evaporation rates on those days showed that the evaporation from the crop followed exactly the energy input curve and demonstrates that the uptake of water by the root system of the crop, its conduction through the stem, and the transfer of water vapor from the interior of the leaves to the atmosphere are, in this particular case, not controlling the rate of evaporation. There is, for example, no indication of any flattening out of the evaporation curve during the day nor the existence of what is sometimes referred to as a midday depression in transpiration. Following the cutting off of the tall crop on 28 July evaporation rates dropped to 2 mm per day and exhibited a slow recovery which took about 30 days until the end of August.

No irrigation was applied after 8 August until 14 September. At the end of this period, some 200 mm of water had been depleted from the soil profile, but moisture content was still relatively high, particularly at depths below 2 feet. The evaporation rate from the crop shows little if any effect of the decline of soil moisture content

even though immediately after the irrigation of 14 September the evaporation rate seemed to increase slightly. It was not possible to protract the drying period any more to study the effect of a continued depletion of soil moisture.

Detailed aspects of the evapotranspiration from sudangrass such as the energy balance at different stages of development and attempts to measure the evaporative flux aerodynamically will be reported elsewhere.

SUMMARY AND CONCLUSIONS:

Sudangrass was grown on the lysimeter field from 10 May 1962 until 17 September 1962. The crop was frequently irrigated and mowed to maintain a height of 30 to 50 cm. In two instances the crop was allowed to attain full height (150-200 cm) and achieve maturity, after which it was mowed low again.

Daily and hourly amounts of evapotranspiration were routinely obtained, greater detail being studied for selected situations.

When the soil surface was significantly exposed and, presumably, evaporation from the surface was important during early development of the crop, irrigation resulted in a subsequent increase in water loss. However, on a fully developed stand the opposite took place on the day of irrigation and the following days showed no increase in evapotranspiration rate.

Four weeks without irrigation during August had no measurable effect on evapotranspiration, however, the period was not long enough to exhaust more than one-half of the available soil moisture supply.

Special tests showed that the ability of the crop to extract, transport and transpire water never limited the water loss. The determining factor was the ability of the evaporating surfaces to extract the required energy from radiant and sensible heat sources.

PERSONNEL: C. H. M. van Bavel, L. J. Fritschen, W. E. Reeves.

TABLE 1. Evapotranspiration in mm from sudangrass in 1962.

Month	Decade	Amount			Management
May	2	48.5	49.1	36.9	Irrigated frequently.
	3	41.6	42.9	39.2	Irrigated frequently.
Jun	1	48.3	45.9	41.8	Mowed, irrigated.
	2	60.2	55.1	51.5	Mowed 1 and 2, irrigated twice.
	3**	76.3	72.4	57.6	Mowed 1 and 2.
Jul	1	66.1	72.1	53.8	Mowed 1, irrigated.
	2	95.0	88.2	57.7	Mowed 3, irrigated.
	3	80.0	88.1	63.4	Mowed 2*, irrigated.
Aug	1	98.2	45.7	83.2	Irrigated.
	2	107.3	54.0	83.0	Mowed, irrigated.
	3	82.1	77.7	83.1	Mowed.
Sep	1	59.3	63.8	70.7	Mowed.
	2	60.1	59.1	66.4	Irrigated.
Total		923.0	814.1	788.3	

* #2 was isolated for 3 days giving abnormally high values.

**Data partially estimated due to equipment failure.

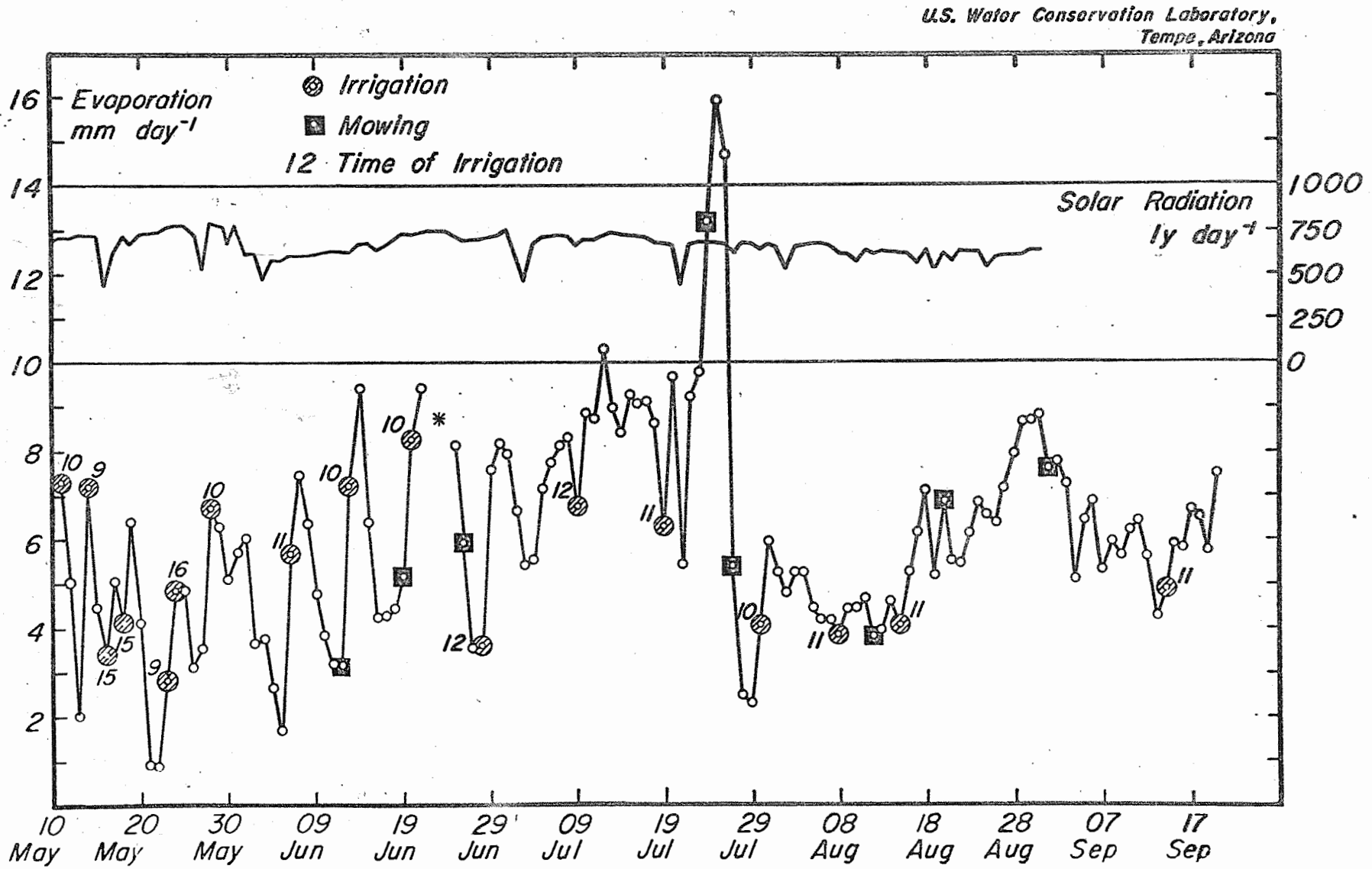

Figure 1. Daily rate of evapotranspiration from sudangrass as measured on lysimeter No. 2 and solar radiation as measured at Sky Harbor Airport (Phoenix Weather Bureau data).

Annual Report of the U.S. Water Conservation Laboratory

TITLE: MEASUREMENT OF EVAPOTRANSPIRATION.

LINE PROJECT: SWC 4-gG2 CODE NO.: None

INTRODUCTION:

For many practical applications it is sufficient to measure evapotranspiration over periods of one to several days. Methods sometimes used to this end are soil moisture measurement or a percolation type lysimeter. Neither method has, however, the required precision. Also, the data can be seriously biased. A weighing lysimeter, properly exposed and operated, is the only reliable method whereby evapotranspiration (or consumptive use) can be found over short periods of time.

Based on experience gained with the precision lysimeters at the Laboratory, a design was sought that would meet the requirements stated, that would, mechanically, be as simple as possible, and that would, in installation and operation, cost no more than other methods that can give comparable results.

As an acceptable design criterion it was required that the instrument should have a precision of 2% in determining weekly amounts of evapotranspiration. It will be shown that, even during periods of low evapotranspiration, this criterion can be met by the proposed design.

Construction details. The lysimeter consists of 2 square containers that fit into one another. The inner bin is 100 × 100 × 100 cm inside dimensions and the outer bin has 1 cm clearance around and 25 cm clearance underneath (Figure 1). Both bins are made from 2.7 mm (12 gauge) galvanized sheet metal. The outer bin is reinforced by four horizontal angle iron ribs (1 1/2 inches × 1/8 inch) placed approximately 25 cm apart; and the inner bin is reinforced by two similar angle iron ribs, one 18 cm from the top and the other at 58 cm. The bottom of the inner bin is reinforced by two similar angle iron ribs, one 18 cm from the top and the other at 58 cm. The bottom of the inner bin is reinforced by 8.0 mm channel iron (2 inches × 6 inches) in order to give the required rigidity when filled with soil. The total weight of the empty bin is 162 kg. Filled with air-dry soil, it weighs about 1400 kg.

A lifting device consists of two steel rods (5/8 inch) in a center position on two opposite sides of the bin. These rods are threaded on both ends and pass through the center of the angle iron reinforcements and bottom of the bin. They are fastened to the channel iron with lock washers and two nuts, one on each side of the channel iron. Removable sleeve connections and eyebolts are attached to the tops of the rods when the bin is to be lifted. The tops of the rods are about 10 cm deep to allow for cultivation. By passing the rods through the angle iron, the bin is prevented from tipping sideways when being lowered into position. The lifting was accomplished by passing a steel rod (1 inch) through the eyebolts and utilizing a fork lift truck.

The load cell (see "Weighing Procedure") is mounted on a 20- × 20- × 2-cm steel base plate using four bolts (1 × 1/4 inch) tapped into the base of the load cell. The bolts are counter-sunk so that the heads of the bolts are flush with the bottom of the base plate. This assures a uniform distribution of the load. The base plate rests in the center of the bottom of the outer bin, and the outer bin rests on a footing. The latter consists of about 10 cm of gravel and a 130- × 130- × 15-cm cement slab.

The inner bin is prevented from tipping to the sides by placing 7.5- × 2.5-cm fiber glass tape straps (Scotch brand) from the inside of the inner bin to the outside of the outer bin. Three straps in three locations on each of the four sides was sufficient to maintain the bin in a stable position. These fiber glass tapes have no effect on the vertical movement of the inner bin but are successful in preventing side movements. They function effectively as stabilizing flexures.

Both bins, inside and outside, were painted with two coats of asphalt paint and then sun-dried to prevent rust. The paint remained somewhat sticky but this did not affect the operation of the lysimeter in any way. A catalyzed coal tar epoxy (#78 Amercoat Corp.) may be better and will be used in the future.

A permanent butyl gasket 9 cm wide and 1 mm thick was installed. This gasket is sealed air tight with butyl cement and the lysimeter can be flooded over during irrigation. A copper tube (1/4 inch) air breather about 17 cm high was attached to the outer bin to prevent the build-up of pressure between the bins. This also serves as a means for detecting leaks in the gasket by applying with a mouth tube a vacuum or pressure and noting if there is any change on the strain indicator dial when the tube is closed (see "Weighing Procedure"). If a leak is present, the dial will return rapidly to the original balance position.

Drainage System and Fill. The drainage system consists of two filter candles (Selas), each 5 cm in diameter and 25 cm long. They are placed about 48 cm apart and 25 cm from the sides of the bin. On the bottom there is 145 kg of fine sand and a 1-cm layer of 28μ glass beads. The glass beads also surround the filter candles. The filter candles are connected to polyethylene tubing (1/2-inch ID) which runs horizontally to the side of the bin where it is joined to a female reducer elbow (Swagelok). From there polyethylene tubing (1/2-inch ID) runs vertically to about 10 cm above the ground surface.

The bubbling pressure of the filter candle is 240 mb. Water is extracted by employing a vacuum pump set. The water from each filter candle is collected in a suitable container and can be measured by placing the containers on the lysimeter and noting the difference in readings. The total drainage system is 11 cm deep and the materials (candles, sand, and glass beads) weigh 172 kg. The density is 1.56 gm cm^{-3}.

The soil was removed from the pit in 30-cm layers, air dried, and then sifted with a 1.3-cm sieve. The remaining 85 cm of the inner bin was packed in 5-cm layers to a density of 1.42 gm cm^{-3}. The total depth of the soil column and drainage system is 96 cm, with 4 cm left on the top for irrigation water. The oven dry weight of the soil column plus the drainage system is 1361 kg and the total volume occupied is 0.958 m^3, not counting the angle iron and rods. The air space in this column is 0.444 m^3. Thus the maximum (saturated)

weight should be 162 + 1361 + 444 = 1967 kg, well under load cell capacity. The weight after wetting and drainage is about 1810 kg, indicating a moisture content of about 287/.958 = .30 volume fraction.

Weighing Procedure. For the weight measuring device, a Baldwin SR-4 type CXX load cell with a 5,000-lb (2,250 kg) capacity was used. The total weight of the inner bin can thus be measured directly, eliminating the use of a balance and counterweights. The inner bin rests on one pivot point, the load cell button. This required a hardened steel plate of Rockwell C-40 hardness and RMS-63 finish mounted in the center position of the reinforcing channel iron using four bolts (1 × 3/8 inch) tapped into the channel iron. The plate is 10 × 10 × 1.3 cm sufficiently dimensioned that it will not crack under the concentrated load.

The cable from the load cell runs underground and the end is located at ground level about 1 m from the lysimeter. At predetermined time intervals, a portable strain indicator (Baldwin SR-4 Type "N") is attached and the reading is attained in microinches per inch with a sensitivity of .1 microinch per inch. By setting the gauge factor at 1.77, the difference between readings, when multiplied by 5, gives the weight change in kg or mm.

Installation and Results. The inner bin was filled with soil during the period from 24 September 1962 to 5 October 1962. After final preparation of the pit and reinforcing of the outer bin, the lysimeter was installed on 24 October 1962. A calibration check was made by adding 25 kg increments up to 75 kg. The readings showed an increase of 74.5 kg when the total amount was added and a decrease of 75.0 kg when taken off. This is within the sensitivity of 0.5 kg. Rye grass was planted on 21 November 1962 and then the lawn and lysimeter was flooded over. The installation functioned properly.

Daily readings were started on 1 November 1962 and were taken Monday and Friday at 0800. The data over the weekend were averaged from 0800 Friday to 0800 Monday or for three days. The daily evaporation rates are for a 24-hour period extending from 0800 to 0800. Table 1 gives the daily evaporation rate for weekly periods during December.

The rainfall data is taken from the data supplied by three Bytrex lysimeters, but a recording raingauge could also be used. On 26-30 November 1962 the lysimeter was drained. About 122 mm of water was extracted, bringing the lysimeter to field conditions, a moisture content of about 25.7 percent by volume.

SUMMARY AND CONCLUSIONS:

A simple and economical weighing lysimeter has been designed, based on the use of a single, precision load cell and a portable strain indicator. The total weight is read directly without the use of a balance and counterweights. Evapotranspiration over a period from one to several days is found by periodic weighings.

The total weight of the 1 m^3 lysimeter is about 1800 kg at field capacity and is found with a precision of .5 kg, equivalent to 0.5 mm of water. To insure normal drainage, the lysimeter is provided with two filter candles on the bottom for water extraction. Stabilization of the inner bin is accomplished with fiber glass tape flexures. The lysimeter is sealed with a butyl gasket which enables it to be flooded over during an irrigation.

The lysimeter was installed in a rye grass lawn in October 1962. After preliminary adjustments, reliable daily data are being routinely obtained without difficulty.

PERSONNEL: C. H. M. van Bavel.

TABLE 1. Daily Evaporation Rate for Weekly Periods from Ryegrass as Found with Tempe Field Lysimeter.

Date	Readout	Change of Previous	mm	Rain	Total	mm/day
03 Dec	1465.5	--	--	--	--	--
10 Dec	1463.3	-2.2	11.0	0.0	11.0	1.6
17 Dec	1461.3	-2.0	10.0	0.0	10.0	1.4
26 Dec	1461.0	-0.3	1.5	12.1	13.6	1.5
31 Dec	1459.5	-1.5	7.5	0.0	7.5	1.5

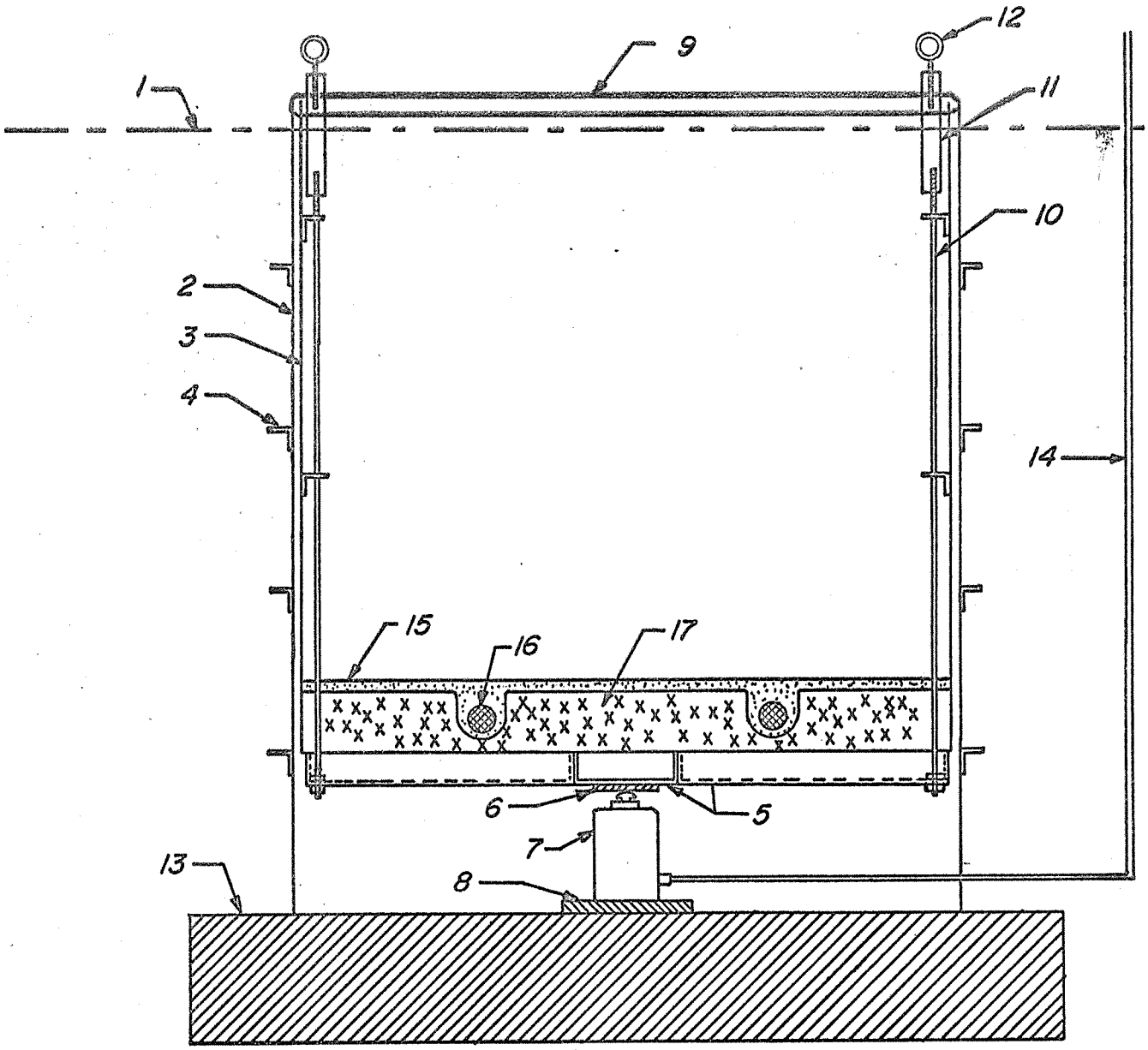

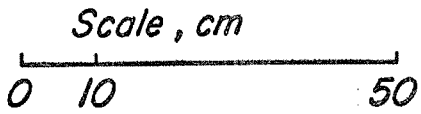

1. Ground level.
2. Outer bin.
3. Inner bin.
4. Angle iron.
5. Channel iron.
6. Load plate.
7. Load cell.
8. Base plate.
9. Butyl gasket seal between bins.
10. Lifting rod.
11. Sleeve connection
12. Eyebolt.
13. Footing.
14. Cable to indicato
15. 28μ glass beads.
16. Filter candle.
17. Fine sand.

Figure 1. Lysimeter assembly.

TITLE: APPLICATION OF HEXADECANOL - OCTADECANOL MONOFILMS TO SMALL PONDS

LINE PROJECT: SWC 4-gG2 CODE NO: Ariz.-WCL-9

INTRODUCTION:

See Annual Report - 1960.

The work conducted in the last two years has shown there are many problems encountered while applying the tallow alcohol in floating, wire-mesh rafts. Bacterial action sometimes damaged the alcohol, and stranding of the rafts as the water level declined was a problem on some ponds. An alternate method of applying the tallow alcohol in a liquid form was investigated.

Other research workers have succeeded in emulsifying the alcohol but have encountered problems in obtaining a stable emulsion while still retaining the ability of the monolayers to form. With limited laboratory studies, we were able to develop an extremely stable emulsion of tallow alcohol with a commercially available emulsifier which was designated E-1.

PROCEDURE:

The emulsified tallow alcohol was evaluated by measuring evaporation of distilled water from 600 ml beakers with a water surface area of 62.05 cm^2. The emulsion was applied to the water surface with a pipette or dropper. The pipette discharged 30 drops of diluted emulsion per gram; therefore, a rate of one drop of emulsion per beaker per day of 0.1 per cent tallow alcohol is the equivalent to 1.45 pounds of tallow alcohol per acre per month. The dropper discharged 20 drops per gram and one drop of emulsion per beaker per day is equivalent to 2.15 pounds of tallow alcohol per acre per month. The treatments were run in triplicate, and the amount of water lost was determined by weighing the beakers daily. Location effects were minimized by daily rotation of beaker positions. Treatment effectiveness was evaluated by comparing evaporation from treated and untreated beakers.

RESULTS AND DISCUSSION:

The beakers were first located indoors where the air temperature and vapor pressure deficit were essentially constant at 24° C and

20.29 millibars respectively during the 22 day test period. Emulsion was applied to one set of beakers at an equivalent rate of 1.45 pounds of tallow alcohol per acre per month. Flakes of alcohol were continuously floated on the water surface in another set of beakers. For the test period the loss was: untreated - 272.19 grams, flakes - 174.08 grams, and emulsion - 164.58 grams. Percentage reductions in evaporation were: flakes - 39.5 per cent, emulsion - 36.0 per cent.

The beakers were next placed on the roof of the main laboratory building with emulsion applied at the following rates to four sets of beakers: 21.5, 10.75, 6.45, and 2.15 pounds per acre per month. A fifth set of beakers was continuously treated with flakes and a sixth set was used as an untreated control. The air temperature and vapor pressure deficit ranged from 15 - 50° C and 6.82 - 111.0 millibars respectively. Evaporation loss for the 12 day test period was determined by weighing the beakers daily. Evaporation losses and evaporation reduction data were as follows for the 12 day measurement period from 5-25-62 to 6-6-62.

Treatment	Loss (grams)	Reduction (per cent)
Untreated	1237.50	[illegible]
Flakes	781.76	36.8
Emulsion - 21.5 pounds/acre/month	599.77	54.0
Emulsion - 10.75 pounds/acre/month	691.55	44.1
Emulsion - 6.45 pounds/acre/month	876.71	29.2
Emulsion - 2.15 pounds/acre/month	1171.05	5.5

The higher rates of emulsion were more effective than the flakes in reducing evaporation. Although evaporation from beakers cannot be compared directly to evaporation from larger bodies of water, the measurements show that it is possible for tallow alcohol emulsions to effectively reduce evaporation.

Storage and temperature fluctuation tests showed the emulsion to be very stable. No separation occurred in samples which had been stored for 11 months, heated to 60° C, and frozen solid.

These preliminary tests indicate that the emulsion will reduce evaporation as well or better than flakes and is very stable. The liquid material will be easier to apply than flakes or powders. Additional testing in larger tanks and in the field seems justified, and the necessary procedures and facilities are being developed.

SUMMARY AND CONCLUSIONS:

A stable emulsion of tallow alcohol has been developed which may be more effective than flakes or powders for reducing evaporation from water surfaces. This indication was obtained with tests utilizing small glass containers of water exposed on a building roof. The continuous presence of flakes reduced evaporation by 37 per cent over a 10 day period while emulsion, applied at a rate of 11 pounds per acre per month, reduced evaporation by 44 per cent. Stability of the emulsion is excellent and it has not broken down during heating to 60° C, freezing, or storage for 11 months. These test results appear quite promising, particularly when the opportunities for simple application devices are considered.

PERSONNEL:

Lloyd E. Myers, Gary W. Frasier.

TITLE: SOIL TREATMENT TO REDUCE INFILTRATION AND INCREASE PRECIPITATION RUNOFF

LINE PROJECT: SWC 4-gG3 CODE NO: Ariz.-WCL-7

INTRODUCTION:

See Annual Report for 1960.

Controlled penetration of asphaltic materials sprayed on the soil surface is desirable for two reasons. First, the asphalt would be protected by the soil against deterioration caused by the combined effects of radiation, oxygen, and heat. Second, creation of a strong pavement would reduce requirements for fencing and other protective measures against mechanical damage. A desirable treatment would result in a uniform penetration of 5 to 10 per cent asphalt, by weight of soil, to a depth of from one-half to one inch. Previous construction methods have produced such a pavement by mechanical mixing. We have initiated work aimed at producing a strong but inexpensive pavement with surface spray applications.

The Granite Reef Test Site is now completed and provides fifteen 100 square foot plots, seven 2,500 square foot plots, and three small natural watersheds of 5,000 square feet. Figure 1 shows the general layout.

We have been fortunate in initiating a cooperative field program with the Bureau of Indian Affairs. Experimental treatments are being installed on operational water harvesting structures used to obtain water for livestock. These operational trials have already provided invaluable information.

PROCEDURE:

Procedures were the same as outlined in the 1960 and 1961 Annual Reports with the following additions.

The penetration of soil stabilizing compounds was evaluated in shallow 10 x 10 x 1.5-inch cake tins. The soil was air dried and mixed for 10 minutes in a blender with sufficient quantity of water to bring the moisture content to 10 per cent by weight. The wetted soil was compacted into the cake tins by dropping a 2-pound weight a distance of 25 inches, 6 times on the center of a 7.25 x 7.25-inch,

0.75-inch thick plywood board which was placed on the smoothed soil surface. Treatments were sprayed on the soil surface and the actual rate of application was determined by weighing the pans before and after spraying. The depth of penetration was determined 24 hours later by removing slices of soil from 3 locations in each pan, measuring the depth of penetration to the nearest 0.125 inch, and averaging the 3 measurements.

Runoff from the 2,500 square foot plots and the small watersheds is measured with household-type water meters. Laboratory tests showed that water will flow through these meters without recording unless the meters are started by a slight pressure surge. Once the meters are started, they will record a flow as small as 0.5 gallons per minute with an error less than 2 per cent. Two-stage float valves were designed and constructed which do not open until 4 inches of head have built up in the reservoirs, remain open until the reservoirs drain, and then reset for the next rain. These valves have been installed on all water meters at the Granite Reef Site. The meters still stop on occasion because of silt. A new measuring system is being designed. Runoff measured to date represents a minimum value.

RESULTS AND DISCUSSION:

The work in 1962 has related primarily to field testing of materials which seemed promising in laboratory tests. Considerable effort was devoted to the development of field testing sites, application procedures and equipment, and systems for measuring rainfall runoff.

Water Repellents: All water repellents tested to date have deteriorated under high soil temperature conditions. A new repellent designated R-8 was found to waterproof soils to a depth of one inch where other repellents were surface treatments only. Temperatures exceeding 60° C will cause R-8 to break down, however, it has not been completely destroyed on a 100 square foot plot at Granite Reef. This plot, number 6 on Table 2, was treated on December 22, 1961, at a rate of 250 pounds per acre and has consistently produced higher runoff than the untreated control plots. During the period January 13, 1962

to December 24, 1962, precipitation totalled 5.35 inches. Runoff from the R-8 treated plot was 50.6 per cent of the total as compared to 9.9 per cent runoff from the untreated plot.

Additional work with R-8 is planned in addition to work on a new repellent R-9 which should be more heat resistant.

Soil Stabilization: Penetration of soil by cationic asphalt emulsion, designated S-1, was obtained by modifying it with additional solvent, water, and surface active agents. The unmodified cationic emulsion will not penetrate most soils because of rapid bonding to the surface soil particles. We believe that the modification permits penetration by temporarily neutralizing the positive charge on the asphalt particles. Typical penetration data are presented in Figure 2. Penetration increased with increasing application rates for all modifications suitable for field use and was not appreciably different for the two test soils. Additional testing is in progress to measure the mechanical strength of the treated soil layer.

Asphalt - Aluminum Foil: A new treatment has been developed which consists of 1-mil aluminum foil bonded to the soil surface with cationic asphalt emulsion. The foil is unrolled from a spindle mounted just ahead of a foam rubber roller which presses the metal sheet against the soil. Asphalt emulsion is sprayed on the soil surface immediately ahead of the unrolling foil which is laid down in overlapping 4-foot wide strips. The treatment has been installed on a 2,500 square foot plot at Granite Reef for over one year with no sign of deterioration, although some of the lap joints have required resealing. This problem has not been serious and can be solved by using a modified asphalt material to seal the laps. Cost of materials is about 18 cents per square yard. The aluminum foil is surprisingly strong when bonded to the soil and the life of the treatment will depend primarily upon the durability of the foil-asphalt-soil bond.

Granite Reef Field Plots: The 100 square foot plots covered with butyl and polyethylene sheeting have consistently caught more rainfall than a close-by, calibrated, recording raingage. These

data, shown in Table 2, raise some interesting questions concerning raingage measurements. An additional raingage is being installed to verify these results.

Treatments applied to the 100 square foot plots are listed in Table 1 and the runoff data are given in Table 2. The butyl rubber shows no sign of deterioration. All plots treated with asphalt emulsion S-1 are deteriorating with runoff decreasing with increasing exposure time. Plot 6, treated with water repellent R-8, has been previously discussed. Plot 5 was covered with 1.5-mil black polyethylene on July 26, 1962, and the material showed signs of deterioration within six months. No repairs will be made.

Treatments applied to the 2,500 square foot plots are listed in Table 3 and runoff data are presented in Table 4. The butyl rubber on Plot 4 shows no sign of deterioration. Observations of the asphalt aluminum foil on Plot 3 were given previously. Observations of other plots are as follows.

Plot 1, treated January 17, 1962, with a light surface coat of asphalt emulsion S-1 and water repellent R-8, had deteriorated noticeably by July. A network of fine surface cracks developed with slight curling on the edges of the cracks. This problem was the result of almost zero penetration. Observation of the deterioration was continued during 1962. The plot will be retreated with a light spray of S-1 and will be maintained with additional applications as needed. These applications are inexpensive, about 4 cents per square yard, and the interval between maintenance treatments may increase as continued applications are made.

Plot 2, rough shaped with a road patrol and hand smoothed to a 5 per cent slope at a cost of about 4 cents per square yard, has shown no sign of erosion and produced 16.0 per cent runoff from the total of 4.99 inches rainfall during 1962. Runoff from a small untreated watershed, with an average slope of about 10 per cent and covered with desert pavement, has averaged about 6 per cent. Under favorable site conditions the smoothed soil treatment may deserve consideration.

Plot 5 was cleaned and retreated on September 18, 1962, after the failure of the S-1 and R-8 treatment. The new treatment was S-1 modified to penetrate into the soil. A strong, tough pavement about one-half inch thick was produced which was slightly porous as expected from laboratory testing. Although a seal coat will be applied, we allowed the base coat to remain exposed throughout the remainder of 1962. After four months exposure, only slight weathering could be visually observed.

Hualapai Indian Reservation: Two field size operational catchment areas were installed in cooperation with the Bureau of Indian Affairs on the Hualapai Indian Reservation near Peach Springs, Arizona. These installations gave us an opportunity to observe problems encountered under actual field conditions and provide weathering information for a climate including severe wind and freezing conditions.

The Blue Mountain Catchment Area is 100 x 100 feet, constructed in a diamond shape, and arranged on a 5 to 6 per cent slope. It is divided into two treatments on its downslope diagonal. One treatment consists of aluminum foil and fiberglass matting bonded together and to the soil with S-1. The other half of the plot was covered with 1.5-mil black polyethylene glued to the soil with asphalt. The soil in this area was very rocky and, to prepare a smooth plot, the entire area had been covered with one-half inch of sand. The sand covering was loose and it was difficult to obtain good bonding between the soil and the sheetings. The polyethylene was destroyed by wind within a month. A new covering of polyethylene was installed with edges buried every 12 to 16 feet. Again the wind destroyed the covering. During the next year, this area will be treated with a new treatment selected from laboratory studies. We found that even a slight wind can hinder the laying of the aluminum or plastic sheetings. It was necessary to repair a small section of the aluminum foil-fiberglass two weeks after installation. A "dust-devil" or whirlwind apparently loosened the lap joints before the S-1 had time to set properly.

The second site installed on the Hualapai Reservation is designated the Nelson Road Catchment Area. This catchment was constructed as a square, 100 x 100 feet, o n a 6 to 7 per cent slope

with a storage pit across the lower side. The storage pit is 50 x 100 feet by 8 feet deep, excavated with a bulldozer. A pipe leads from the bottom of the pit to a watering tank with a float valve to control outflow from the pit. The pit was lined with fiberglass matting and S-1 which laboratory studies had indicated were capable of holding a 13 foot head of water. The pit provides storage for 125,000 gallons of water at a total cost of $600.00. This catchment area is also divided into two treatments each with an area of 50 x 100 feet. One-half of the plot is covered with S-1 and the other half is aluminum foil with S-1 as a binder. Several weeks after installation, a section 20 x 20 feet of the aluminum foil was damaged by wind. This area was repaired and appears to be withstanding further damage by wind. The asphalt S-1 treatment area deteriorated quite rapidly and was resprayed 3 months after the original treatment.

Equipment: The 25-foot spray boom has performed beautifully and will treat 1,250 square feet per minute with excellent uniformity. Nozzles with swirl plates were originally used to spray water and unmodified cationic emulsion. These nozzles would not handle materials of higher viscosity, such as modified emulsions, and were replaced with deflector-type nozzles which provide an adequate spray pattern, operate at lower discharge pressures, and are relatively trouble-free.

We have had to make a number of modifications in application equipment since our operations are somewhat non-standard. For example, considerable difficulty was encountered in spraying cold asphalt emulsion at high altitudes with a small gasoline powered gear pump. This problem was solved by installing a small scooter transmission between the engine and the pump. We believe that most of the field equipment problems have now been solved.

SUMMARY AND CONCLUSIONS:

Recent work has shown that a strong, inexpensive, and potentially durable pavement for water harvesting can be created by spraying modified asphaltic compounds on the soil surface. Laboratory findings were confirmed by field testing when a 2,500 square foot plot was

sprayed with modified cationic asphalt emulsion to produce a tough, 3/4-inch thick pavement. The application was made in two minutes spraying time. Previous methods have relied on mechanical mixing to produce such a pavement. Our work is aimed at modifying asphalt compounds to improve durability and to provide controlled distribution of the asphalt within the depth of soil penetrated by the asphalt. Results to date are promising.

A new ground cover has been developed which consists of aluminum foil bonded to the soil with cationic asphalt emulsion. The foil is unrolled from a spindle mounted in front of a foam rubber roller which presses it against the soil which is sprayed with emulsion immediately ahead of the spindle. No deterioration has been detected in a 2,500 square foot plot exposed at Granite Reef for one year. Additional plots are under test in northern Arizona under conditions of freezing and high winds. The foil is surprisingly strong when bonded to the soil. Should the foil-asphalt-soil bond prove sufficiently durable, this will be an excellent treatment for water harvesting.

Runoff from bare soil plots, with and without a water repellent, have produced more runoff at Granite Reef than was expected. A 2,500 square foot plot smoothed to a 5 per cent slope with a road grader and hand labor has produced 16 per cent runoff from an annual total of 5.99 inches during 1962. No erosion has been observed. Runoff from a 100 square foot plot, with 3 per cent slope, no surface preparation, and sprayed with a water repellent in December 1961, was 51 per cent. Runoff from a 5,000 square foot untreated area was about 6 per cent. The cost of the smoothed soil and water repellent treatments is low, from 2 to 4 cents per square yard, and both treatments deserve additional attention.

Plots treated with surface sprays of cationic asphalt emulsion began to deteriorate within six months of almost zero soil penetration. One plot will be maintained by additional top sprays as required. The applications are inexpensive, about 4 cents per square yard, and the interval between maintenance treatments may increase as the surface

is built up by continued maintenance.

Two experimental water harvesting structures have been installed on the Hualapai Indian Reservation in cooperation with the Bureau of Indian Affairs. Valuable experience has been obtained in construction methods required under conditions of high wind. The wind rapidly destroyed a polyethylene ground cover and caused problems in applying asphalt and aluminum foil treatments. As a direct result of this experience, we have initiated work to develop treatments which will not be damaged by wind.

PERSONNEL:

L. E. Myers, G. W. Frasier.

Table 1. Treatments of 100 square foot test plots at Granite Reef.

Plot	Treatment Date	Treatment
1	1-5-61	S-1 at 0.45 lb/yd^2
		R-1 at 0.021 lb/yd^2
	8-25-61	Retreated with R-1 at 0.021 lb/yd^2
2B	5-18-61	30-mil butyl rubber sheet
3B	9-15-61	S-1 at 0.90 lb/yd^2 upper half
		S-1 at 1.80 lb/yd^2 lower half
4	9-15-61	Untreated
5A	9-22-61	S-1 at 0.90 lb/yd^2 upper half
		S-1 at 0.45 lb/yd^2 lower half
		R-1 at 0.021 lb/yd^2 right half
		R-8 at 0.031 lb/yd^2 left half
6	12-22-61	R-8 at 0.052 lb/yd^2
5B	7-26-62	1.5-mil black polyethylene

Table 2. Runoff data from 100 square foot plots at Granite Reef.

Date	Rainfall Total	Rainfall Intensity	Plot 1 Runoff		Plot 2B Runoff		Plot 3B Runoff		Plot 4 Runoff		Plot 5A Runoff		Plot 5B Runoff		Plot 6 Runoff	
	(in.)	(in/hr)	(in.)	(%)	(in.)	(%)	(in.)	(%)	(in.)	(%)	(in.)	(%)	(in.)	(%)	(in.)	(%)
1-13-62 1-21-62	.92	.15	.433	47.3	.964	105.4	.564	59.7	0	0	.578	63.2			.290	31.7
1-23-62	.14	.07	.064	45.7	.161	115.0	.089	63.8	0	0	.112	80.0			*.032	22.9
1-24-62	.06	.06	.016	26.7	.081	135.0	.010	16.7	0	0	.010	16.7			.010	16.7
1-26-62	.18	.18	.096	53.3	.193	107.2	.129	71.7	.064	35.6	*0	0			.145	80.6
2-07-62	.15	.05	.048	32.0	.161	107.3	.129	86.0	0	0	.129	86.0			.096	64.0
2-11-62	.06	.02	0	0	.096	160.0	.048	80.0	0	0	.032	53.3			.032	53.3
2-19-62	.24	.20	.112	46.7	.242	100.8	.177	73.8	0	0	.179	74.6			.169	70.4
2-21 2-25-62	.38	.20	.273	71.8	.450	118.4	.337	88.7	.096	25.3	.369	97.1			.321	84.5
2-27-62	.15	.10	.048	32.0	.153	102.0	.096	64.0	0	0	.112	74.7			.096	64.0
3-09-62	.12	.12	.048	40.0	.137	114.2	.087	72.5	0	0	.089	74.2			*.032	26.7
3-19-62	.61	.15	.273	44.8	.690	113.1	.433	71.0	.048	7.9	.450	73.8			*.290	47.5
3-21-62	.06	.15	.016	26.7	.081	135.0	.056	93.3	.003	5.0	.064	106.7			.040	66.7
6-28-62	.14	.20	.016	11.4	.145	103.6	.064	45.7	.003	2.1	.064	45.7			.024	17.1
7-21-62	.04	.02	0	0	.048	120.0	.008	20.0	0	0	0	0			.003	7.5
7-28-62	.31	1.20	.154	49.7	.321	103.5	.154	49.7	.112	36.1			.353	113.9	.306	98.7
9-20-62	.40	.50	.169	42.3	.474	118.5	.257	64.3	.064	16.0			.530	132.5	.145	36.3
9-23-62	.33	.10	.064	19.4	.369	111.8	.161	48.8	.032	9.7			.385	116.7	.169	51.2
9-25-62	.11	.05	.016	14.5	.129	117.3	.048	43.6	.008	7.3			.129	117.3	.003	2.7
10-17 10-18-62	.21	2.00	.064	30.5	.233	111.0	.137	65.2	.024	11.4			.242	115.2	.104	49.5
11-15-62	.08	.04	.008	10.0	.104	130.0	.016	20.0	.003	3.8			.081	101.3	0	0
12-3-62	.12	.20	0	0	.153	127.5	.040	33.3	.008	6.7			.129	107.5	.061	13.3
12-18-62	.33	.25	.193	58.5	.402	121.8	.177	53.6	.064	19.4			*.201	60.9	.281	85.2
12-19-62	.07	.07	0	0	.081	115.7	.016	22.9	0	0			.048	68.6	.008	11.4
12-24-62	.14	.20	.032	22.9	.169	120.7	.056	40.0	0	0			.112	80.0	.048	34.3
TOTAL	5.35		2.143	40.1	6.037	112.9	3.289	61.5	.529	9.89	2.189	67.4	2.210	105.24	2.705	50.6

* Leak at bottom of plot, not repaired.

Table 3. Treatments of 2,500 square foot test plots at Granite Reef.

Plot	Treatment Date	Treatment
1	1-17-62	R-8 at 0.052 lb/yd^2 mixed with S-1 at 0.90 lb/yd^2
2	11-30-61	Untreated
3	1-19-62	1-mil aluminum foil
4	11-30-61	30-mil butyl rubber sheeting
5A	1-9-62	S-1 at 0.90 lb/yd^2 R-8 at 0.052 lb/yd^2 applied as top spray
5B	9-18-62	Modified S-1 at 2.70 lb/yd^2

Table 4. Runoff data from 2,500 square foot plots at Granite Reef.

Date	Rainfall Intensity	Rainfall Total	Plot 1 Runoff		Plot 2 Runoff		Plot 3 Runoff		Plot 4 Runoff		Plot 5A Runoff		Plot 5B Runoff	
	(in/hr)	(in.)	(in.)	(%)	(in.)	(%)	(in.)	(%)	(in.)	(%)	(in.)	(%)	(in.)	(%)
1-21-62	.15	.87			.08	9.2	.55	63.2	.88	101.1	.87	100.0		
1-23-62	.07	.14			0	0	.17	121.4	.15	107.1	.14	100.0		
1-24-62	.05	.06	.06	100.0	0	0	--	--	.08	133.3	.06	100.0		
1-26-62	.10	.18	.11	61.1	.02	11.1	.13	72.2	.19	105.6	.17	94.4		
2-07-62	.05	.15	.10	66.7	0	0	.12	80.0	.16	106.7	.13	86.7		
2-11-62	.02	.06	.02	33.3	0	0	.06	100.0	.07	116.7	.02	33.3		
2-21-62	.10	.08	.03 1/	37.5	.01 1/	12.5	.05 1/	62.5	.09 1/	112.5	.06 1/	75.0		
2-25-62	.20	.30	.25	83.3	.14	56.0	.29	96.7	.22	73.3	.18	60.0		
3-09-62	.12	.12	.10	83.3	.01	8.3	.13	108.3	.12	100.0	.06	50.0		
3-19-62	.15	.61	.43	70.5	.11	18.0	.56	91.8	.60	98.4	.29	47.5		
3-21-62	.15	.06	.05	83.3	.01	16.7	.06	100.0	.06	100.0	.05	83.3		
6-28-62	.20	.14	0 2/	0	0	0	.13	92.9	.13	92.9	0	0 2/		
7-21-62	.02	.04	.01	25.0	0	0	.02	50.0	.02 4/	50.0	.01	25.0 3/		
7-28-62	1.20	.31	.18	58.1	.14	45.2	.23	74.2 3/	.29 4/	93.5	.17	41.5		
8-22-62	.15	.08	.01	12.5	0	0	.04	50.0	.07 4/	87.5				
9-20-62	.50	.40	.06	15.0	.06	15.0	.24 4/	60.0	.41	102.5				
9-23-62	.10	.33	.06	18.2	.05	15.2	.28	84.8	.33	100.0				
9-25-62	.05	.11	.01 4/	9.1	0	0	.10	90.9	.12	109.1				
10-17-62 10-18-62	2.00	.21	.08	38.1	.07	33.3	.21	100.0	.17 4/	81.0			.18	85.7
11-15-62	.04	.08	0	0	0	0	.06	75.0	.04 4/	50.0			.04	50.0
12-03-62	.20	.12	0	0	0	0	.13	65.0	.11	91.7			.11	91.7
12-18-62	.25	.33	.05	15.2	.10	30.3	.33	100.0	.14 4/	42.4			.30	90.9
12-19-62	.07	.07	0	0	0	0	.04	57.1	.07	100.0			0	0
12-24-62	.20	.14	.02	14.3	0	0	.10	71.4	.13	92.9			.08	57.1
TOTAL		4.99	1.63	41.0	.80	16.0	4.03	80.8	4.65	93.2	2.21	70.83	.71	74.7

1/ Meter not working properly prior to 2-20-62
2/ Crack at lower edge of asphalt plots
3/ Plot 3 and 5 catchment leak
4/ Meter not working properly

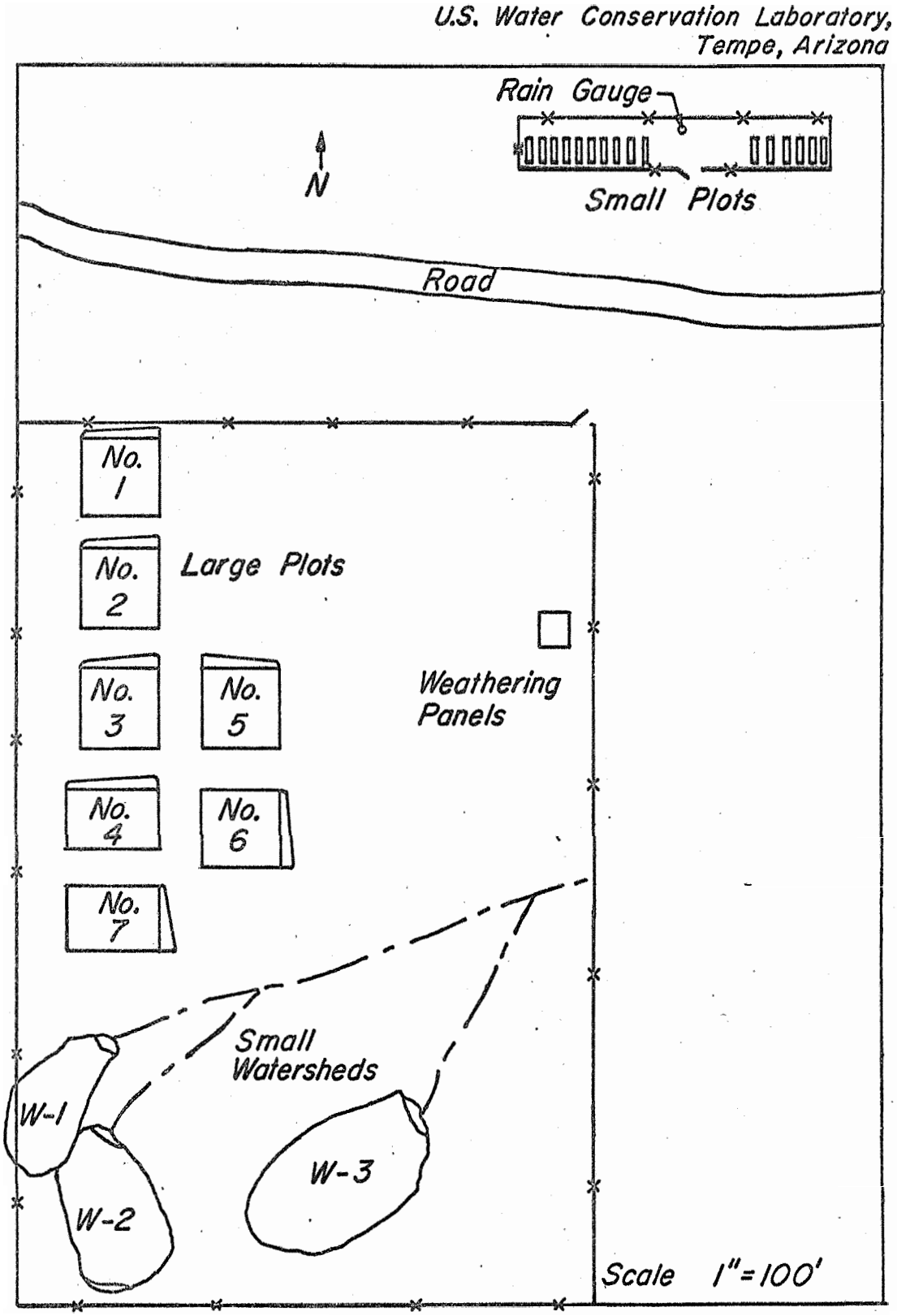

Figure 1. Granite Reef testing site.

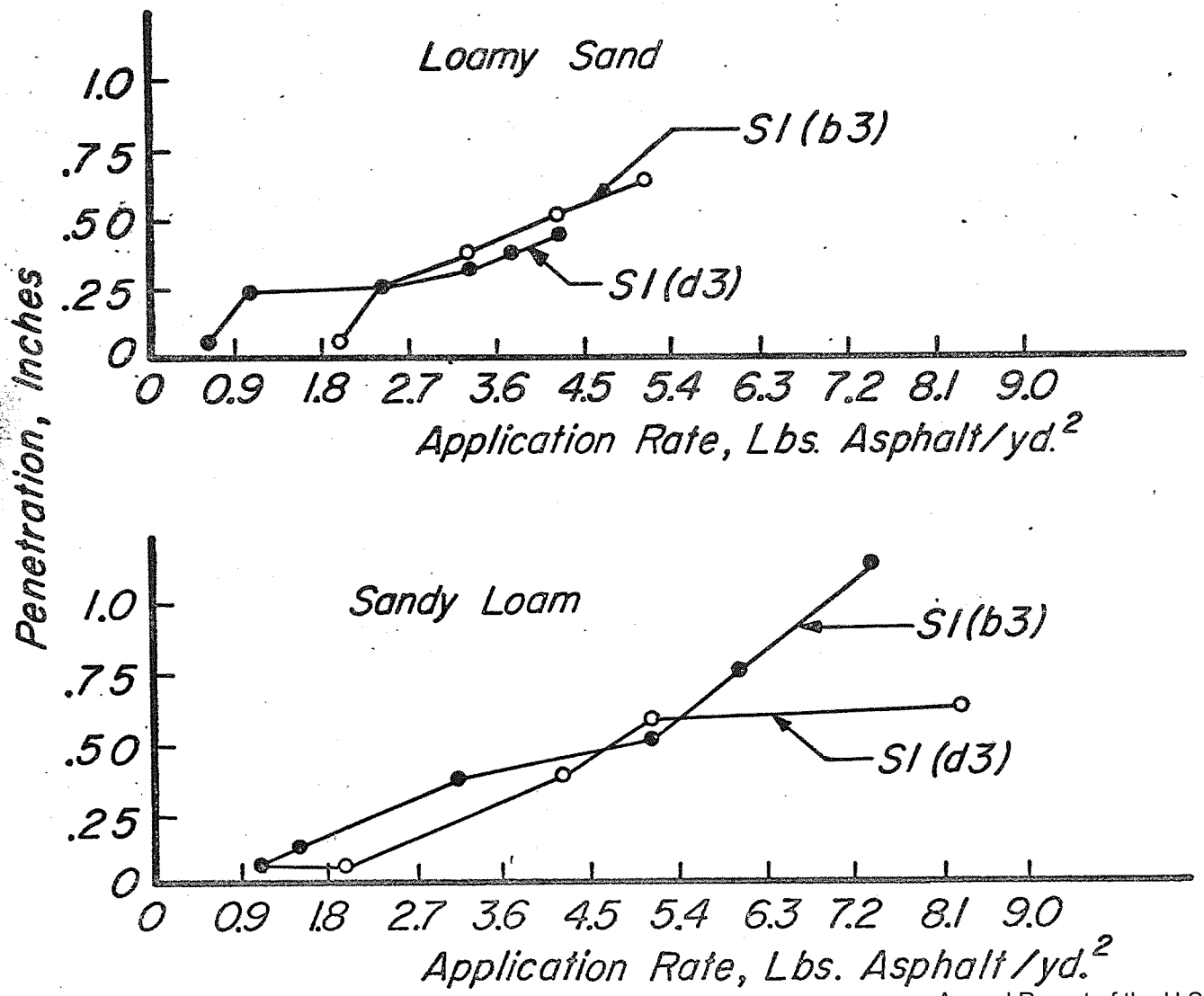

Figure 2. Penetration of modified S-1 into soil.

TITLE: ANALYZING GROUND WATER MOUND FORMATION BY RESISTANCE NETWORK ANALOGS

LINE PROJECT: SWC 4-gG3 CODE NO.: Ariz.-WCL-15

INTRODUCTION:

The studies on ground-water mound analysis by resistance network analogs were completed and published (see Annual Report 1961 and (42)). A further interpretation of the results was made, however, particularly on the effect on mound formation of the moisture content in the percolation zone below the recharge system being higher than that in the rest of the soil above the water table. Also, the effect that a rising mound itself may have on the recharge rate was studied. This effect was analyzed in conjunction with the effect on recharge of water depth in the recharge system and that of clogging of bottom material. The resulting equations and conclusions were verified with a laboratory study on soil columns. A paper has been prepared in which the studies are described in detail (73).

PROCEDURE:

Semi-equilibrium mound

Since the moisture content in the zone of percolation below the recharge basin tends to be higher than the original moisture content of the soil, the fillable pore space above the ground-water mound can be expected to be lower than above the water table adjacent to the mound. This would cause the center region of the mound to rise more rapidly than would be predicted by considering the fillable porosity as uniform. Since under sustained recharge in uniform soil the moisture content in the percolation zone may be close to saturation, the difference between the fillable porosity f_p in the zone above the mound and the fillable porosity f adjacent to the mound, can be quite large. Thus, the center region of the mound can be expected to exhibit a relatively high initial rate of rise to a semi-equilibrium position, after which subsequent rates of rise are relatively slow and more caused by a general buildup of the water table adjacent to the percolation area. The semi-equilibrium height of the mound can be expected to be approximately the same as the equilibrium height H_∞ of the

mound if the water table at some distance from the mound were kept at its original elevation. An equation is presented in (42) which permits calculation of the equilibrium height H_{∞} of the mound center. Thus, this equation can be used to predict the height to which the ground water mound will rise rather rapidly after the wetting front reaches the water table.

Recharge rates

The effect of water depth in the recharge basin, of clogging of the bottom material, and of a rising mound on recharge was analyzed by considering a one-dimensional system of vertical flow with a water depth h, a clogged bottom layer with conductivity K_s and thickness L_s, a water table at distance L below the clogged layer, and a conductivity K of the soil between the clogged layer and the water table. Assuming continuous flow, the Darcy equation was then applied to express the vertical flow rate V in terms of the factors just mentioned. The condition of vertically downward flow assumed in this analysis may be approached by the flow under the center portion of the recharge facility.

Laboratory studies

The laboratory studies were carried out in a 5-inch diameter vertical column using glass beads as porous medium. First, 55 cm of 201 micron beads were packed in the column. Next, the restricting layer was placed which consisted of 76 micron beads. This layer was initially 7.6 cm thick to permit study of the saturated case (see equation (1) under RESULTS AND DISCUSSION). The restricting layer was then increased to 20.6 cm thickness to permit study of the unsaturated case described by equation (2) under RESULTS AND DISCUSSION. The column was equipped with piezometers, tensiometers and air inlets to measure pressures, tensions and to permit drainage of pore space below the restricting top layer. De-aired distilled water with 0.1% phenol was used. Constant-level devices were used to maintain constant head and tail water levels in the recirculating system. The outflow from the column was measured for a range of

water depths. Pressures and tensions were measured to calculate hydraulic conductivity of the two materials and to measure the tension below the restricting layer.

RESULTS AND DISCUSSION:

Semi-equilibrium mound

On the basis of equation (5) in (42), a graph was constructed (Figure 1) which shows H_{∞}/W as a function of W/D for different values of V_a/K, where W is the width of the recharge strip for percolation zone, D is the original height of the saturated material above the impermeable layer, V_a is the recharge rate, and K is the hydraulic conductivity of the soil. This graph is only valid if $\frac{W}{D} < 4$. For example, if D is 50 ft, W is 40 ft, V_a is 5 ft/day, and K is 10 ft/day, Figure 1 shows that H_{∞}/W is 0.8 or H_w is 32 ft. Thus, after the wetting front reaches the original water table below the recharge basin, the mound can be expected to rise rather rapidly for a distance of 32 ft, after which much slower rates of rise of the mound can be expected.

Recharge rates

The one-dimensional vertical flow between the recharge basin and the ground-water table in the presence of a clogged bottom can be described by

$$V = \frac{h + L_s + L}{\frac{L_s}{K_s} + \frac{L}{K}} . \qquad (1)$$

To investigate the effect of L on V, all other terms considered constant, equation (1) is differentiated with respect to L, or

$$\frac{dV}{dL} = \frac{\frac{L_s}{K_s} - \frac{h + L_s}{K}}{\left(\frac{L_s}{K_s} + \frac{L}{K}\right)^2}$$

The following relationships can now be written:

(1) if $K_s < \frac{K L_s}{h + L_s}$, $\frac{dV}{dL} > 0$,

(2) if $K_s = \frac{K L_s}{h + L_s}$, $\frac{dV}{dL} = 0$,

(3) if $K_s > \frac{K L_s}{h + L_s}$, $\frac{dV}{dL} < 0$.

Thus, the manner in which V is affected by L depends on the relative magnitude of L_s, K_s, h, and K. In case of uniform soil conditions, $K_s = K$, and since $\frac{L_s}{h + L_s} < 1$, condition (3) will exist and V increases with a rising water table. Since the percolation zone is essentially saturated, the water table can be expected to rise quite fast and its effect on V may not be noticed until the water table extends above the bottom and V decreases. If, however, air space occurs in the percolation zone, a rising water table may increase V because of the increased gradients and possibly also because of an increase in K due to air space being reduced by the increased soil-water pressures caused by the rising water table.

If K_s is considered to vary from K to 0, condition (3) will be maintained until $K_s = \frac{K L_s}{h + L_s}$, whereby V is unaffected by the position of the water table. If K_s becomes less than $\frac{K L_s}{h + L_s}$, condition (1) is reached and V decreases with a rising water table. If the expression for condition (2), i. e., $K_s = \frac{K L_s}{h + L_s}$, is substituted in equation (1), the result is $V = K$. Thus, at condition (2), the flow below the restricting layer occurs under unit hydraulic gradient and the pressure below the restricting layer is atmospheric (the entire water depth in the basin is dissipated through the restricting layer).

If condition (1) exists, the effect of L on V is complicated by the unsaturated hydraulic-conductivity characteristics of the soil material below the restricting bottom soil. Since $K > K_s$, the soil

pores in the soil below the bottom layer are of larger size than the pores in the bottom layer. Thus, the soil below the bottom layer will be the first to become unsaturated in case negative pressures develop between the recharge basin and the water table in the soil. The pressure head of which the pores of the lower soil drain is called p_c. When this pressure head, which has been called the displacement pressure or critical pressure, is reached, the hydraulic conductivity undergoes a drastic reduction, particularly if the soil is of uniform pore size. It will be assumed here that K of the soil below the restricting layer is instantaneously reduced to an insignificantly small value as soon as the pressure in the soil water has dropped to p_c. Numerical values of p_c may be of the order of -1 ft of water, ranging from approximately -0.5 ft for sands to -1.5 ft or less for fine-textured soils. The role of p_c in the effect of L on V for condition (1) can best be explained by considering the effect on recharge of lowering the water table. According to condition (1), V increases with increasing L. However, V cannot increase indefinitely because the pressure head in the soil below the bottom layer can not be less than p_c (at pressure heads less than p_c, the underlying soil is considered to be at essentially zero hydraulic conductivity). Thus, the flow rate through the restricting layer can never exceed a flow V_c whereby the total head dissipated through the restricting layer equals $h + L_s - p_c$ 1/. According to Darcy's equation, this flow can be written as

$$V_c = \frac{K_s}{L_s} (h + L_s - p_c). \qquad (2)$$

The L-value whereby V reaches V_c, symbol L_c, can be calculated by substituting V_c and L_c for V and L in equation (1) and equating the resulting expression to equation (2). This yields the following expression for L_c

---

1/ Since p_c is negative, this maximum head is actually the sum of the numerical values of h, L_s, and p_c.

$$L_c = \frac{p_c}{\frac{K_s}{K\,L_s}(h + L_s - p_c) - 1} \qquad (3)$$

Thus, if the restricting layer is of sufficiently low hydraulic conductivity for condition (1), the pressure below the restricting layer will be p_c as long as L exceeds L_c and V will be V_c. If the water table rises above L_c, the pressure in the soil below the restricting layer will now become greater than p_c and the recharge rate will undergo a reduction.

Laboratory studies

The results of the tests are shown in Table 1 and in Figure 2. Equation (1) shows that, for the saturated case, a plot of V against h should yield a straight line with a slope of $1/(\frac{L_s}{K_s} + \frac{L}{K})$. The intercept of the line is $(L_s + L)/(\frac{L_s}{K_s} + \frac{L}{K})$. From the slope and intercept values of Figure 2, the equation $V = 0.0154h + 0.94$ is derived. Calculating the slope and intercept values for the measured values of K_s and K (from flow rate and piezometer measurements) and L_s and L for the column gives $V = 0.0156h + 0.98$, which is a good agreement as could be expected.

The equation for the unsaturated condition for the material below the restricting layer (Equation (2)) shows that a straight line in a plot of V_c against h can only yield a straight line if p_c is constant. As has been argued previously, a relatively constant value of the pressure below the restricting layer can be expected for a range of h-values if the underlying soil is relatively uniform. For such soils the conductivity reduction with drainage of pore space is rather drastic and quite a range of K-values occurs within a relatively small range of pressure. Therefore, there can be quite a range in V within a small range of pressure. The graph in Figure 2 shows that the points fall indeed on a straight line. Equation (2) shows that the impedance of the restricting layer is equal to the reciprocal of the slope of the line, whereas p_c can be calculated as L_s minus the intercept times

the impedance. The values thus obtained are shown in the fourth column of Table 1. Good agreement between these values and the impedance calculated from individually measured L_s and K_s appears to exist. The same is true for the p_c-value calculated from the intercept and that measured with a tensiometer below the restricting layer.

Thus, if thin, slowly permeable layers in canals or ponds or recharge pits are underlain by relatively uniform soil and if the impedance of the slowly permeable layer is high enough to yield unsaturated conditions in the underlying material, the pressure below the restricting layer can be considered to be constant and equal to the negative pressure where the conductivity undergoes a rather drastic reduction. As a matter of interest, the air entry value of the coarse glass beads was measured as 33 cm of water.

SUMMARY AND CONCLUSIONS:

The flow system between a recharge basin and the lower mound may consist of a number of perched mounds and percolation zones. The flow conditions governing formation and recession of individual mounds can be of considerable complexity. With a resistance network analog, non-uniformities and complexities in soil and boundary conditions can be taken into account. Solutions may be obtained regarding rise, fall, or equilibrium state of mounds above original water tables and perching layers for two-dimensional or axially symmetrical flow systems.

Of the various mounds that may be formed below a recharge system, the upper and lower mounds are the most important. The upper mound can affect the recharge rate from the basin, whereas the lower mound determines the storage and recovery of the recharge water. Due to the high moisture content in the zone of percolation below the recharge basin, mounds can be expected to rise rapidly to a semi-equilibrium condition when the wetting front reaches the water table or perching layer, after which lower rates of rise tend to occur. A graph is presented to estimate the height of this semi-equilibrium position for mounds above original water tables and two-dimensional systems.

The effect of the upper mound on the recharge rate from the basin is considered in relation to the hydraulic conductivity of the bottom

of the basin, which has a tendency to decline with prolonged recharge. It is shown that a rising mound can increase, decrease, or not affect at all, the recharge rate from the basin, depending on the hydraulic conductivity of the bottom material compared to that of the rest of the soil. If the bottom material is sufficiently clogged for the underlying soil to become unsaturated, the pressure below the slowly permeable bottom material is negative and, for soil with relatively uniform pore size, approximately equal to the negative pressure whereby pore space is being drained and the conductivity undergoes a rather drastic reduction. This was verified with a laboratory study where an observed pressure of -30 cm water below the restricting layer in a vertical column compared favorably with a critical pressure of -33 cm water, and a pressure of -32.7 cm water calculated from a plot of recharge rate versus water depth in the basin.

PERSONNEL: Herman Bouwer, R. C. Rice.

Table 1. Results of studies of flow through restricting surface layer (all lengths in cm and K in cm/min).

	Underlying material saturated		Underlying material unsaturated	
	Measured	Calculated from V-h graph	Measured	Calculated from V-h graph
L_s	7.6		20.6	
K_s	0.21		0.19	
L_s/K_s	36.3		108.2	117.4
L	55.1		55.1	
K	1.99		1.87	
L/K	27.7			
$L/K + L_s/K_s$	64.0	65.0		
$\frac{L + L_s}{\frac{L}{K} + \frac{L_s}{K_s}}$	0.98	0.94		
P_c			-30	-32.7

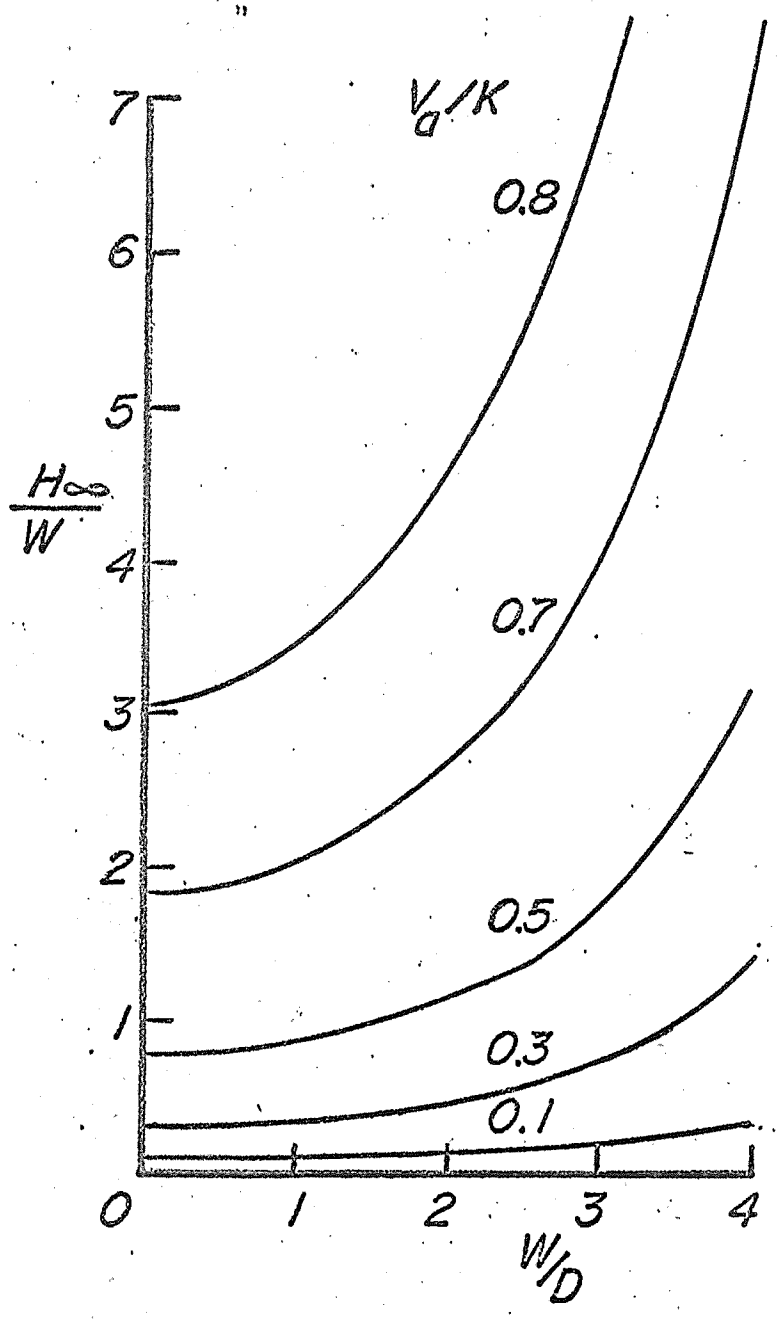

Figure 1. Graph showing H_∞/W as a function of W/D for different values of V_a/K (on the curves).

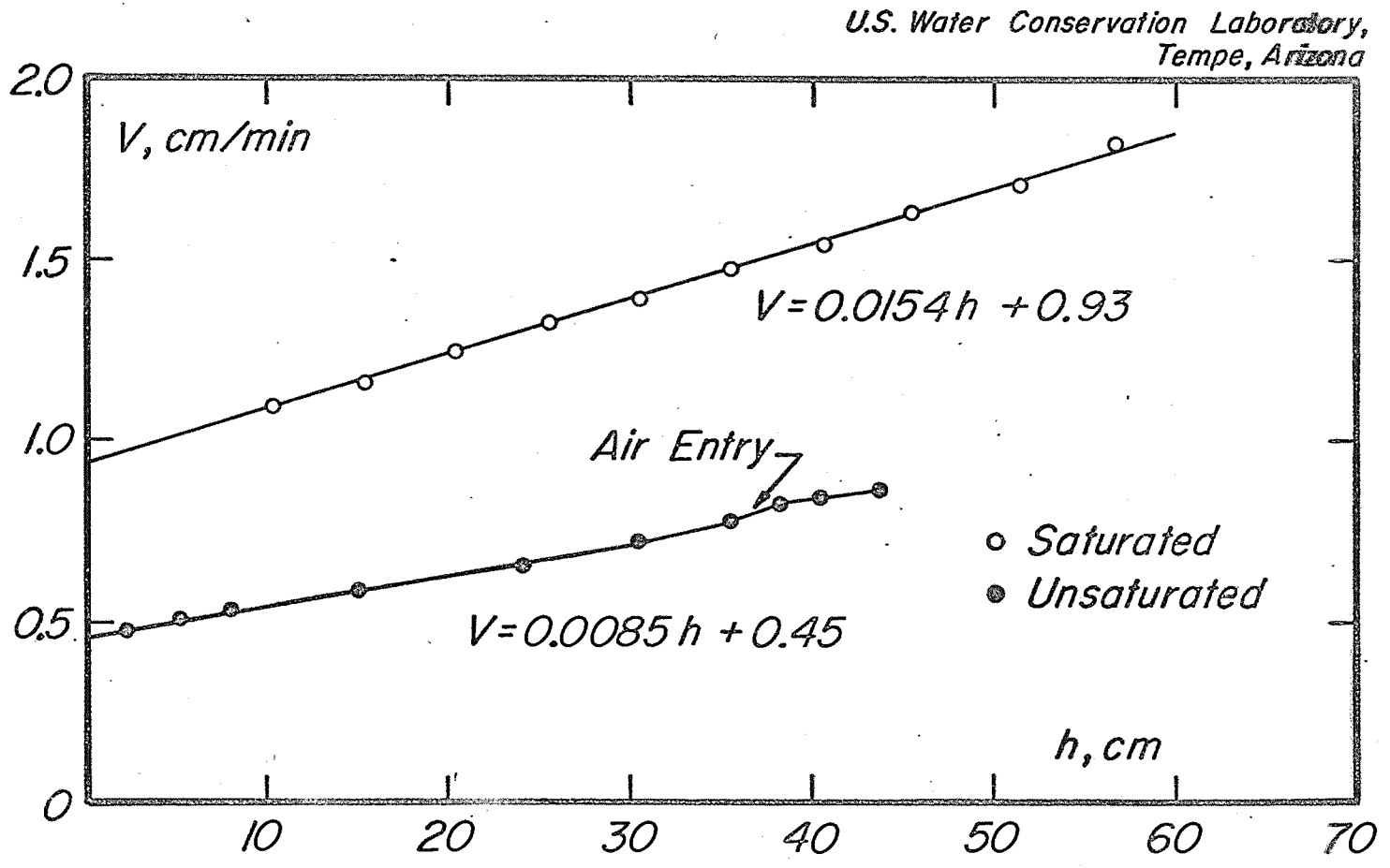

Figure 2. Flow rate as a function of water depth in glass-bead column with slowly permeable top layer.

TITLE: THE USE OF SALTY WELL WATER FOR THE PRE-PLANTING IRRIGATION ON SILTY CLAY SOILS

LINE PROJECT: SWC 4-gG3 CODE NO.: Ariz.-WCL-22

INTRODUCTION:

For need of study see Annual Report 1958. The objective of the experiment is to determine the amount of water to apply at the pre-planting irrigation to maintain economic production. The experiment was initiated April 1, 1958.

PROCEDURE:

The experiment is located at the University of Arizona Experiment Farm, Safford Branch, Safford, Arizona. The experiment was conducted on Field "I" borders 1-18.

Plots were plowed in January 1962, and allowed to dry out. On March 12, 1962 the following amounts of pre-planting and leaching water (2496 ppm) were applied.

1. 8 inches of well water - plots 4, 6, 12, 17.
2. 12 inches of well water - plots 3, 8, 10, 16.
3. 16 inches of well water - plots 2, 7, 11, 14.
4. 17 inches of well water - plots 5, 9, 13, 15.

On April 12, 1962, all plots were furrowed out and planted to New Mexico 1517D (short staple) and Pima S-2 (long staple) varieties. Difficulty in placement of the seed in moisture was noted at this time. On April 23, 1962, plots were replanted and a light irrigation given to germinate the seed. On May 9, 1962, another light irrigation was given to enhance seedling breakthrough.

Soil salt measurements were made on all plots previous to and after the leaching irrigation. A final measurement was made at the harvest date.

All water applied in regular irrigations was measured. Only that amount necessary for consumptive use was given. Areas for yield measurements were marked off prior to harvest. Irrigation dates. Leaching irrigation 3/12. Irrigations for consumptive use purposes. 5/25, 6/22, 7/13, 8/13 and 9/8.

RESULTS AND DISCUSSIONS:

A good stand of cotton was obtained after the second planting. Early season growth was slow because of cold weather and rhizotonia.

Yield Seed Cotton (1517D) in Pounds Per Plot

Trts.	Reps. 1	2	3	4	Mean
8"	23.0	26.0	22.0	22.0	23.3
12"	28.0	23.0	22.0	24.0	24.3
16"	26.0	25.0	27.0	23.0	25.3
17"	32.0	26.0	25.0	22.0	26.3

No sig.

Yield Seed Cotton (Pima S-2) in Pounds Per Plot

Trts.	Reps. 1	2	3	4	Mean
8"	17.0	18.0	15.0	18.0	17.0
12"	18.0	19.0	22.0	19.0	19.5
16"	21.0	18.0	14.0	17.0	17.5
17"	17.0	17.0	17.0	21.0	18.0

No sig.

Numerous fall and winter rains apparently partially took care of our leaching in the top foot and can be noted from the leaching data. At the time of the leaching irrigation March 12, the subsoil was still quite wet. Considerable difficulties were encountered when trying to force water through the soil.

Soil-salt conditions at leaching time between treatments were very similar. The addition of leaching water did not significantly affect the salts in the top foot but did significantly reduce salts in the second and third foot. Yields were always lowest in the 8" leaching treatment but not significantly so.

SUMMARY AND CONCLUSIONS:

There were no significant differences in yield; however, the 8-inch leaching treatment was lower than the others on both varieties.

There was less than a 10% reduction in yield by the 8-inch leaching treatment, which is less than in previous years. Considerable rain fell from October 19, 1961 until March 12, 1962 (5.65 inches) accomplishing leaching in the top foot, thus bringing the salt content down by pre-planting time.

After leaching, very little difference in salt content existed between treatments in the top foot, with a slightly greater difference in the second and third foot. The 8-inch leaching treatment was higher at the second and third foot depths. The leaching data shows a tremendous buildup of salts during the growing season at all depths.

PERSONNEL: Leonard J. Erie.

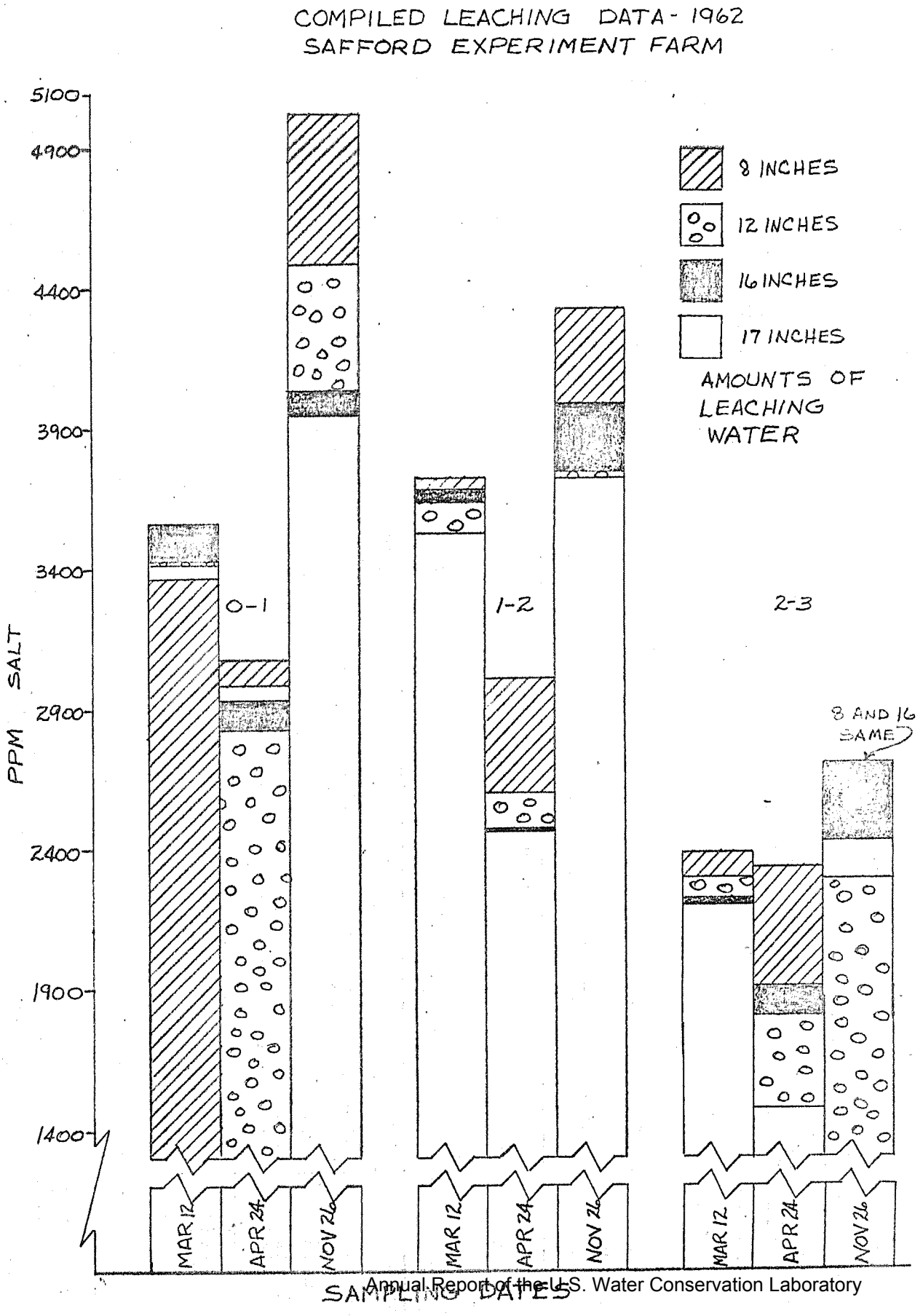
COMPILED LEACHING DATA - 1962
SAFFORD EXPERIMENT FARM
8 INCHES
12 INCHES
16 INCHES
17 INCHES
AMOUNTS OF LEACHING WATER
PPM SALT
5100
4900
4400
3900
3400
2900
2400
1900
1400
0-1
1-2
2-3
8 AND 16 SAME
MAR 12
APR 24
NOV 26
SAMPLING DATES

TITLE: MEASUREMENT AND CALCULATION OF UNSATURATED CONDUCTIVITY AND SOIL-WATER DIFFUSIVITY

LINE PROJECT: SWC 4-gG4 CODE: Ariz.-WCL-13

INTRODUCTION:

The objectives and need for study for this project were reported in the 1961 Annual Report of the U. S. Water Conservation Laboratory. In that report the initial work concerning the measurement of soil-water diffusivity at several bulk densities for several soils was reported. This work, and a study concerning temperature and soil-water diffusivity relations, was completed during 1962. Additional work involved a theoretical and experimental examination of the pressure plate outflow method for measuring capillary conductivity and a discussion of Fick's laws for diffusion applied to porous media.

PART I. SOIL-WATER DIFFUSIVITY MEASUREMENTS.

The experimental technique of measuring soil-water diffusivity was given in the 1961 Annual Report. A brief introduction and the results and discussion of the measurement of soil-water diffusivity at several porosities and several temperatures are reported here under separate headings. Literature citations are appended at the end of this section.

Concentration-dependent diffusion analysis has been used to describe unsaturated water flow in soils (1, 4, 7, 10). The applicability of diffusion analysis, however, has been shown, by the experiments of Nielsen et al. (7), to be limited to the case of water entering the soil at very nearly atmospheric pressure. In this case, three quantities are of interest: the soil-water diffusivity, the cumulative infiltration, and the distance that water penetrates into the soil.

Diffusion theory predicts that, for sorption of water by a horizontal column, the cumulative infiltration is proportional to the square root of time. The proportionality constant has been termed "sorptivity," denoted by the symbol S, by Philip (10). For sorption by an initially air-dry soil, the wetting front is sharp

and can usually be visually observed. Assuming that this visible wetting front is a plane of constant water content, the advance of this plane should also be a linear function of the square root of time. The proportionality constant that relates the advance of this front to the square root of time is a convenient parameter to use in describing the horizontal distance of penetration of water into soil. For lack of existing terminology this parameter will be called "penetrability." The utility of this nomenclature is restricted since a sharp visible wetting front cannot always be observed due (among other things) to soil color or to high initial water contents. It is used here for convenience.

PART I a. POROSITY AND SOIL-WATER DIFFUSIVITY RELATIONS.

INTRODUCTION:

The extreme complexity of pore configurations in soil precludes a quantitative theoretical approach to the description of porosity and water flow relations. Qualitative aspects of these relations are well known, but it remains for experiment to describe them quantitatively.

Measurements of soil-water diffusivity, sorptivity, and penetrability were made on Adelanto loam, Pachappa loam, and Pine silty clay, each at three porosities, each porosity in duplicate.

RESULTS AND DISCUSSION:

Some physical properties of the soil materials used in this study are given in Table 1. Density, porosity, and other pertinent data are given in Table 2. For the three soil materials the range of bulk densities is about 0.13 g cm^{-3} and the range of porosities is about 0.05.

For sorption of water by air-dry soils, the water-content distribution curves are of such a shape that accurate measurements of diffusivities cannot be made at the lower water contents nor at water contents near θ_s. This is because the slopes approach zero at the lower water contents and become very large near θ_s. Although precise measurements of diffusivities can be made at intermediate water contents, the diffusivity-water content relationship must

be known, or at least reasonably estimated, over the entire water content range, and particularly near θ_s, if these data are to be useful in predicting water-content distributions.

Soil-water diffusivities measured for the three soil materials are shown in Figures 1, 2, and 3, as a function of relative water content. Diffusivities were measured for the two lengths of water-content distributions for each porosity at the same volumetric water content. The resulting diffusivity values for each water content were averaged and plotted as a function of relative water content.

Since values of water content exist at higher porosities that do not exist at lower porosities, the relative water content parameter allows better comparisons of diffusivity at different porosities than the volumetric water content. For example, in Pine silty clay, diffusivity data were obtained at 0.47 and 0.48 volumetric water content for 0.556 porosity, but 0.463 was the highest water content attained for 0.509 porosity. Sufficient data are given in Table 2 to convert the diffusivities in Figures 1, 2, and 3 to a volumetric water content basis.

Data for Adelanto loam, given in Figure 1, show that diffusivities decrease with decreasing porosity. At a given water content diffusivity values changed from twofold to threefold when the porosity was changed 0.049. For Pachappa loam (Figure 2) the diffusivities are about the same for the three porosities. Only at lower water contents can a difference be observed. At 0.55 relative water content, the diffusivity is lower at the lower porosity but the difference is not as great as that shown by Adelanto. For Pine silty clay, porosity and soil-water diffusivity relations are shown in Figure 3. As with Adelanto loam, diffusivities decrease with decreasing porosity, the change being slightly more than twofold throughout the range of water contents for which measurements were made.

The two soil materials that show marked differences in diffusivity due to porosity differences (Adelanto and Pine) both have

considerably higher clay contents (Table 1) than does Pachappa. Although Pine has almost twice as much clay as does Adelanto, the relative differences in diffusivity due to porosity are about the same. Table 2 shows that the water content at the source θ_s for Pachappa changed only 0.006 for a porosity change of 0.05, whereas θ_s for Adelanto and Pine changed 0.026 and 0.037 respectively.

Some inferences concerning the influence of texture on soil-water diffusivity can be deduced by comparing the texture data in Table 1 with the diffusivity data of Figures 1, 2, and 3. The silt fractions of the three soil materials are similar whereas the clay fractions are in the order Pine > Adelanto > Pachappa. For the sand fraction the order is, of course, reversed. The slopes of the ln D_θ versus θ' plots are indicative of the rate at which the diffusivity changes with water content. In general the slopes are in the order Pine > Adelanto > Pachappa. This indicates that the diffusivity changes more rapidly with water content in fine textured soils than in coarse textured soils. Gardner and Mayhugh's (4) data show the opposite order. Slopes of the lines drawn through their data points would indicate that coarse textured soils exhibit a greater rate of change of diffusivity with water content than does fine textured soils. However, their data were obtained in a somewhat different manner than those reported here. Furthermore, the data in Figures 1, 2, and 3 are for a limited water content region. Therefore, the statements inferred from this data may not apply to other water contents.

An exponential function of the type $D = D_o \exp \beta\theta$ has been proposed to describe diffusivity-water content relationships (5). Inspection of Figures 1, 2, and 3 would suggest that diffusivities for the three soil materials could be represented by an exponential function. Indeed, within the water content region where accurate measurements can be made, this type of function adequately represents the data. Data for the lowest porosity of the three soil materials were used to obtain the constants β and D_o in the expression $D = D_o \exp \beta\theta'$ by the method of least squares. The broken lines in Figures 1, 2, and 3 are plots of these functions.

If the exponential function obtained from the measured data will describe the diffusivity-water content relationship over the entire range of water contents, then water content distributions calculated using this function should coincide with the experimentally determined distribution. Using the determined exponential diffusivity functions, the broken lines in Figures 4, 5, and 6 were computed by the numerical method of Philip (8). The symbols are experimental data. It is apparent that the water content distributions were not successfully predicted by using the exponential function obtained from diffusivity data measured for a limited water content region. As an example, for Adelanto, porosity 0.438, water can penetrate 30.3 cm in 900 minutes whereas using the determined exponential diffusivity function, 21.4 cm would be predicted.

As a test of the applicability of diffusion theory to the description of water flow into these soil materials and under these experimental conditions, the relative water contents were plotted versus $xt_o^{-1/2}$ in Figures 4, 5, and 6. If diffusion theory is applicable, then water content data obtained on duplicate columns of the same porosity, but with the water allowed to penetrate different distances, will coincide when plotted versus $xt_o^{-1/2}$. In Figures 4, 5, and 6 the open symbols are data for columns of one length and the soild symbols are for columns of a different length. In all cases the agreement is good.

For Pachappa (Figure 5) the values on the abscissa are twice those of Pine and Adelanto. This makes the small difference that exists between the two columns of Pachappa less noticeable. The use of the Boltzmann transformation to obtain the desired form of the diffusion equation requires that a plane of constant water content advance proportional to the square root of time. Thus, if it is assumed that the visible wetting front is a plane of constant water content, then a plot of the distance of this front from the source versus $t^{1/2}$ should yield a straight line that pierces the origin. For Pachappa, such plots yielded straight lines after the first few centimeters, but each exhibited a small positive intercept on the order of 0.5 to 0.8 cm. When the values of $xt_o^{-1/2}$ in

Figure 5 are corrected for this small intercept, the data points for the two columns fall perfectly on one line. Since a non-zero intercept is not accounted for by the mathematical model, soil-water diffusivity analysis will not exactly describe water movement through this soil material under these experimental conditions.

Figure 7 shows advance of the wetting front versus the square root of time plots for one porosity of each soil material. The open and solid symbols represent data from duplicate columns. The small positive intercept for Pachappa as shown by the figure has been observed on all columns of Pachappa reported here and in subsequent experiments. The cause of this is obscure but it is doubtful that it is due to experimental technique.

The slopes of the lines shown in Figure 7 are the ratios $xt^{-1/2}$ (neglecting the intercept for Pachappa). These ratios and those for the other porosities are given in Table 2. Also shown in Table 2 are values of $qt^{-1/2}$, where q is the quantity of water imbibed per unit area. The ratios $xt^{-1/2}$ and $qt^{-1/2}$ are the penetrability and sorptivity respectively.

Inferences concerning distance of penetration and cumulative infiltration in horizontal columns as influenced by porosity differences can be drawn from the values of sorptivity and penetrability given in Table 2. For Adelanto an increase in porosity of 0.049 will cause water to penetrate 39% farther and 49% more water to be imbibed than would occur at the lower porosity during the same time period. For Pachappa a porosity increase of 0.051 will cause water to penetrate 12% farther and 15% more water to be imbibed than would occur at the lower porosity during the same time period. For Pine, the magnitudes are about the same as for Adelanto. A porosity increase of 0.047 will cause 40% farther penetration and 50% more imbibition than what would occur at the lower porosity during the same period. As an example, for Pine, in 900 minutes water will penetrate 31.5 cm for porosity 0.556 and 22.5 cm for porosity 0.509.

If the time necessary for water to penetrate a given distance and the time required for a given amount of water to be imbibed is considered, 92% more time would be required for water to penetrate Adelanto to a given distance and 122% more time for the same quantity of water to be imbibed when porosity is decreased by 0.049. For Pachappa the percentages are 24 and 33 for distance and quantity, respectively, for a porosity decrease of 0.051. For Pine, these values are 96% and 125%, respectively, for a porosity decrease of 0.047. As an example, for Adelanto, 901 minutes are required for 10 cm of water to be imbibed for porosity 0.438 while 406 minutes are required for the same quantity to enter when the porosity is 0.487.

SUMMARY AND CONCLUSIONS:

Water at -2mb pressure was absorbed by horizontal columns of three soil materials of differing texture each at three porosities, each porosity in duplicate. The soil materials were Adelanto loam, Pachappa loam, and Pine silty clay. From the water content distributions, soil-water diffusivities were calculated, assuming applicability of diffusion theory. For a total porosity change of about 0.05, Pachappa loam exhibited little change in soil-water diffusivity but Adelanto loam and Pine silty clay exhibited twofold to threefold changes in diffusivity at the same relative water content. Cumulative infiltration and distance of penetration of water into horizontal soil columns decreased 50% and 40%, respectively, for Adelanto and Pine, and 15% and 12%, respectively, for Pachappa when the total porosity was decreased 0.05.

Water content distributions were calculated using exponential diffusivity-water content functions obtained by a least squares fit to the diffusivity data measured over a limited water content region. Predictions of water contents based on these functions were considerably in error.

Table 1. Physical properties of soil materials used.

Soil	Particle size > 50μ	2 - 50μ	< 2μ	15-bar retentivity
	%	%	%	% by weight
Adelanto	31.6	46.1	22.3	10.4
Pachappa	41.6	49.9	8.5	4.7
Pine	2.6	54.9	42.5	14.7

Table 2. Density, porosity, and other pertinent data. Values shown are averages of duplicate columns.

Soil	Bulk density	Particle density	Porosity	Water content at source θ_s	Initial water content θ_i	Penetrability $xt^{-1/2}$	Sorptivity $qt^{-1/2}$
	$g\ cm^{-3}$	$g\ cm^{-3}$		$cm^3\ cm^{-3}$	$cm^3\ cm^{-3}$	$cm\ min^{-1/2}$	$cm\ min^{-1/2}$
Adelanto	1.375	2.68	.487	.413	.034	1.40	.496
	1.446	2.68	.460	.395	.036	1.15	.392
	1.505	2.68	.438	.387	.038	1.01	.333
Pachappa	1.257	2.71	.536	.426	.014	2.03	.752
	1.339	2.71	.506	.421	.015	1.88	.684
	1.396	2.71	.485	.420	.015	1.82	.652
Pine	1.195	2.69	.556	.500	.045	1.05	.441
	1.238	2.69	.540	.484	.047	.936	.380
	1.322	2.69	.509	.463	.050	.750	.294

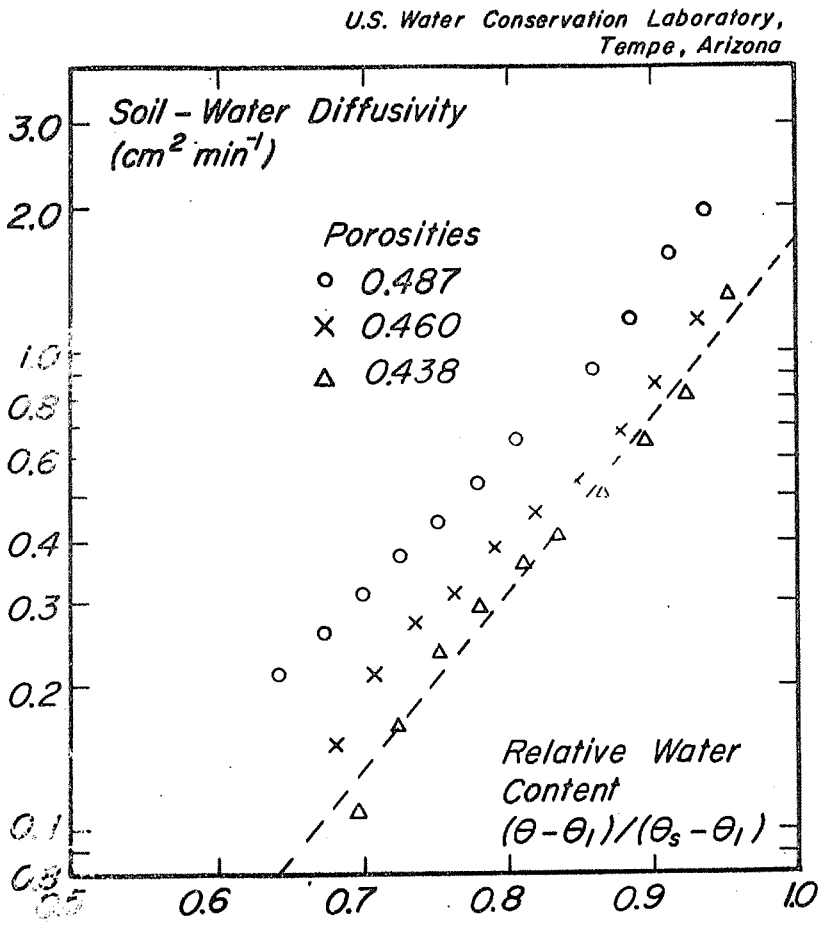

Figure 1. Soil-water diffusivity versus relative water content for Adelanto loam at three porosities. The broken line is the least squares fit to the data at the lowest porosity.

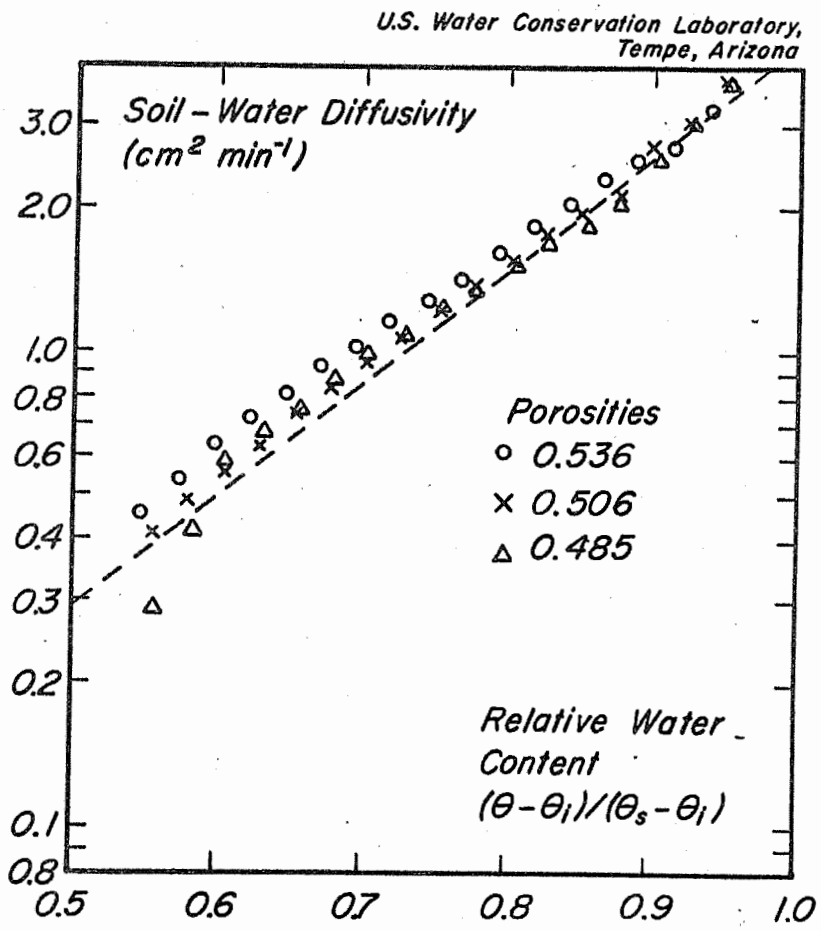

Figure 2. Soil-water diffusivity versus relative water content for Pachappa loam at three porosities. The broken line is the least squares fit to the data at the lowest porosity.

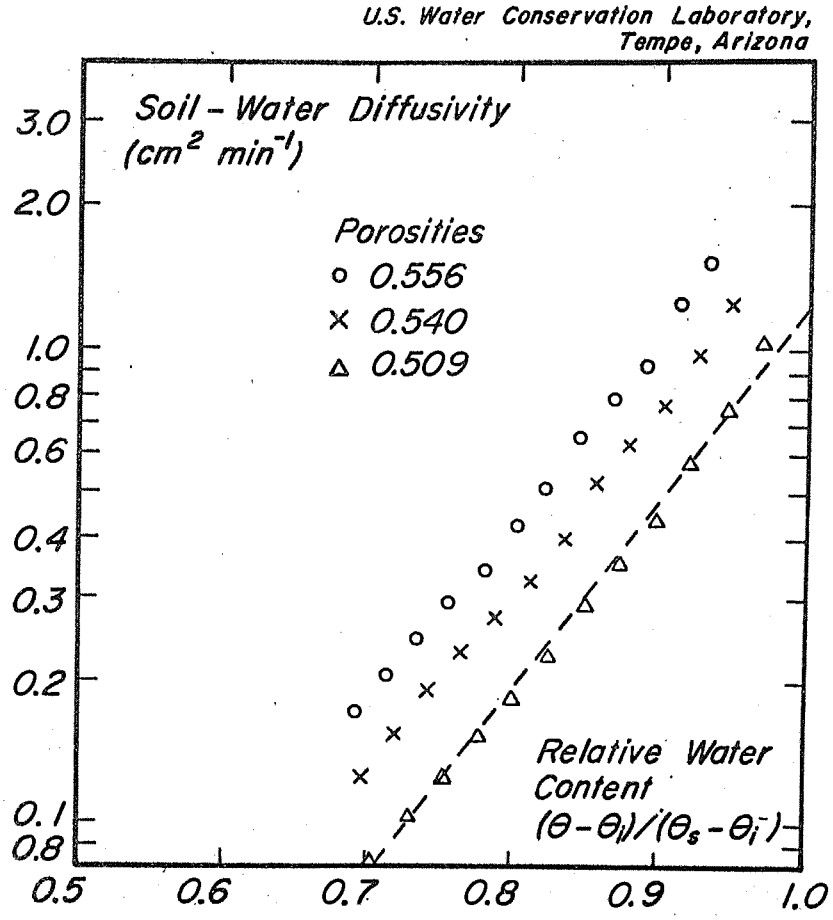

Figure 3. Soil-water diffusivity versus relative water content for Pine silty clay at three porosities. The broken line is the least squares fit to the data at the lowest porosity.

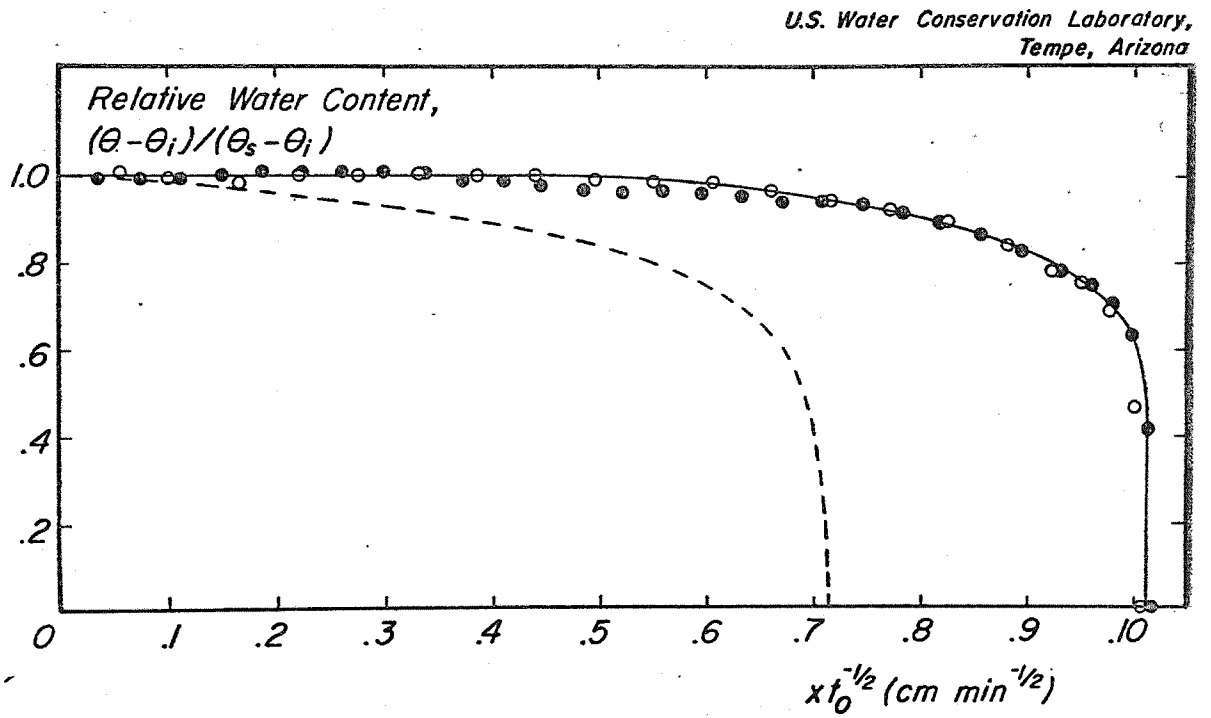

Figure 4. Water-content distribution curves for Adelanto loam, porosity 0.438. The broken line was calculated using an exponential function obtained from the measured diffusivity data.

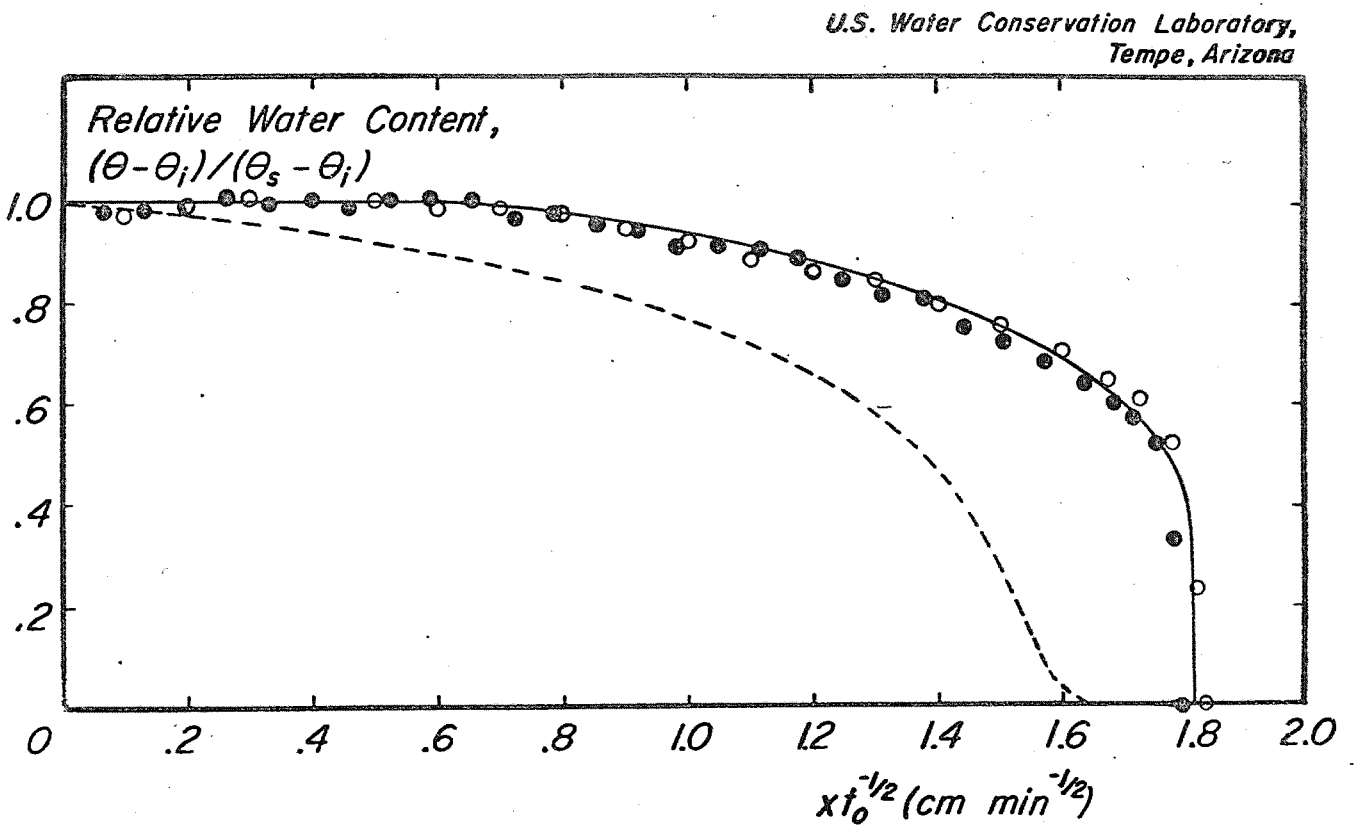

Figure 5. Water-content distribution curves for Pachappa loam, porosity 0.485. The broken line was calculated using an exponential function obtained from the measured diffusivity data.

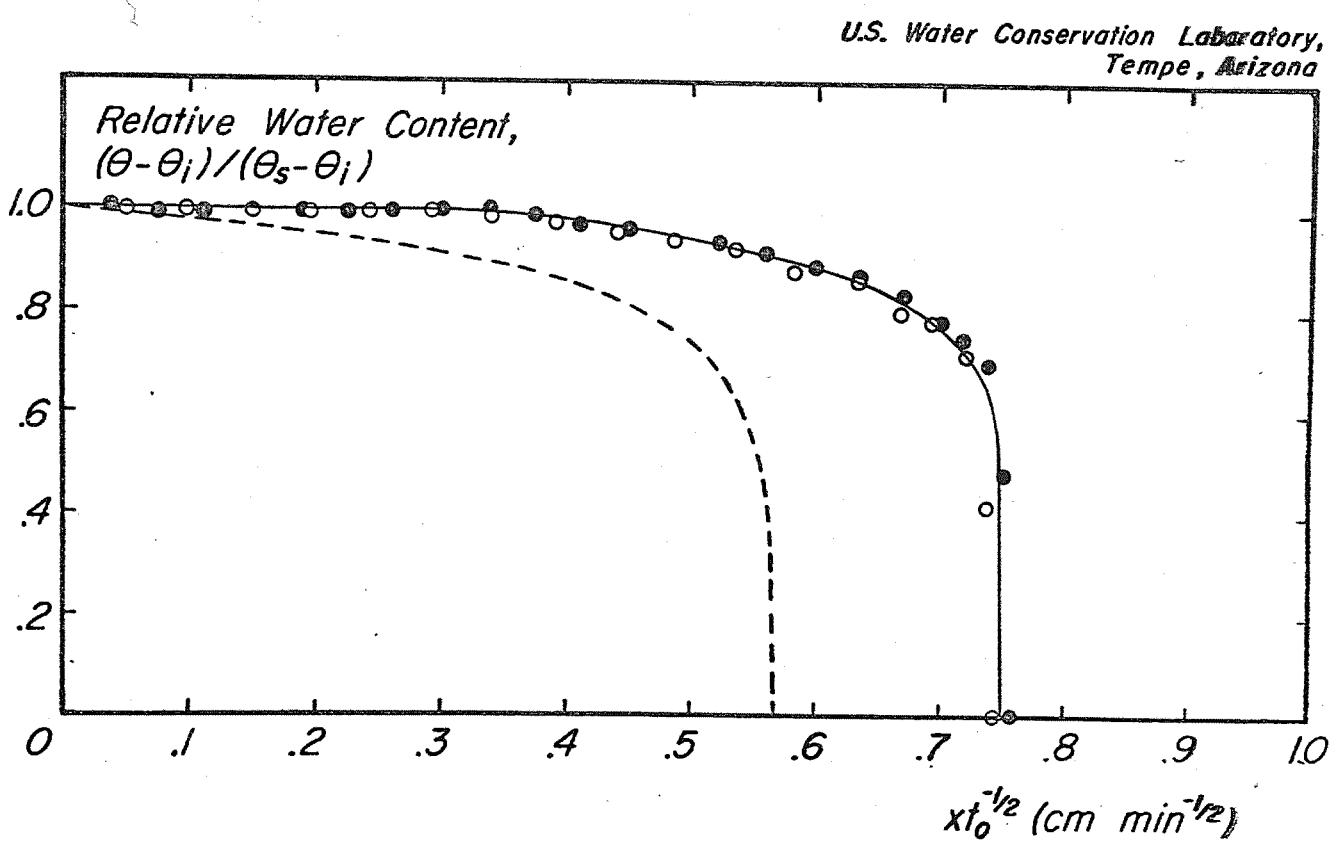

Figure 6. Water-content distribution curves for Pine silty clay, porosity 0.509. The broken line was calculated using an exponential function obtained from the measured diffusivity data.

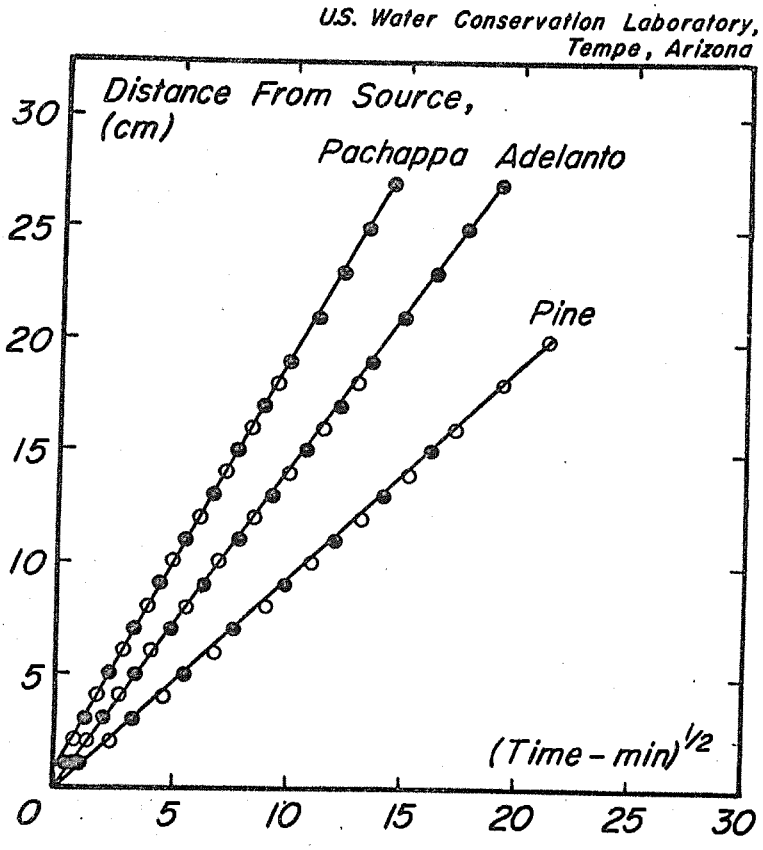

Figure 7. Distance to the wetting front versus the square root of time for Pachappa loam, porosity 0.506, Adelanto loam, porosity 0.487, and Pine silty clay, porosity 0.540. The different symbols on each line are data for duplicate columns.

PART I b. TEMPERATURE AND SOIL-WATER DIFFUSIVITY RELATIONS.

INTRODUCTION:

One can infer from capillary theory that the temperature dependence of soil-water diffusivity is a result of the temperature dependence of viscosity and surface tension. By analogy to water flow in a capillary tube an inverse relation between soil hydraulic conductivity and viscosity can be derived. Capillary theory states that the pressure potential of soil water is directly proportional to the surface tension. Thus, since the diffusivity (D_θ) can be written $D_\theta = k_\theta(d\psi/d\theta)$ where k_θ is the unsaturated hydraulic conductivity, ψ the pressure potential, and θ the volumetric water content, the diffusivity should be directly proportional to the surface tension and inversely proportional to the viscosity of water. This relationship was proposed during the early stages of the development of soil-water diffusion theory.

Experimental verification of the inverse relationship between unsaturated hydraulic conductivity and viscosity is limited. The temperature dependence of pressure potential cannot be entirely explained by the temperature dependence of surface tension. Gardner (5) measured soil-water diffusivities at several temperatures and concluded that the temperature effect was not large. His data indicated that, at air-dry water contents, the temperature coefficient of diffusivity may be positive or negative, depending upon the soil texture.

Soil-water diffusivity and penetrability data were obtained for duplicate samples of Pachappa loam, Adelanto loam, and Pine silty clay at temperatures of 5.0, 13.5, 24.0, 33.0, and 42.5° C. The data are interpreted on the basis of the temperature dependence of the ratio of surface tension to viscosity.

THEORETICAL FORMULA:

Philip (10) was apparently the first to explicitly state the relation between soil-water diffusivity, surface tension, and viscosity. He proposed the term <u>intrinsic diffusivity</u> to denote a diffusivity which is a function of the medium geometry but

independent of the properties of the liquid. The relationship between the intrinsic diffusivity (D'_θ) and the soil-water diffusivity is

$$D_\theta = [(\sigma/\eta) \cos H] \, D'_\theta \quad , \qquad [1]$$

where σ is the surface tension, η is the viscosity, and H is the angle of contact between the fluid and the solid. The units of intrinsic diffusivity are length, in contrast to length^{2}time^{-1} for classical diffusivity.

Philip (10) also proposed the term intrinsic sorptivity (S') whose relationship to sorptivity (S) is

$$S = [(\sigma/\eta) \cos H]^{1/2} \, S' \quad . \qquad [2]$$

The sorptivity is the coefficient of the $t^{1/2}$ term in Philip's vertical infiltration equation (9). Infiltration into horizontal columns can be described by the relation

$$q = 2(\theta_s - \theta_i) \, (\bar{D} \, t/\pi)^{1/2} \qquad [3]$$

where q is the quantity of water imbibed per unit area, θ_s is the water content at the source, θ_i the initial water content, t the time, $\pi = 3.14 \ldots$, and $\bar{D}$ is a weighted-mean diffusivity as used by Gardner (5). Equation [3] is a solution of the parabolic, second order, diffusion equation with constant diffusivity. A derivation is given by Kirkham and Feng (6), and is discussed in standard texts on diffusion such as Crank (2). Kirkham and Feng consolidated the constants in their equation and wrote $q = At^{1/2}$, hence, $A = S = 2(\theta_s - \theta_i) \, (\bar{D}/\pi)^{1/2}$.

Swartzendruber et al. (11) preceded Philip (10) in analysing the effect of surface tension and viscosity on infiltration. They developed a capillary tube model from which the same result as equation [2] was obtained. They also found that the penetrability would be affected by surface tension and viscosity in the same manner as infiltration. Thus

$$x = P' \, [(\sigma/\eta) \cos H]^{1/2} \, t^{1/2} \quad , \qquad [4]$$

where x is the distance to the wetting front from the source and P' is the intrinsic penetrability.

Assuming that the contact angle, whatever its value, remains constant irrespective of temperature changes, then the term cos H can be included in the intrinsic factors. Thus, equations [1], [2], and [4] become:

$$D_\theta = (\sigma/\eta)\, D_\theta^o \quad , \qquad [5]$$

$$S = (\sigma/\eta)^{1/2}\, S^o \quad , \qquad [6]$$

$$P = (\sigma/\eta)^{1/2}\, P^o \quad , \qquad [7]$$

where D_θ^o, S^o, and P^o are modified intrinsic factors.

RESULTS AND DISCUSSION:

Some physical properties of the soil materials used in this study are given in Table 1, Part I a, and Table 1 in this section. In Table 1, the water content at the source θ_s was obtained by extrapolating the water content distribution curves of Figure 1 to x = 0.

The water content distribution curves are shown in Figure 1 for the three soil materials. The lines were drawn through the mean water content of ten samples at each x. The water content ranges of the ten samples at each x are shown by the vertical lines. All five temperatures yielded essentially the same water content distribution curve. No trend whatsoever was observed between water contents for any particular x and temperature. The difference between the average water content of duplicate samples at any x at 5° C and the average of duplicates at the same x at 42.5° C was no greater than the difference between duplicates at the same temperature. Therefore, under these experimental conditions, the effect of temperature on water retention could not be measured. However, the times necessary for water to penetrate the specified distances were considerably different for the different temperatures.

Since temperature effects on the water content distribution curve could not be measured, the line drawn through the mean water

content at each x was used to evaluate $dx/d\theta$ and $\int x d\theta$ in equation [8],

$$D_\theta = -\frac{1}{2t}\frac{dx}{d\theta}\int x d\theta \quad , \qquad [8]$$

which is used to calculate the diffusivity. As noted previously, accurate measurements of $dx/d\theta$ cannot be made at water contents near θ_s nor at the lower water contents. Within the region of measurement the only term in equation [8] that varied with temperature was the time required for water to advance a given distance in the soil columns. These times are given in Table 2 for the three soil materials, and pertain to x = 20.3 cm for Pachappa and Adelanto and to x = 15.3 for Pine.

Soil-water diffusivities for the three soil materials at three temperatures are shown in Figures 2, 3, and 4. For Pachappa and Adelanto, diffusivities were twofold higher at 42.5° C than at 5° C. Diffusivities for Pine changed about threefold over the same temperature interval. Diffusivities at 13.5 and 33.0° C are not shown, but can be calculated using diffusivities at one of the temperatures shown in Figures 2, 3, and 4 and from the times in Table 2.

Figure 5 shows weighted-mean diffusivities, calculated using a rearrangement of equation [3], versus temperature. Since q (measured volumetrically and by numerically evaluating $\int x d\theta$) and $(\theta_s - \theta_i)$ were not measurably influenced by temperature, time was again the only term that changed with temperature.

The weighted-mean diffusivity is a weighted average of the entire diffusivity-water content function [see Crank (2) p. 256]. Since this diffusivity and the measured diffusivities shown in Figures 2, 3, and 4 varied with temperature in identically the same manner, it appears that the same may be true for diffusivities at the water contents near θ_s and the lower water contents where measurements of D are uncertain. If this is so, then we can conclude that the diffusivity at any water content is affected by temperature in the same manner as the diffusivity at any other water content. We can, therefore, examine the diffusivity-temperature

relations for one diffusivity, say $\bar{D}$, and apply the conclusion to the other diffusivities.

Using $\bar{D}$ for D_θ in equation [5], the ratio $\bar{D}/(\sigma/\eta) = \bar{D}^o$ was calculated for each temperature. Values of σ and η for five-degree intervals in the range 0 to 45° C are given by Dorsey (3). Values for temperatures not specifically given in the tables were obtained by linear interpolation. The five values of $\bar{D}^o$ thus obtained for each soil material were averaged and the result was multiplied by (σ/η) at several temperatures to obtain the three lines shown in Figure 3. The symbols represent experimental data. Comparison of the data points and the lines show how well the temperature dependence of soil-water diffusivity can be explained on the basis of the temperature dependence of the surface tension-viscosity ratio.

In the derivation of equation [8] it was assumed that a plane of constant water content advances proportional to $t^{1/2}$. Assuming that the visible wetting front is a plane of constant water content, plots of distance of this wetting front from the source versus $t^{1/2}$ should be linear. Figure 6 shows the distance to the visible wetting front versus $t^{1/2}$ for the three soil materials at the highest and the lowest temperatures. Data for the remaining three temperatures are similar. Duplication was excellent, as indicated by the different symbols for duplicate samples, and straight lines obtained. The slopes of these lines are the penetrabilities. Note that for Adelanto and Pine the lines pierce the origin, but for Pachappa a small positive intercept (about 0.5 cm) obtains. This was observed and discussed in Part I a.

Figure 7 shows the penetrabilities for the three soil materials as a function of temperature. The points are experimental data. The lines were obtained by calculating $P(\sigma/\eta)^{-1/2} = P^o$, again assuming the contact angle to be independent of temperature. Values of P^o were calculated for each temperature, averaged, and the result multiplied by $(\sigma/\eta)^{1/2}$ at several temperatures to obtain the lines.

As discussed earlier, the sorptivity S is directly proportional to $(\bar{D})^{1/2}$, hence values of S are proportional to the square root of

the values in Figure 3. The temperature dependence of sorptivity is the same as that for penetrability and could be illustrated by Figure 7 if the ordinate were suitably labeled. Comparing data points with the theoretical lines in Figures 5 and 7 indicate that, at least in the first approximation, the effect of temperature on soil-water diffusivity, sorptivity, and penetrability can be explained on the basis of the temperature dependence of surface tension and viscosity. The data are sufficiently good to substantiate the assumption that the contact angle does not vary appreciably with temperature within this temperature range.

In equations [5], [6], and [7] the modified intrinsic factors can be evaluated by measuring D, S, and P at one temperature, knowing σ/η at that temperature. Estimates of D, S, and P can then be obtained for other temperatures by multiplying by σ/η or $(\sigma/\eta)^{1/2}$ for that temperature. These conclusions are based on data obtained in the region 5 to 42.5° C and may not be valid outside of this temperature interval.

From the practical point of view, it is of interest to infer from the above discussion the effect of temperature on the vertical infiltration of water into soil. Philip (10) has shown that the equation

$$q = St^{1/2} + At \qquad [9]$$

describes vertical infiltration fairly well for all except very large times. In equation [9], A is approximately proportional to the saturated hydraulic conductivity and should therefore be proportional to the inverse of viscosity. Since $S > A$ for small times, the sorptivity term is dominant and infiltration should vary with temperature as $(\sigma/\eta)^{1/2}$ varies with temperature during the early stages. As time progresses to the point where the A term becomes dominant, the infiltration should vary with temperature as $(1/\eta)$ varies with temperature.

SUMMARY AND CONCLUSIONS:

Water at -2mb pressure was absorbed by horizontal columns of three soil materials of differing texture at temperatures 5.0, 13.5,

24.0, 33.0, and 42.5° C. From the water content distributions, soil-water diffusivities were calculated, assuming applicability of diffusion theory. Twofold to threefold differences were observed between diffusivities at 5.0° and 42.5° C. The water content distribution curves were not measurably influenced by temperature, thus, in the equation used to calculate diffusivity, the time required for water to penetrate the given distance was the only term differing with temperature.

The temperature dependence of the ratio of surface tension to viscosity appears to be the dominant factor in describing the temperature dependence of soil-water diffusivity. The square root of the surface tension viscosity ratio adequately accounts for the temperature dependence of penetrability and sorptivity.

Table 1. Density, porosity and volumetric water content data for soil materials used.

Soil	Bulk density	Porosity	Water content at source θ_s	Initial water content θ_i
Pachappa	1.377 ± .009	.492	.420	.012
Adelanto	1.378 ± .018	.486	.418	.030
Pine	1.257 ± .007	.533	.476	.035

Table 2. Times required for water to advance 20.3 cm in Pachappa loam and Adelanto loam, and 15.3 cm in Pine silty clay. Values are averages of duplicate columns.

Temperature	Time		
	Pachappa	Adelanto	Pine
°C	min	min	min
5.0	191	414	534
13.5	144	349	428
24.0	114	274	346
33.0	104	261	262
42.5	92	199	191

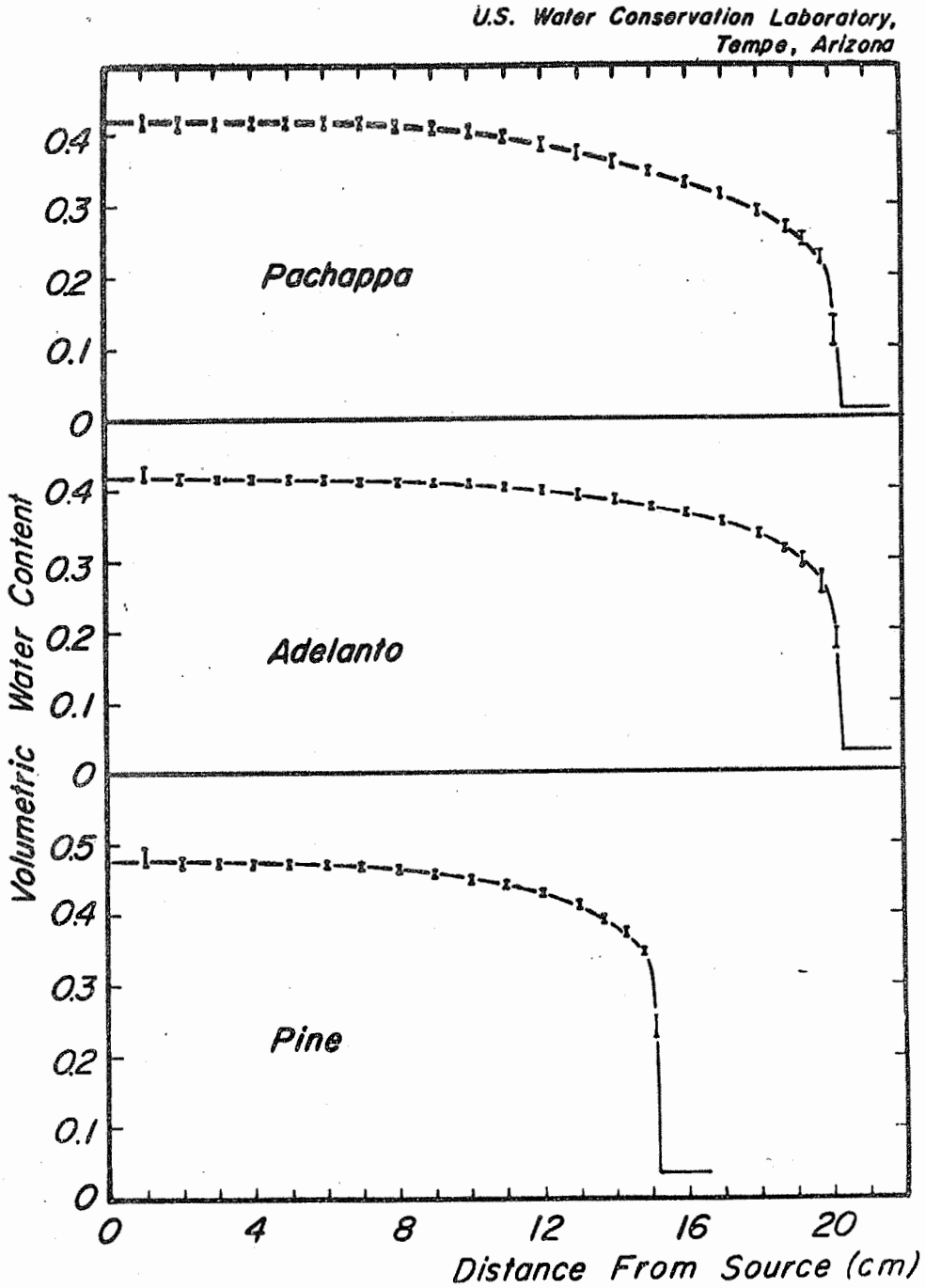

Figure 1. Water content distribution curves for duplicate samples of three soil materials at five temperatures. The length of the vertical lines indicates the range of water contents for the ten samples. The line was drawn through the means.

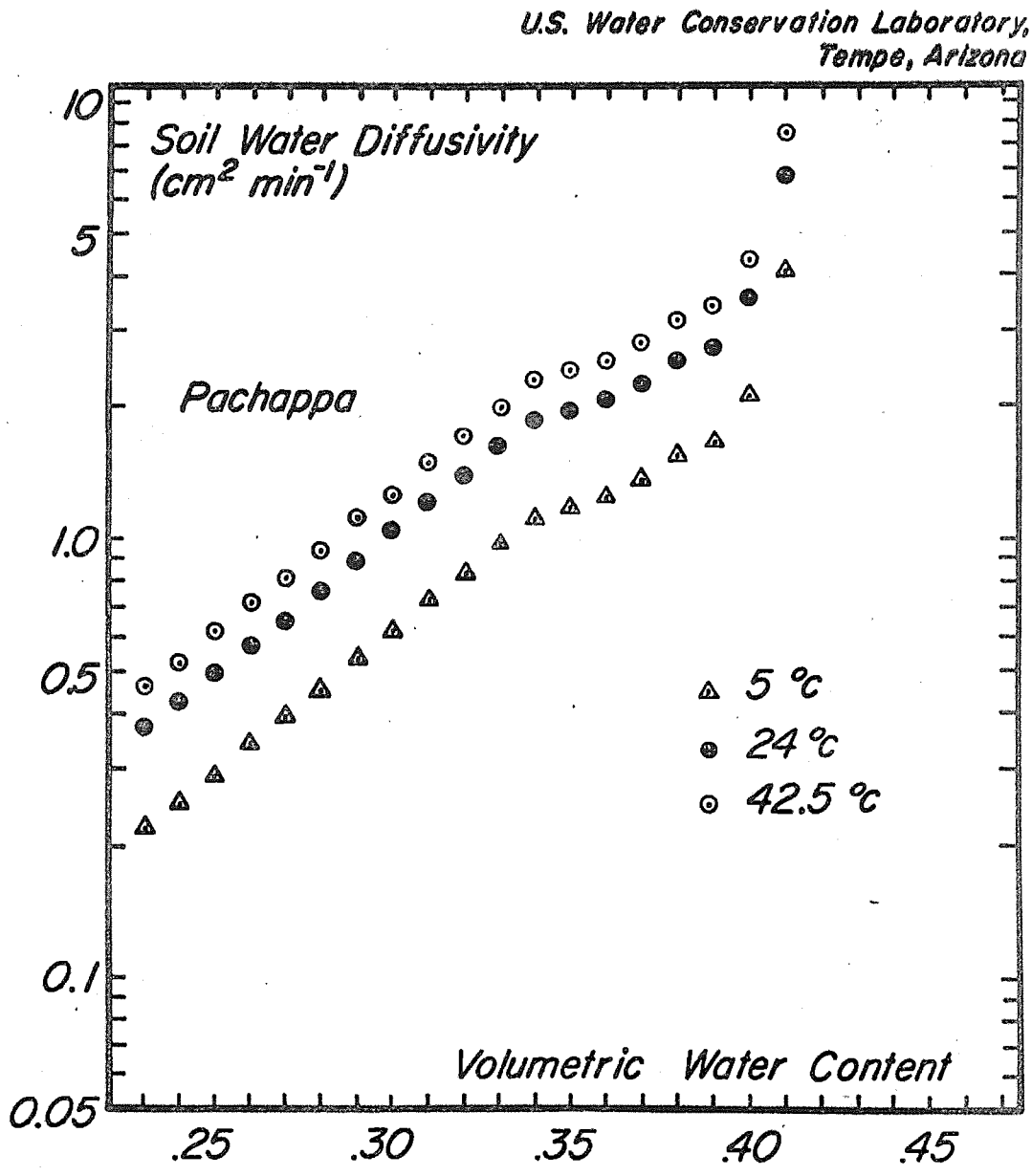

Figure 2. Soil-water diffusivity versus volumetric water content for Pachappa loam at three temperatures.

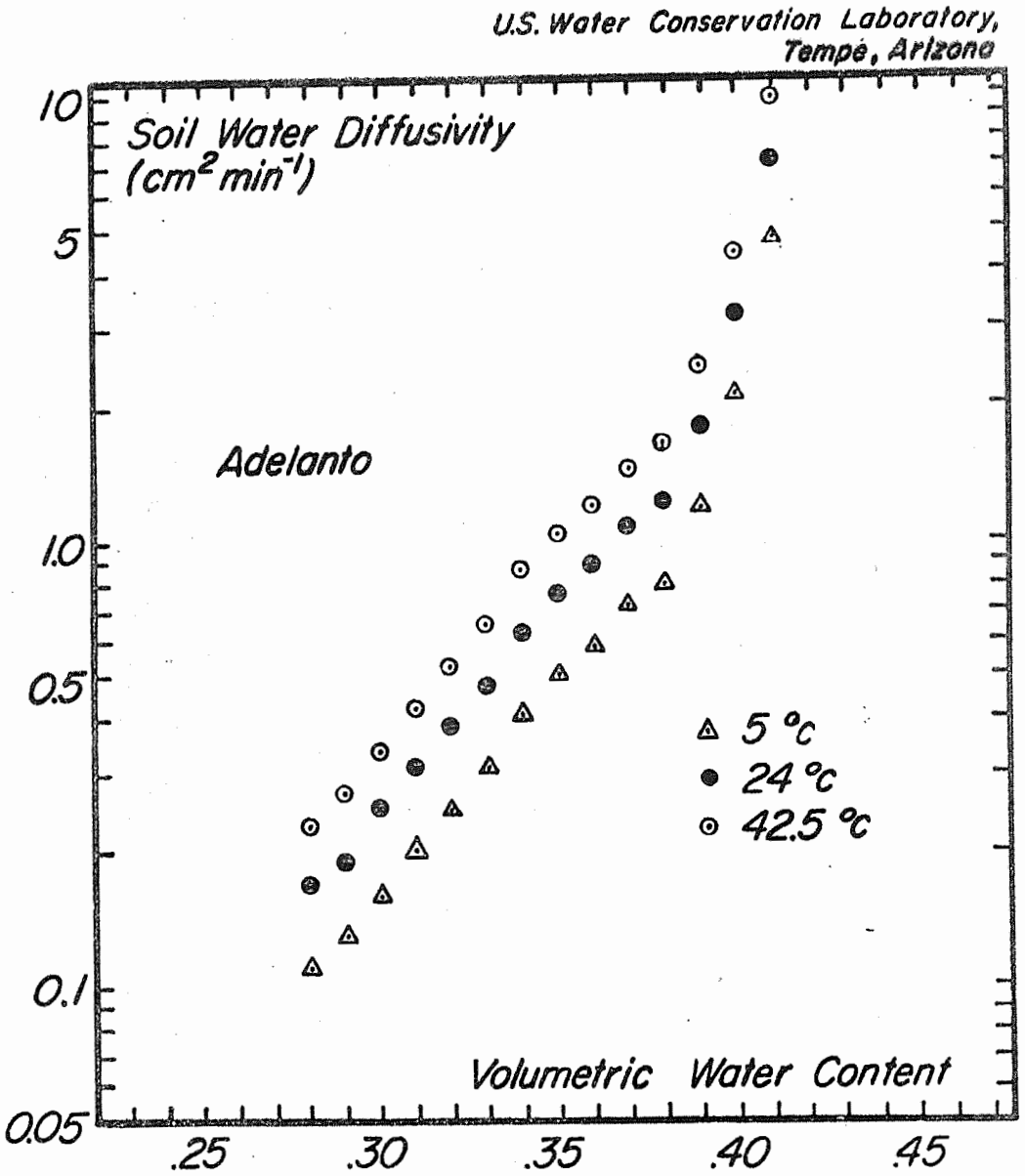

Figure 3. Soil-water diffusivity versus volumetric water content for Adelanto loam at three temperatures.

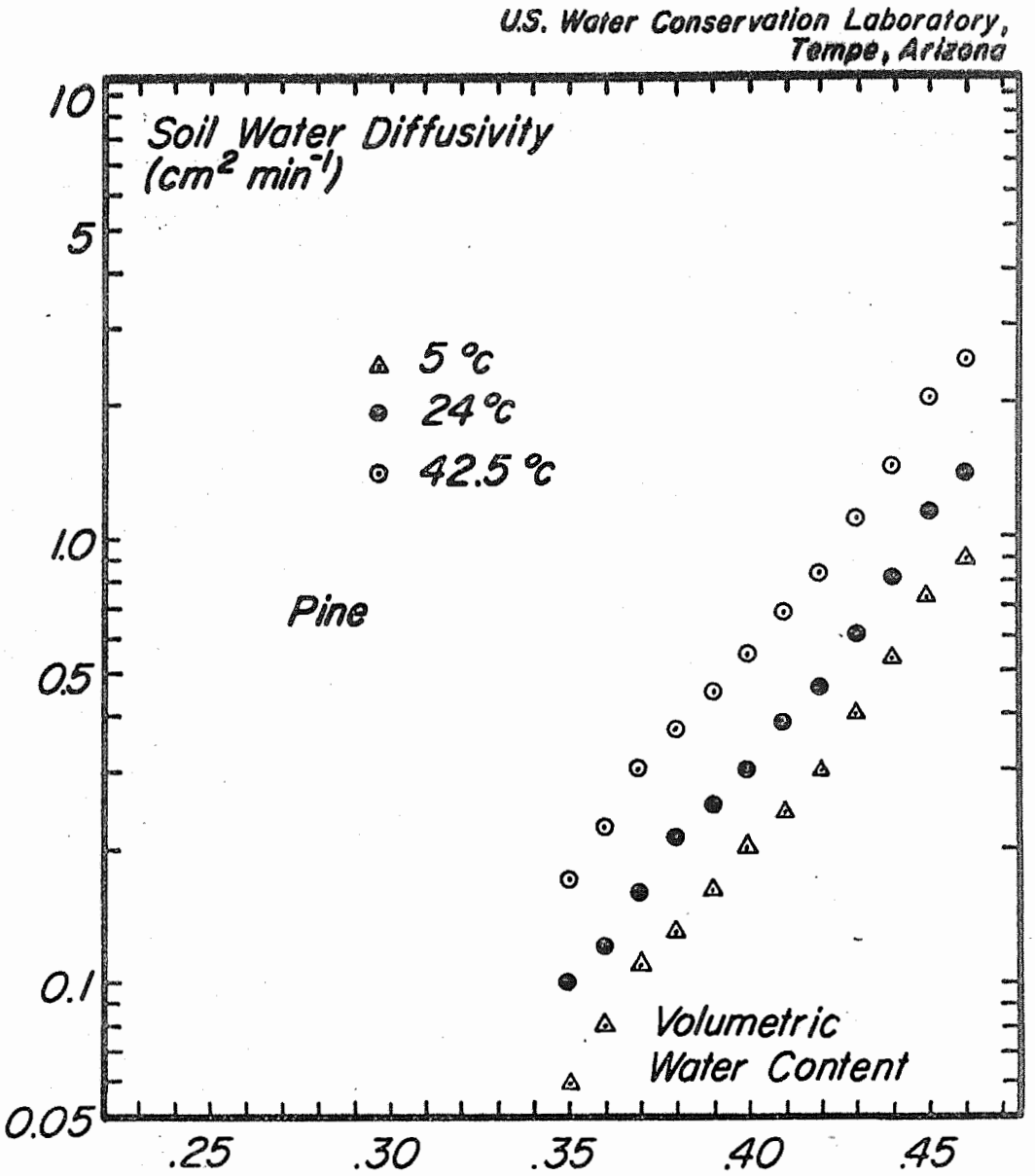

Figure 4. Soil-water diffusivity versus volumetric water content for Pine silty clay at three temperatures.

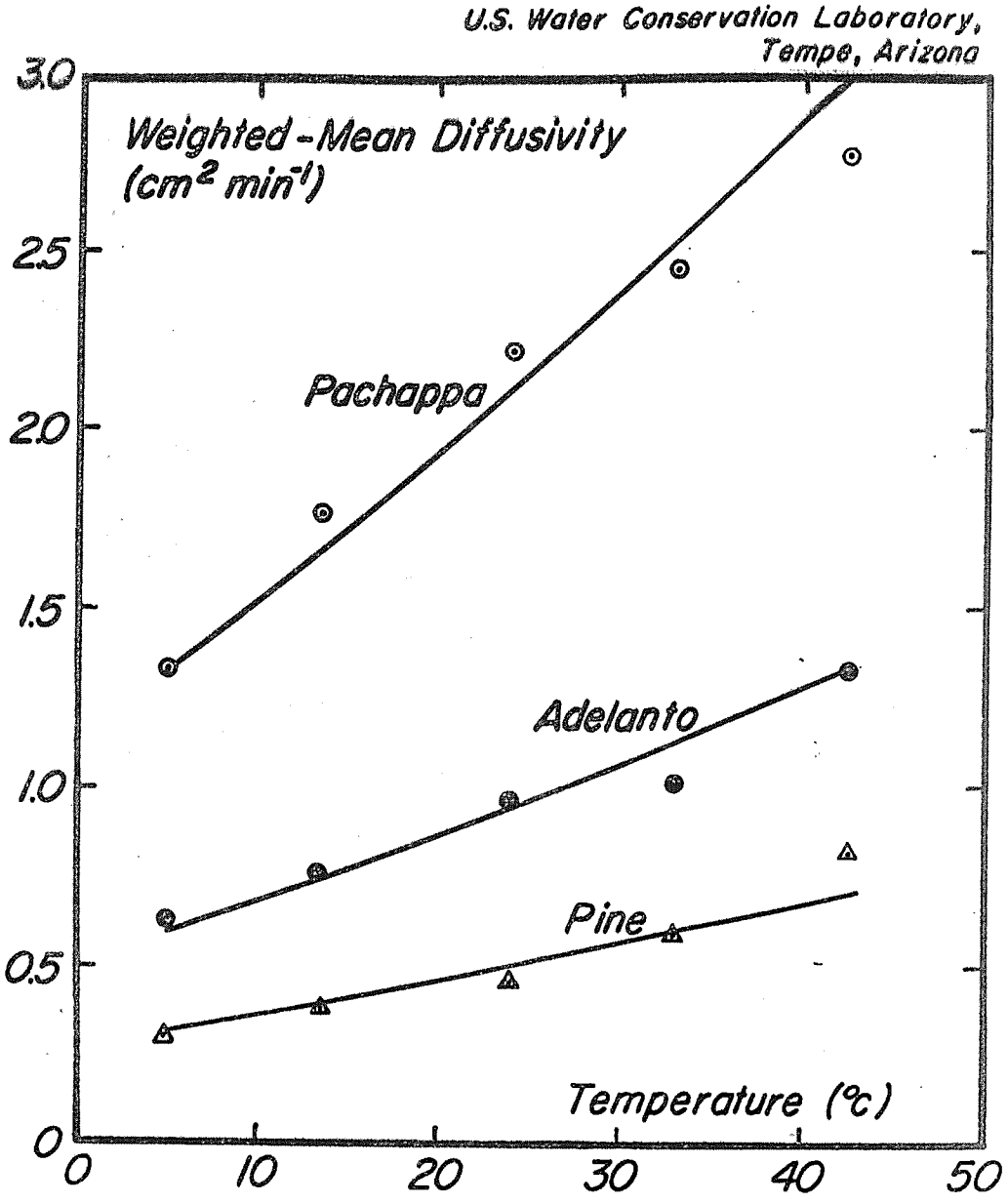

Figure 5. Weighted-mean diffusivity versus temperature. The symbols are experimental whereas the lines were obtained from considerations of the temperature dependence of surface tension and viscosity.

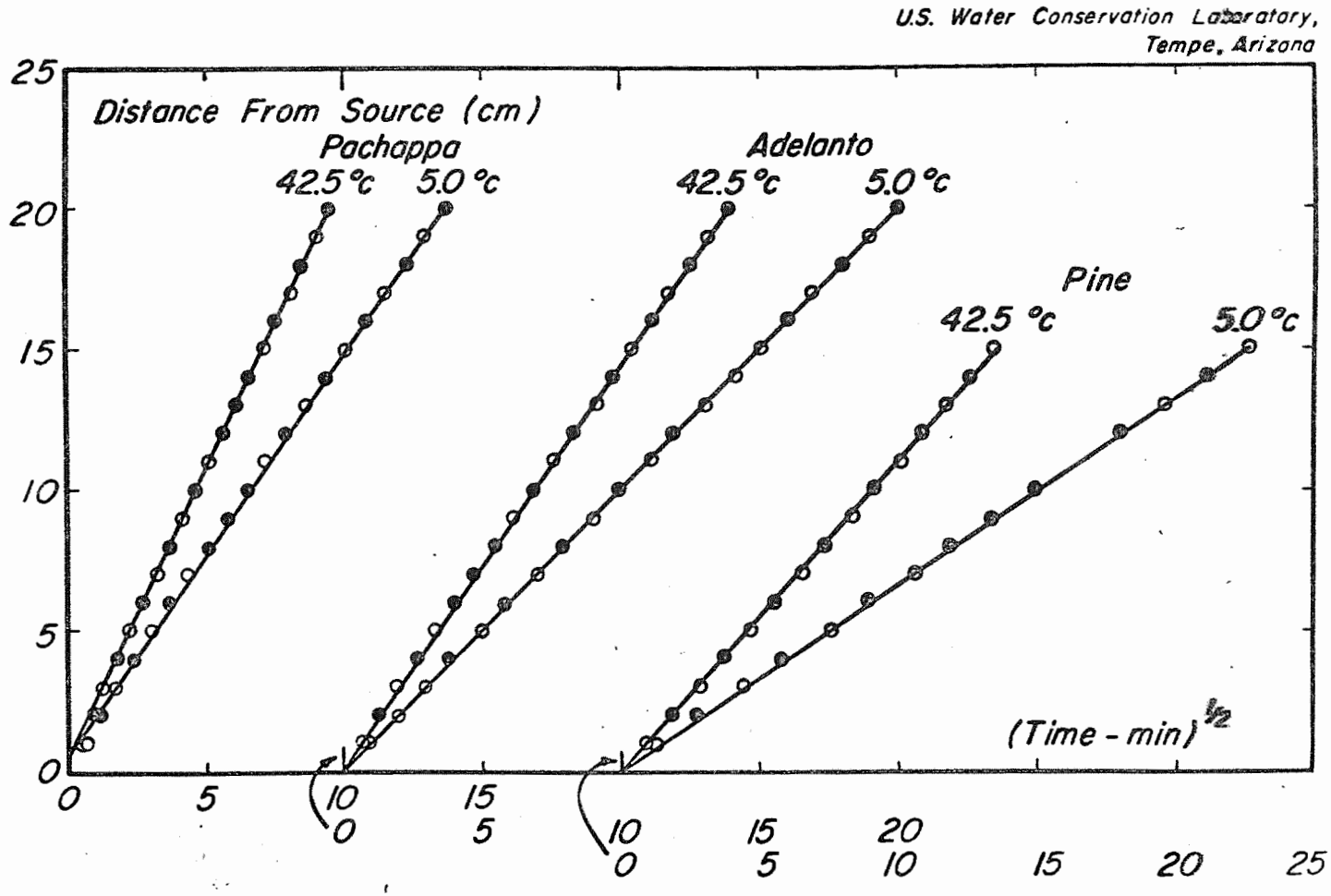

Figure 6. Distance to the wetting front versus the square root of time for three soil materials, each in duplicate at the highest and lowest temperatures.

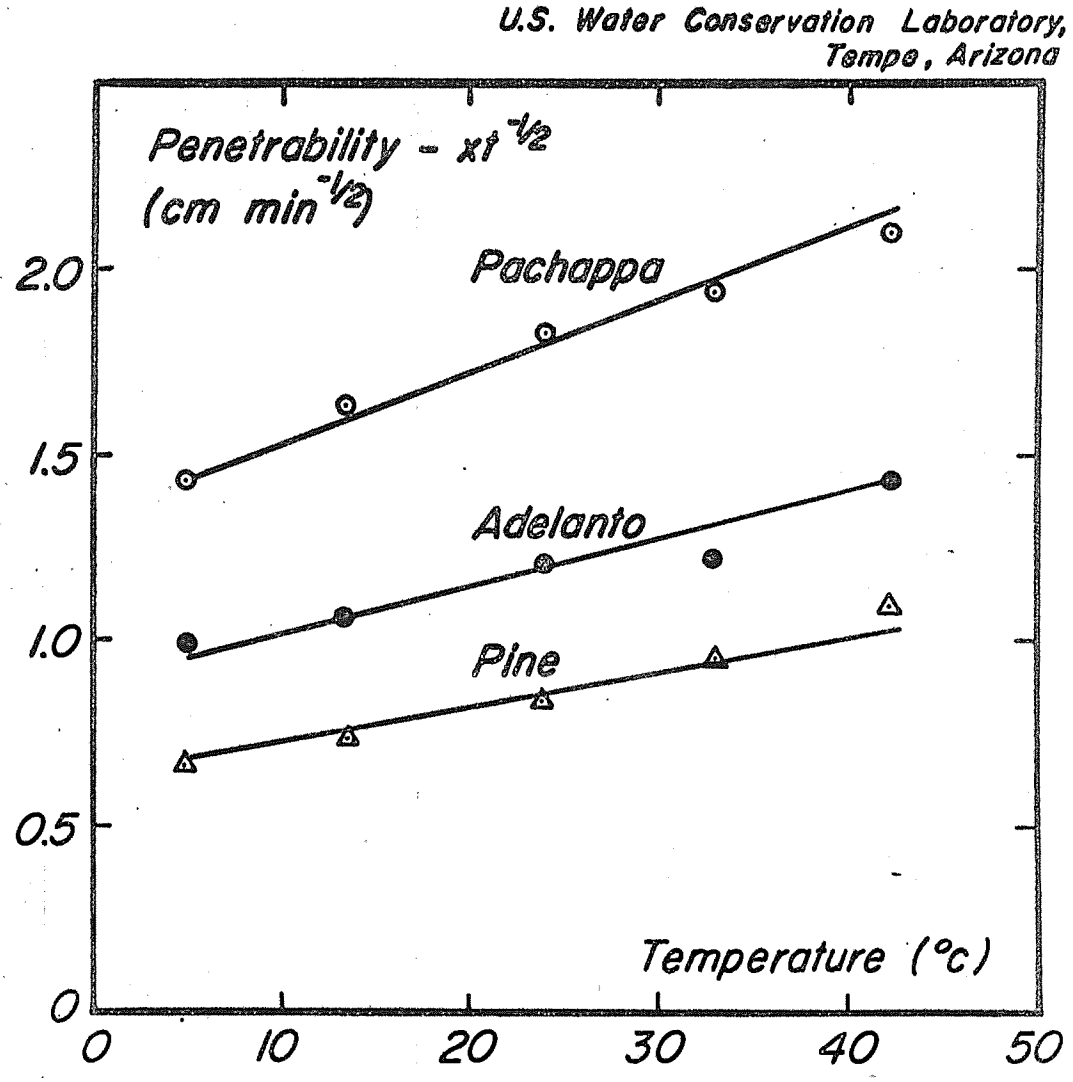

Figure 7. Advance of wetting front versus temperature. The symbols are experimental whereas the solid line was obtained from considerations of the temperature dependence of surface tension and viscosity.

REFERENCES:

1. Bruce, R. R., and Klute, A. The measurement of soil-moisture diffusivity. Soil Sci. Soc. Amer. Proc. 20:458-462. 1956.
2. Crank, J. The Mathematics of Diffusion. Oxford University Press. 1956.
3. Dorsey, N. E. Properties of Ordinary Water-Substance. Reinhold Publishing Corp., New York, pp. 183, 514-515. 1940.
4. Gardner, W. R., and Mayhugh, M. S. Solution and tests of the diffusion equation for the movement of water in soil. Soil Sci. Soc. Amer. Proc. 22:197-201. 1958.
5. Gardner, W. R. Diffusivity of soil water during sorption as affected by temperature. Soil Sci. Soc. Amer. Proc. 23: 406-407. 1959.
6. Kirkham, D., and Feng, C. L. Some tests of the diffusion theory, and laws of capillary flow, in soils. Soil Sci. 67: 29-40. 1949.
7. Nielsen, D. R., Biggar, J. W., and Davidson, J. M. Experimental considerations of diffusion analysis in unsaturated flow problems. Soil Sci. Soc. Amer. Proc. 26:107-111. 1962.
8. Philip, J. R. Numerical solutions of equations of the diffusion type with diffusivity concentration dependent. Trans. Faraday Soc. 51:885-892. 1955.
9. Philip, J. R. The theory of infiltration. 1. The infiltration equation and its solution. Soil Sci. 83:345-347. 1957.
10. Philip, J. R. The theory of infiltration. 4. Sorptivity and algebraic infiltration equations. Soil Sci. 84:257-264. 1957.
11. Swartzendruber, D., de Boodt, M. F., and Kirkham, D. Capillary intake rate of water and soil structure. Soil Sci. Soc. Amer. Proc. 18:1-7. 1954

PERSONNEL PART I: R. D. Jackson

PART II. EXAMINATION OF THE PRESSURE PLATE OUTFLOW METHOD FOR MEASURING CAPILLARY CONDUCTIVITY.

This investigation was undertaken to ascertain the reliability of the pressure plate outflow method for measuring soil-water diffusivity. The method, as proposed by Gardner (3), assumed constant diffusivity and negligible plate or membrane impedance. The diffusivity was obtained by plotting fractional outflow yet to come ($1 - Q_t/Q_o$) versus time on semi-log paper and calculating D from the slope of the line. Methods proposed to account for membrane impedance were reported by Miller and Elrick (5), Rijtema (7), and Kunze and Kirkham (4). Of the three, Kunze and Kirkham's method appears the most useful.

Experimental results obtained using this method were disappointing. Reproducible results were not obtained and difficulties arose in the interpretation of data. This led to a theoretical and experimental examination of the method, the results of which constitute this report.

EXAMINATION OF THEORY:

The assumption of constant diffusivity appears to be the weak point in the outflow method. Authors of previous literature on this method have carefully pointed out that this assumption is essential to mathematical development of the method, but none have shown that it is experimentally attainable, nor to what degree it must be attained to permit agreement between experiment and theory. Experimentally, outflow increments of sufficiently small size to validate the assumption of constant D appear impractical, because small increments require high measurement precision and necessitate a large number of increments to cover a given range of water contents.

An indication of the effect of the nonconstant diffusivity on outflow curves was obtained by assuming a particular diffusivity--water content relationship and calculating outflow curves, assuming no membrane impedance ($\underline{a} = 0$; the symbol $\underline{a}$ refers to the ratio of membrane impedance to the soil impedance). Theoretical outflow

curves for an exponential diffusion coefficient $D = D_o \exp \beta\theta$ are given by Crank (2). The curves are for $D_i/D_o = 10$ and $D_i/D_o = 25$, where D_i is the diffusivity at the initial (highest) water content, and D_o is the diffusivity at the final (lowest) water content, and θ is the volumetric water content. The solution for the ratio $D_i/D_o = 2$ was obtained by interpolation.

Figure 1 shows outflow curves for $D_i/D_o = 2, 10, 25$, assuming $D = D_o \exp \beta\theta$ and $\underline{a} = 0$. For $D_o t/L^2 > 0.2$ the latter graph is linear and the slope can be easily determined. Also shown are two lines illustrating the effect of membrane impedance on outflow curves with constant diffusivity. Note that for $D_o t/L^2 > 0.2$ the graphs are linear and the extrapolated linear portion has an intercept greater than $8/\pi^2$.

For $D_i/D_o = 2$, 10, and 25, there is no linear portion from which "the" slope can be calculated. Bear also in mind that the intercept cannot be less than $8/\pi^2$. Thus the method of Gardner (3) and of Rijtema (7) are not applicable if $D_i/D_o \not\approx 1$. The same applies to the method of Miller and Elrick (5) even if $\underline{a} = 0$, because the exponential tails of experiment and theory cannot be matched. Kunze and Kirkham (4) stated that they frequently observed twofold to fivefold changes in conductivity (and hence diffusivity) with water content changes of only 1 to 2 percent.

Kunze and Kirkham (4) utilize the initial portion of the outflow curves and assume D constant within this region of water contents. In Figure 2, the effect of nonconstant D on initial outflow without membrane impedance is shown when plotted according to Kunze and Kirkham. Also on the plot are three lines for $D_i/D_o = 1$ but for three different values of membrane impedance. This shows that with either nonconstant diffusivity or with appreciable membrane impedance the relation between outflow and time is initially linear on a log-log plot. However, if both effects are present simultaneoulsy, there is, for lack of an appropriate mathematical solution, no assurance that a theoretical model will exhibit a linear portion and afford a method of data analysis.

Plots of Q_t/Q_o versus $(D_o t/L^2)^{1/2}$, (according to the $t^{1/2}$ method) as discussed by Crank (2) are shown in Figure 3 for $D_i/D_o = 2$, 10, and 25, with $\underline{a} = 0$. The initial linear portions are evident. Membrane impedance makes the initial portion of the curves nonlinear and shifts them to the right as shown in the curves for $\underline{a} = 0.0667$ and 0.2, $D_i/D_o = 1$. Therefore, the $t^{1/2}$ method is not applicable when membrane impedance is not negligible.

EXPERIMENTAL:

To perform careful tests of present theories, nonhomogeneous packing and poor contact between the porous material and the plate had to be minimized. This consideration required a graded, uniformly packed, porous material.

The porous plates used were two monel plates 0.255 cm thick and one stainless steel plate 0.196 cm thick. The plates were selected because of their low impedance, relatively high bubbling pressure, and rigidity.

The pressure cell developed by Reginato and Van Bavel (6) was used for this measurement. The cell is sufficiently small that it can be weighed at the beginning and the end of a measurement to obtain the total outflow. A stopcock arrangement was added to the outflow tube to prevent water from re-entering the porous material while the air pressure was disconnected during weighing.

The porous plates were saturated with water in a vacuum desiccator, then placed in the pressure cell. The cells were assembled and the impedance of each plate was measured with the cell complete except for the porous material. The measured impedances (z_p) were: Cell 1, monel plate, $z_p = 12.8$ min; Cell 2, monel plate, $z_p = 10.8$ min; Cell 3, stainless steel plate, $z_p = 4.5$ min.

After measuring the impedances, the cells were taken apart and the 50-500μ sand was packed, under water, into each cell. The cells were assembled and 60 mb of air pressure was applied for an overnight period. A pressure of 60 mb was sufficient to bring

air into contact with the plate but only a small amount of outflow resulted.

The bulk densities, measured at the end of the experiment, were 1.57 g cc for each sample. This agreement in bulk densities is an indication that the samples were packed sufficiently uniformly.

Outflow measurements were made by placing the cell near a direct-reading balance (readable to 0.01 g) and collecting the outflow directly on the balance. The time associated with outflow increments was observed on a timer accurate to 0.01 minute. During the initial outflow period two people were required to obtain the measurements, one noted the outflow, the other the time. The cell was weighed immediately prior to each measurement, allowed to equilibrate for 24 hours after completion of the measurement and reweighed to obtain the total outflow. After equilibration at the final pressure, the cell weight was taken and the sample removed and dried to obtain the final water content and bulk density. The air pressure to the cell was controlled by a regulator accurate to 0.3 mb. Measurements were made during three pressure increments of 10 mb from 60 to 90 mb and one 20-mb increment from 90-110. Samples then were resaturated, equilibrated at 60 mb, and another identical series of measurements were made.

At the completion of the experiment, the impedances of the monel plates were so high that accurate measurements of the impedances were not attempted. The stainless steel plate had a $z_p = 6.85$, about 50 percent higher than at the beginning of the experiment. The increases in impedance were possibly due to bacterial activity and corrosion in the plates. If the theory adequately accounts for membrane impedance, the increase in impedance should not affect the calculation of diffusivity.

RESULTS AND DISCUSSION:

Results of the total outflow and volumetric water content measurements are presented in Table 1. If all experimental and

theoretical conditions were perfectly met, the values for Q_o and θ_i for the three cells would be identical at each pressure increment. However, these quantities vary considerably between cells and with reruns of the same cell. Regardless of the reason for the differences, consistent results were not obtained from samples intended to be replicates.

Of primary interest are the diffusivity data presented in Table 2. Diffusivities calculated from Q_t/Q_o versus $t^{1/2}$ plots show considerable variation between replicates and between reruns of the same sample. The large differences between reruns with the cells containing monel plates can be explained partially on the basis of increased plate impedance for which the $t^{1/2}$ method does not account. However, with the cell containing the stainless steel plate an increased plate impedance would not account for the higher D obtained during the second series of runs.

When the data were plotted on log-log paper according to Kunze and Kirkham (4) not all data could be matched satisfactorily with a theoretical curve and hence, account for membrane impedance. Considerable difficulty was encountered in fitting some curves as evidenced by the fact that, in some instances, ranges instead of single values are given in Table 2. More variability occurred when data were interpreted in this manner than by using the $t^{1/2}$ method.

The difficulty in matching experimental points to theoretical curves to account for plate impedance is depicted in Figure 4, where data for cell 2 (monel plate), 80 to 90 mb pressure increment, are presented. There are six data points within the first 15 percent of the total outflow—the region Kunze and Kirkham suggest using. The solid circles show the match of theory and experiment if the first two points are considered in error, hence neglected. The open circles show the fit if the first five points are used and the remainder neglected. It is difficult to decide which theoretical curve the points best fit. If the curve for

$\underline{a}$ = 0.5 is chosen, then D = 0.27. Additional uncertainty arises if the curve for $\underline{a}$ = 1000 is chosen. The family of curves for $\underline{a}$ = 10 to $\underline{a}$ = 1000 are nearly coincident [see (4) Table 1], making the selection of the proper curve difficult. For $\underline{a}$ = 10, α_1^2 = 0.097, and for $\underline{a}$ = 1000, α_1^2 = .001, thus for these data, D would be somewhere between 4 and 40, considerably higher than if the curve for $\underline{a}$ = 0.5 is used. This shows some of the difficulties one may encounter when membrane impedance is large.

In contrast, Figure 5 shows data obtained when membrane impedance was negligible. These data are for cell 3 (stainless steel plate). The data match the theoretical curve and the calculated D is the same as that calculated from Q_t/Q_o versus $t^{1/2}$ plots. Figure 6 shows Q_t/Q_o versus $t^{1/2}$ plots for the same data shown in Figures 4 and 5. The open circles are for cell 3 (stainless steel plate). Note that the initial portion is linear and pierces the origin. The D calculated from the slope of the line is the same as the D obtained in Figure 5. The solid circles are the same data as shown in Figure 4. Note the sigmoid-shaped curve. Only a portion near the center approaches linearity. The D calculated from the slope of this portion is 0.119, one-half of the lowest value obtained from the plots of Figure 4. This shows the difficulty in using the $t^{1/2}$ method when plate impedance is present.

Figure 7 shows the same data (negligible membrane impedance) as are in Figure 5 and the open circles of Figure 6 plotted semi-logarithmically according to Gardner's method. Comparing the curve with Figure 1 suggests that D was not constant within this pressure increment. The straight line was calculated assuming D constant (D = 0.069 as obtained from Figure 5 or 6) using equation [3], neglecting all terms in the series but the first. It is obvious that D cannot be calculated from plots of this type using methods of Gardner, Rijtema, or Miller and Elrick. In the latter case a matching theoretical curve cannot be obtained.

SUMMARY AND CONCLUSIONS:

1. The assumption of constant diffusivity puts a severe limitation on the pressure-plate outflow method. It does not appear practical from an experimental point of view to take increments sufficiently small to make this assumption valid.

2. When diffusivity is not constant and membrane impedance not negligible, methods accounting for membrane impedance may be inapplicable because theoretical and experimental curves may not match.

3. When diffusivity is not constant and membrane impedance is negligible, plots of Q_t/Q_o versus $t^{1/2}$ yield initially linear portions from which a weighted-mean diffusivity can be calculated. The method of Kunze and Kirkham is also applicable in this case.

4. It is extremely difficult experimentally to obtain replicated results of diffusivity measurements.

5. Considering the various theoretical and experimental aspects, we conclude that data obtained from the outflow method, in its present state of development, may be uncertain by an order of magnitude.

Table 1. Outflow and water content data for 50-500μ sand, bulk density 1.57 g cm^{-3}. The a and b columns are reruns of the same sample.

A. Total outflow (Q_o in grams).

Pressure increment (mb)	Cell 1 (monel plate)		Cell 2 (monel plate)		Cell 3 (stainless steel plate)	
	a	b	a	b	a	b
60-70	2.57	3.08	1.58	2.47	3.97	4.04
70-80	5.17	3.49	4.39	4.28	5.98	4.51
80-90	--	3.64	--	3.99	--	3.00
90-110	4.87	4.20	4.87	4.14	2.91	2.86

B. Initial volumetric water content (θ_i, cm^3 cm^{-3}).

60-70	.345	.308	.335	.308	.301	.288
70-80	.309	.265	.313	.274	.254	.231
80-90	--	.216	--	.214	--	.168
90-110	.173	.165	.170	.158	.126	.126

Table 2. Reproducibility of diffusivity data for 50-500μ sand, bulk density 1.57 g cm^{-3}. Units of diffusivity are cm^2 min^{-1}. The a and b columns are reruns of the same sample.

A. Using square root of time method.

Pressure increment (mb)	Cell 1 (monel plate)		Cell 2 (monel plate)		Cell 3 (stainless steel plate)	
	a	b	a	b	a	b
60-70	2.50	.438	1.45	.463	1.68	3.60
70-80	1.64	.542	2.10	.161	1.49	1.89
80-90	--	.272	--	.119	--	.493
90-110	.553	.087	.477	.046	.069	.093

B. Using Kunze and Kirkham's (4) method.

60-70	--	1.45	--	--	1.78	4.12
70-80	3.13	14.3	3.33	--	1.70	2.87
80-90	--	.64-1.1	--	.27-4.0	--	.490
90-110	1.47	.249	.602	.114	.069	.098

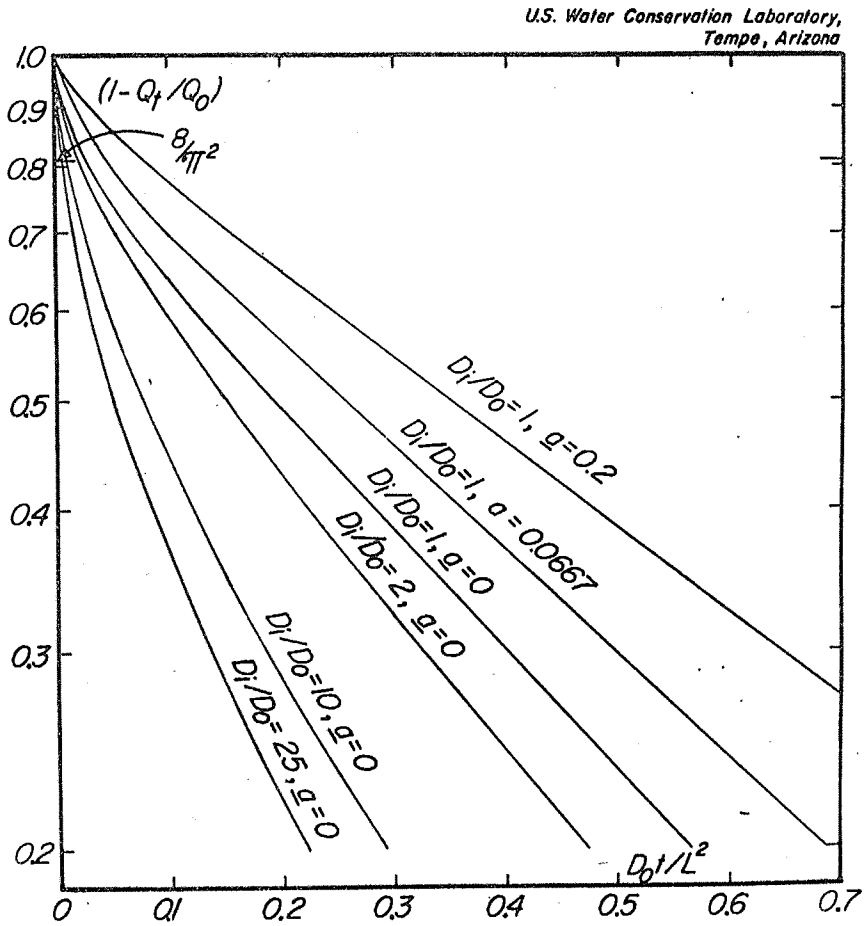

Figure 1. Theoretical outflow curves plotted according to Gardner's method.

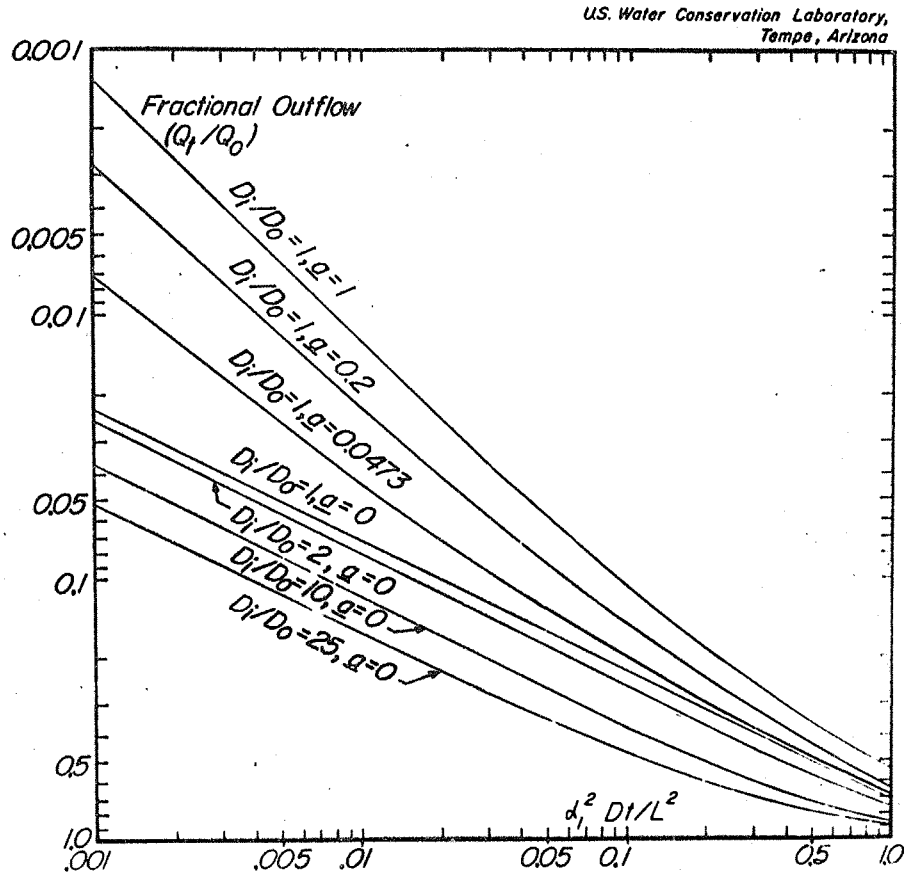

Figure 2. Theoretical outflow curves plotted according to Kunze and Kirkham's method.

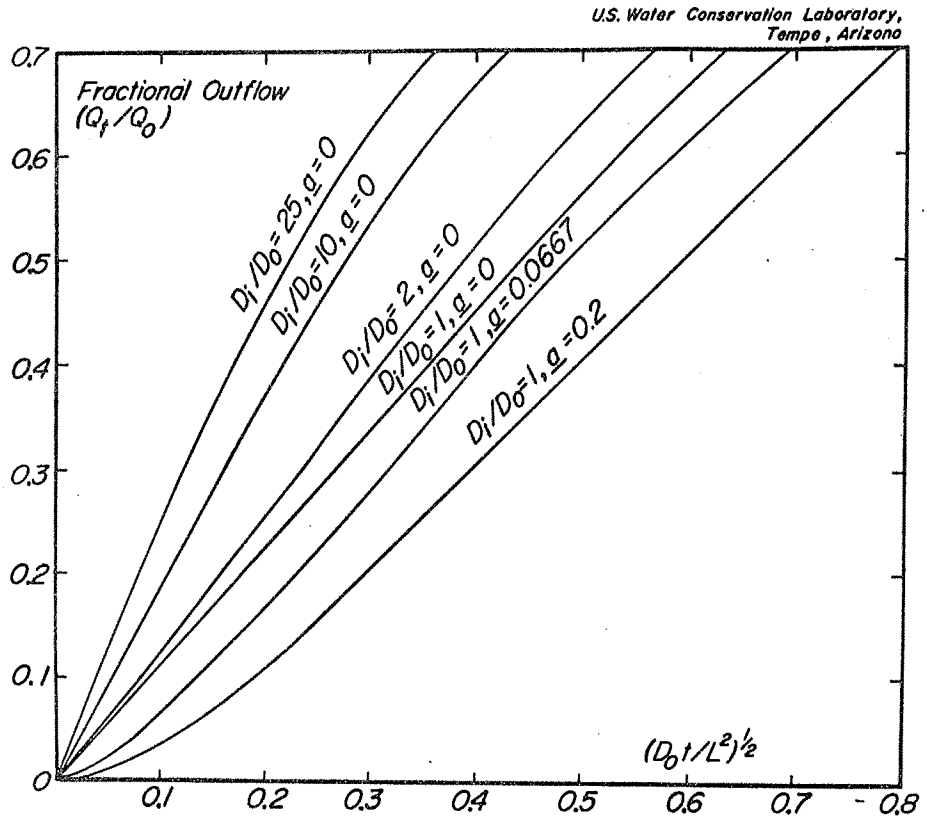

Figure 3. Theoretical outflow curves plotted according to the square root of time method.

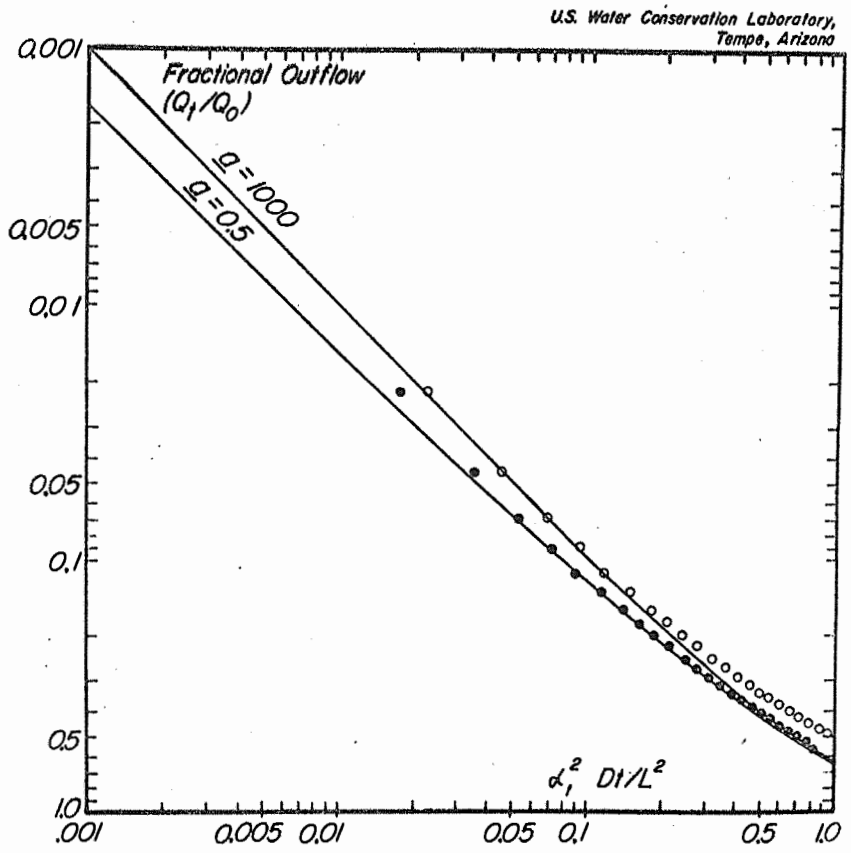

Figure 4. Comparison of experimental data from samples having membrane impedance with theoretical outflow curves of Kunze and Kirkham.

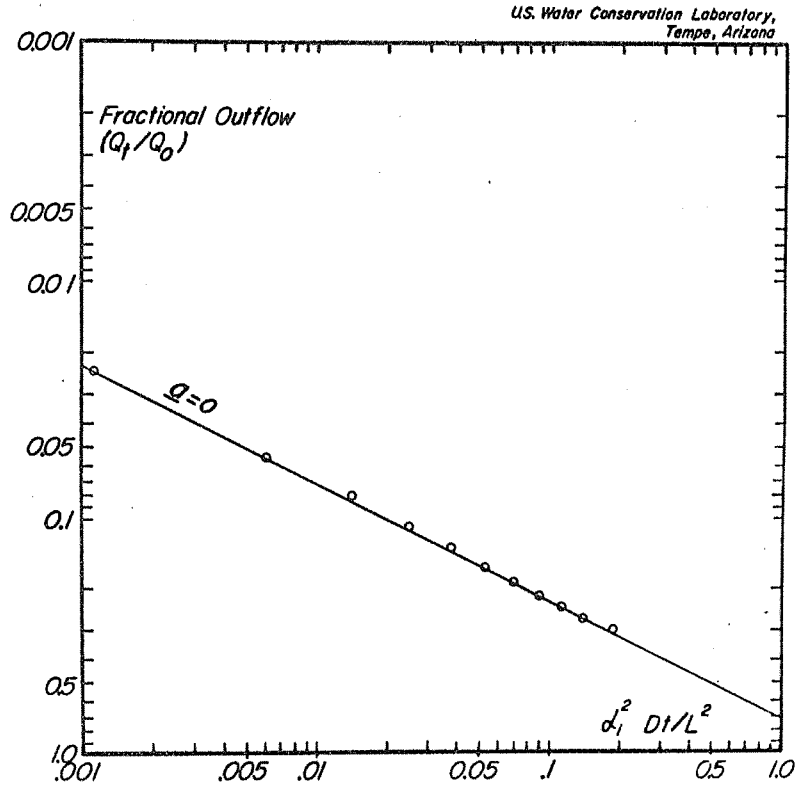

Figure 5. Comparison of experimental data from sample without membrane impedance with theoretical outflow curve of Kunze and Kirkham.

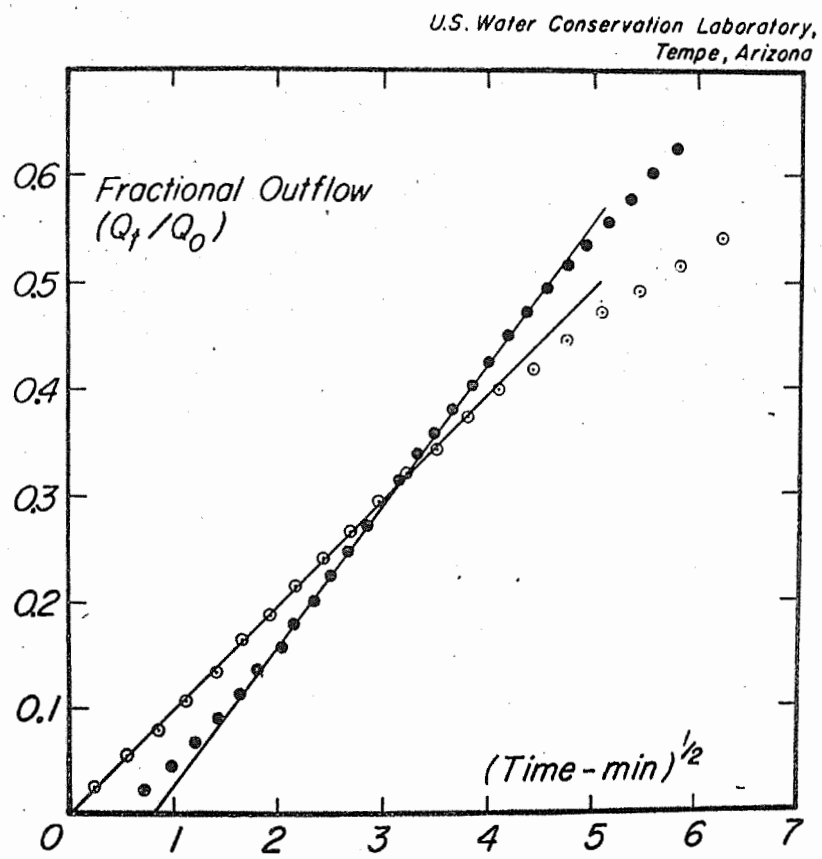

Figure 6. Data from samples without (open circles) and with (solid circles) membrane impedance plotted according to square root of time method.

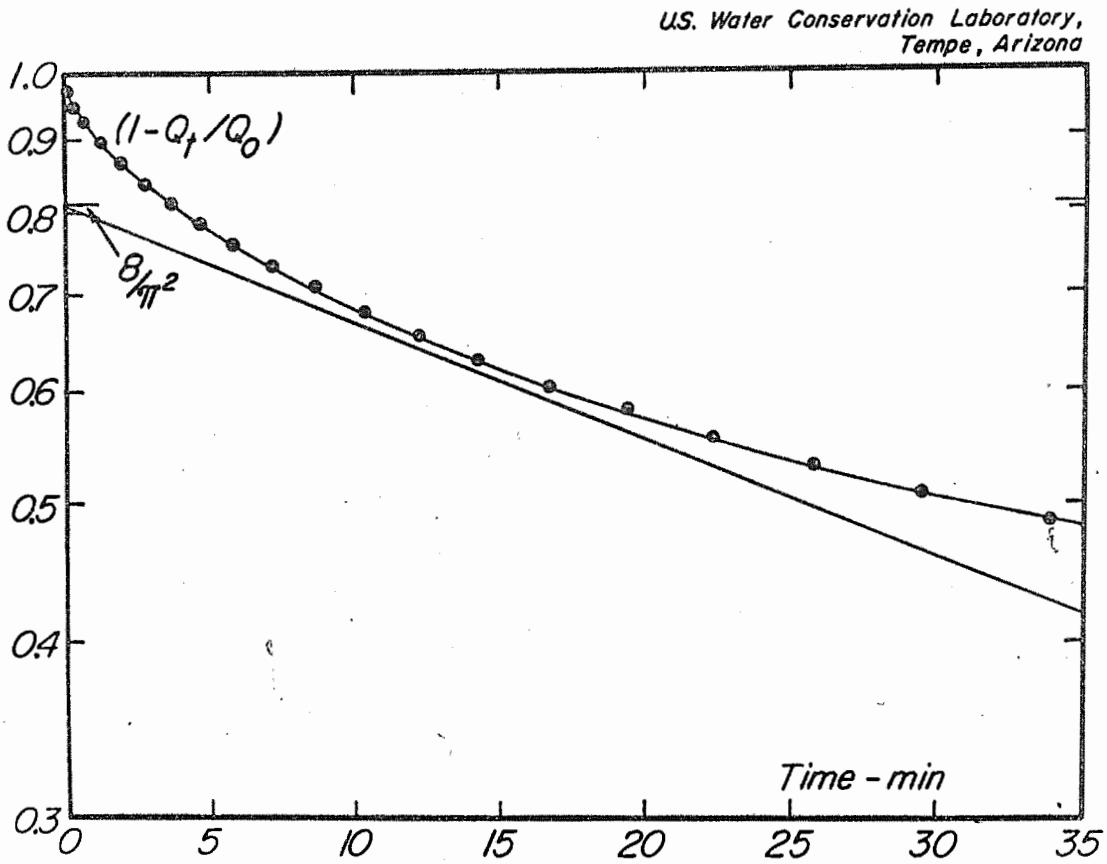

Figure 7. Experimental data without membrane impedance but with non-constant diffusivity plotted according to Gardner's method.

REFERENCES:

1. Butijn, J., and Wesseling, J. Determination of the capillary conductivity of soils at low moisture tensions. Netherlands J. Agr. Sci. 2:155-163. 1959.

2. Crank, J. Mathematics of Diffusion. Oxford University Press, London. 1956.

3. Gardner, W. R. Calculation of capillary conductivity from pressure plate outflow data. Soil Sci. Soc. Amer. Proc. 20:317-320. 1956.

4. Kunze, Raymond J., and Kirkham, Don. Simplified accounting for membrane impedance in capillary conductivity determinations. Soil Sci. Soc. Amer. Proc. 26:421-426. 1962.

5. Miller, E. E., and Elrick, D. E. Dynamic determination of capillary conductivity extended for non-negligible membrane impedance. Soil Sci. Soc. Amer. Proc. 22:483-486. 1958.

6. Reginato, Robert J., and Van Bavel, C. H. M. Pressure cell for soil cores. Soil Sci. Soc. Amer. Proc. 26:1-3. 1962.

7. Rijtema, P. E. Calculation of capillary conductivity from pressure plate outflow data with non-negligible membrane impedance. Netherlands J. Agr. Sci. 7:209-215. 1959.

PERSONNEL PART II: R. D. Jackson, C. H. M. van Bavel, R. J. Reginato

PART III. A DISCUSSION OF FICK'S LAWS FOR DIFFUSION APPLIED TO POROUS MEDIA.

Fick's laws - originally stated for one-phase media - apply also to diffusive transport through fluids (gases and/or liquids) contained in porous media. The solid matrix complicates matters by altering the diffusion path length and the cross-sectional area available for diffusion. In such applications both the diffusion coefficient and the concentration of the diffusing substance can be expressed either on the basis of the bulk volume of the medium or of its fluid phase. There exists no universally adopted usage in this regard. Also, both modes of expression are, at times, used in the same treatment and, indeed, in the same equation, all this being conducive to errors and confusion.

This discussion compares and relates both modes of expression as regards to their usage.

FICK'S FIRST LAW:

When expressed on the basis of the bulk medium, the first, or steady-state, law for the one-dimensional case reads:

$$\frac{dQ}{dt} = -D_m A_m \frac{dc_m}{dx_m} , \qquad [1]$$

where $\frac{dQ}{dt}$ is the mass flux, D the diffusion coefficient, A the cross-sectional area, c the concentration of the diffusing substance, and x the distance. The subscript m refers to the bulk medium, the subscript f to the fluid.

If ϵ is the relative volume occupied by the particular fluid in question (V_f/V_m), we have

$$c_m = \epsilon \, c_f , \qquad (0 < \epsilon < 1). \qquad [2]$$

In the case of a single fluid completely occupying the pores of the medium, ϵ is the porosity of the medium. If β is defined as a tortuosity, we may write

$$x_m = \beta\, x_f \quad , \qquad (0 < \beta < 1). \qquad [3]$$

In some cases the area applicable to the fluid (A_f) has been taken to be $\epsilon\, A_m$, but this is true only for diffusion paths of constant cross-section passing straight through the medium. From $A = V/x$ and equation [3] it follows that

$$A_m = A_f\, (\epsilon\, \beta)^{-1} \quad . \qquad [4]$$

Substituting [2], [3], and [4] into [1], we obtain Fick's first law expressed on the basis of the fluid phase:

$$\frac{dQ}{dt} = D_f\, A_f\, \frac{dc_f}{dx_f} \quad , \qquad [5]$$

where

$$D_f = D_m\, \beta^{-2} \quad , \qquad [6]$$

a relation that does not contain ϵ, the relative volume of the fluid.

Often it is convenient to use [1] but to measure and express the concentration as c_f. Using [2] in [1], the first law becomes:

$$\frac{dQ}{dt} = -\, D_p\, A_m\, \frac{dc_f}{dx_m} \quad , \qquad [7]$$

where D_p is still another diffusion coefficient. It follows that

$$D_p = D_f\, \epsilon\, \beta^2, \qquad [8]$$

where, in contrast to [6], ϵ is explicit.

FICKS'S SECOND LAW:

In applying Fick's second law to a porous medium, and using quantities referring to the bulk medium,

$$\frac{\partial c_m}{\partial t} = D_m \frac{\partial^2 c_m}{\partial x_m^2} , \qquad [9]$$

describes the transport in one dimension. When, for convenience, fluid-based concentrations are used, we find the same form:

$$\frac{\partial c_f}{\partial t} = D_m \frac{\partial^2 c_f}{\partial x_m^2} , \qquad [10]$$

From [6] and [8], we see that

$$\frac{\partial c_f}{\partial t} = \frac{D_p}{\epsilon} \frac{\partial^2 c_f}{\partial x_m^2} , \qquad [11]$$

a form often found in the literature.

Upon integrating equations [9], [10], or [11] for a particular solution, c should be expressed in both integral and boundary values on the same, consistent basis.

CONCLUSIONS:

As to preference, equations containing x_f and A_f are impractical because neither can be directly measured. This leaves equations [1] and [9] as the most consistent and perhaps most rigorous and equations [7] and [11] as the most practical in some situations. Whatever choice is made, the terms used in diffusion equations and their measurement should be unambiguously described.

PERSONNEL PART III: R. D. Jackson, C. H. M. van Bavel, F. S. Nakayama.

TITLE: DEVELOPMENT AND USE OF GAMMA TRANSMISSION EQUIPMENT FOR THE MEASUREMENT OF SOIL DENSITY AND MOISTURE CONTENT.

LINE PROJECT: SWC 4-gG4 CODE NO.: Ariz.-WCL-20

INTRODUCTION:

Evaporation from the soil surface is, in part, determined by the distribution and content of moisture in superficial layers. Within these, extreme gradients of moisture content occur changing rapidly with time. A study of these conditions requires a type of measurement that can be made repeatedly, without disturbing the site, and in thin layers of soil. It has been demonstrated that the gamma transmission method is suited for such a purpose to the exclusion of all other methods.

There are no commercial sources of suitable equipment nor are adapted designs readily available. For developing a better understanding of evaporation, detailed studies of surface moisture conditions are necessary and this project proposes to supply equipment to such ends.

The specific objectives involved are the design and testing of equipment for non-destructive measurement of soil density and moisture content using gamma radiation transmitted by thin soil layers and to use this method for the detailed study of moisture content of surface layers.

When investigating the transmission method the assumption is usually made that when a gamma point source is placed in a body of material, the radiation intensity is subject to the following law:

$$\frac{I_x}{I_0} = \exp\left(-{}_{\lambda}\mu_0 \rho x\right) \qquad [1]$$

Where I_x is the radiation intensity at a distant x from the source, I_0 is the radiation intensity at the point source, x is the distance from the source (cm), ${}_{\lambda}\mu_0$ is the mass attenuation coefficient ($cm^2 g^{-1}$), and ρ is the total or wet density ($g\ cm^3$).

It must be remembered however, that this equation applies only to monochromatic, primary radiation, that is, radiation of one wave length emitted by a source and transmitted to the detector without alteration.

Equation [1] will be used in this work by empirically evaluating the mass attenuation coefficient for various soils. Then, by maintaining a fixed distance between the source and detector, the density can be calculated by measuring the radiation intensities, I_x and I_0. This calculation can then be compared to the gravimetrically measured density.

PROCEDURE:

Equipment. The source and detector probes and access tubes are all constructed from brass, as this tubing is held to very close tolerances and the probes fit snugly in the access tubes.

The source tube was designed and built to accommodate a 5 mc Cs^{137} source capsule, 1.270 cm in diameter and 1.905 cm long. In order to position the source in the access tube within 0.1 cm, a positioning tube was built and attached to the source probe. Holes with a diameter of 0.326 cm were drilled 1.0 $\pm$ 0.1 cm apart vertically.

The detector probe was designed to house the NaI(Th) scintillation crystal, the multiplier phototube, DuMont K1780, the preamplifier and related connectors. A positioning tube for the detector was built to match the one for the source probe.

The source and detector probe layout and the dimensions of the two probes are shown in Figure 1.

The electronic system used to count the number of pulses transmitted from the source to the detector consists of a non-overloading linear amplifier which is connected into a pulse height analyzer and from there into a timer, scaler, and rate meter. A separate high voltage supply is used to furnish the necessary voltage required by the multiplier phototube. A pulse height analyzer is adjusted to discriminate against all secondary or scattered radiation and therefore the scaler counts only the primary radiation. Equation [1] then gives the mass attenuation coefficients of soil and water.

Calibration. In order to apply equation [1] to this experiment it is necessary that the exact distance between the point source and the detector probe be known. However, if this distance is once known and remains constant, the calculations are much easier. Therefore,

an alignment jig has been constructed so that when placing access tubes in the soil the jig will insure that the tubes are always at a fixed distance apart. The construction layout for the alignment jig is shown in Figure 2.

In order to assure that the electronic part of the system is functioning properly at all times a count rate through a magnesium rod was taken and the electronic equipment was adjusted so that the count rate in the magnesium would be of a constant value at all times. Figure 3 shows the source and detector probes, the access tubes, the alignment jig, a lucite standard, a magnesium standard and a soil column. Initially, the two probes are lowered so that the point source and detector are at the mid point of the magnesium rod. The count rate in magnesium was adjusted electronically to a set value. This could also be done for the lucite rod.

The probes were then moved up to obtain a count rate in the soil column and a total of five separate count rates were made on each column. This was done by obtaining a count rate in the center of the soil column, 1 cm above and 1 cm below the center and then rotating the column 90° again counting 1 cm above and 1 cm below the center of the column. Thus, the five count rates in the soil column were averaged to obtain a single value count rate to correspond with the average bulk density of the column.

Columns were packed with five separate soils to different densities and with varying moisture contents. An empirical relationship is thus obtained between the count rate, density, and moisture content and compared with the results predicted by equation [1].

RESULTS AND DISCUSSION:

At this time the electronic equipment is still being perfected to make the detector probe work satisfactorily, that is, a preamplifier is being designed to make the system do the job for which it was intended. When this is completed, a complete calibration will be run for the five different soils and the empirical relationships mentioned above can be obtained. As soon as the electronic equipment is functioning properly, the detailed calibration as described above will be carried out.

SUMMARY AND CONCLUSIONS:

Equipment was designed for the non-destructive measurement of soil density and moisture content using gamma radiation transmitted by thin soil layers. This equipment is to be used in the field to determine the moisture content distribution in the superficial soil layers and to determine what effect this distribution has on evaporation.

The equipment consists of a 5 mc Cs^{137} source in the source probe and a scintillation detection unit in the detector probe. The two access tubes which hold the probes are set 30 cm apart in the soil with the aid of an alignment jig. The electronic equipment in the detector probe has not had the stability necessary for accurate and precise measurements and this problem is currently being remedied.

PERSONNEL: R. J. Reginato, C. H. M. van Bavel.

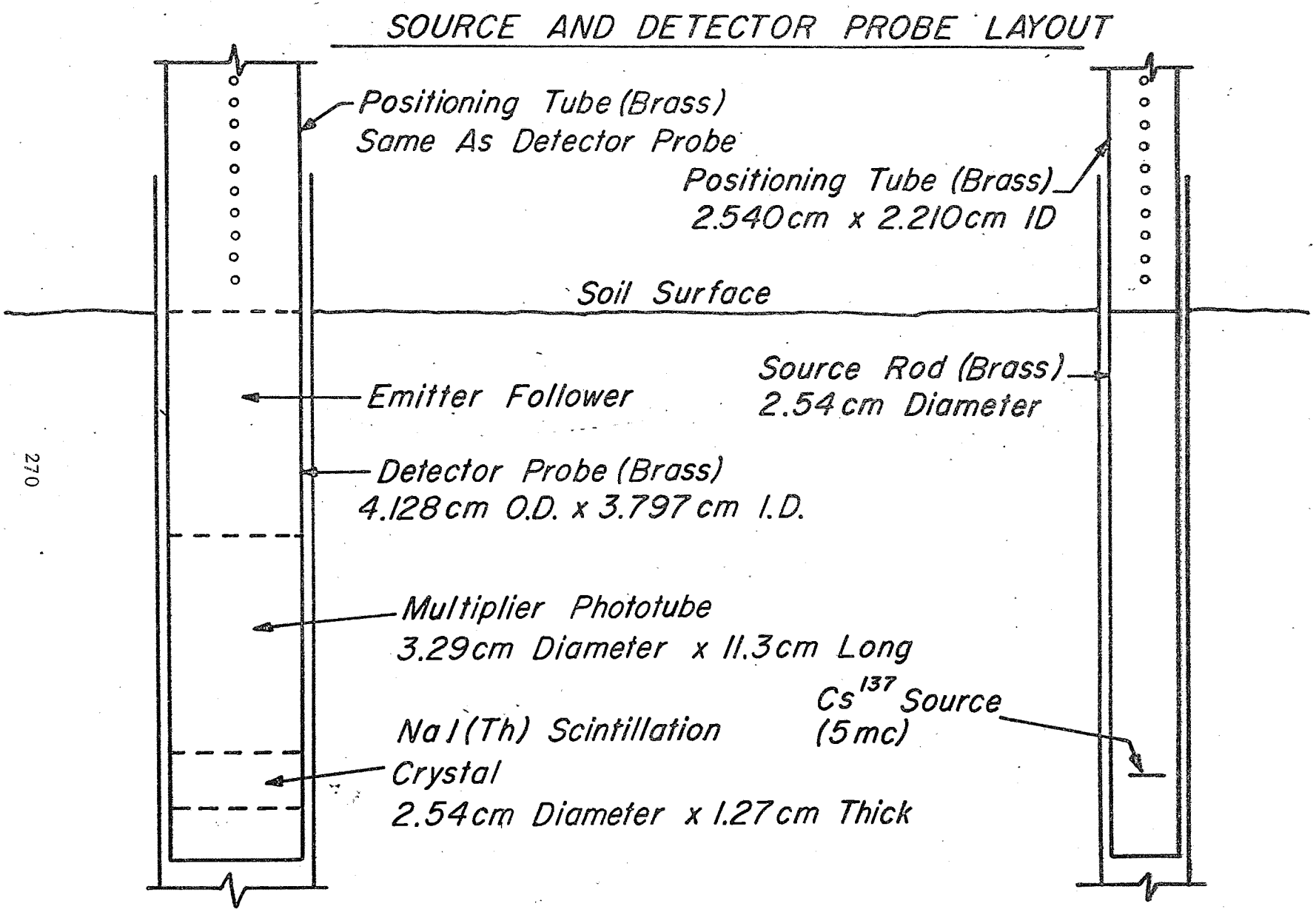

Figure 1. Source and detector probe layout for gamma transmission apparatus.

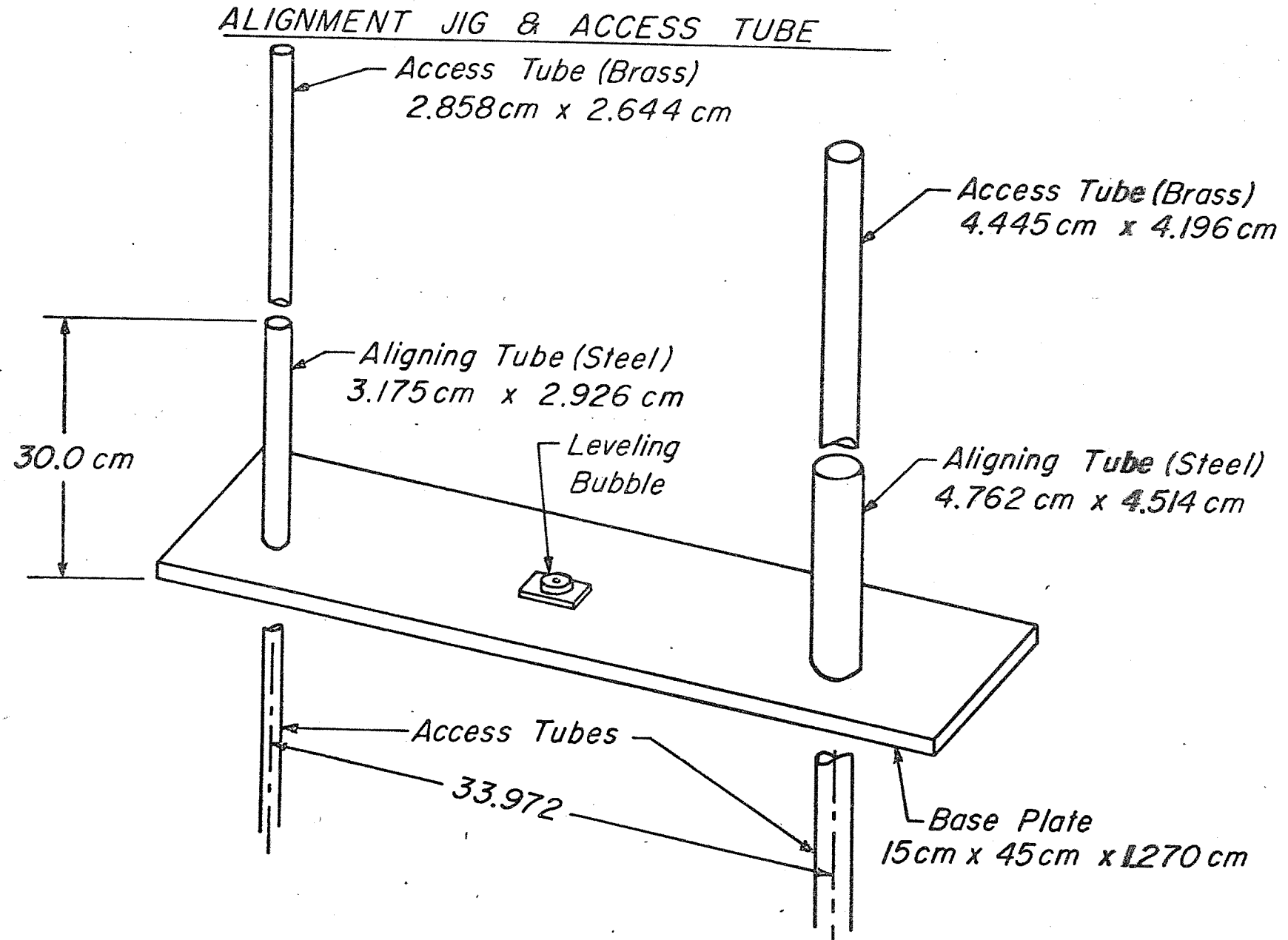

Figure 2. Alignment jig and access tube layout for gamma transmission apparatus.

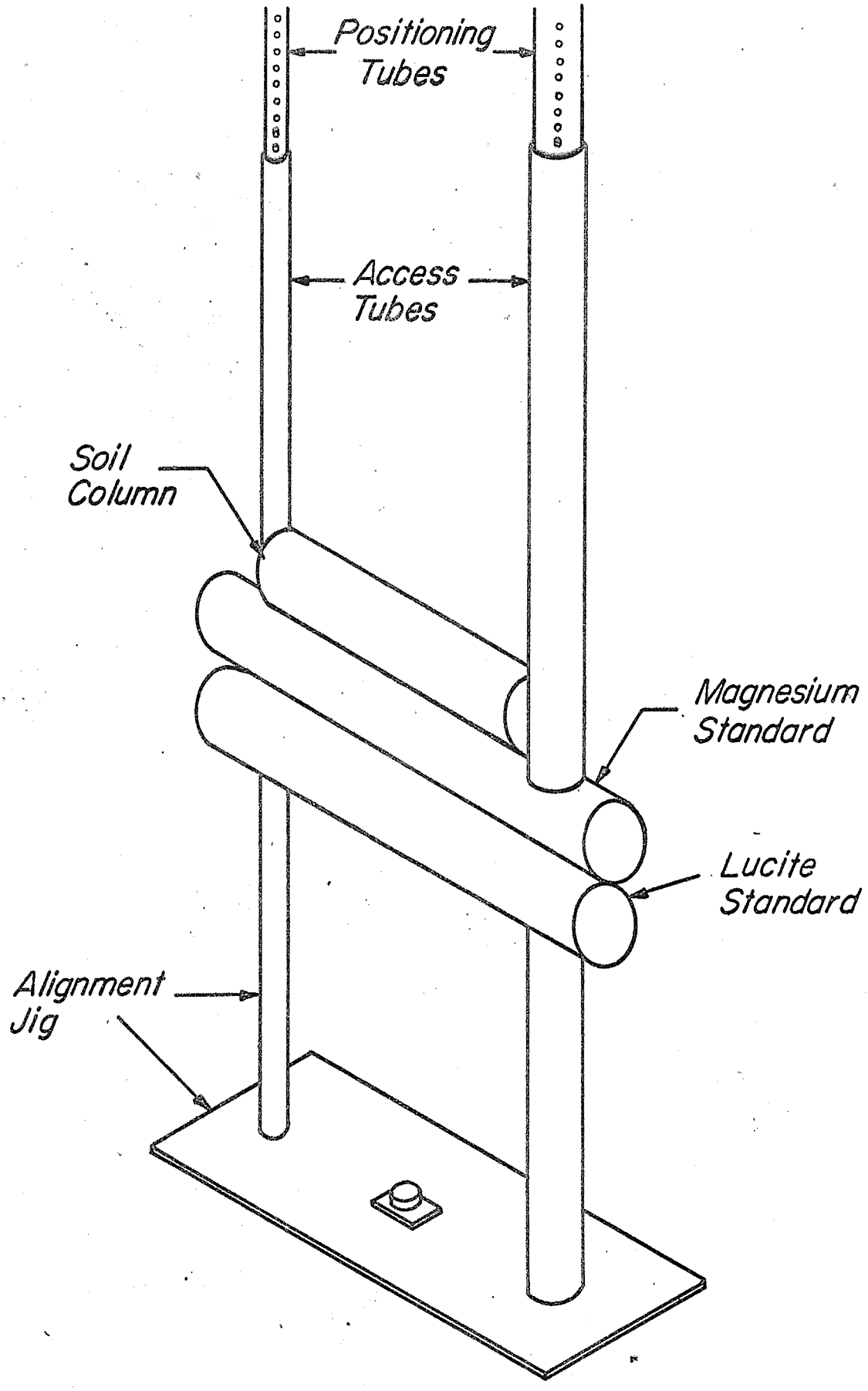

Figure 3. Laboratory setup for calibration of gamma transmission apparatus.

TITLE: DYNAMIC SIMILARITY IN ELBOW FLOW METERS

LINE PROJECT: SWC 4-gG5 CODE NO.: Ariz.-WCL-2

INTRODUCTION:

The discharge equation for an elbow meter can be written as

$$Q = C\ A(2gh)^{0.5}$$

where A is the cross sectional area of the elbow, h is the difference in head between the piezometer taps, and C is the discharge coefficient. For dynamic similarity, the discharge coefficient C varies with the Reynolds number and geometry of the elbow. Calibration of the commercial, 3-inch diameter, flanged, cast iron elbows during 1961 showed C is relatively constant above a minimum velocity of approximately 3 feet per second. Then for velocities above this minimum, the discharge equation can be written as

$$Q = C\ (h)^{0.5} \tag{1}$$

where the discharge coefficient C varies only with the geometry of the elbow.

Using Lansford's analysis, assuming uniform velocity and concentric flow through the bend, the theoretical discharge coefficient is

$$C = \left(\frac{R_c}{2D}\right)^{0.5} A\ (2g)^{0.5} \tag{2}$$

where R_c is the radius of curvature and D the diameter of the elbow. The value of C was calculated using dimensions obtained in three different ways for each of the commercial, short radius elbows and compared with the measured calibration discharge coefficients. (Also see Annual Report for 1960 and 1961).

PROCEDURE:

Dimensions for calculating the theoretical discharge coefficients were obtained in three ways.

1. Standard dimensions indicated by manufacturing specifications were used to obtain diameter and radius of curvature.

2. Diameters were determined from an average of sixteen face diameter measurements made with an inside micrometer. Radii of curvature were determined from graphic plots, as indicated in Figure 1,

made from measurements of actual elbow profiles with a dial indicator. All measurements were accurate to 0.001-inch.

3. Diameters were determined as in method 2. Volumes of the elbows were determined by using suitable end plates and filling the elbows with 30° C water measured with class A volumetric flasks and pipets. Radii of curvature were then computed by assuming the elbow to be a true quarter torus

$$R_c = \frac{8\Delta V}{\pi^2 D^2} \tag{3}$$

where ΔV is the measured volume less the volume of the measured tangent lengths.

Theoretical discharge coefficients were computed with equation 2 and were compared to the coefficients obtained from actual calibration data.

RESULTS:

Measurements showed that the elbows are not uniform. This should be expected for unmachined, sand-mold castings. Diameters were not constant for a given elbow, cross-sections were not circular, inner and outer radii were not concentric or of consistent length, and radii were not truly tangential to the straight sections of the elbows. Measurements used for computations are presented in Table 1. Average diameters did not vary greatly but tangent lengths varied from 0.80 to 2.00 inches, volumes varied from 61.0 to 67.5 cubic inches, and graphically measured radii of curvature varied from 3.67 to 4.55 inches.

Discharge coefficients calculated from manufacturers dimensions (American Standard for Cast Iron Flanged Fittings, Class 125) varied from actual discharge coefficients by 2.5 to 10.3 per cent using the dimensions D = 3.00 inches, R_c = 4.75 inches. The 10 per cent error agrees with Lansford's estimate for errors in computed coefficients.

Coefficients of discharge computed from measured D and graphically determined R_c varied from actual discharge coefficients by 0.3 to 4.3 per cent. The maximum error was therefore only slightly more than 4 per cent.

Coefficients of discharge computed from measured D and R_c calculated from volume measurements varied from actual discharge coefficients by 0.0 to 4.3 per cent as given in Table 2.

The accuracy of methods 2 and 3 for computing the discharge coefficient are comparable. Measurements used in method 2 are difficult and require special equipment. Measurements used in method 3 are not difficult and can be made with relatively simple equipment. Our work indicates that method 3 offers a relatively simple means of calculating discharge coefficients for 3-inch diameter, short radius, flanged, cast iron elbow flow meters with a maximum error of less than 5 per cent.

Method 3 will be tested on elbow flow meters with different dimensions.

SUMMARY AND CONCLUSIONS:

Methods were developed for computing discharge coefficients for commercial, 3-inch diameter, flanged, cast-iron elbow flow meters with a maximum error of less than 5 per cent. Theoretical discharge coefficients were calculated with the equation proposed by Lansford:

$$C = \left(\frac{R_c}{2D}\right)^{0.5} A\ (2g)^{0.5}$$

where R_c is the radius of curvature, D is the elbow diameter, and A is the cross-sectional area. Dimensions were obtained in three ways.

1. R_c and D were determined from standard manufacturing specifications.

2. D was measured and R_c was determined from accurate interior profile measurements.

3. D was measured and R_c was computed from measured elbow volumes by assuming the elbow to be a quarter torus.

Computed coefficients were compared to coefficients determined by actual calibration of the elbows. Deviations were: method 1 - 2.5 to 10.3 per cent, method 2 - 0.3 to 4.3 per cent, method 3 - 0.0 to 4.3 per cent. Methods 2 and 3 provide comparable accuracy with

maximum errors less than 5 per cent. Method 3 can be utilized with relatively simple measuring equipment and is recommended on that basis.

PERSONNEL: L. E. Myers, K. J. Brust.

Table 1. Measured and calculated dimensions of commercial, 3-inch, cast iron, flanged, short radius, 90° elbows.

Elbow No.	Face Diameter	Tangent Length		Volume	Average Diameter	Radius of Curvature	
		Inner Bend	Outer Bend			Calculated	Graphic
	(in.)	(in.)	(in.)	($in.^3$)	(in.)	(in.)	(in.)
1	2.909	0.80	1.20	60.98	2.901	4.60	4.55
Reversed	2.893	0.80	1.20	60.98			
2	2.905	Not	Available		2.905		
Reversed	2.905						
3	2.997	1.80	2.20	66.67	2.999	3.65	3.67
Reversed	3.002	1.60	1.80	66.67			
4	3.017	1.60	2.00	67.52	3.017	3.72	3.71
Reversed	3.016	1.60	2.00	67.52			
5	2.979	0.80	1.20	65.16	2.983	4.66	4.55
Reversed	2.988	1.00	1.00	65.16			
6	2.967	1.00	1.20	63.30	2.971	4.54	4.42
Reversed	2.975	0.80	1.00	63.30			
7	3.014	0.80	1.40	67.28	3.005	4.51	4.37
Reversed	2.996	1.40	1.20	67.28			
8	3.001	1.20	1.10	67.14	2.999	4.43	4.31
Reversed	2.997	1.30	1.50	67.14			
9	2.983	1.20	1.40	65.59	2.981	4.07	4.03
Reversed	2.979	1.80	1.60	65.59			
10	2.989	1.60	1.60	66.11	2.981	3.99	3.94
Reversed	2.993	1.60	1.60	66.11			

Table 2. Discharge coefficients, and per cent deviation in discharge coefficients of 3-inch, cast iron, flanged, short radius, 90° elbows.

Elbow No.	Discharge Coefficients		Deviation in Discharge Coefficients
	Theoretical	Calibration	
	($ft.^{5/2} sec.^{-1}$)	($ft.^{5/2} sec.^{-1}$)	Per cent
1	0.328	0.325	+0.9
Reversed		0.325	+0.9
2		0.329	
Reversed		0.328	
3	0.307	0.321	-4.3
Reversed		0.320	-4.0
4	0.313	0.326	-4.0
Reversed		0.320	-2.1
5	0.344	0.348	-1.1
Reversed		0.347	-0.8
6	0.338	0.339	-0.2
Reversed		0.338	0.0
7	0.342	0.330	+3.7
Reversed		0.333	+2.7
8	0.339	0.329	+3.0
Reversed		0.328	+3.3
9	0.321	0.323	-0.7
Reversed		0.328	-2.2
10	0.318	0.330	-3.6
Reversed		0.326	-2.4

LEGEND

A. Upstream face diameter
B. Outer curve tangent length
C. Average tangent length
D. Inner curve tangent length
E. Measured radius of curvatures
F. Downstream face diameter

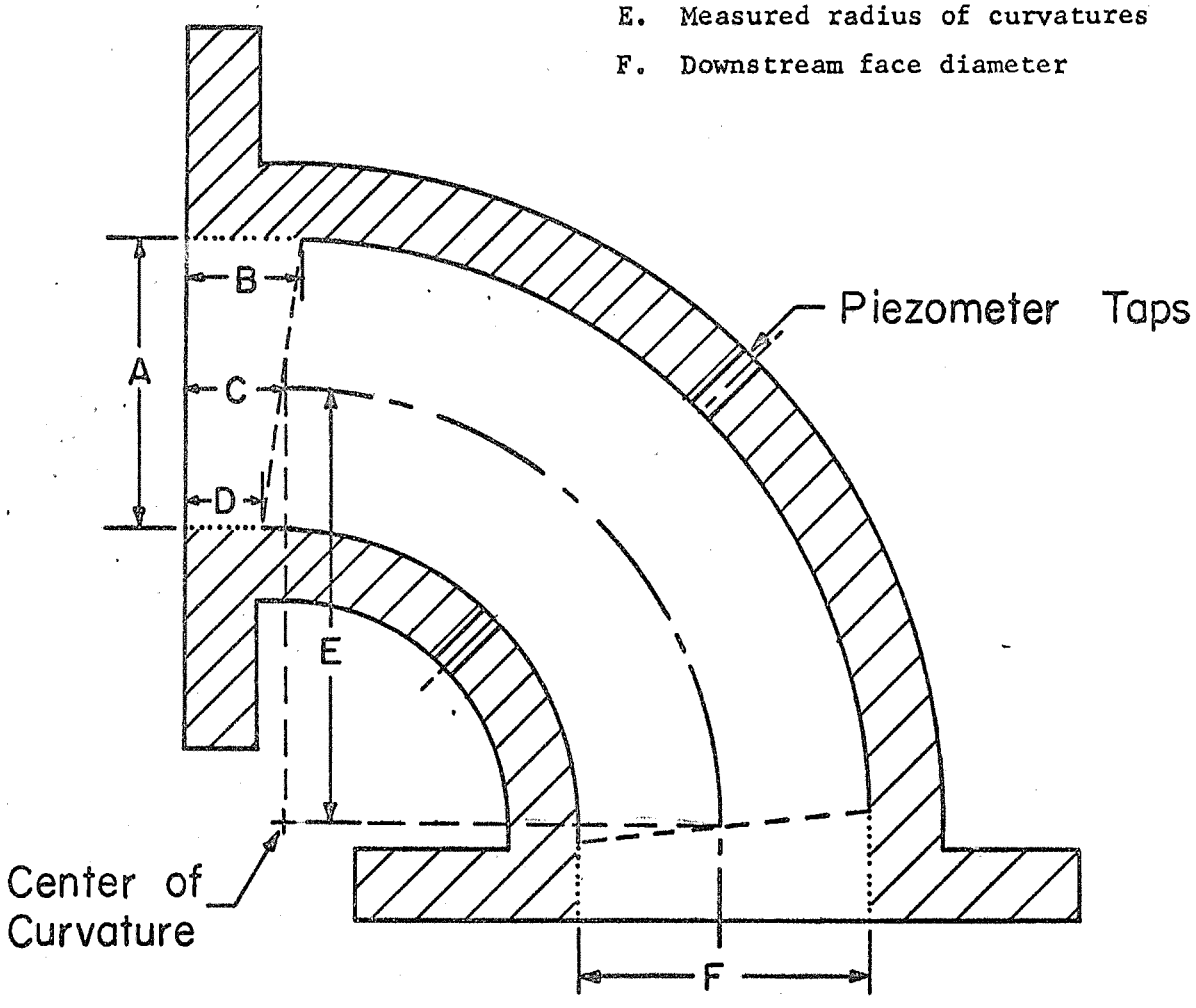

Figure 1. Radial-section typical of the commercial, 3-inch diameter, flanged, cast iron elbows.

TITLE: QUANTITATIVE MEASUREMENT OF WATER FLOW WITH CHEMICAL TRACERS

LINE PROJECT: SWC 4-gG5 CODE NO: Ariz.-WCL-30

INTRODUCTION:

Efficient use of irrigation water requires accurate flow measurement. Many irrigation systems have no flow measuring devices as such but have existing structures satisfactory for flow measurement if accurately field calibrated. Many structures designed for flow measurement have never been accurately calibrated. Present field calibrating methods have shortcomings which have retarded their use. Simpler and more accurate field calibrating methods would permit the use of existing structures in irrigation systems for reasonably accurate flow measuring devices.

Tracer flow measurement has several important advantages over commonly used open channel flow measuring methods such as: requiring no flow restricting device, no measurement of channel dimensions, and large flow measuring range. Recent developments in fluorescence assay have made possible quantitative tracer measurements in the 0.1 ppb range. Experiments using a commercial organic pigment, Rhodamine B, have shown it can be used as a water tracer in very low concentrations. On the basis of these developments, a project was initiated to develop a tracer flow measuring technique for field use.

PROCEDURE:

Rhodamine B was evaluated as a water tracer using a Turner Model III fluorometer. The sensitivity of detection of Rhodamine B with this instrument is specified as about 0.05 ppb and the instrument is readable to 0.5 per cent. Evaluation included accuracy of quantitative detection, adsorption on naturally occurring substances, and effect of temperature.

Accuracy of quantitative detection was checked with 20, 10, and 5 ppb concentrations of Rhodamine B in deionized water. Concentrations were prepared from a precisely prepared 10 ppm concentration of Rhodamine B in deionized water using a 1 ml T.D. micro transfer pipette with class A T.C. volumetric flasks. The concentrations of 20, 10,

and 5 ppb were each prepared three times and fluorescent readings were obtained in a constant temperature room.

Adsorption of Rhodamine B on soil was determined by allowing a 50 ppb concentration to drain through a 2-inch thick layer of soil and measuring the concentration of the effluent.

Adsorption in a soil suspension was investigated by comparing fluorescent readings of a standard concentration of Rhodamine B in deionized water with fluorescent readings of soil suspensions with and without Rhodamine B.

The effect of temperature on fluorescence of Rhodamine B was determined over a temperature range from 10 to 30° C using 100, 50, 25, 5, 1, and 0.5 ppb concentrations of Rhodamine B in deionized water. Fluorescent readings were obtained for each concentration at 5 degree temperature intervals.

The equipment for field testing the Rhodamine B tracer included the Turner Model III fluorometer, a portable generator, sampling pumps and tubing, sample containers, and a stopwatch.

The integrated sample flow measuring technique as suggested by A. Barbagelata was used. In this technique, a known amount of tracer, S, is added to the stream being measured. At a downstream point, located sufficiently distant from the point of addition to insure complete mixing, a sample of the entire tracer wave is collected at a steady sampling rate. The concentration of this sample, $\bar{C}$, times the sampling interval, Δt, is the integral of the tracer wave

$$\bar{C}\ (\Delta t) = \int_0^{\Delta t} C\ dt \qquad (1)$$

where C is the concentration of the tracer wave at any time. The amount of tracer, S, added at the upstream point should equal the amount passing the sampling point

$$S = Q\ \bar{C}(\Delta t) \qquad (2)$$

so the discharge, Q, is equal to the amount of tracer added divided by the integral of the tracer wave. In the field tests, the tracer was added about 3 feet upstream from a Cipolletti weir. The tracer

and stream flowed over the weir and through an 80 foot concrete channel of varying cross section. Two sampling pumps just upstream from the discharge end of the concrete channel were used to collect a sample of the tracer wave at a steady rate and the sampling interval was recorded. In the field tests, the concentration of the sampled tracer waves was determined by comparing fluorescent readings with standards prepared by diluting the Rhodamine B in 62.5 liters of water taken from the channel. The flow rate was then calculated by using equation 2 and compared with the flow rate measured with the Cipolletti weir.

RESULTS AND DISCUSSION:

Accurate quantitative detection must be realized before reliable tracer flow measurements can be achieved. The first attempts to achieve accurate quantitative detection proved that extreme care must be observed in preparing and handling standards. Volumetric preparation of standards using a 1 ml T.D. micro transfer pipette with class A T.C. volumetric flasks enabled concentrations of 5, 10, and 20 ppb to be prepared quite accurately. The field standards preparation technique using 62.5 liters of water enabled standards to be duplicated within $\pm$ 1 per cent.

Adsorption of Rhodamine B when filtered through soil reduced the 50 ppb concentration of Rhodamine B in deionized water to an effluent concentration of about 1 ppb. This is of sufficient magnitude to eliminate Rhodamine B as a groundwater tracer. Flow measurements in a soil-lined channel may be influenced by adsorption of Rhodamine B on the wetted perimeter. This should not be a problem unless the measurement reach is long, but the phenomena will be investigated in a laboratory flume. Other tracers with less affinity for soil will also be investigated.

Adsorption of Rhodamine B in a soil suspension could be detected but was relatively small, and it is believed the adsorption effect is compensated by preparing standards with the background water being measured. The standards are prepared at concentrations which are both higher and lower than the concentration being measured. The effect

of adsorption in a soil suspension is receiving further study.

The effect of temperature on the fluorescence of a 100 ppb concentration of Rhodamine B in deionized water is shown in Figure 1. The increase in temperature from 10.5 to 30° C caused a linear decrease in fluorescent readings from 68 to 45. Similar results were found for all other concentrations and a temperature correction factor was developed which is independent of concentration. The problem can be eliminated by making readings on the sample and the standards at the same temperature.

The first field tests showed several problems in instrument operation, standards preparation, and sampling technique. The fluorometer was found to be sensitive to intense outdoor light and temperature variations. This problem was solved by enclosing the fluorometer, except for the control face, in a light-tight case which incorporates a supplemental ventilating blower. The low concentrations of the integrated samples required preparing precise standards with a large volume of water. Weighing the water with a 200 pound scale readable to 1 ounce enabled field standards as low as 16 ppb to be duplicated within ± 1 per cent. Sampling the tracer wave at a steady rate was exceedingly difficult. Foreign matter in the irrigation water lodged at restrictions in the control valves and varied the sampling rate. This problem was solved by designing a new sampling system which does not include any localized flow restrictions.

Comparison of flow rates measured with the weir and with the integrated sample method resulted in discrepancies which were too large to attribute to error in the weir measurement. Visual observation indicated that complete mixing of the tracer was not occurring in the 80 foot long concrete channel under conditions of shallow, high velocity flow. Future tests will include measures to obtain adequate mixing, however, the tests indicated that mixing will be the major problem encountered in the use of the tracer flow-measurement method.

SUMMARY AND CONCLUSIONS:

Field equipment and techniques have been developed for the precise quantitative measurement of fluorescent tracers used in integrated sample or dilution methods of measuring the flow of water in pipes and channels. Quantitative measurements in the 16 parts per billion range can be made with less than ± 1 per cent error by comparing fluorescence of the sample with the fluorescence of known standards. Readings are affected by temperature fluctuations and suspended sediment in the water being measured but methods have been developed to correct or eliminate these effects. Adsorption of tracer on the channel perimeter may be a problem with some tracers, but fluorescent materials are available which are not readily adsorbed on soil. Instrumentation and procedures have been developed to permit fluorescence to be measured in the field with accuracy equivalent to that obtained in the laboratory. Limited field tests have indicated that uniform mixing of tracers in the water being measured will not occur under certain flow conditions. Future work will be primarily concerned with the study and definition of mixing problems in the field.

PERSONNEL: L. E. Myers, K. J. Brust, F. S. Nakayama.

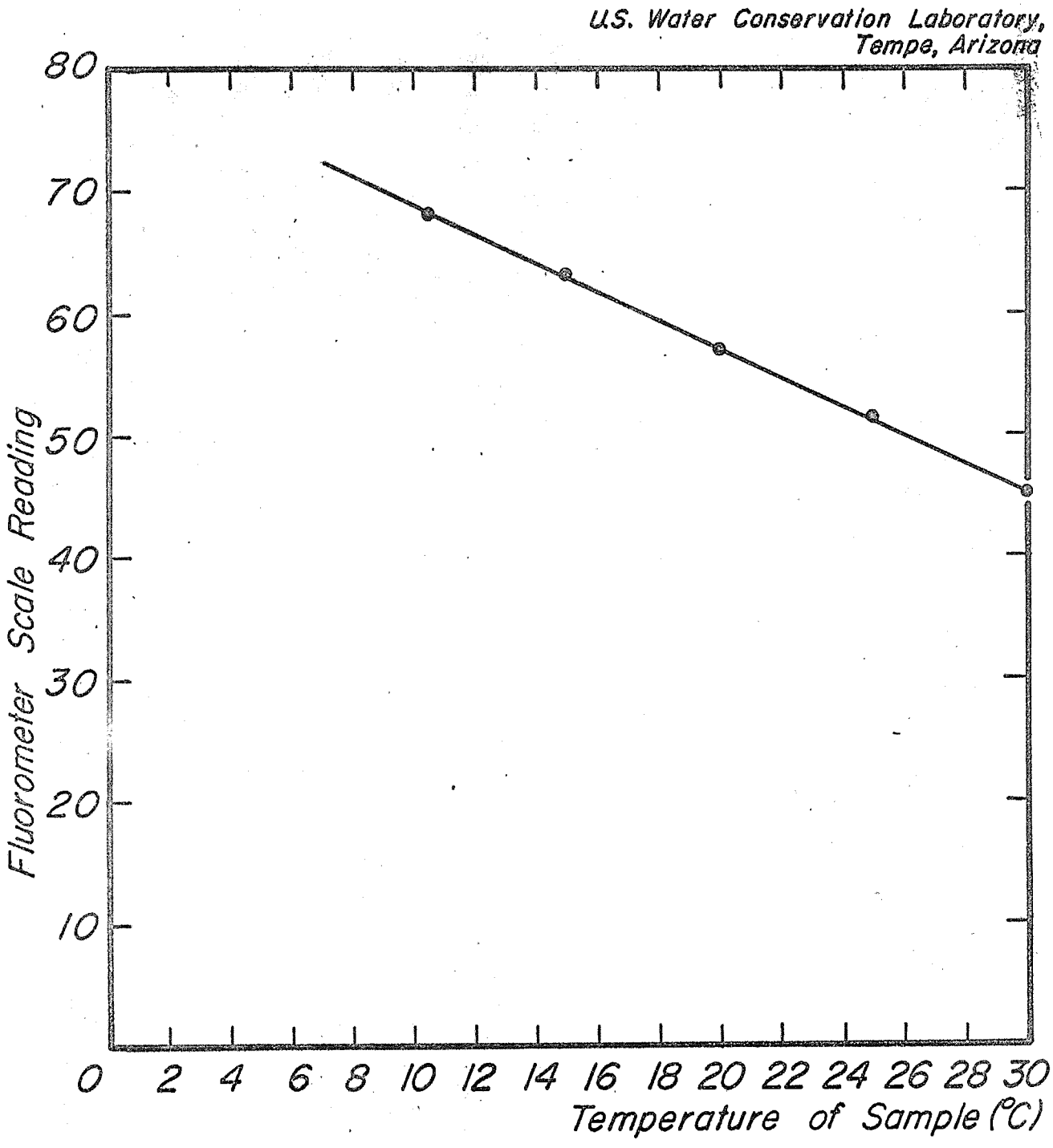

Figure 1. Fluorescence of 100 ppb Rhodamine B in deionized water over a 10 to 30° C temperature range.

TITLE: UTILIZATION OF LIMITED WATER SUPPLIES FOR THE GREATEST ECONOMIC RETURN IN THE IRRIGATION OF COTTON

LINE PROJECT: SWC 4-gG5 CODE NO.: Ariz.-WCL-21

INTRODUCTION: See previous Annual Reports.

OBJECTIVES:

1. To study the influence of various soil-moisture treatments on certain visible plant symptoms for possible use in indicating need for irrigations on Deltapine Smooth Leaf and Pima S-2 cotton.

2. To correlate the mean soil moisture in the root zone with desirable irrigation schedules.

3. To study the blossom and boll characteristics under various irrigation schedules.

PROCEDURE:

The experiment was located at the University of Arizona Cotton Research Center, Tempe, Arizona. Deltapine Smooth Leaf and Pima S-2 cotton were planted in 4-row plots with 7 different irrigation treatments replicated 5 times. Fifty pounds of nitrogen were applied uniformly at the first irrigation.

Irrigation treatments

1. Irrigate when 50% of the available water has been used from the top three feet of root zone until approximately July 1, then at 65% thereafter. 5/17, 6/12, 6/26, 7/11, 8/2, 8/24, 9/13.
2. Irrigate when 75% used. 5/17, 6/26, 7/25, 8/24.
3. Irrigate when 65% used. 5/17, 6/21, 7/11, 8/2, 8/24, 9/13.
4. Irrigate when 50% or less is used. 5/17, 6/12, 6/26, 7/11, 7/25, 8/9, 8/28, 9/13.
5. Irrigate at 65% used but do not fully replenish root zone with 8/2 irrigation. 5/17, 6/21, 7/11, 8/2, 8/24, 9/13.
6. Irrigate when 65% used with final irrigation in August. 5/17, 6/21, 7/11, 8/2, 8/24.
7. Irrigate when 50% or less used with final irrigation in August. 5/17, 6/12, 6/26, 7/11, 7/25, 8/9.

Tagging treatments

1. All blossoms were tagged every day during the fruiting season on treatments 1, 3 and 4 on both varieties. Each mature boll was harvested separately for processing to determine blossom and boll efficiency.

2. The blossoms on all other treatments except 6 and 7 in Pima S-2 were counted every day until mid-August. At this time treatments 5, 6 and 7 on Deltapine Smooth Leaf and treatment 5 on Pima S-2 were tagged for the remainder of the fruiting season. All bolls on all treatments were harvested, counted and weighed.

   Soil moisture measurements were made in all treatments on Deltapine Smooth Leaf and treatments 3 and 4 on Pima S-2.

   Prior to the planting of the cotton the field had been in alfalfa. It was plowed twice, the second time to eliminate volunteer alfalfa plants that had come up after the first plowing. Previous to furrowing out, the land was disked to get rid of weeds. The cotton was planted on April 8 and an excellent stand was obtained. Cotton was thinned by hand chopping.

   Cultural practices included 8 aerial and 2 ground rig applications for insect control. One ground rig application of herbicide was applied. In addition, the field was cultivated 5 times.

   Yield measurements were made on 2 rows, 250 feet long within all irrigation treatments on Deltapine Smooth Leaf. Two rows, 200 feet long were picked in all Pima S-2 plots. Yield plots were hand picked twice.

DISCUSSION:

The cotton got off to a normal start this year but due to rhizotonia in the early season and cool weather in the later part of May and early June, the first blossoms were delayed 7 to 10 days. The effect of delayed blossoming continued throughout the fruiting season as the September blossoming period was also set back 7 to 10 days.

However, no real killing frost occurred until early January which permitted harvesting of many late set bolls. Considerable variability existed between replications. Even though about 40 rows on the north

side were considered as buffers, the soil under replications 4 and 5 was underlain with large rocks within 4 feet of the surface. This cut down the water-holding capacity and thus overall average moisture conditions were dryer than planned. Replication 1 and the upper 1/4 of the field were also in this category because the top soil had been cut off in the leveling operation.

SUMMARY AND CONCLUSIONS:

Analysis of variance showed high significance between irrigation treatments, also between replications. The significance between replications was thought to be due to the previously mentioned soil variabilities.

Again this year treatment 5 was irrigated on the same dates as treatment 3. On one irrigation, August 2nd, treatment 5 received water only half as long as treatment 3. Yields were significantly reduced on treatment 5 because of this shortened irrigation time (Table 1).

13.7% reduction in main plot yields 13.7% reduction in tagged areas	Deltapine
26.3% reduction in main plot yields 29.0% reduction in tagged areas	Pima S-2

There was no difference in yields between treatments 3 and 6 on either variety (Table 1). The last irrigation on treatment 6 was given late enough in August that apparently an additional irrigation in September on treatment 3 had no effect upon the yield of treatment 3.

Yields on treatment 7 were reduced from treatment 4 in both varieties (Table 1). Treatment 7 received its last irrigation on August 9, but treatment 4 received two more irrigations. Reduction in yields on Deltapine Smooth Leaf was due to less blossoms and bolls on treatment 7. Yield reduction in Pima was due to reduced boll size. Percent boll set on all treatments in the short staple was quite similar (average 48%).

From previous years' data, extremely dry treatments produced less total blossoms and usually had a higher percent set. This would partially explain why treatment 2 was somewhat higher in boll set. Pima set averaged 72%.

Treatments 4 and 7 in both varieties were kept wet during the main part of the blossoming season. Table 2 shows these treatments produced heavier bolls. Treatment 3 (short staple) set on a greater number of blossoms than wetter treatments. These blossoms are late and bolls are small, thus the weight per boll is reduced. Figure 1 shows the effect of water on blossoms as related to growing season.

Table 3 shows the consumptive use measurements made in 1962. Deltapine Smooth Leaf used approximately the same amount of water as Pima S-2 on treatments compared. For maximum production either variety used about 40 inches of water. Treatment 6 used about 4 inches less water than treatment 3. It was not given a September irrigation. From a yield standpoint, the September irrigation was not necessary in 1962.

Figures 2, 3, 4 and 5 show an average of 40, 20, 18, 11, 5 and 6 percent water used, respectively, in the first through sixth foot soil profile. Treatment 4 was given 2 irrigations more than 3 and used only 1 inch more of consumptive use water and yielded about .1 of a bale more. Nearly 1/2 bale difference occurred on the Pima S-2 on these irrigation treatments.

PERSONNEL: L. J. Erie.

Table 1. Plot Yields in Pounds of Lint Cotton

Deltapine Smooth Leaf

Trts.	Reps. 1	2	3	4	5	Mean	Bales/Acre
1	46.2	52.0	47.7	48.6	39.0	46.7	2.45
2	38.3	52.1	46.6	37.4	35.7	42.0	2.20
3	52.1	51.2	58.7	52.5	38.1	50.5	2.65
4	57.5	53.3	56.7	52.7	45.4	53.1	2.78
5	42.4	47.3	49.0	44.4	34.9	43.6	2.28
6	54.7	53.7	58.6	47.5	38.9	50.7	2.66
7	50.1	49.0	49.5	48.9	38.6	47.2	2.47

Pima S-2

Trts	Reps. 1	2	3	4	5	Mean	Bales/Acre
1	21.3	17.0	14.3	18.5	18.4	17.9	1.17
2	17.2	17.2	13.6	18.1	17.8	16.8	1.10
3	23.8	19.6	16.6	16.8	22.2	19.8	1.29
4	28.9	27.5	20.0	27.8	27.0	26.2	1.71
5	14.7	18.3	15.3	10.6	14.1	14.6	0.95
6	22.6	21.0	16.0	21.0	20.2	20.2	1.32
7	24.7	24.6	20.6	20.2	22.0	22.4	1.46

Table 2. Blossom and Boll Data

Deltapine Smooth Leaf

Trt.	Total Blossoms	Total Bolls	Bulk Wt. (Gms.)	Boll Wt. (Gms.)	% Set
1	3940	1792	7219.1	3.77	45.5
2	3140	1691	6394.6	3.74	53.9
3	4052	1926	7790.8	3.79	47.5
4	3733	1786	8085.4	4.18	47.8
5	3649	1713	6726.3	3.87	46.9
6	3864	1875	7525.2	3.88	48.5
7	3450	1611	7141.7	4.26	46.7

Pima S-2

Trt.	Total Blossoms	Total Bolls	Bulk Wt. (Gms.)	Boll Wt. (Gms.)	% Set
1	2536	1898	4646.3	2.40	74.8
2	2755	1954	4373.2	2.24	70.8
3	2893	2179	5545.4	2.49	75.3
4	3184	2274	6071.8	2.60	71.4
5	2488	1727	3935.5	2.28	69.4
6	--	2159	5069.4	2.35	--
7	--	2213	5197.0	2.35	--

Table 3. Consumptive use by cotton 1962.

Treatments	Deltapine Smooth Leaf	Pima S-2
1	39.40	
2	29.48	
3	40.83	40.39
4	41.73	41.35
5	37.76	
6	36.14	
7	31.42	

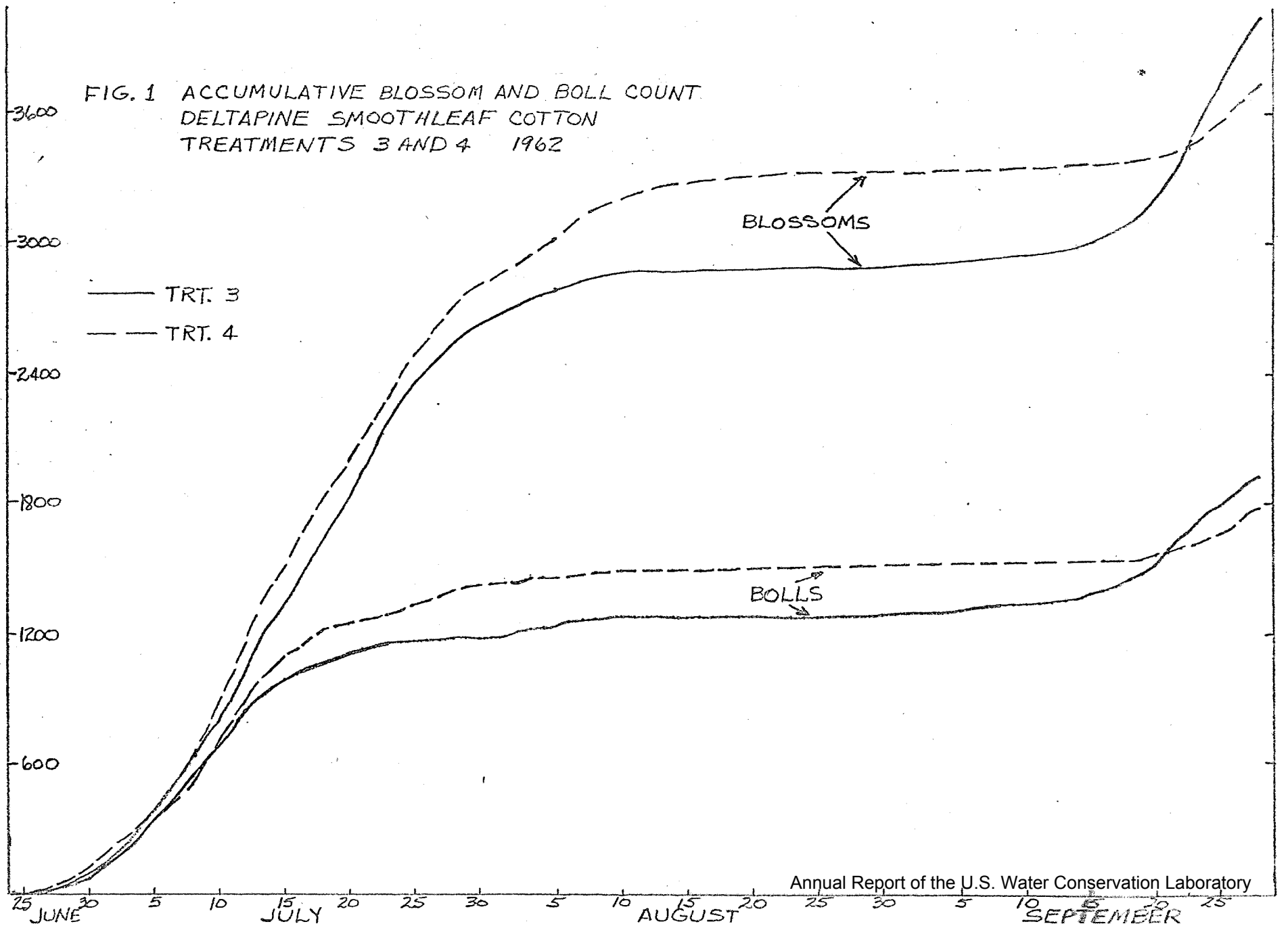
FIG. 1 ACCUMULATIVE BLOSSOM AND BOLL COUNT
DELTAPINE SMOOTHLEAF COTTON
TREATMENTS 3 AND 4 1962
3600
3000
2400
1800
1200
600
TRT. 3
TRT. 4
BLOSSOMS
BOLLS
25
JUNE
30
5
10
15
JULY
20
25
30
5
10
15
AUGUST
20
25
30
5
10
15
SEPTEMBER
20
25

FIG. 2 CONSUMPTIVE USE - COTTON
CRC TRT. 3 1962

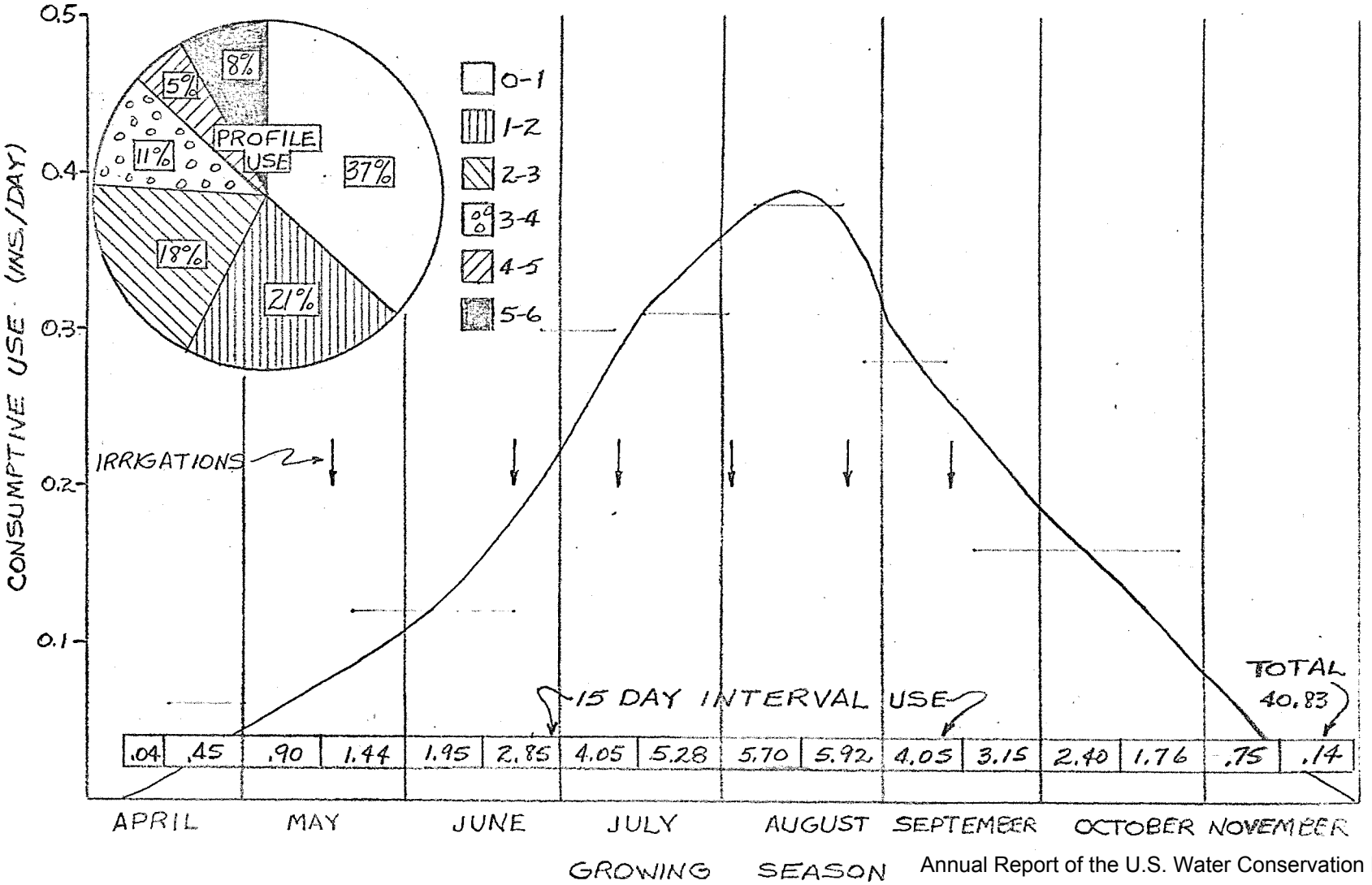

FIG. 3 SOIL MOISTURE PERCENTAGE
COTTON CRC TRT.-3 1962

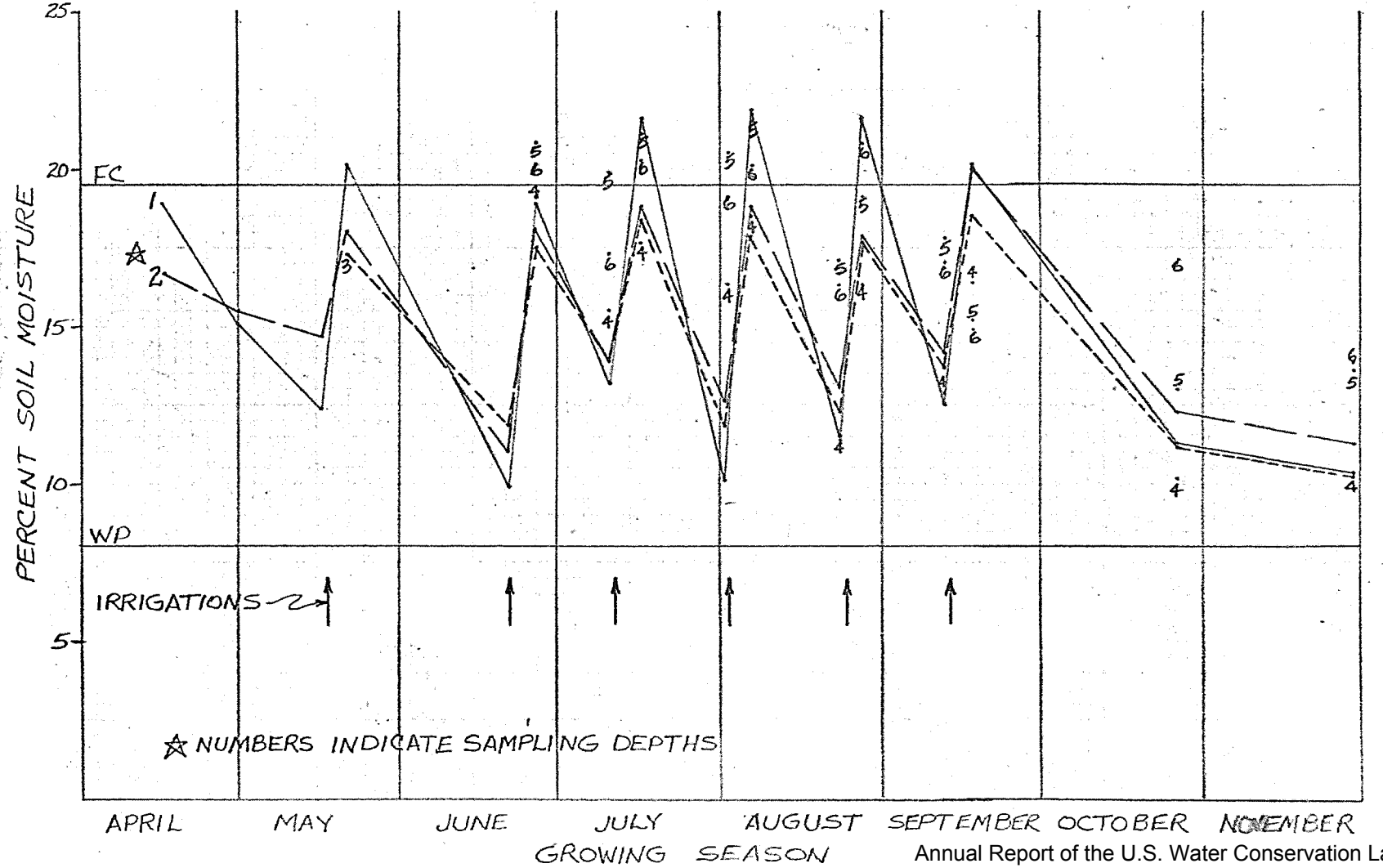

FIG. 4 CONSUMPTIVE USE - COTTON
CRC TRT. - 4 1962

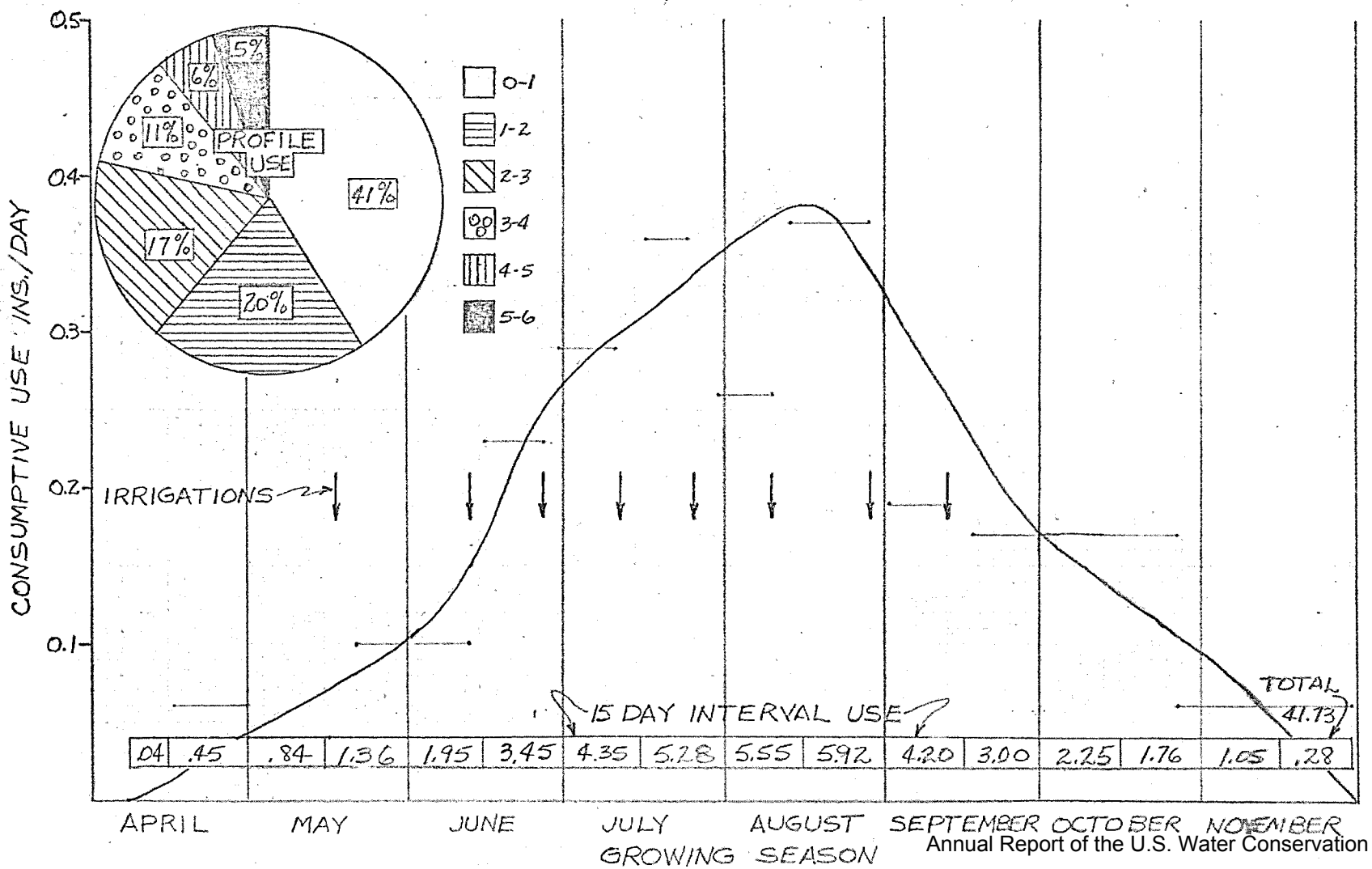

FIG. 5 SOIL MOISTURE PERCENTAGE
COTTON CRC TRT-4 1962

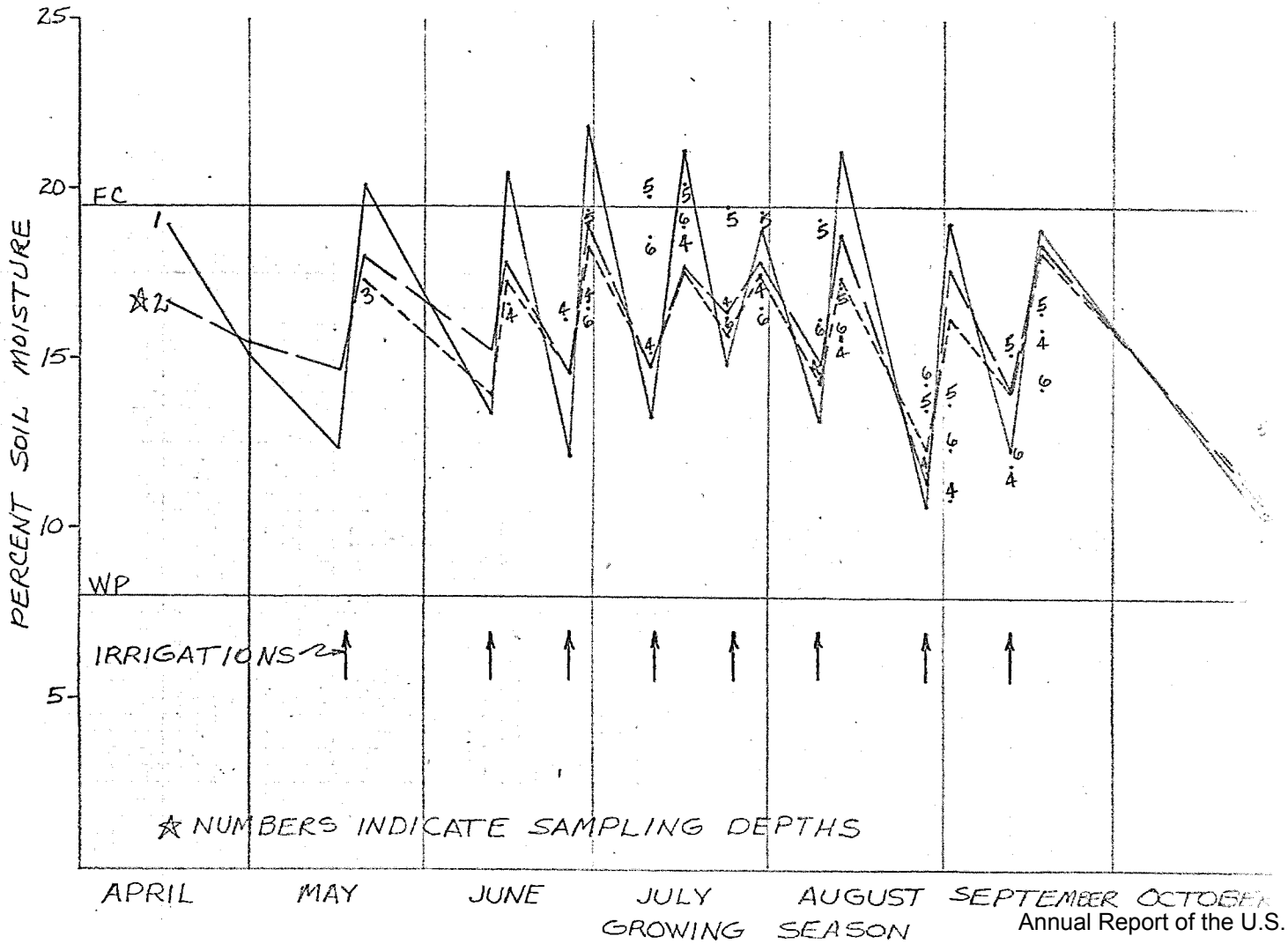

TITLE: SIMPLIFIED PREDICTION METHOD FOR THE FALL OF THE WATER TABLE IN DRAINED LAND.

LINE PROJECT: SWC 6-g1 CODE NO.: None.

INTRODUCTION:

The steady-state condition in tile- or ditch-drained land is adequately described in the literature and satisfactory solution methods are available for determining depth and spacing of drains to meet a specified drainage requirement. This has not been true for the transient case, however, which may be the condition that is more often encountered in practice. The difficulty in applying steady-state drainage solutions to the transient case is that the flux per unit area of water table, which is uniform for the steady-state case, varies with distance from the drain for the transient case. The non-uniformity of the flux for the transient case is herein accounted for by the introduction of a correction coefficient. Using this correction coefficient, steady-state drainage solutions are integrated analytically or numerically to predict the rate of fall of the water table midway between the drains. The procedure is based on abrupt drainage of pore space. A detailed description of the development, including examples and comparisons with other transient drainage solutions, is presented in (87).

PROCEDURE:

The basic equation is

$$P = -fC \frac{dm}{dt}, \tag{1}$$

where P = instantaneous drainage rate or coefficient for the steady-state

f = drainable porosity

C = a correction coefficient to account for the non-uniformity of flux for the falling water table

m = height of water table midway between drains above tile center; and

t = time.

Assuming that the average of a non-uniform flux at the water table gives the same drainage flow as when that average were uniformly

distributed across the water table, C can be determined as the ratio of the average drop of the entire water table between drains to the drop midway between drains. Thus, C will be in excess of 1 for the falling water table immediately following ponded conditions, where the water table falls faster near the drains than midway between the drains. After having receded faster near the drains for some time, the water table can be expected to fall for some time without appreciable change in shape, in which case C = 1. During the final stages of water table recession, the water table falls faster midway between the drains than near the drains, so that near C-values of less than one can be expected. From the literature it appears that C-values between 0.8 and 1.0 can be used, except for the first stages of water table recession after the ponded case.

From steady-state drainage solutions, relationships between P and m may be available in terms of an equation or in tabular or graphical form. If P versus m is available as an equation, this equation can be substituted into equation (1) for analytical integration. If the relation between P and m is in tabular or graphical form, for instance, from numerical, model, analog, or field studies, equation (1) can be integrated numerically.

RESULTS AND DISCUSSION:

To exemplify the analytical integration of equation (1), Hooghoudt's equation is selected for the steady-state relation between P and m. This gives, after integration and rearrangement of terms,

$$\frac{Kt}{f} = \frac{2.3\ CS^2}{8d_e} \log \frac{m_o(m_t + 2d_e)}{m_t(m_o + 2d_e)} , \qquad (2)$$

where K = the hydraulic conductivity,

S = the spacing between drains, and

d_e = Hooghoudt's equivalent depth to the impermeable material to be evaluated from tables or a graph (87).

For practical purposes, a C-value of 0.9 will be valid for most cases. Equation (2) can be used to calculate the time required for the water table to drop from m_o to m_t for a given spacing S. This process is

repeated for various spacings until the S-value giving the specified rate of fall of the water table is found.

A more general approach that does not depend on equations describing the relation between P and m and which also eliminates the trial-and-error procedure for finding the desired spacing, utilizes P versus m curves for a number of drain spacings. An example of such a family of curves is shown in Figure 1, where P/K is plotted against m/d for different values of S/d. This graph was obtained from nomographs by Ernst and Boumans. In using plots as Figure 1, the tile depth must be selected first so that d can be evaluated. A certain distance of fall of the water table from m_o to m_t is then selected and the corresponding m_o/d and m_t/d are marked on the graph. From the specified time Δt for the water table to fall from m_o to m_t, $\bar{P}$ is calculated with equation (1) in finite-difference form, or $\bar{P} = \frac{Cf\Delta m}{\Delta t}$. Knowing the hydraulic conductivity of the soil, $\bar{P}/K$ is computed and the S/d-curve for which the average P/K between m_o/d and m_t/d is equal to the computed value of $\bar{P}/K$ is determined from Figure 1. Since d is known, the spacing S can then be computed.

The integrated Hooghoudt equation was compared with another integrated steady-state equation (by Toksöz and Kirkham) and with an equation developed by van Schilfgaarde for the transient case. The results show excellent agreement between all three equations.

SUMMARY AND CONCLUSIONS:

Steady-state drainage solutions relating drainage rate to water table height are analytically or graphically integrated to predict the rate of fall (or rise) of the water table midway between tile-lines or ditches. The procedure assumes abrupt drainage of pore space. A factor C is introduced to account for the non-uniformity of flux per unit area of water table if the water table changes in shape during recession. Except for a falling-water table immediately following a ponded condition, a C-value of 0.9 will be satisfactory for most cases. The procedure is amenable to steady-state formulas or to graphical or tabular solutions obtained by analogs, models, numerical procedures, field experiments, or others.

Comparison of two integrated steady-state drainage equations with an equation developed specifically for the transient case shows good agreement. The simplicity, general applicability and apparent accuracy of the procedure favor its adoption in routine drainage design.

PERSONNEL: Herman Bouwer.

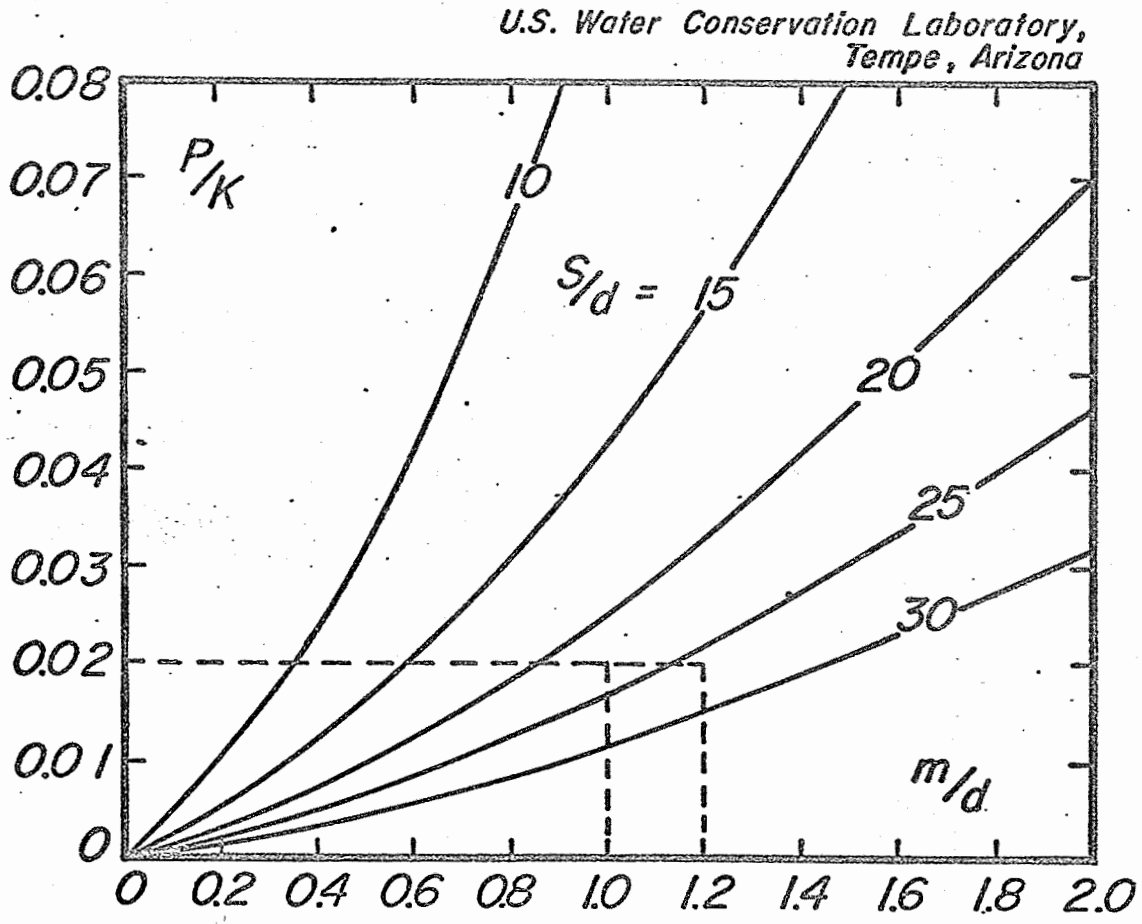

Figure 1. Family of curves of P/K versus m/d for different S/d-values for direct evaluation of desired drain spacing (curves obtained from nomographs by Ernst and Boumans).

TITLE: SOIL MOISTURE POTENTIALS AND WATER UPTAKE BY ROOTS

LINE PROJECT: SWC 11-gG1 CODE NO.: Ariz.-WCL-3

I. DIFFUSION STUDIES WITH TRITIATED WATER (THO OR $H^3H^1O^{16}$)

INTRODUCTION:

The objectives, theory and techniques, and methods of analysis used in this phase of the study have been pointed out in the Annual Reports of 1960 and 1961.

RESULTS AND DISCUSSION:

Diffusion coefficients of THO in different concentrations of dilute agar gel were determined to obtain the diffusion coefficient of the tracer in liquid water. These results are shown in Figure 1. Between 0.3 to 1% agar concentration, the D_{THO} shows an inverse linear relation to the gel concentration. The D_{THO} in pure water, extrapolated to infinite dilution of gel, is $2.41 \pm 0.055 \times 10^{-5}$ cm^2 sec^{-1} and compares with that of $2.44 \pm 0.057 \times 10^{-5}$ cm^2 sec^{-1}, the widely accepted value of D_{THO}, which has been determined by a different method (3). Our value, as far as it can be determined by literature searches, will be the only other one presenting the diffusion coefficient of tritiated water in liquid water to be reported in the literature.

The nature of the apparent diffusion coefficient of tritiated water in a Pachappa loam as a function of the water content of the soil material was firmly established (Preliminary results were presented in the 1961 Annual Report). As can be seen in Figure 2, the D_{THO} shows a complexed relation to the water content. The D_{THO} is nearly constant for volumetric water contents of 10 to 40%. As the water content decreased below 10%, the D_{THO} rapidly increased to a maximum at about 4% water content, then rapidly decreased as the water content was further reduced. The maximum value of D_{THO} is 3.5 times greater than the D_{THO} at 40% water content. The sharp rise in D_{THO} starting at 10% and continuing to 4% water content was probably the result of an increase in the number of continuous pores available for vapor diffusion; the sharp decrease in D_{THO} below 4% is probably the result of the

adsorptive force field of the particles acting upon the diffusing tracer molecules. These forces are present throughout the entire moisture range, but manifest themselves to a greater degree at the low water contents, where the tracer molecules diffusing in the vapor phase have a greater probability of colliding and exchanging with the adsorbed molecules. Surface area calculation indicates that for this soil, two molecular layers of water are present on the particle surface when the water content is about 4%.

If diffusion were solely in the liquid phase, one might expect D_{THO} to decrease with a decrease in water content. This would be because the path length through the liquid would increase as water content decreased. However, as the water content decreases, air enters the larger pores. The ensuing vapor phase provides an additional pathway for the diffusion of THO. Diffusion can proceed in series and in parallel within the two phases. Since the diffusion coefficient of water vapor in air is 10^4 greater than in liquid water, one might expect a rapid increase in diffusion as the pores become air-filled. As stated earlier, neither situation was the case for Pachappa loam between 10 to 40% water content. Apparently, within this water content range, vapor diffusion increased with decreasing water content in the same proportion as liquid diffusion decreased. At this time, we can only speculate on the mechanism involved.

Note also the need for detailed measurements in this type of study. For example, if the diffusion coefficient for THO had been measured only at 1.5, 10, 20, 30, and 40% water contents, the D_{THO} peak would have been missed and one might have erroneously concluded that the D_{THO} was essentially constant over the entire water content range.

The occurrence of the type of D_{THO}-water content relationship for Pachappa loam shown in Figure 2 does not necessarily mean that the same condition will exist for other soil materials. This means that, if THO is to be used as a tracer for water in a particular soil-water system, the diffusive behavior of THO must be determined in that system to evaluate properly the results.

II. ROOT WATER UPTAKE MEASUREMENTS WITH TRITIATED WATER

INTRODUCTION:

A method was investigated in which tritiated water was used for tracing and measuring the amount of water absorbed by roots during short time intervals, the main objective being the determination of the instantaneous water uptake by roots without a change in the water potential of the soil (See Annual Report for 1960).

Sorghum (RS-610) and corn (WD 456 × KB 397) were grown in 3-ounce, wax-lined paper cups. Each set of containers was made of two parts, an inner cup with its bottom removed, held within an outer cup with one-half its top removed. A single sheet of Saran film was placed between the inner and outer cups to prevent sticking of the roots to the outer cup. Plants were grown in the inner cup, and, when the roots formed a complete mat at the "false bottom" between the two cups, the outer container was removed and the exposed root-mat placed directly in contact with a tracer-treated soil material (1, 2). The growth medium consisted of 180 g of 2:1 sand to Adelanto soil mixture. This mixture was found to be the best medium for plant growth under our environmental conditions. Plants were irrigated with 1/2-strenth Hoagland nutrient solution. The weight of the containers with the soil and plants was checked so that the approximate water potential of the soil at any time could be known from a previously determined moisture characteristic curve of the soil-sand mixture. The plants were grown in the greenhouse for approximately 6 weeks, at which time a thick root mass was formed at the bottom of the inner cup. A second cup of the same capacity containing 65 g of sand-soil mixture was brought to a predetermined moisture potential on the pressure cooker apparatus. This potential was similar to that of the medium in which the plants were grown. The soil material was treated with 0.25 ml of 100 μc/ml tritiated water and allowed to equilibrate until the THO was distributed evenly throughout the soil material.

The cup containing the plants and root mat was pressed firmly in contact with the THO-treated soil and allowed to stand for predetermined contact periods of 15 minutes to 6 hours (see Figure 3 for diagrammatic sketch). Blank runs were made simultaneously consisting of the moist soil-sand mixture only without the root mats. After the predetermined contact periods, the cup with the root mat was separated from the THO source and the plant cut at the base of the stem. The plant, the soil-sand mixture containing the roots, the blank, and the THO treated soils were analyzed for THO by the method developed and described in the 1960 Annual Report.

RESULTS AND DISCUSSIONS:

Figure 3 shows the total activity in the tops of sorghum plants, where the plant roots were in contact with the THO-treated soil at the times noted. Two to six replicates were run per contact period in this series. A slightly higher amount of THO in the plant is noted at the 4-hour contact period and a significant increase is measured only at the 6-hour period. For contact periods of less than 4 hours, the THO activities in the plant tops were essentially the same.

The total activity of tracer THO that moved into the sections which had the plant roots and soil, and also that moved into the sections with only the soil, is presented as a function of time in Figure 4. The plant and soil materials correspond to those of the preceding figure. The activity increased almost linearly with time and did not have the sharp increase noted in the plant tops. Note also that in several cases the THO activity in the soil without plants had approximately the same, and sometimes higher, activity than that in which the roots were present. The gain in THO in the plant top resulting in a consequent loss of THO in the soil section cannot account for all the differences between the "soil and plant" and the "soil only" containers.

The presence of accentuated upward transport of THO in the soil section in which roots are present is shown in Table 1. In

this case, the soil container was cut in two equally thick horizontal layers and analyzed for THO.

In every treatment except the 2- and 6-hour periods, the upper sections in which roots were present had a higher THO activity than the comparable sections without the roots. In these analyses the THO concentrations in the root and soil mass were determined together. Separation of the root and soil materials was not possible because of the intimate association of the two. For the 6-hour periods, the lower value possibly may be caused by the absorption and consequent transport of THO out of the upper half into the plant tops. The translocation of the tracer via the root from the contact points at the lower half to, and through, the upper half is apparently the cause of the higher amount of THO in the upper section.

An exploratory experiment using corn plants was conducted in which one of the treatments consisted of placing a 2 mm air gap between the root mat and the THO treated soil. This was run to ascertain the contribution of tracer vapor movement to the THO absorption activity. The results are listed in Table 2 for two treatment periods.

The results show that, even with the air gap which prevents liquid phase THO movement between the THO source and the root mass, a considerable amount of THO has moved to the upper sections. Thus, the total activity measured must be corrected for the effect of THO vapor movement, and since it is of significant magnitude, accurate evaluation of tracer water absorption by roots is difficult to make.

Further investigations to ascertain the source of the water being absorbed under the previously described experimental conditions were conducted. The experimental procedure was similar, except that in this case the weight changes were followed in the various sections, instead of the THO activity. These results are shown in Figure 5 in which the weight losses are compared for the treatments where the root mat was in direct contact with the thin soil-sand

mixture and where an air gap was interposed between the two materials. In both cases the plant and soil section and also the bottom section lost weight in a similar manner. It is evident that the roots present above the root mat were absorbing the bulk of the water, and that very little water was being absorbed by the root mat in contact with the additional source of water. It is also apparent that the section ordinarily treated with THO is losing water primarily by vapor transfer to the atmosphere and not by water absorption by the roots.

SUMMARY AND CONCLUSION:

The diffusion coefficient of tritiated water (THO or $H^3H^1O^{16}$) in liquid water was determined by the gel technique and found to be 2.41×10^{-5} cm^2 sec^{-1}. This value confirms the only other data reported in the literature and which was obtained by another type of experimental technique.

Detailed measurements of the apparent diffusion coefficient of THO in Pachappa loam soil showed a complex relation between the diffusion coefficient and the water content of the soil material. A maximum diffusion coefficient of 4.16×10^{-5} cm^2 sec^{-1} was obtained at 4% water content by volume when about two molecular layers of water were present on the soil particle surface. At water contents between 40 and 10%, the D_{THO} was nearly constant, rising gradually from 1.10×10^{-5} to 1.37×10^{-5} cm^2 sec^{-1}. At water contents below 4% the D_{THO} values decreased sharply from the maximum.

The root-mat technique in the form used to study mineral uptake by roots is not applicable for investigating water absorption by roots, where tritiated water is utilized as a tracer for soil water. The quantity and rate of tracer water absorbed directly from the soil-tracer water system cannot be accurately separated from that moving to and into the plant by diffusive processes.

REFERENCES:

1. Dean, L. A., and Gledhill, W. H. Influence of soil moisture on phosphate absorption by an excised root technique. Soil Sci. 82:71-79. 1956.

2. Stanford, G., and De Ment, J. D. A method for measuring short-term nutrient absorption by plants. I. Phosphorus. Soil Sci. Soc. Amer. Proc. 21:612-617. 1957.

3. Wang, J. H., Robinson, C. V., and Edelman, I. S. Self-diffusion and structure of liquid water. III. Measurement of the self-diffusion of liquid water with H^2, H^3, and O^{18} as tracers. Jour. Amer. Chem. Soc. 75:466-470. 1953.

PERSONNEL: F. S. Nakayama, R. D. Jackson, C. H. M. van Bavel

Table 1. THO activity in horizontal layers of soil and soil and plant sections.

Contact period	Material	Total THO activity, μc	
		Lower section	Upper section
15 min.	plant & soil	.616	.027
	soil only	.588	.005
30 min.	plant & soil	.879	.027
	soil only	.945	.006
1 hr.	plant & soil	1.14	.178
	soil only	1.47	.013
2 hr.	plant & soil	2.16	.072
	soil only	2.42	.082
3 hr.	plant & soil	3.72	.353
	soil only	3.21	.125
4 hr.	plant & soil	3.47	.350
	soil only	3.49	.154
6 hr.	plant & soil	3.88	.516
	soil only	3.96	.627

Table 2. The effect of direct contact and air gap between root mass and THO source in the THO activity in the horizontal layers of soil and plant and soil sections.

Contact period	Material	Total THO activity, µc		
		Lower section	Upper section	Plant top
2 hr. (direct contact)	plant & soil	2.67	.126	.061
	soil only	2.42	.082	--
2 hr. (air gap)	plant & soil	1.58	.111	.016
4 hr. (direct contact)	plant & soil	3.65	.208	.194
	soil only	2.98	.189	--
4 hr. (air gap)	plant & soil	3.01	.155	.175

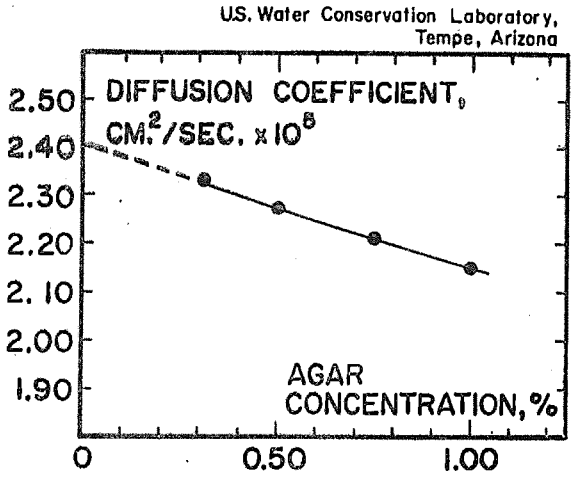

Figure 1. Diffusion coefficient of tritiated water in agar gel at different agar concentrations.

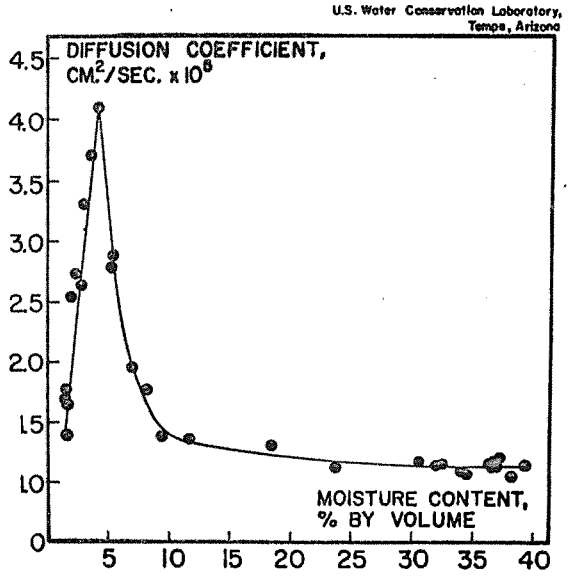

Figure 2. Apparent diffusion coefficient of tritiated water in Pachappa loam at different water contents.

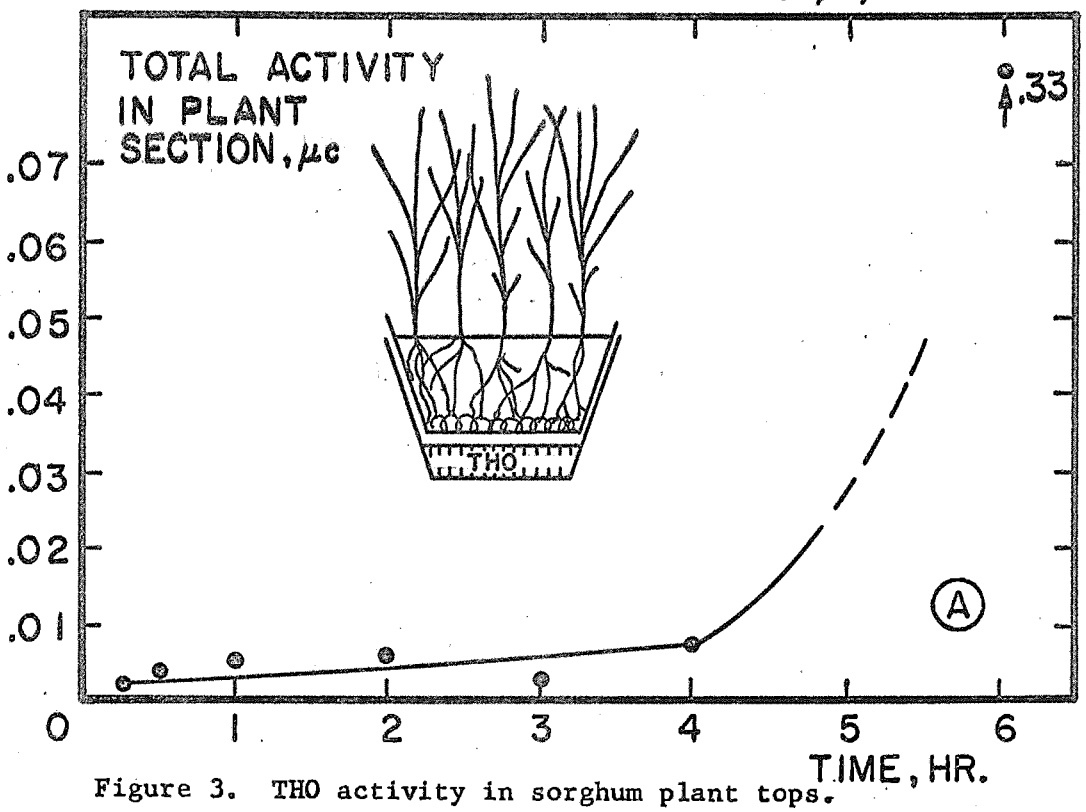

Figure 3. THO activity in sorghum plant tops.

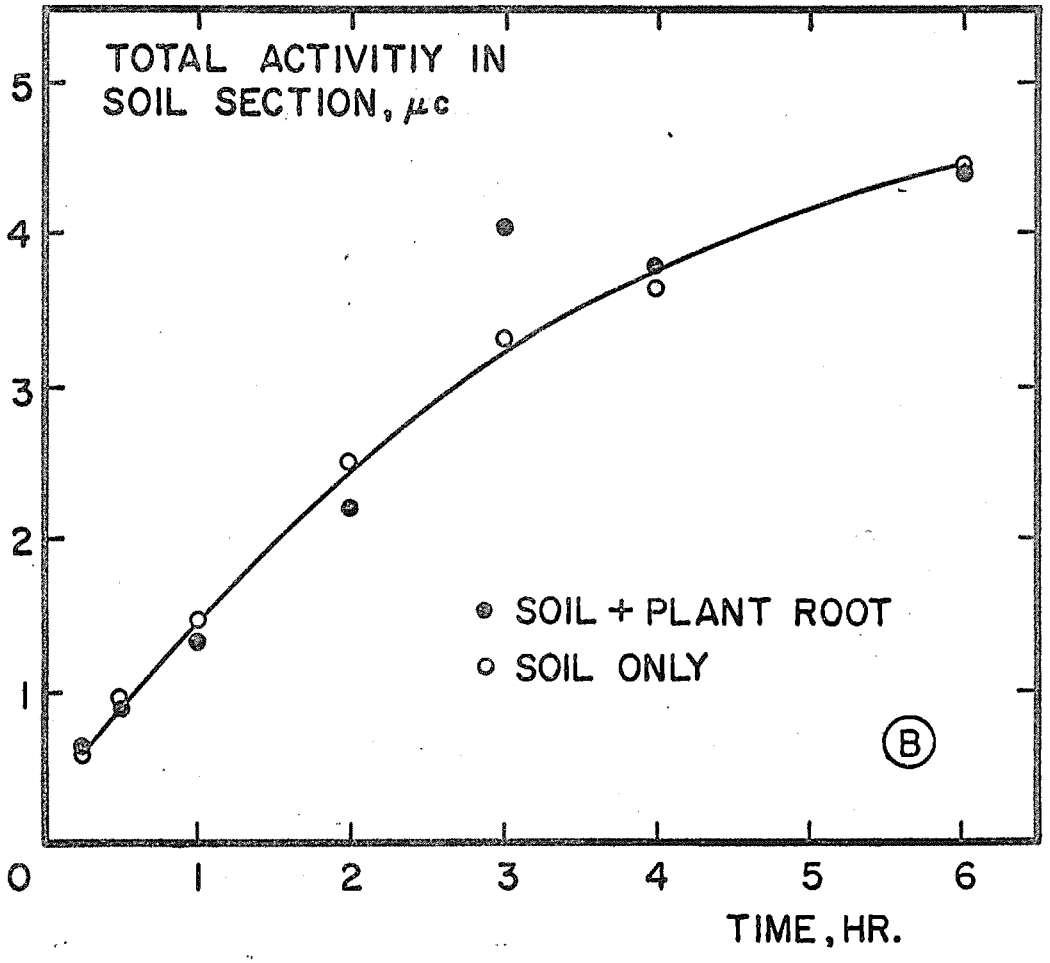

Figure 4. THO activity in soil and soil + plant sections.

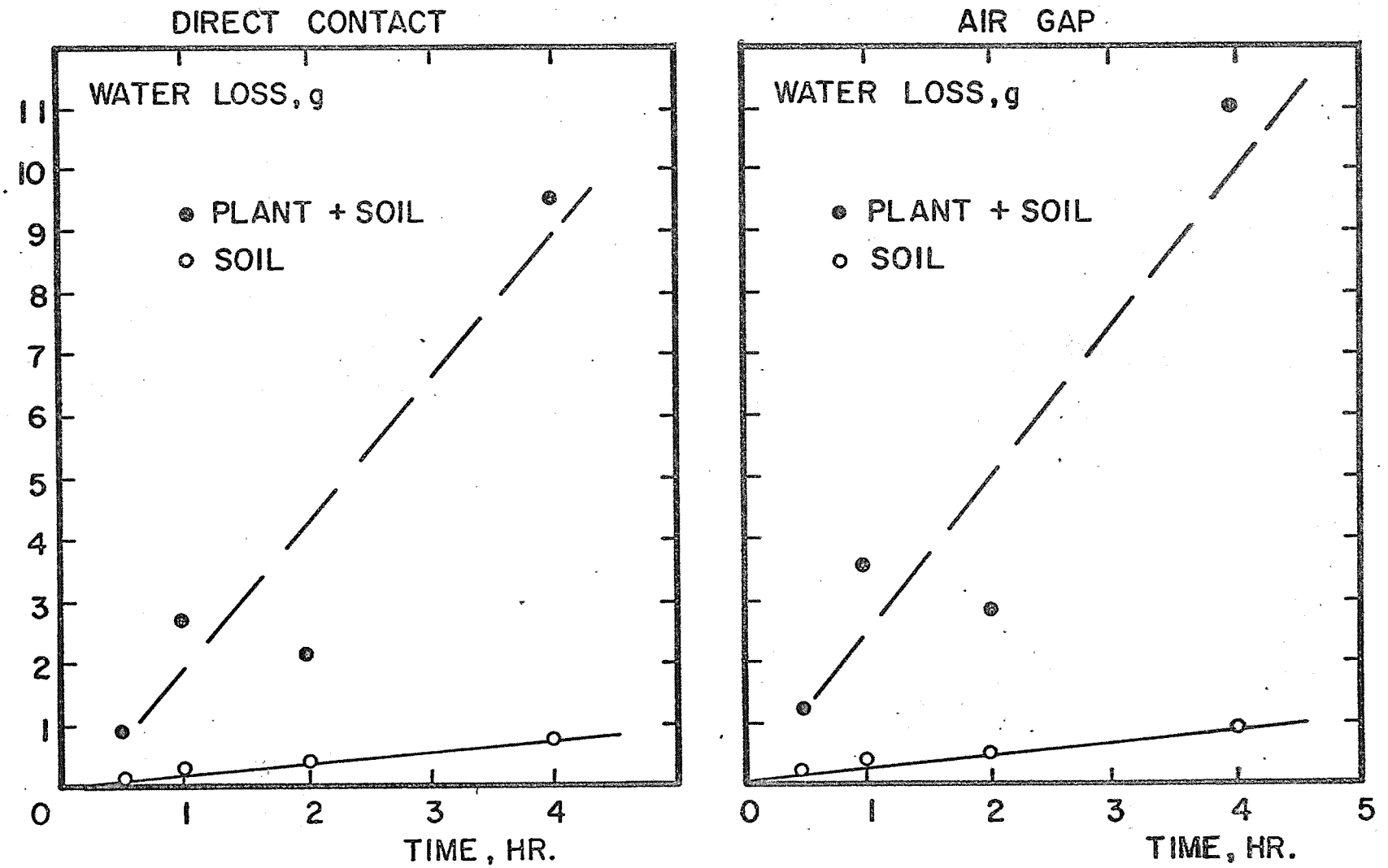

Figure 5. Weight loss of soil and soil + plant sections with air gap and direct contact.

TITLE: NONDESTRUCTIVE BETA RAY TRANSMISSION METHOD FOR MEASURING WATER CONTENT IN PLANTS

LINE PROJECT: SWC 11-gG1 CODE NO.: Ariz.-WCL-26

INTRODUCTION:

There is no reliable quantitative method for measuring the water content and stresses of intact plants directly. Most methods require sacrificing a portion of the plant and, thus, resulting in a probably adverse effect upon the moisture status of the rest of the plant. In other cases the techniques are workable only in the laboratory under stringent environmental control and their application for field use is extremely remote at present.

It is, therefore, the objective of this study to investigate the applicability of the nondestructive beta ray gauging technique for determining the water content and moisture status of plant leaves and the changes they undergo under various environmental conditions. By such studies it may be possible to evaluate more adequately the water economy of plants. In addition, the development of equipment and methods is contemplated which are suitable for field use with different types of irrigated crops.

Principle. The basic principle of the beta ray gauging technique involves the measurement of the attenuation of the beta ray radiation by matter. It is known that the greater the amount of material present in the beta ray path, the greater is the resulting attenuation. The transmission behavior is characterized by the following exponential relation:

$$I = I_o e^{-\mu d} , \qquad [1]$$

where

I = intensity of the transmitted radiation

I_o = intensity of the incident radiation

μ = mass absorption coefficient, $cm^2 g^{-1}$

d = absorber thickness, $g\ cm^{-2}$

"I_o" and "μ" can be kept as constants by using a single beta ray source, and by maintaining the same counting geometry. Thus,

"I" would be a function only of "d," the quantity of material interposed between the source and the detector.

In the case of the plant leaves, the absorber material will be primarily water, since a large fraction of the leaf is water. Any changes in the water content of the leaf, when it is used as the beta ray absorbing medium, will affect the intensity of the transmitted radiation.

Choice of isotope. Several factors were considered in making the choice of the isotope, namely that of the beta ray energy, half-life, availability, and thickness of leaf material to be encountered. The various properties of several isotopes which were investigated as possible choices are listed in Table 1.

It was expected in general to encounter, with plant samples, absorber thicknesses ranging from 10 to 40 mg/cm^{-2}, with the majority in the lower ranges, and changes in thicknesses of 1 to 4 mg/cm^{-2}. Thus, primarily on the basis of this, promethium-147, with its apparent greater flexibility in regard to range and to sensitivity than the other radioisotopes, was selected for our use. It was also readily available and its cost was reasonable.

Carbon-14, which has been used previously (1), can also be used. Sulfur-35 and calcium-45 have beta ray energies which are also applicable, but, because of their short half-lives, are not particularly useful. Technetium-99 is also suitable, but the isotope is not readily available commercially. Krypton-85 and thallium-204 both have more energetic beta emissions and they will be useful for the thicker leaves, but they will not reflect small changes in leaf water content as well as the isotopes with the lower beta ray energy for the thinner leaves.

METHOD:

1. Construction and testing of beta ray gauge.

The construction details of the beta ray gauge are presented in Figure 1. A photograph (Figure 2) shows the complete model. Section A is used to hold the 1" diameter × 3/8" thick disc with a 2μc promethium-147 beta ray source which was obtained from the

New England Nuclear Corporation. Section B is used to hold the end-window G. M. counter tube. Figure 2 shows the Model 10107 thin-window detector tube (Radiation Counter Laboratories, Inc.). The stainless steel bodied Model 10108 was later found to be more applicable than the 10107 Model for our work and the results are based on this detector tube. The detector-beta ray source distance was set at 3/32 inch.

The equipment used for the study included the Baird-Atomic Corporation Model 930 Timer, Model 134 Scaler, Model 212 Amplifier, and a modified Model 319 High Voltage Supply. In addition, the Nuclear-Chicago Corporation Model 2800 Portable Scaler was utilized. The detection systsms were operated following the prescribed procedures outlined by the manufacturers.

For the measurement of absorber thickness, the sample was placed between the beta ray source and the detector and the attenuated radiation measured for one minute. A test of the equipment was made using different thicknesses of aluminum foil absorber as the attenuator. These results are plotted in Figure 3. The count rates are plotted on semi-logarithmic paper as a function of the aluminum absorber thickness. The data show that the beta rays of Pm-147 are attenuated following the exponential equation of equation 1. The counting rates of 500 to 50,000 counts per minute, covering the range in absorber thickness of 40 to 20 mg/cm^2 are of sufficient magnitude to give reliable counting statistics. The low count rates can be increased, if necessary, by placing the detector closer to the beta ray source and also by using a detector with a thinner end window.

2. Use of beta ray gauge with plants.

A calibration curve was made with leaf material where the detector count rates were related to the absorber thickness and also the relative turgidity. Leaf materials were brought to 100 per cent relative turgidity by floating them in distilled water in a petri dish at 25° C and fluorescent illumination (30 ft-candles) for

approximately 15 hours. Excess water on the leaf was removed with absorbent paper and the leaf weighed, placed in the beta ray gauge, and the transmission recorded. The leaf was further dried, weighed, and counted; the procedure was repeated until a moisture level in the leaf beyond the wilt stage was attained. Care was taken in the counting process to replace the leaf in the same position on the holder. The absorber thickness was obtained for leaf discs from the ratio of fresh weight to the area of the discs. For whole leaves, the area was measured by first making a photocopy of the leaf on the Xerox copy machine and then determining the area with a planimeter.

Examples of the calibration curves relating to the absorber thickness and relative turgidity are presented in Figures 4 and 5. Note that for a given absorber thickness or relative turgidity the count rate is not the same. This is the result of differences in the structure of the leaf, causing differences in the geometry of the absorber. It was also found that a slight shift in position of the leaf affected the count rate, and the variations noted are partly the result of failure to reposition the leaf at the same place in the gauge. Therefore, for precise work a calibration curve should be run for the individual leaf.

Both curves show linearity on the semilogarithmic plot following the empirical exponential relation of equation 1. Although the linear portions of the three curves are displaced, calculations using the data for the absorber thickness-count rate relations give slopes or μ values of 0.112, 0.110, and 0.110 mg/cm^2 for a, b, and c, respectively.

The similarity of slopes for the leaves at similar stages of plant development can be used to advantage, particularly in the field. For example, by getting the count rate with the beta ray gauge on a test leaf, and obtaining the relative turgidity by the leaf-punched method on an adjacent leaf, we can get a reference point on the absorption curve. Then by drawing a line with the slope previously determined for similar leaves, through this point,

other count rates for the test leaf can be immediately converted into relative turgidity values in the field. Similar procedures can be used to obtain changes in absorber thickness or leaf water content.

The equipment was further checked under laboratory conditions, using whole plants to determine its responses to changes in the water status. Fifteen-week old cotton plants (Pima S-2) grown in the greenhouse in 1/2-strength Hoagland nutrient solution were used. The experiment to be reported was conducted in the environmentally controlled growth chamber at 30° C and a water deficit of the atmosphere of 29 mb. The plant was preconditioned overnight in the growth chamber before use.

The first fully formed leaf from the top (leaf number 19 from the cotyledonary node out of a total of 24 leaves in this experiment) was selected for the beta ray gauge measurements. The leaf was slipped between the source and the detector, and then positioned securely with tape so that no movement of the leaf occurred relative to the gauge holder during the experiments. The gauge was also located so that the larger veins were not placed within the counting geometry.

The results showing plant response to alternate dark and light periods as measured by the beta ray gauge are illustrated in Figure 6. Light intensity at the top of the plant was 3500 foot-candles and decreased progressively to a value of 2200 foot-candles near the lowest leaf. The data are presented in terms of count rates to give the magnitude of the range encountered for the experimental conditions present. The count rates ranged from 24,000 cpm for the "normal" leaf to 27,000 cpm for the "wilted" leaf. Standard deviation of the count rates at these levels was ± 180 cpm as measured separately using aluminum absorbers. Results are also plotted in terms of relative turgidity and absorber thickness, both of which were obtained from calibration curves of the test leaf similar to those shown in Figures 4 and 5.

As can be seen in Figure 6, the cotton plant responded rapidly to alternate dark-light periods, and the beta ray gauge was able to follow the changes that occurred during these periods. The relative turgidity changed in response to light and ranged from a high of 78 per cent to a low of 73 per cent within one-half hour. Plant-wilt occurred within the narrow range of relative turgidity. The first indication of wilt was observed by an increase in count rate of the gauge. The plant was able to regain its turgor even in the light. Part of the reason for the recovery in this instance is the fact that the moisture deficit of the atmosphere changed from 29 to 26 mb during the early portion of the light period. The recovery behavior was accentuated when the lights were turned off, and the period involved for full recovery was approximately one-half hour.

Water loss of 1 mg/cm^2 of leaf surface occurred during the one-half hour interval after the light was turned on. This indicates rapid response of the stomatal opening to light. Assuming that the rest of the plant leaves behaved in a similar fashion as the test leaf, and by using the measured total leaf area of 3480 cm^2, an estimate of 3.5 g water loss for the entire plant is obtained. Note that this value is the loss from the plant which results when transpiration exceeds absorption, and is not the total transpirational loss for which it might be easily mistaken.

During the last light period and at the minimum leaf water content, all leaves except the test leaf with the beta ray gauge were removed simultaneously from the plant. The single leaf was able to return to its original water content within 8 minutes. Again, by assuming the equal redistribution of water in the leaf, we find that approximately 0.2 g of water was translocated into the leaf. This information gives us some idea regarding the water conductive capacity of the petiole and associated leaf parts.

SUMMARY AND CONCLUSION:

The beta ray gauging technique for determining leaf water content and the internal water status of plants was investigated. The promethium-147 radioisotope was found to provide the right beta ray energy resulting in suitable response to leaf water changes in leaves with density-thicknesses of 10 to 40 mg/cm^2.

Equipment was constructed and the gauge performance checked with plants under controlled environmental conditions. The instrument showed reliable and good response to rapid changes in water conditions which can occur in plants. Furthermore, with light-weight portable equipment, the method should be readily applicable for investigating internal water status and the amount of desiccation and rehydration in the leaves of field crops.

REFERENCE:

1. Mederski, H. J. Determination of internal water status of plants by beta ray gauging. Soil Sci. 92:143-146. 1961.

PERSONNEL: F. S. Nakayama, W. L. Ehrler, C. H. M. van Bavel

Table 1. Properties of several beta emitting radioisotopes considered for beta ray gauging.

Radioisotope	Half-life	Maximum energy, Mev	Range, mg/cm^2
Hydrogen-3	12.3 y	.018	.6
Nickel-63	85 y	.067	7.0
Carbon-14	5570 y	.155	28
Sulfur-35	87.1 d	.167	32
Promethium-147	2.6 y	.223	50
Calcium-45	163 d	.254	60
Technetium-99	2×10^5 y	.29	74
Krypton-85	10 y	.695	250
Thallium-204	4.0 y	.765	280

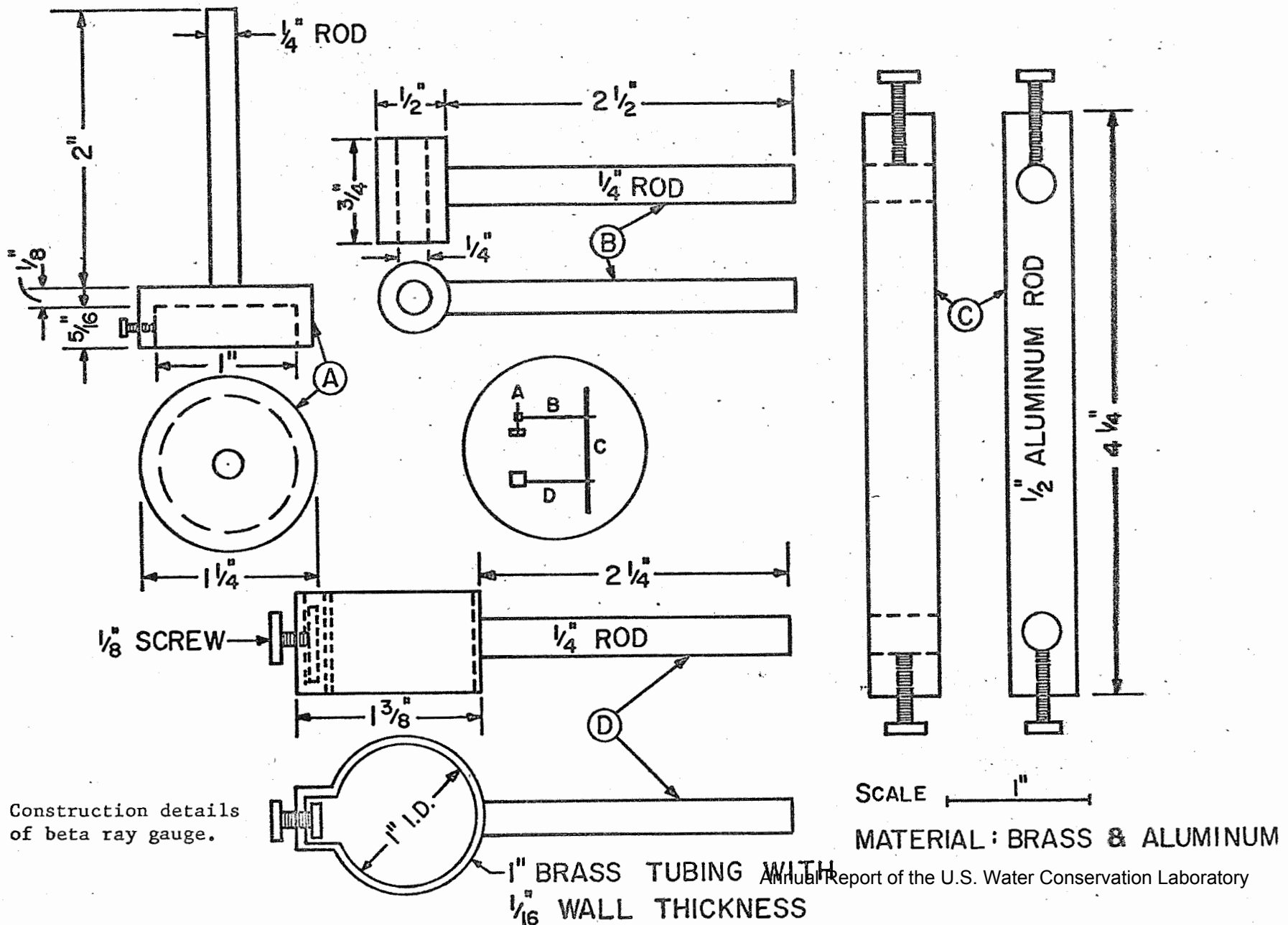

gure 1. Construction details of beta ray gauge.

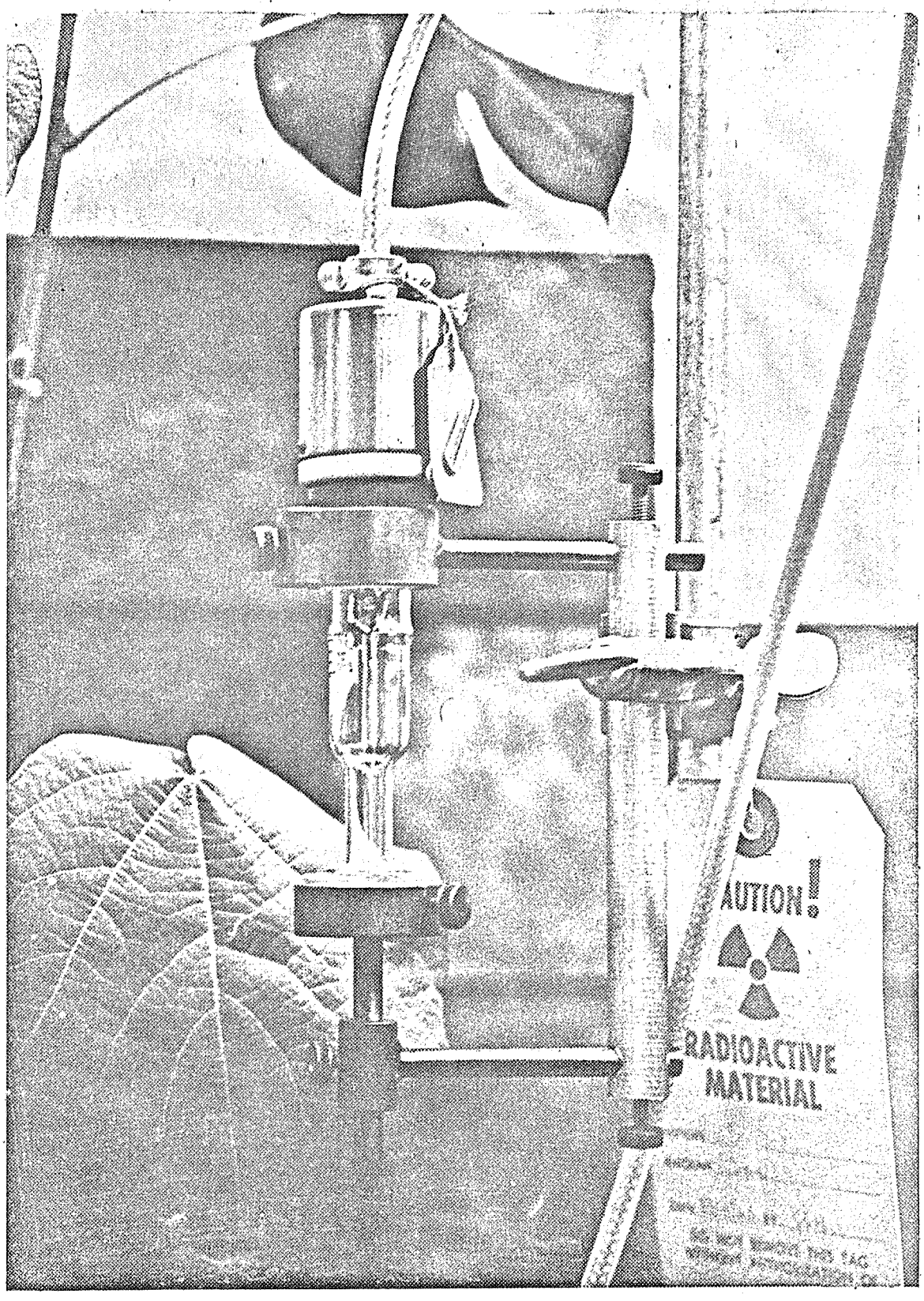

Figure 2. Photograph of beta ray gauge.

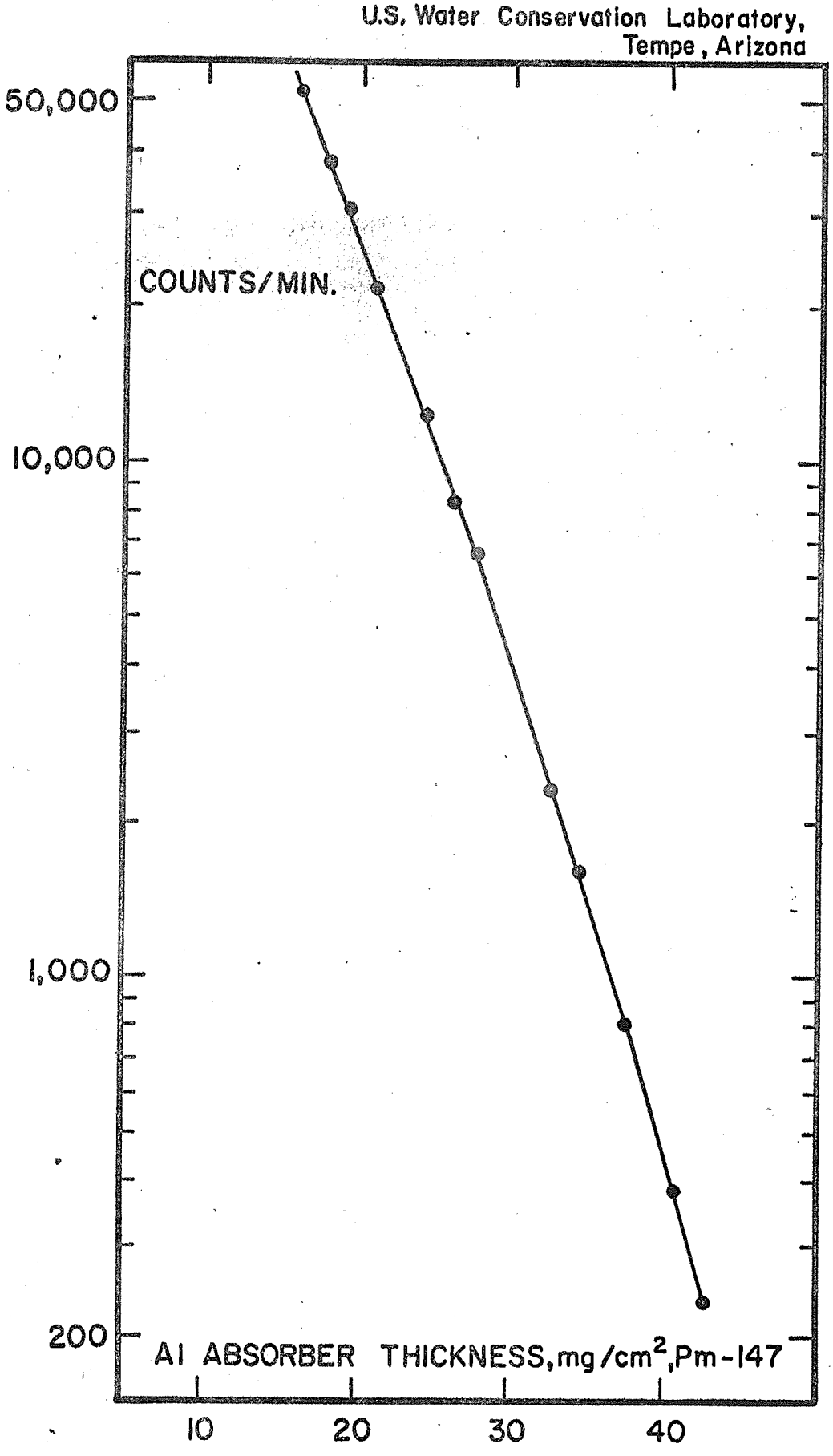

Figure 3. Absorption curve for promethium-147 beta ray in aluminum.

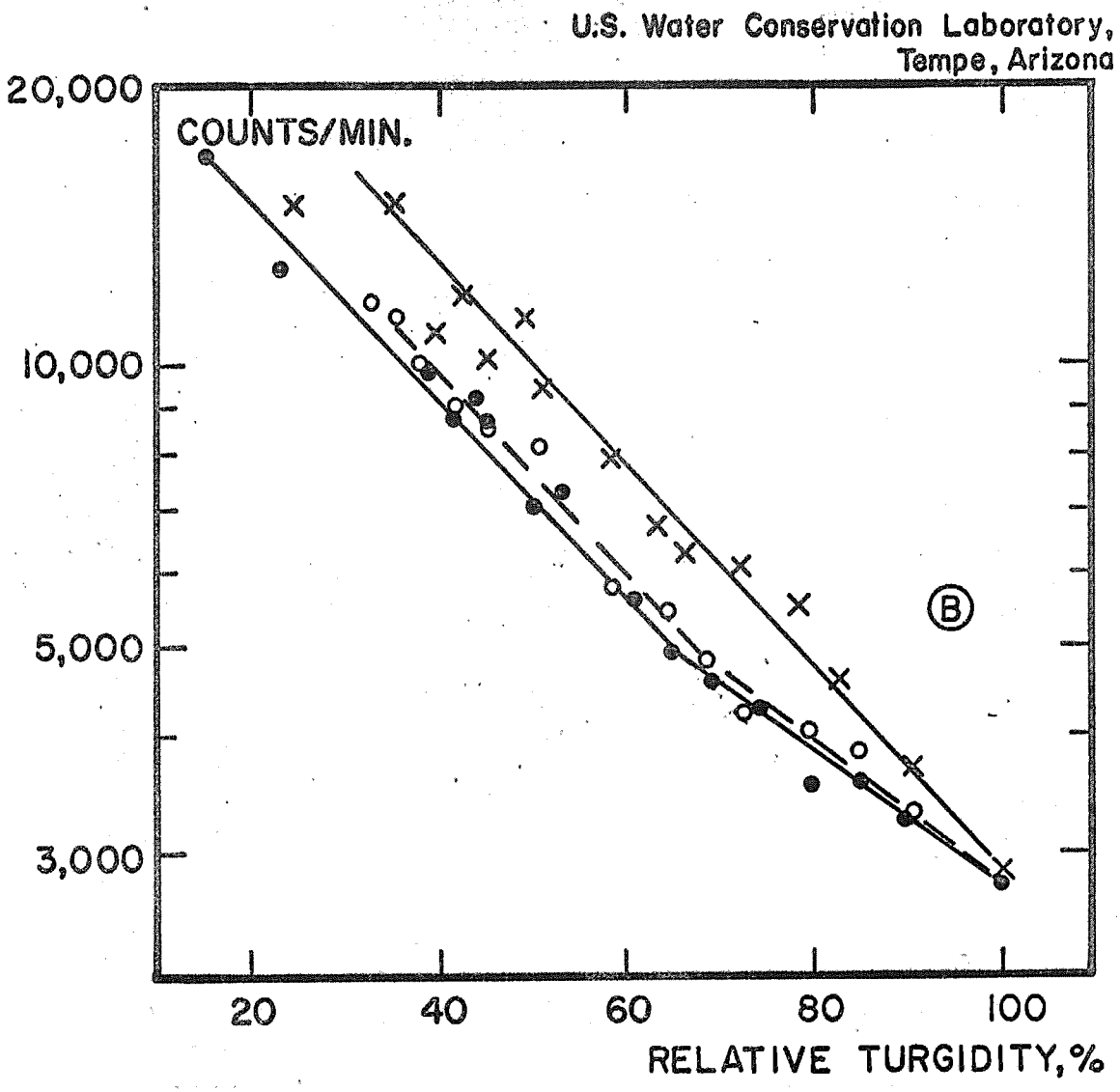

Figure 4. Absorption curve for promethium-147 beta ray in moist leaf related to relative turgidity.

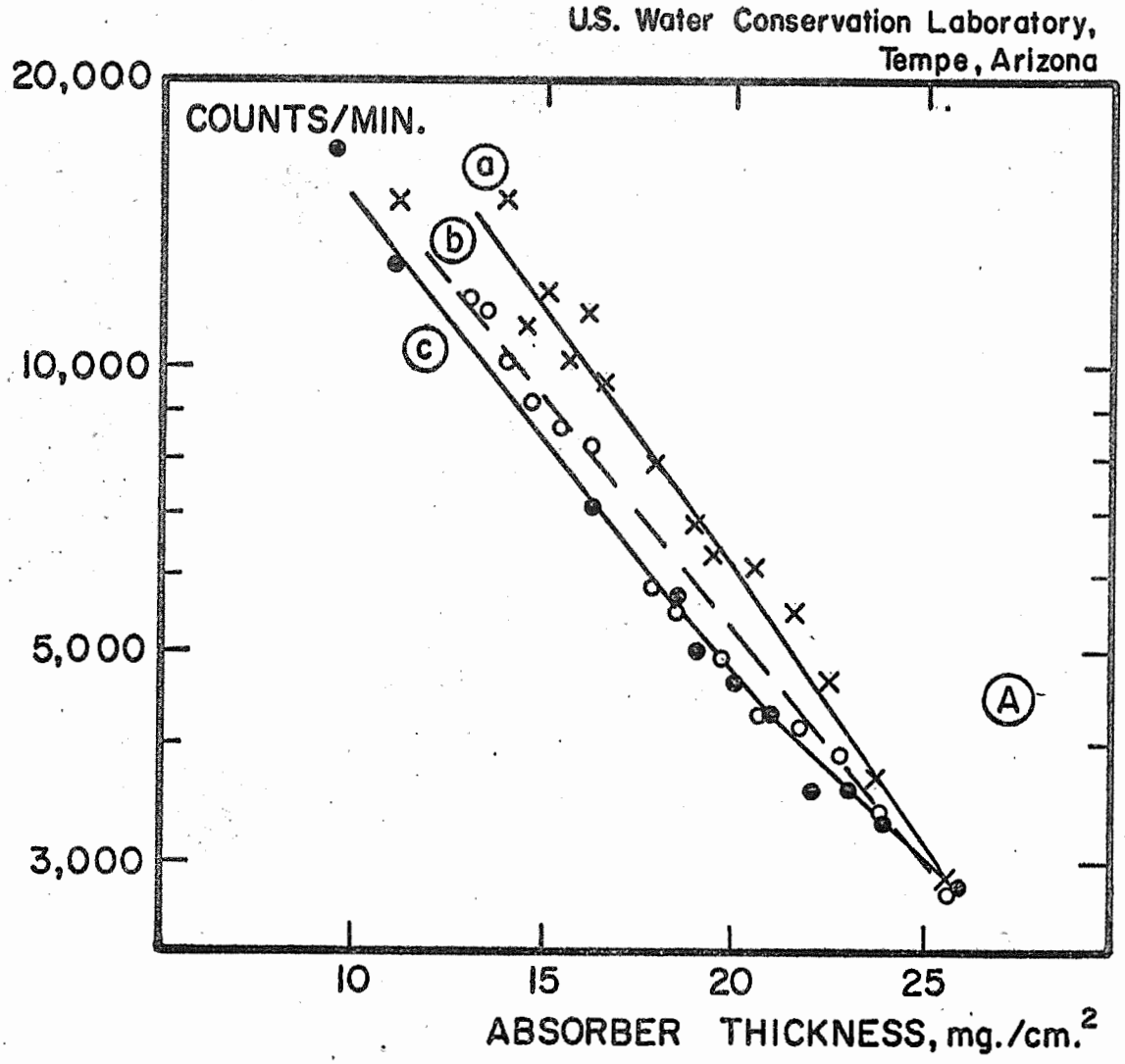

Figure 5. Absorption curve for promethium-147 beta ray in moist leaf related to absorber thickness.

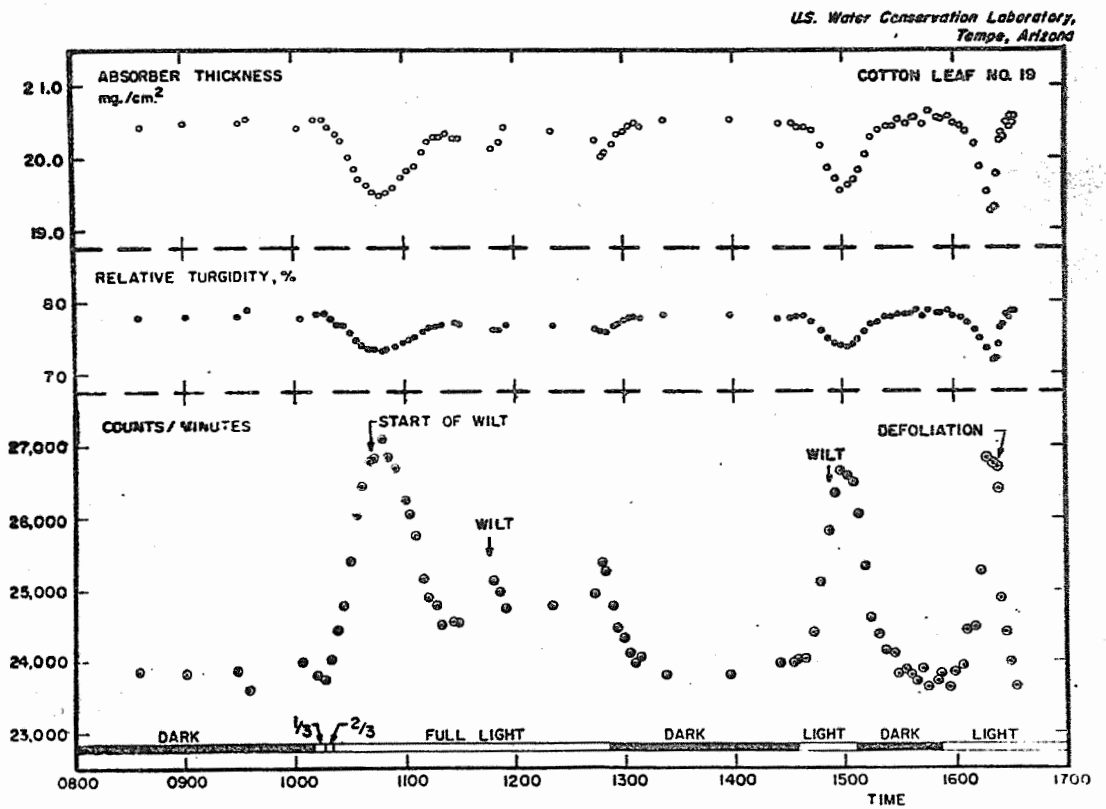

Figure 6. Response of cotton leaf to variable light conditions as measured with the beta ray gauge.

TITLE: WATER LOSS FROM PLANTS AS RELATED TO STOMATAL DIFFUSIVE RESISTANCE

LINE PROJECT: SWC 11-gG1 CODE NO.: None

INTRODUCTION:

Transpiration affects the water economy of plants. To understand this process, one of the things we must investigate is the escape path of the water vapor. Previous studies on stomatal behavior in relation to water vapor loss have one serious shortcoming, namely, that of the disturbance of the stomate and its environment. For example, to measure the stomatal aperture, the leaf must be observed under the microscope. This involves the use of high light intensity and other disturbing artificial conditions in the process of preparing the materials.

It is quite obvious that an accurate method, which has minimum effect on the leaf environment, for following vapor loss in leaves and concomitant water loss to the atmosphere must be developed. An isotopic tracer technique, using a water tracer, should lend itself to the solution of some of the problems. In this case, we propose to follow ordinary water vapor movement through stomates with tritiated water (THO or $H^3H^1O^{16}$). Investigators have attempted to give physical interpretation of diffusive processes to the stomate (1, 2). It would be of interest, then, to apply some of the data obtained from the tracer technique to some of the theories developed.

The objectives of the study then are (a) to develop a method for the direct and absolute measurement of the diffusive resistance of stomates to water vapor, (b) to relate the stomatal diffusive impedance of plant leaves to various environmental conditions, and (c) to calibrate empirical methods for characterizing stomatal aperture by means of the method developed under (a).

The first phase of the study was strictly of an exploratory nature to develop equipment, methods, and techniques. This consisted of exposure of leaves and materials simulating plant leaves to tritiated water vapor, analysis of tritiated water

concentration in the exposed material, and determination of optimum tracer concentration and exposure periods.

PROCEDURE:

Moist blotter paper, 6 x 8 cm, cut from green desk blotters was used to simulate leaves.

Corn plants (WD 456 × KB 397) were grown for 3 to 4 weeks in 3-oz wax-lined paper cups containing 180g of 2:1 sand-soil mixture. Plants were irrigated with 1/2-strength Hoagland nutrient solution. On the day prior to THO vapor treatment, normal irrigation was terminated and proportionately different amounts of nutrient solution were added to the cups to obtain different water contents in the soil material.

The plant materials were placed in a chamber for exposure to tritiated vapor. This treatment chamber was made from 1/4-inch lucite and was 20 inches wide, 12 inches deep, and 18 inches tall. The two 10" x 18" front panels were latched to the rest of the box for fast demounting. Rubber gasket seals were used to make the box as leak-free as possible. The chamber was equipped internally with a 50 CFM squirrel cage blower. The blower drive was mounted on the outside of the box to prevent heating of the internal chamber. The treatment chamber was placed in a laboratory gloved box and manual operations were carried out with this protective device.

For treatment of the plant with THO vapor, the material was placed in the chamber with a glass flask containing 100 ml of 2 or 10 μc/ml tritiated water. The air stream from the recirculating blower was directed over the surface of the tritiated water. During the treatment periods, the plants were illuminated with fluorescent lamps at 200 foot-candles. Chamber and water temperatures were maintained at 26 to 29° C.

After the prescribed exposure times, the plant leaves were analyzed for THO activity by the method developed and described in the 1960 Annual Report. Plants from the same set of plants as

the treated one, but unexposed to THO, were photocopied on the Xerox copier and the leaf area measured and related to the leaf weight.

RESULTS AND DISCUSSIONS:

Figure 1 shows the THO activity of moist blotter papers exposed to tritiated water. The results indicate a linear relation (r^2 = .98) between the THO activity in the blotters and the exposure periods of 15 minutes to 2 hours. Equilibration of THO activity on the blotter and the tritiated water source did not occur within the 2-hour exposure period. The 15 minutes exposure gives THO activities that can be measured accurately with our existing analytical equipment.

Blotters were used to check the exposure techniques and also to be a standard for normalizing results of experiments conducted at different times. Exploratory study in this regard showed that air leakage and poor recirculation within the treatment chamber may cause inconsistent replications.

The results for three replicates of corn plants at different soil water contents exposed to 10μc/ml tritiated water are shown in Figure 2. An exposure time of 15 minutes was used in these studies. Blotters were also exposed at the same time as the plants and the mean activities of 7 blotters per replicate in A, B, and C were 0.66, 0.72, and 0.69 μc/ml. This indicates that the THO exposure condition in the three replicates were quite similar, but the results with the plants, however, show some variation. The data show a decrease in THO exchange between the atmosphere and the internal leaf water as the soil water content decreases, and the linear relation does not indicate an abrupt closure of the stomates at any particular soil moisture content. The leaves at the 5% water content level and lower were badly wilted (permanent wilting at 3.6% water content), and yet evidence of exchange of tracer vapor is present. This would indicate either incomplete stomatal closure even at wilt, or some amount of cuticular diffusion of THO and consequent exchange with the leaf water. The magnitude

of the activity of the leaf water suggests the former more strongly. There was about 70% decrease in THO activity when the water content was decreased from 25 to 3.5%.

SUMMARY AND CONCLUSION:

Preliminary studies in which plants were exposed to tritiated water ($H^1H^3O^{16}$ or THO) vapor show that the method may be used to evaluate the stomatal behavior of plants. The leaves of corn plants, when grown under different moisture regimes and exposed to tracer vapor, show proportionately higher THO activity at the high than at the low soil water levels. Also, the data indicate differences in stomatal resistance from one soil moisture level to another and also an incomplete closure of the stomates even at the permanent wilting percentage.

REFERENCES:

1. Bange, G. G. On the quantitative explanation of stomatal transpiration. Acta Bot. Neerl. 2:255-297. 1953.
2. Penman, H. L. and Schofield, R. K. Some physical aspects of assimilation and transpiration. Symp. Soc. Exp. Biol. 5:115-129. 1951.

PERSONNEL: F. S. Nakayama, C. H. M. van Bavel.

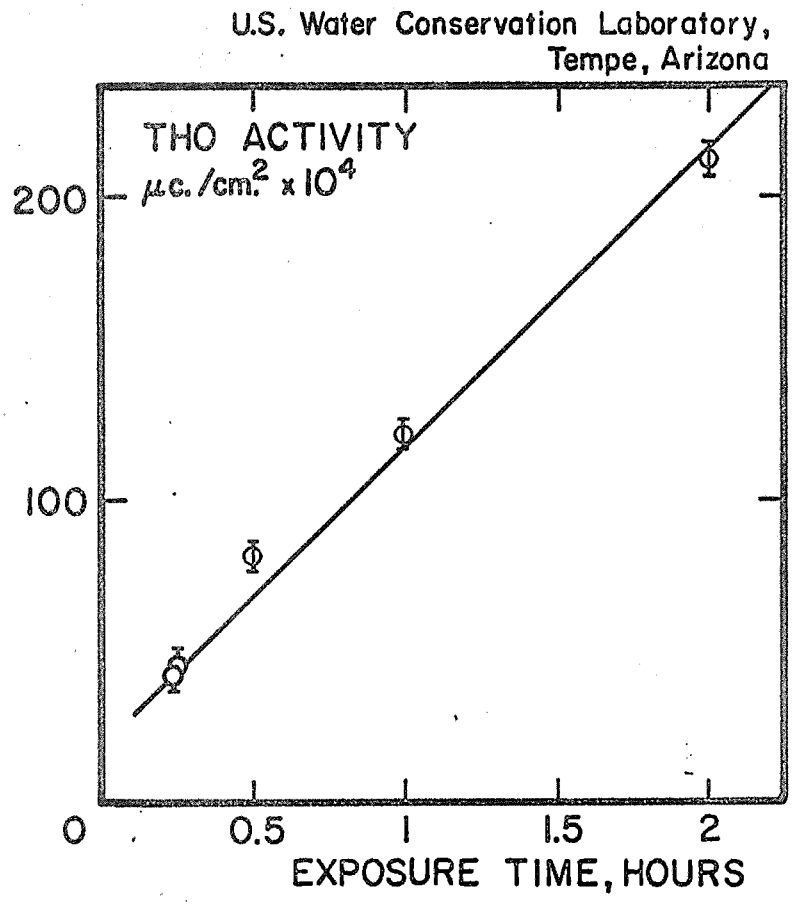

Figure 1. THO activity in moist blotter paper exposed to 2 μc/ml tritiated water.

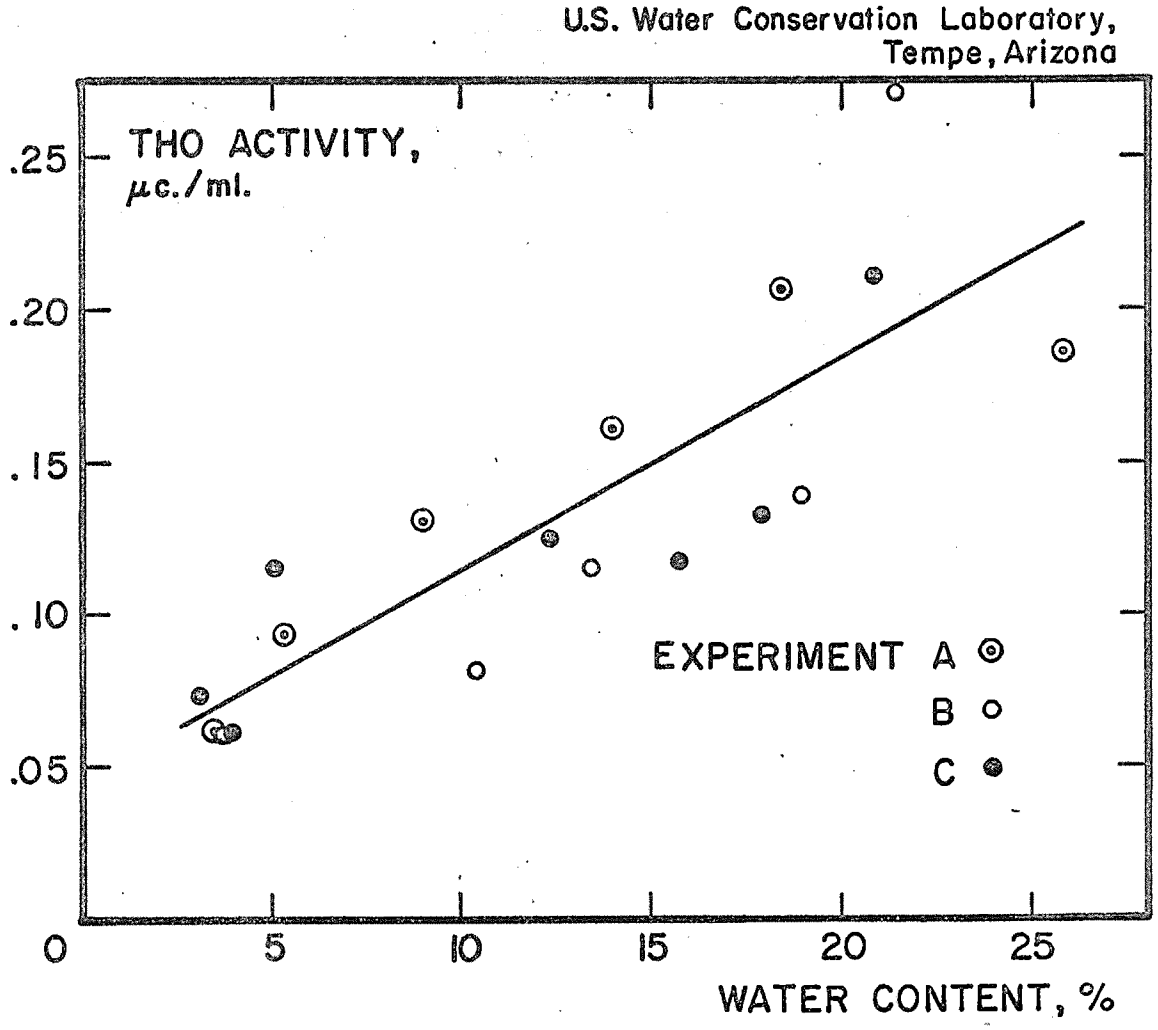

Figure 2. THO activity in corn plants exposed to 10 µc/ml tritiated water.

TITLE: WATER ABSORPTION, TRANSPIRATION, AND INTERNAL WATER BALANCE OF COTTON PLANTS AS AFFECTED BY CHANGES IN EVAPORATIVE DEMANDS

LINE PROJECT: SWC 11-gG1 CODE NO.: Ariz.-WCL-29

INTRODUCTION:

Wise use of irrigation water demands an understanding of plant water-relations. The large quantities of water lost from transpiring plants must be balanced by water absorbed from the substrate in order to avoid wilting and consequent growth impairment or death of plants. Few attempts have been made to measure accurately both transpiration and water absorption over short periods under different environmental conditions.

Precise information is needed about the effects of different magnitudes of water deficit on plant growth and transpiration. To obtain the necessary control of the variables concerned in transpiration, a controlled-environment facility is needed. The objective is to understand plant water-relations better over short periods, and, ultimately, to be able to correlate plant response under controlled conditions with field behavior of crops. The research to achieve such an objective was initiated in April 1962, and is expected to continue until 1967, subject to annual evaluation.

PROCEDURE:

Since the internal water balance of a plant is affected by the relative rates of water absorption and transpiration, cell turgidity can be affected by altering either process. The primary purpose of this investigation is to study the effects on plants of changes in the transpiration rate induced by manipulating evaporative demand. However, first an experiment was performed to determine the effect of root temperature on water absorption at a low transpiration rate. This information permitted all following experiments to be carried out at root temperatures favorable to water absorption. Therefore, any decrease in plant turgidity in response to a higher evaporative demand could be ascribed to a transpiration rate higher than before, rather than to a possible simultaneous decrease in the rate of water absorption.

The general procedure was to grow cotton plants (Pima S-2, long-staple) in nutrient solution in the greenhouse to about the 12-leaf stage, and then to take the required number of plants into the Controlled-Environment Room overnight to equilibrate in aerated nutrient solution in the darkness at the desired dry- and wet-bulb temperatures. The next morning each plant was sealed in a 2-liter, rigid, plastic pot. After the roots were inserted, the stem was fitted with a rubber stopper below the cotyledonary node, and a watertight seal was made by means of cotton batting and wax. A standpipe rising from the pot lid had a reference line 2 cm above the solution level for water absorption measurements. The whole apparatus, including pot and plant, was weighed at intervals for transpiration determinations.

Usually two plants were placed on a bench in the middle of the Controlled-Environment Room so that circulating air moved the leaves only slightly. In several experiments a third plant, similar to the others, was reserved for beta ray gauge measurements of a representative leaf. This plant, placed at the north end of the bench, was not weighed, since precise beta ray gauge monitoring depends on maintenance of the original leaf position in regard to detector and radioactive source. It was assumed that the internal water balance of all three plants would be affected similarly by the experimental variables.

The main variable studied was the diffusive capacity of the stomates as determined by the presence or absence of light. This approach, although a departure from the objective stated in the title, is considered a logical preliminary to changing evaporative demand by varying the wet-bulb temperature; moreover, a change can be effected more quickly and with less temperature reaction of the controls than a change of wet-bulb temperature, since it consists of merely turning the lights on or off.

During the water absorption measurements, forced aeration was not given to the roots. Therefore, the duration of experiments was kept to the minimum consistent with other experimental objectives. Since the internal water balance can change rapidly, experimental measuring periods were short, mostly confined to 30 minutes per period.

The data collected and considered pertinent to this type of experiment deal with light intensity (Weston light meter), integrated saturation deficit (Leeds and Northrup recorder, with dry- and wet-bulb probes located in the return-air duct of the Controlled-Environment Room), evaporation rate (black Bellani plate), leaf area, plant tissue water content (fresh and oven-dry weights), and the relative turgidity (beta ray gauge leaf measurements, counts min^{-1}). See WCL-26 for a detailed account of the beta ray gauge data.

RESULTS AND DISCUSSION:

Root-temperature experiment

Before the standpipe-pot was developed, the weight method was used for measuring both transpiration and water absorption. The determination of transpiration consisted of two successive weighings of the plant and all appurtenances (such as pot and solution, etc.), whereas the absorption measurement was obtained from two weighings of the pot with its nutrient solution, without the plant. Complications involved in blotting the roots dry before weighing and the consequent correction of the water absorption value made an alternate method desirable. However, the root temperature results, which were the only data derived from this method of measurement, pointed to the desirability of maintaining the root temperature above 20°C.

Under conditions conducive to a rather low transpiration rate—DB 28.2, WB 24.0, SD (saturation deficit) 11 mb—a root temperature of 20°C compared to 30°C depressed water absorption 56 percent over a one-hour period, enough to cause wilting of the three youngest leaves in 20 minutes. When 30°C and 10°C root temperatures were compared for one hour, water absorption was depressed 83 percent, the wilting of the upper leaves appearing in 10 minutes. These values are mean data for three pots. When the plants from both low-temperature treatments again were put in nutrient solution at 30°C, water absorption much exceeded transpiration, and recovery from visible drooping was complete in 12 to 20 minutes.

Development of the standpipe-pot described earlier enabled more precise water absorption measurements to be made; therefore, this method

supplanted the weight method used for the root temperature study. Preliminary tests showed an apparent stimulatory effect of hydrostatic pressure on water absorption when the water level in the standpipe was maintained at 40 cm above the pot lid. To avoid a possible additional variable, the standpipe reference level was changed to 2 cm above the lid for all subsequent experiments.

Twenty-four hour experiments

A. Continuous darkness. Two 24-hour experiments were undertaken as a preliminary to the short-term experiments to find out if transpiration and water absorption showed any periodicity. In the first experiment, carried out with 18-week-old plants, transpiration and water absorption were measured in the Controlled-Environment Room for 12 consecutive 2-hour periods in the darkness at a mean air temperature of 34.2°C and a SD ranging from 16.0 to 17.2 mb. The evaporation rate from a Bellani plate, placed 1 meter from the plants, was 0.60 to 0.63 ml hr^{-1}. Plant I transpired from 4.2 to 4.8 g hr^{-1} for the first eight hours (25.0 to 29.0 g m^{-2} hr^{-1}), and absorbed slightly more water than it lost. Plant II transpired from 5.2 to 6.1 g hr^{-1} during the first eight hours (24.0 to 27.0 g m^{-2} hr^{-1}), the measurements beginning at 0900. Water absorption was essentially equal to transpirational losses. After eight hours, both transpiration and absorption declined steadily in the two plants to a rate about one-half that of the initial value. The total absorption for the 24 hours was 15 percent lower than transpiration for plant I, and 10 percent lower for plant II.

Generation of large amounts of bubbles in the mass of roots near the bottom of the pot interfered with the water absorption measurement whenever the bubbles could not be dislodged and replaced with nutrient solution up to the water absorption reference line. This problem occurred with both plants after about eight hours, and at times made an absorption measurement unreliable; therefore, the data are presented only for the first eight hours.

B. Continuous light. In the second 24-hour experiment, two plants were kept in the light (intensity ranging from 2200 ft-c at bench height to 3500 ft-c at the top of the plant, 120 cm), while measurements of both transpiration and water absorption were made for 12 two-hour periods in the Controlled-Environment Room. The mean air temperature was 33.4°C, with a SD ranging from 9.7 to 11.4 mb. The plants were 16 weeks old. Evaporation from the black Bellani plate ranged from 1.02 to 1.18 ml hr^{-1}. It should be noted that this evaporimeter responds to both SD and radiation. The measurements began at 1100, and showed a similar transpiration for each of three 2-hour periods: plant I, about 22 g hr^{-1} (125 g m^{-2} hr^{-1}), with an equal rate of water absorption; plant II, about 27 g hr^{-1} (113 g m^{-2} hr^{-1}), again with absorption equaling transpiration. During the remainder of the 24 hours, however, both plants showed a steady decline in both transpiration and water absorption, finally reaching values only about one-fourth the original rate. Nevertheless, the total absorption equaled the total transpiration. Accumulation of bubbles was a problem after the first six hours.

In both of the 24-hour experiments, confining the plant roots for that duration without forced aeration may have caused abnormal root respiration, although there were no apparent pathic symptoms. The transpired water was replenished with well-aerated nutrient solution in an attempt to alleviate any possible lack of adequate oxygen in the root zone. In each experiment a third plant was exposed to the same conditions as the two plants used for transpiration and absorption measurements, except that it remained immobile. This permitted beta ray gauge monitoring for the thickness of a representative, fully expanded leaf near the tip of the plant. In general, the beta ray gauge readings confirmed the water flux measurements, in that the monitored leaf showed a slight but steady loss of thickness (indicating a net removal of water) in the continuous-darkness experiment, but no net change in thickness in the continuous-light experiment (see WCL-26 for more details).

Short-term experiments

A. At a SD of 6 mb. Three cotton plants, 14 weeks old, were brought from the greenhouse into the Controlled-Environment Room at 1600 the day previous to the experiment. They were put in aerated nutrient solution and kept in darkness at an air temperature of 30°C and a SD of 6 mb until the next morning. Table 1 gives details of the subsequent treatment and results of the experiment. The transpiration-absorption data for the 30-minute period just preceding the first period of light can be considered more typical of the steady-state dark conditions than the first period, in which evaporation of dew from the leaves probably gave abnormally high transpiration values. Allowing for the experimental error in absorption measurements in the dark under very low evaporative demand, the data for the dark period indicate a balance between gain and loss of water by the plants. A sudden large increase in stomatal aperture induced by light brought about a moderate deficit in tissue water content of both plants. During three more 30-minute periods in the light, absorption continued to lag slightly behind transpiration. The upper leaves of both plants wilted slightly in the second period of light. Not until the last of five consecutive 30-minute periods of light did absorption exceed transpiration slightly. Turning off the lights greatly depressed transpiration, but in stages; it sank to one-half the steady-state in light during the first period, and to even lower rates in later dark periods. Absorption exceeded transpiration when the lights were off, but not to an extent sufficient to cancel completely the deficit built up earlier. Nevertheless, the imbalance was decreased sufficiently to overcome the wilting.

As pointed out before, no water balance measurements were made on the plant having the attached beta ray gauge. Moving the plant for periodic weighing might interfere with counter geometry and thus lead to an incorrect count rate. It was assumed that the internal water balance of all three plants was affected equally by the experimental variables. The count rate from a young, fully expanded leaf on the third plant increased when transpiration exceeded absorption in the two plants measured for water balance. Therefore, indications are

that the water content of the single leaf is a reflection of that of the whole plant.

B. At a SD of 15 mb. After a previous night's equilibration in the Controlled-Environment Room at an air temperature of 30°C and a SD of 15 mb, three 14-week-old cotton plants were exposed to the following sequence of 30-minute experimental periods: four dark, six light, and three dark. Pertinent data are found in Table 2. As in the previous experiment, in darkness water absorption was essentially equal to transpiration, but lagged behind when the lights were turned on suddenly. Moreover, the difference was more pronounced than before. Absorption remained behind transpiration for three more periods in plant I, but in plant II absorption began to equal transpiration by the third period of light.

In three periods of darkness after the lights were turned off, absorption far exceeded transpiration. However, this excess was enough to cancel the previous deficit only for plant II. The wilt produced by excess transpiration over absorption was evident in both plants in the second period of light. It was more pronounced than that occurring at 6 mb, but again was reversed by darkness. The beta ray gauge on the third plant confirmed the measurements made on the first two plants.

C. At a SD of 29 mb. Plants 15 weeks old were stabilized overnight in the Controlled-Environment Room in darkness at 30°C and at a SD of 29 mb. The next morning transpiration and absorption were determined for two plants, while the third was monitored by a beta ray gauge. The results (Table 3) show, as before, absorption essentially equal to transpiration in the early dark periods, but reveal a great disparity in the two processes in the light. The reaction speed of these plants was quite different from that in the previous experiments. After a large deficit in net water content induced a wilt during the first period of light, absorption increased so much in the next period as to exceed transpiration, thus curing the wilt in both plants. In the following three periods of light, absorption continued to exceed transpiration, so that the deficit engendered when

the lights first came on was canceled even before the lights were turned off. However, during these succeeding periods of light, the plants again wilted very slightly and recovered, with no obvious correlation with the transpiration-absorption measurements.

The excess water absorption after the lights went off contributed to a total absorption that exceeded transpiration considerably, implying that the plants were better hydrated at the end of the experiment than the start. The beta ray gauge on the third plant did not confirm this fact, but both instances of earlier wilting were corroborated nicely by the beta ray gauge readings of a young, fully expanded leaf.

SUMMARY AND CONCLUSIONS:

Plant growth and water use are closely associated with the internal water balance, which depends on the relative rates of transpiration and water absorption. Experimental induction of an unfavorable internal water balance by an increased evaporative demand may lead to a better understanding of plant water-relations, especially when done over short time increments.

Experiments were performed with long-staple cotton (Pima S-2) in nutrient solution in the Controlled-Environment Room. Both transpiration and water absorption were measured precisely for several consecutive 30-minute periods to determine the effect on the internal water balance of changes from light to darkness. The transpiration-absorption measurements were made on two plants, while a third served for beta ray gauge thickness measurements of a fully expanded leaf (see WCL-26). An integrated value for the SD, as well as the evaporation rate from a black Bellani plate, characterized the evaporative demand of the aerial environment. Light intensity at three elevations was also determined.

Preliminary experiments showed that water absorption was not inhibited at a root temperature of 30°C, and that there was no apparent periodicity of either water absorption or transpiration in a 24-hour period of darkness or light.

Three short-term experiments involved measurement of transpiration and water absorption during sudden changes from darkness to light, carried out under different degrees of evaporative demand (SD of 6,

15, and 29 mb). Turning on the lights suddenly caused transpiration to exceed water absorption, after having been equal to it under steady-state dark conditions. The greater the evaporative demand, the greater the disparity between transpiration and water absorption. However, during succeeding periods of light, a progressively higher rate of absorption compared to transpiration tended to cancel the deficit caused by the first period of light. At 29 mb, for example, water absorption was much less than transpiration in the first 30-minute period after the lights came on, but exceeded transpiration in the next period. Under a lower evaporative demand the difference between water gain and loss was not so pronounced immediately after the lights came on, and there was a correspondingly longer recovery time. At the lower values of evaporative demand it was necessary for the lights to be off for several half-hour periods in order for the deficit to be overcome completely.

This difference in the rate of increase in water absorption during successive periods of light is correlated with the SD. The higher the SD, the faster the plants increased their rate of water absorption after its initial decline in the first period of illumination. A possible explanation is the development of a higher DPD in the leaves of plants that wilted more severely (at 29 mb) than in those with a milder wilt (at 15 and 6 mb). The higher DPD would enhance the gradient for water absorption. This hypothesis can be tested by determining the DPD of leaf tissue before and after wilting under quite different conditions of evaporative demand.

It is concluded that precise measurement of both transpiration and water absorption over short periods in a controlled environment can contribute to an understanding of the internal water balance of cotton plants.

PERSONNEL: W. Ehrler, C. H. M. van Bavel, F. S. Nakayama

Table 1. Cotton transpiration and water absorption in light and darkness at a saturation deficit of 6 mb, 28 December 1962.

Time	Condition	Sat. Deficit	Bellani Evap.	PLANT I (2688 cm^2) Transp.	Absorp.	(A - T)[c]	PLANT II (2518 cm^2) Transp.	Absorp.	(A - T)[c]
		mb	ml hr^{-1}	g hr^{-1}	g hr^{-1}	g hr^{-1}	g hr^{-1}	g hr^{-1}	g hr^{-1}
0930 1000	Darkness	5.9	0.16[a]	6.0[b]	3.6	-2.4	6.0[b]	4.4	-1.6
1000 1030	Darkness	5.5	0.14[a]	2.0	1.6	-0.4	2.0	2.8	+0.8
1030 1100	Light	5.7	0.16[a]	8.0	4.6	-3.4	10.0	6.0	-4.0
1100 1130	Light	4.8	0.64	15.0	14.4	-0.6	22.0	17.4	-4.6
1130 1200	Light	5.6	0.76	21.0	19.6	-1.4	22.0	21.0	-1.0
1200 1230	Light	6.1	0.74	21.0	20.6	-0.4	24.0	23.4	-0.6
1230 1300	Light	6.2	0.78	21.0	21.6	+0.6	23.0	24.0	+1.0
1300 1330	Darkness	5.7	0.67	10.0	12.0	+2.0	10.0	12.0	+2.0
1330 1400	Darkness	5.9	0.32	7.0	5.0	-2.0	5.0	5.0	±0.0
1400 1430	Darkness	5.9	0.19	2.0	4.0	+2.0	3.0	4.0	+1.0
1430 1500	Darkness	4.7	0.26	3.0	3.4	+0.4	4.0	4.0	±0.0
						Σ = -5.6			Σ = -7.0

[a] Liquid water on plate surface
[b] Includes evaporation of extraneous water
[c] Absorption minus transpiration

Table 2. Cotton transpiration and water absorption in light and darkness at a saturation deficit of 15 mb, 19 December 1962

Time	Condition	Sat. Deficit	Bellani Evap.	PLANT I (3032 cm^2) Transp.	Absorp.	(A - T)[a]	PLANT II (3277 cm^2) Transp.	Absorp.	(A - T)[a]
		mb	ml hr^{-1}	g hr^{-1}	g hr^{-1}	g hr^{-1}	g hr^{-1}	g hr^{-1}	g hr^{-1}
0830 0900	Darkness	15.7	---	4.0	5.0	+1.0	4.0	4.0	±0.0
0900 0930	Darkness	15.7	0.40	2.2	3.0	+0.8	4.0	3.4	-0.6
0930 1000	Darkness	15.7	0.64	3.0	2.6	-0.4	2.0	2.4	+0.4
1000 1030	Darkness	15.7	0.74	3.0	3.4	+0.4	3.8	3.0	-0.8
1030 1100	Light	14.3	0.99	17.0	7.4	-9.6	19.6	11.6	-8.0
1100 1130	Light	11.7	0.74	22.0	14.6	-7.4	28.0	25.0	-3.0
1130 1200	Light	12.0	1.15	17.0	16.4	-0.6	26.0	26.0	±0.0
1200 1230	Light	12.2	1.15	16.0	15.0	-1.0	25.0	26.0	+1.0
1230 1300	Light	12.7	1.20	13.0	13.0	±0.0	26.0	26.0	±0.0
1300 1330	Light	11.6	1.24	12.0	10.6	-1.4	24.0	29.0	+5.0
1330 1400	Darkness	11.6	1.06	5.0	9.8	+4.8	7.0	16.0	+9.0
1400 1430	Darkness	14.8	0.79	3.0	7.0	+4.0	2.0	5.0	+3.0
1430 1500	Darkness	14.1	0.89	5.0	6.0	+1.0	7.0	5.0	-2.0
						Σ = -8.4			Σ = +4.0

[a]Absorption minus transpiration

Table 3. Cotton transpiration and water absorption in light and darkness at a saturation deficit of 29 mb, 3 January 1963.

Time	Condition	Sat. Deficit	Bellani Evap.	PLANT I (2755 cm^2) Transp.	Absorp.	(A - T)[a]	PLANT II (3284 cm^2) Transp.	Absorp.	(A - T)[a]
		mb	ml hr^{-1}	g hr^{-1}	g hr^{-1}	g hr^{-1}	g hr^{-1}	g hr^{-1}	g hr^{-1}
0830 0900	Darkness	29.4	2.01	4.0	4.6	+0.6	4.0	5.4	+1.4
0900 0930	Darkness	28.8	1.91	3.0	5.0	+2.0	4.4	4.6	+0.2
0930 1000	Darkness	29.6	2.00	8.0	6.4	-1.6	8.0	6.0	-2.0
1000 1030	Light	29.2	2.09	31.0	19.4	-11.6	38.0	25.0	-13.0
1030 1100	Light	26.1	1.96	35.0	38.0	+3.0	30.0	36.0	+6.0
1100 1130	Light	26.8	2.23	28.0	30.0	+2.0	35.0	34.4	-0.6
1130 1200	Light	27.6	2.30	29.0	35.2	+6.2	33.0	36.0	+3.0
1200 1230	Light	27.4	2.30	31.0	32.2	+1.2	33.0	35.8	+2.8
1230 1300	Darkness	26.8	2.22	9.2	17.2	+8.0	5.8	15.0	+9.2
1300 1330	Darkness	26.5	2.08	5.0	4.0	-1.0	1.0	3.4	+2.4
1330 1400	Darkness	28.6	2.01	6.0	5.6	-0.4	6.0	6.0	±0.0
						Σ = +8.4			Σ = +9.4

[a]Absorption minus transpiration

TITLE: CONSUMPTIVE USE OF WATER BY CROPS IN ARIZONA.

LINE PROJECT: SWC 11-gG1 CODE NO.: Ariz.-WCL-23

INTRODUCTION:

See previous Annual Report.

PROCEDURE:

Consumptive-use measurements were made at the following locations in 1961-1962.

1. Cotton - Cotton Research Center.
2. Alfalfa - Mesa Experiment Farm.
3. Sorghum - (Grain and Forage) Double Cropped - Mesa Experiment Farm.
4. Bermuda lawn - U. S. Water Conservation Laboratory.
5. Cole Crops (Cabbage, Broccoli, Cauliflower) - Mesa Experiment Farm.
6. Potatoes - Mesa Experiment Farm.
7. Sweet Corn - Mesa Experiment Farm.
8. Cantaloupes - Mesa Experiment Farm.
9. Grapes - Robert Frye Ranch, Litchfield Park, Arizona.
10. Other vegetables - (Onions, Carrots, Lettuce) - Mesa Experiment Farm.

RESULTS AND DISCUSSION:

Cotton graphs and data will be found under WCL-21. Vegetable crops require frequent early irrigations to germinate seed, maintain stands and aid in placement of tensiometers. Soil moisture sampling was delayed until a definite irrigation schedule was adhered by or until after tensiometers had been placed. Data was then projected back to the planting date. Consumptive and profile use figured in this manner were thought to be closer to the actual use, thus eliminating deep percolation from early irrigations referred to previously.

Irrigation of grapes was handled under much closer management than in previous years. A more normal pattern of water use was found from data collected under these conditions.

Frequent irrigations on cantaloupes and sweet corn during the high production period may have brought about unavoidable deep

percolation, thereby increasing the total consumptive use.

A large amount of stored water and frequent early irrigations may also have caused considerable deep percolation in the alfalfa. This was the first year for consumptive use in alfalfa, and because of the high consumptive use, additional information will be collected at several locations this coming year.

Tables 1 through 5 represent semi-monthly consumptive use and Blaney-Criddle "K" factors. In addition, seasonal "F" and "K" factors are included for each crop.

Figures 1 through 16 show the consumptive use curves for various crops during the growing season. In addition, the percent water use by soil depth is included.

PERSONNEL: Leonard J. Erie.

TABLE 1

15 DAY INTERVAL USE AND "K" VALUES FOR VARIOUS CROPS IN ARIZONA 1962

	COTTON		ALFALFA		SORGHUM (Grain)		SORGHUM (Forage)	
	CU	K	CU	K	CU	K	CU	K
Jan 1-15								
16-31			1.26	.85				
Feb 1-14			3.36	1.63				
15-28			3.64	2.04				
Mar 1-15			4.35	2.13				
16-31			4.96	1.95				
Apr 1-15	.04	.02	5.10	1.65	.08	.07	.05	.05
16-30	.45	.14	5.70	1.76	.90	.28	1.05	.32
May 1-15	.90	.26	6.30	1.76	2.55	.71	2.85	.80
16-31	1.44	.42	7.36	2.10	4.80	1.37	4.96	1.42
Jun 1-15	1.95	.52	7.80	2.04	6.15	1.61	5.70	1.49
16-30	2.85	.71	8.40	2.04	6.60	1.60	5.85	1.42
Jul 1-15	4.05	1.00	8.70	2.09	3.75	.90	4.35	1.05
16-31	5.28	1.16	9.12	2.01	3.20	.71	3.36	.74
Aug 1-15	5.70	1.40	6.30	1.54	2.40	.59	2.40	.59
16-31	5.92	1.38	3.52	.81	4.16	.96	4.96	1.15
Sep 1-15	4.05	1.15	6.00	1.70	5.85	1.66	6.30	1.79
16-30	3.15	.93	5.70	1.66	4.05	1.18	4.80	1.39
Oct 1-15	2.40	.86	4.35	1.54	2.55	.90	3.00	1.10
16-31	1.76	.62	2.88	1.01	1.92	.67	2.08	.73
Nov 1-15	.75	.36	.84	.74	1.35	.56	1.35	.56
16-30	.14	.08			.90	.44	.90	.44
Dec 1-15					.30	.24	.20	.16
16-31								
Total	40.83		105.64*		51.51		54.16	
Seasonal "F"		53.66				54.81		54.81
Seasonal "K"		.76				.94		.99

* Considerable deep percolation up until August 15.

TABLE 2

15 DAY INTERVAL USE AND "K" VALUES FOR VARIOUS CROPS IN ARIZONA 1962

	BERMUDA		CANTALOUPES		SWEET CORN		GRAPES	
	CU	K	CU	K	CU	K	CU	K
Jan 1-15								
16-31								
Feb 1-14								
15-28								
Mar 1-15								
16-31					.15	.06	.18	.35
Apr 1-15			.14	.05	.75	.24	1.05	.34
16-30			.60	.19	1.35	.42	2.70	.83
May 1-15	.90	.43	1.35	.38	4.65	1.30	5.25	1.47
16-31	2.88	.85	3.68	1.05	7.36	2.10	8.96	2.53
Jun 1-15	3.90	1.04	7.95	2.08	8.40	2.20	5.70	1.49
16-30	4.65	1.15	6.45	1.57	5.64	1.71	6.80	1.61
Jul 1-15	5.10	1.26	4.29	1.39			5.25	1.24
16-31	5.76	1.26					.72	.86
Aug 1-15	4.95	1.22						
16-31	4.32	1.01						
Sep 1-15	3.75	1.06						
16-30	3.15	.93						
Oct 1-15	2.55	.81						
16-31								
Nov 1-15								
16-30								
Dec 1-15								
16-31								
Total	41.91		24.46*		28.30*		36.61*	
Seasonal "F"		40.33						
Seasonal "K"		1.04						

* Wet treatment - deep percolation involved.

TABLE 3

15 DAY INTERVAL USE AND "K" VALUES FOR VARIOUS CROPS IN ARIZONA 1962

	LATE CABBAGE		BROCCOLI		CAULIFLOWER		EARLY CABBAGE	
	CU	K	CU	K	CU	K	CU	K
Jan 1-15	1.80	1.07	2.25	1.34	2.25	1.34	1.95	1.16
16-31	1.76	.87	2.40	1.18	1.95	1.04	1.80	.96
Feb 1-14	1.54	.75	1.92	1.00				
15-28	1.40	.79						
Mar 1-15	1.20	.59						
16-31	.36	.40						
Apr 1-15								
16-30								
May 1-15								
16-31								
Jun 1-15								
16-30								
Jul 1-15								
16-31								
Aug 1-15								
16-31								
Sep 1-15	.09	.04	.05	.02	.05	.02	.05	.02
16-30	.45	.14	.23	.07	.30	.09	.30	.09
Oct 1-15	1.05	.37	.90	.32	1.05	.38	1.05	.38
16-31	1.92	.71	2.40	.88	2.56	.94	2.72	1.00
Nov 1-15	3.00	1.48	3.60	1.78	4.20	2.08	3.00	1.48
16-30	2.25	1.20	2.55	1.36	3.45	1.83	2.55	1.35
Dec 1-15	1.95	1.10	2.25	1.27	3.00	1.70	2.25	1.27
16-31	1.92	1.05	2.40	1.31	2.72	1.50	2.24	1.22
Total	20.69		20.95		21.53		17.91	
Seasonal "F"		28.83		23.96		21.89		21.89
Seasonal "K"		.72		.87		.98		.82

TABLE 4

15 DAY INTERVAL USE AND "K" VALUES FOR VARIOUS CROPS IN ARIZONA 1962

	DRY ONIONS		LETTUCE		GREEN ONIONS		CARROTS	
	CU	K	CU	K	CU	K	CU	K
Jan 1-15	.60	.36			2.10	1.25	1.65	.98
16-31	.96	.47			.48	1.45	1.76	.87
Feb 1-14	1.12	.54					1.26	.61
15-28	1.54	.87					.98	.55
Mar 1-15	3.30	1.62					.60	.29
16-31	5.12	2.02					.06	.07
Apr 1-15	6.60	2.14						
16-30	5.70	1.76						
May 1-15	3.63	1.34						
16-31								
Jun 1-15								
16-30								
Jul 1-15								
16-31								
Aug 1-15								
16-31								
Sep 1-15			.09	.04	.04	.02	.09	.04
16-30			.30	.09	.30	.09	.60	.19
Oct 1-15			1.05	.37	.90	.32	1.35	.48
16-31	.01	.01	2.40	.88	3.04	1.12	2.56	.93
Nov 1-15	.12	.06	1.95	.97	2.85	1.41	3.00	1.48
16-30	.15	.08	1.80	.96	2.40	1.28	2.10	1.12
Dec 1-15	.30	.17	1.65	.93	1.80	1.02	1.65	.93
16-31	.48	.26	1.40	.87	1.76	.96	1.60	.87
Total	29.63		10.64		15.67		19.26	
Seasonal "F"		29.75		18.11		20.34		28.83
Seasonal "K"		1.0		.59		.77		.67

TABLE 5

15 DAY INTERVAL USE AND "K" VALUES FOR VARIOUS CROPS IN ARIZONA 1962

		POTATOES	
		CU	K
Jan	1-15		
	16-31		
Feb	1-14		
	15-28	.07	.04
Mar	1-15	.30	.15
	16-31	.96	.38
Apr	1-15	3.90	1.26
	16-30	5.55	1.71
May	1-15	6.90	1.94
	16-31	6.40	1.83
Jun	1-15	4.20	1.10
	16-30	2.64	.80
Jul	1-15		
	16-31		
Aug	1-15		
	16-31		
Sep	1-15		
	16-30		
Oct	1-15		
	16-31		
Nov	1-15		
	16-30		
Dec	1-15		
	16-31		
Total		30.92	
Seasonal "F"			26.89
Seasonal "K"			1.15

Figure 1.

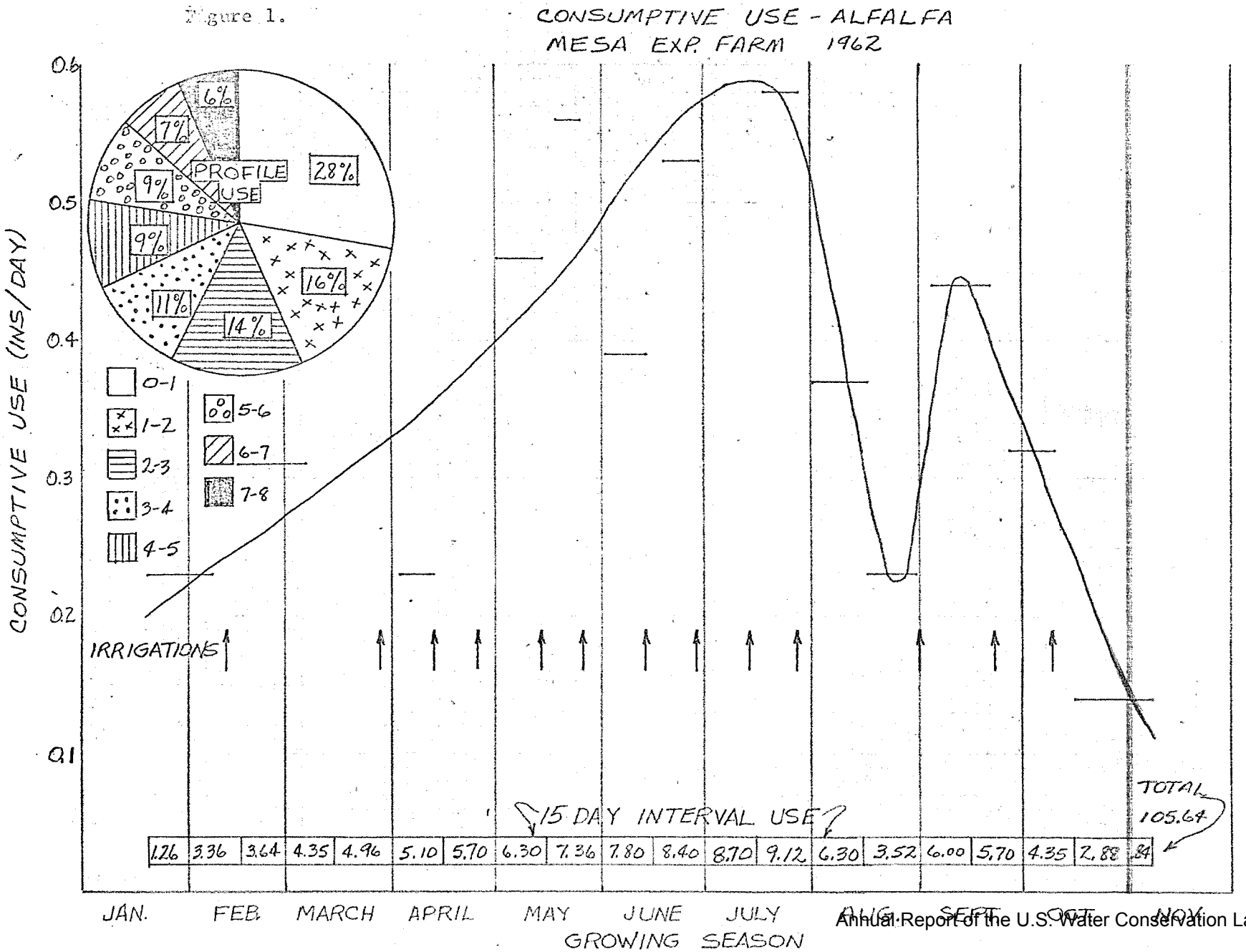
CONSUMPTIVE USE - ALFALFA
MESA EXP. FARM 1962
CONSUMPTIVE USE (INS/DAY)
0.6
0.5
0.4
0.3
0.2
0.1
PROFILE USE
6%
7%
9%
9%
11%
14%
16%
28%
0-1
1-2
2-3
3-4
4-5
5-6
6-7
7-8
IRRIGATIONS
15 DAY INTERVAL USE
1.26
3.36
3.64
4.35
4.96
5.10
5.70
6.30
7.36
7.80
8.40
8.70
9.12
6.30
3.52
6.00
5.70
4.35
2.88
.84
TOTAL
105.64
JAN.
FEB.
MARCH
APRIL
MAY
JUNE
JULY
AUG.
SEPT.
OCT.
NOV.
GROWING SEASON

Figure 2.

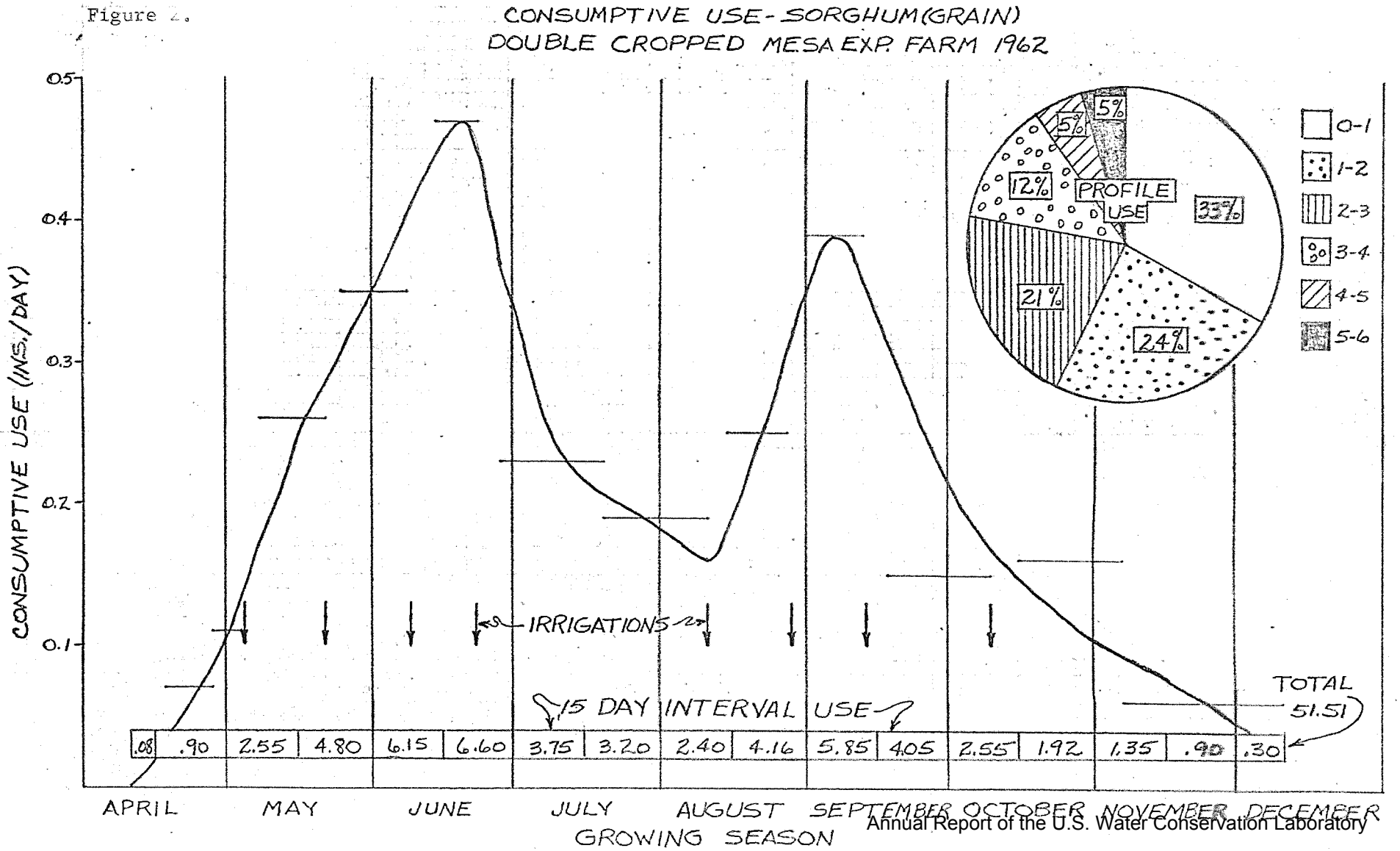
CONSUMPTIVE USE-SORGHUM(GRAIN)
DOUBLE CROPPED MESA EXP. FARM 1962
CONSUMPTIVE USE (INS./DAY)
0.5
0.4
0.3
0.2
0.1
IRRIGATIONS
15 DAY INTERVAL USE
.08 .90 2.55 4.80 6.15 6.60 3.75 3.20 2.40 4.16 5.85 4.05 2.55 1.92 1.35 .90 .30
TOTAL 51.51
APRIL
MAY
JUNE
JULY
AUGUST
SEPTEMBER
OCTOBER
NOVEMBER
DECEMBER
GROWING SEASON
PROFILE USE
5%
5%
12%
33%
21%
24%
0-1
1-2
2-3
3-4
4-5
5-6

Figure 3.

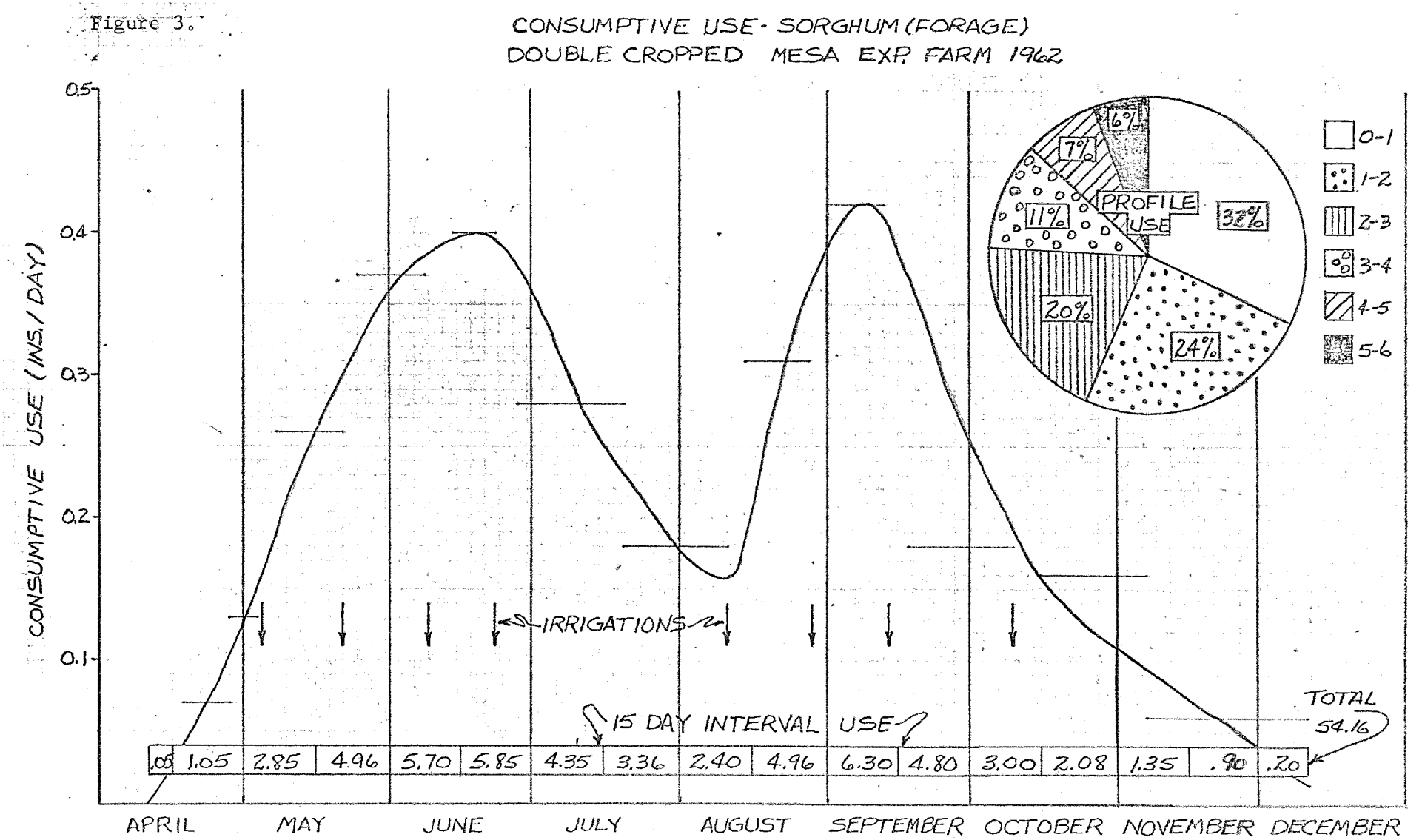
CONSUMPTIVE USE - SORGHUM (FORAGE)
DOUBLE CROPPED MESA EXP. FARM 1962
CONSUMPTIVE USE (INS./DAY)
0.5
0.4
0.3
0.2
0.1
IRRIGATIONS
15 DAY INTERVAL USE
TOTAL 54.16
.05 1.05 2.85 4.96 5.70 5.85 4.35 3.36 2.40 4.96 6.30 4.80 3.00 2.08 1.35 .90 .20
APRIL
MAY
JUNE
JULY
AUGUST
SEPTEMBER
OCTOBER
NOVEMBER
DECEMBER
GROWING SEASON
PROFILE USE
6%
7%
11%
32%
20%
24%
0-1
1-2
2-3
3-4
4-5
5-6

Figure 4.

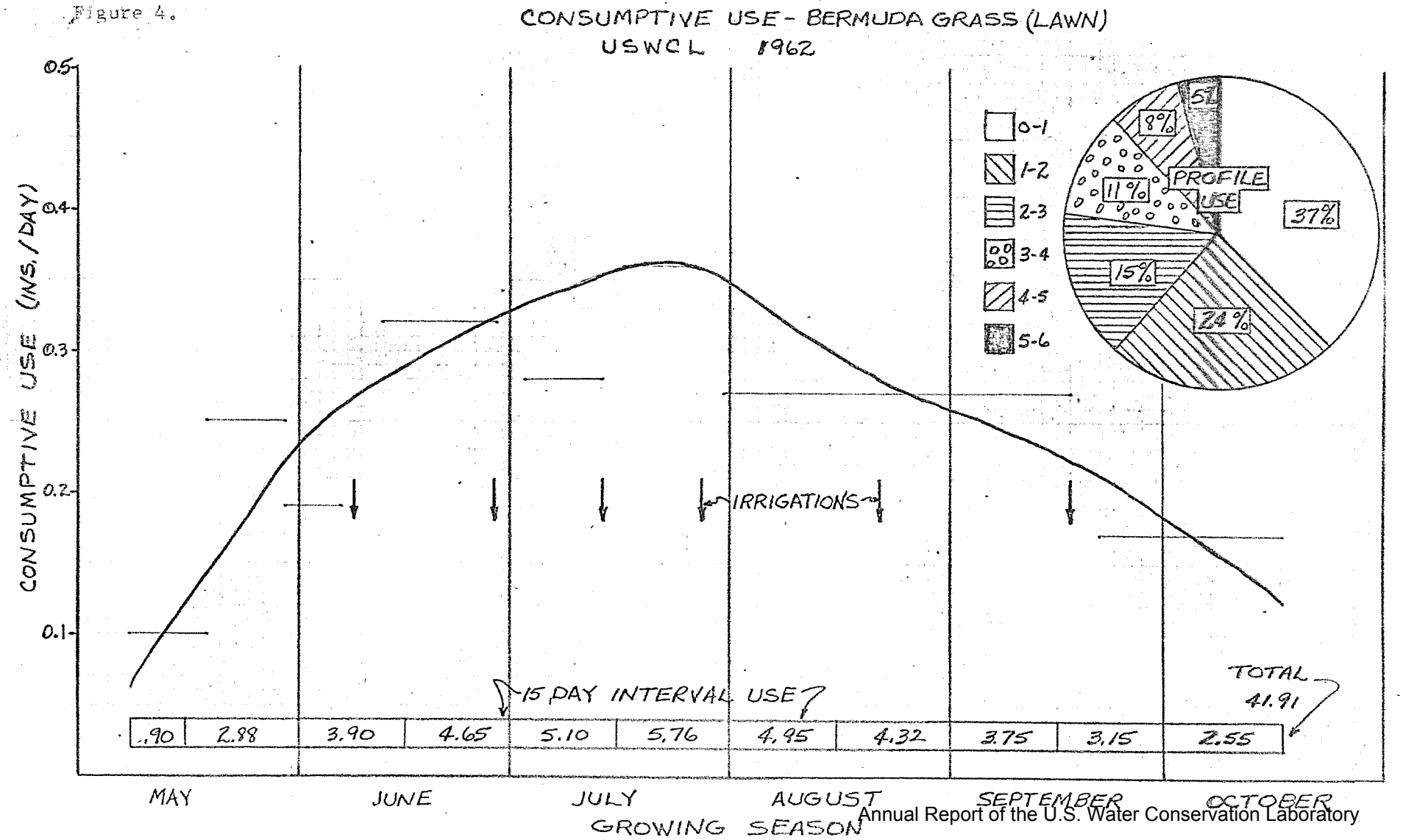
CONSUMPTIVE USE - BERMUDA GRASS (LAWN)
USWCL 1962
CONSUMPTIVE USE (INS./DAY)
0.5
0.4
0.3
0.2
0.1
0-1
1-2
2-3
3-4
4-5
5-6
PROFILE USE
5%
8%
11%
37%
15%
24%
IRRIGATIONS
15 DAY INTERVAL USE
TOTAL 41.91
.90
2.88
3.90
4.65
5.10
5.76
4.95
4.32
3.75
3.15
2.55
MAY
JUNE
JULY
AUGUST
SEPTEMBER
OCTOBER
GROWING SEASON

Figure 5.

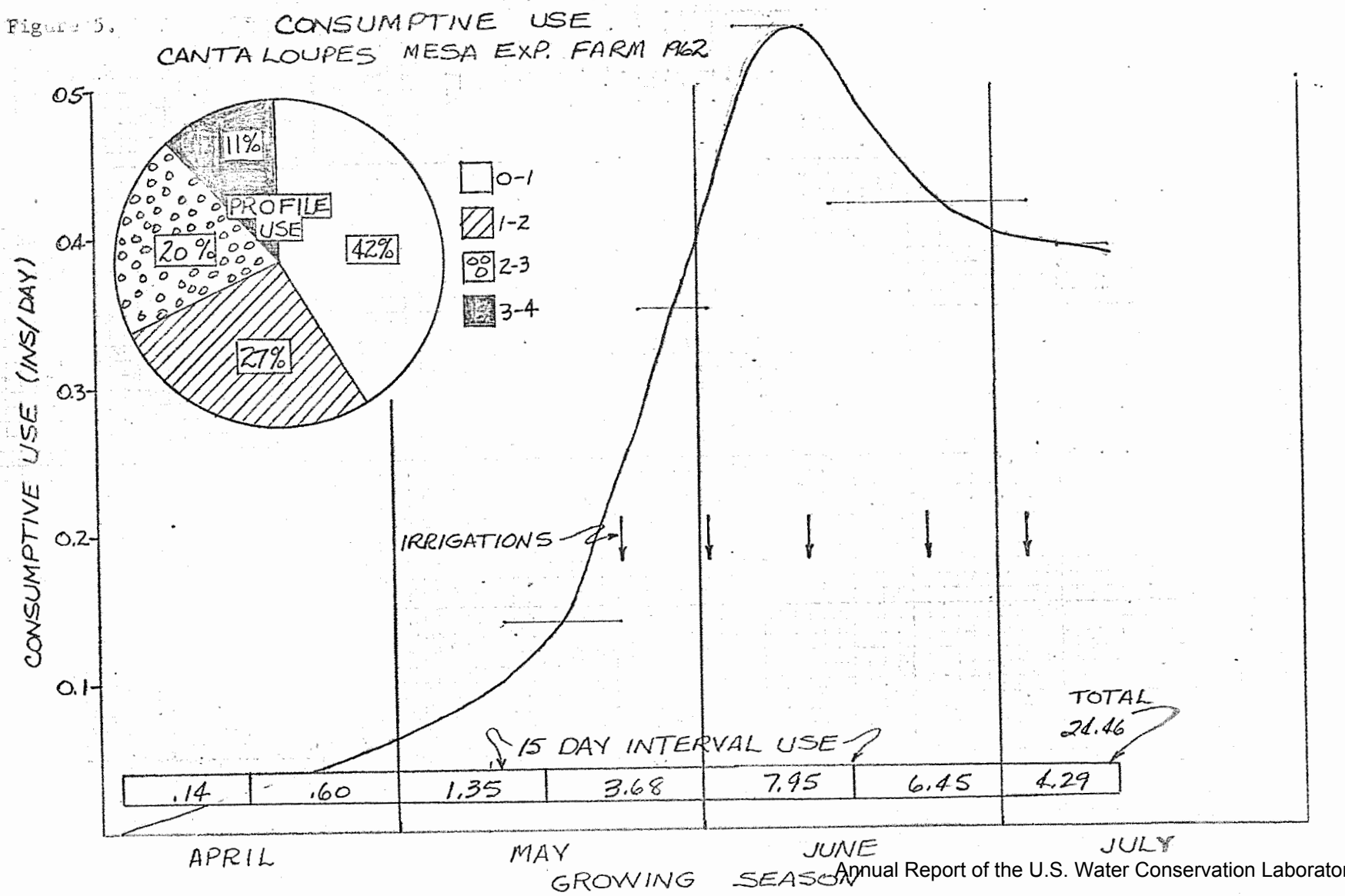
CONSUMPTIVE USE
CANTALOUPES MESA EXP. FARM 1962
CONSUMPTIVE USE (INS/DAY)
0.5
0.4
0.3
0.2
0.1
PROFILE USE
11%
20%
42%
27%
0-1
1-2
2-3
3-4
IRRIGATIONS
15 DAY INTERVAL USE
TOTAL
24.46
.14
.60
1.35
3.68
7.95
6.45
4.29
APRIL
MAY
JUNE
JULY
GROWING SEASON

Figure 6.

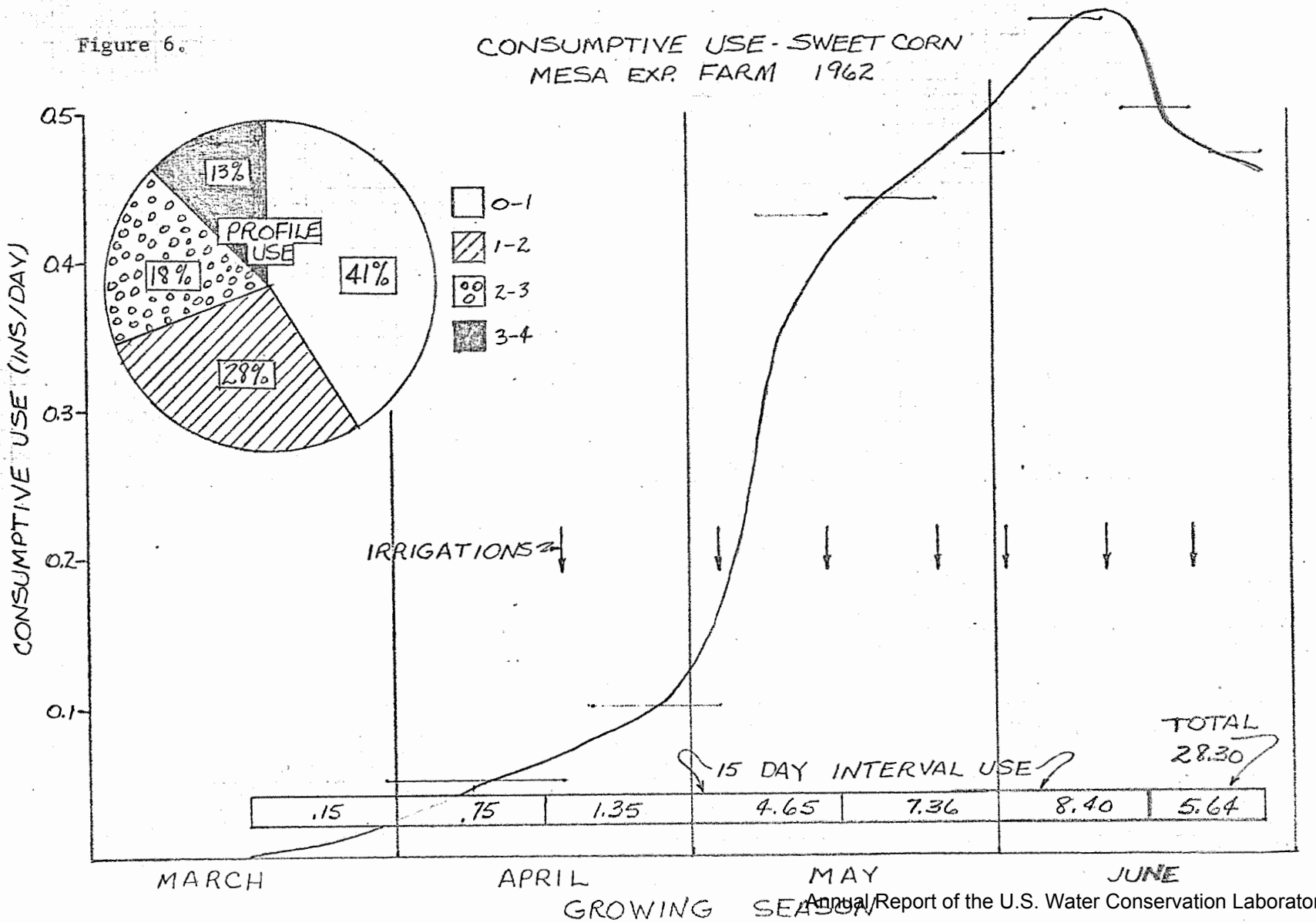
CONSUMPTIVE USE - SWEET CORN
MESA EXP. FARM 1962
CONSUMPTIVE USE (INS/DAY)
0.5
0.4
0.3
0.2
0.1
13%
PROFILE USE
18%
41%
28%
0-1
1-2
2-3
3-4
IRRIGATIONS
15 DAY INTERVAL USE
TOTAL 28.30
.15
.75
1.35
4.65
7.36
8.40
5.64
MARCH
APRIL
MAY
JUNE
GROWING SEASON

Figure 7.

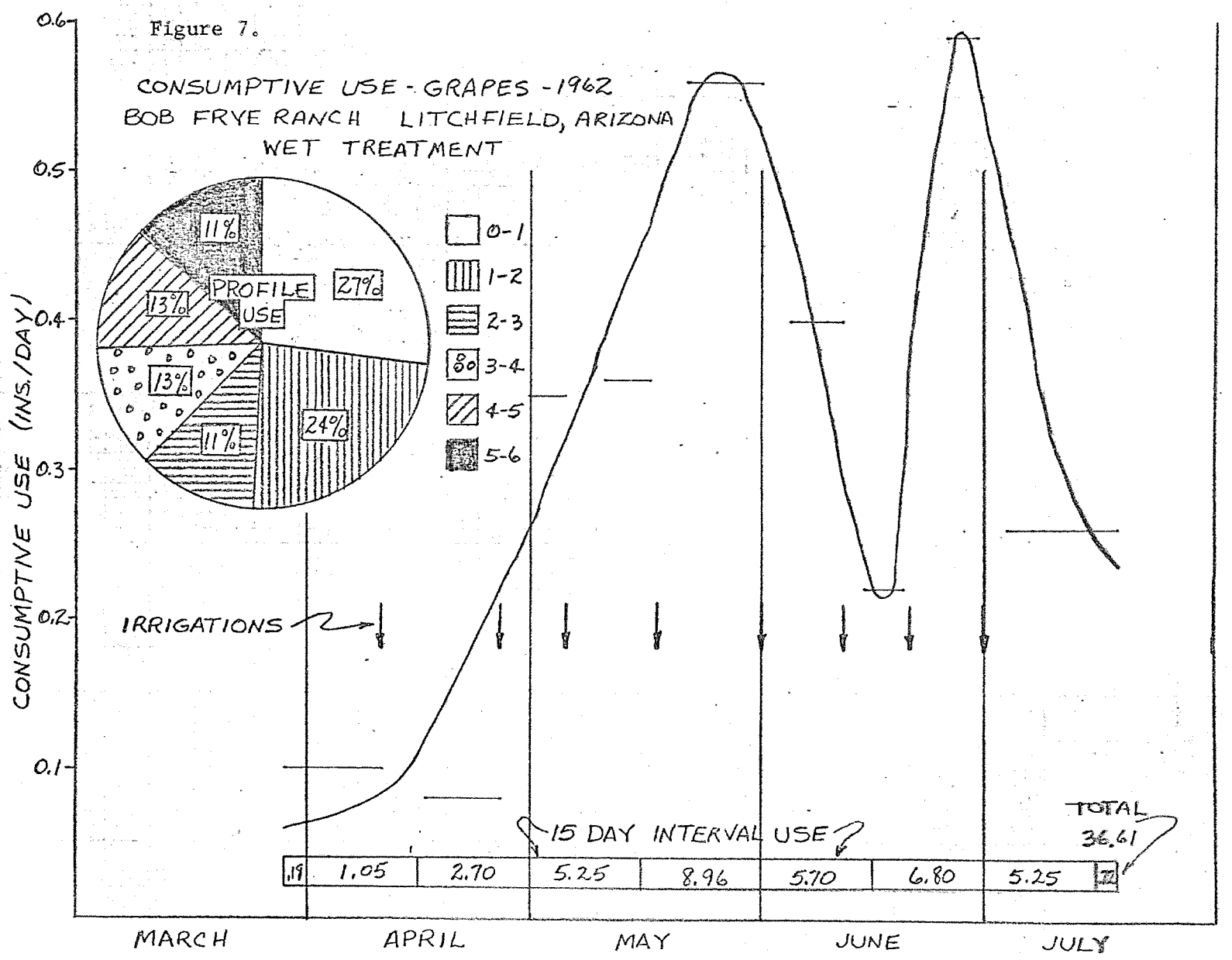
CONSUMPTIVE USE - GRAPES - 1962
BOB FRYE RANCH LITCHFIELD, ARIZONA
WET TREATMENT
CONSUMPTIVE USE (INS./DAY)
0.6
0.5
0.4
0.3
0.2
0.1
11%
13%
PROFILE USE
27%
13%
11%
24%
0-1
1-2
2-3
3-4
4-5
5-6
IRRIGATIONS
15 DAY INTERVAL USE
.19
1.05
2.70
5.25
8.96
5.70
6.80
5.25
.72
TOTAL
36.61
MARCH
APRIL
MAY
JUNE
JULY
GROWING SEASON

Figure 8.

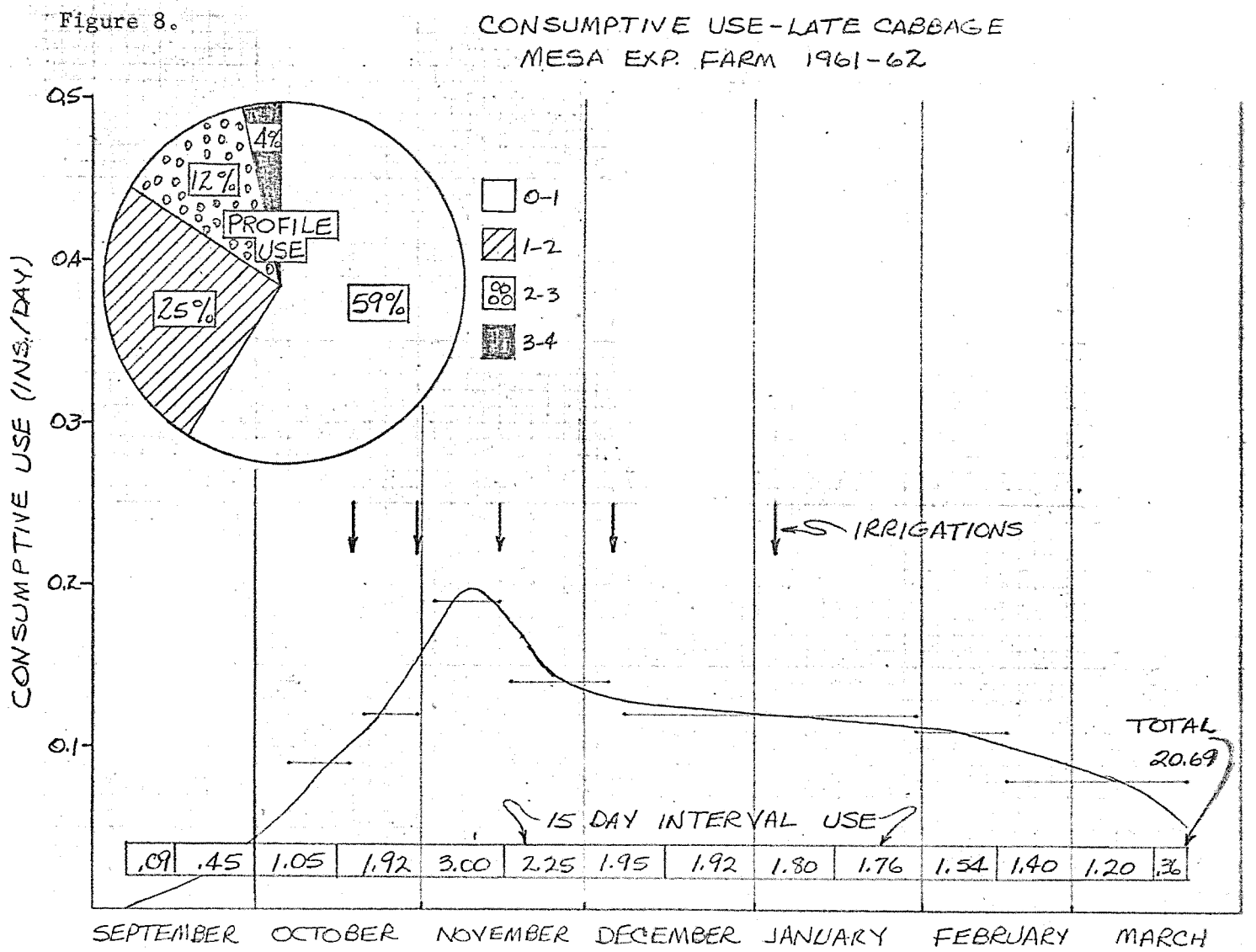
CONSUMPTIVE USE - LATE CABBAGE
MESA EXP. FARM 1961-62
CONSUMPTIVE USE (INS./DAY)
0.5
0.4
0.3
0.2
0.1
4%
12%
PROFILE USE
25%
59%
0-1
1-2
2-3
3-4
IRRIGATIONS
TOTAL 20.69
15 DAY INTERVAL USE
.09
.45
1.05
1.92
3.00
2.25
1.95
1.92
1.80
1.76
1.54
1.40
1.20
.36
SEPTEMBER
OCTOBER
NOVEMBER
DECEMBER
JANUARY
FEBRUARY
MARCH
GROWING SEASON

Figure 9.

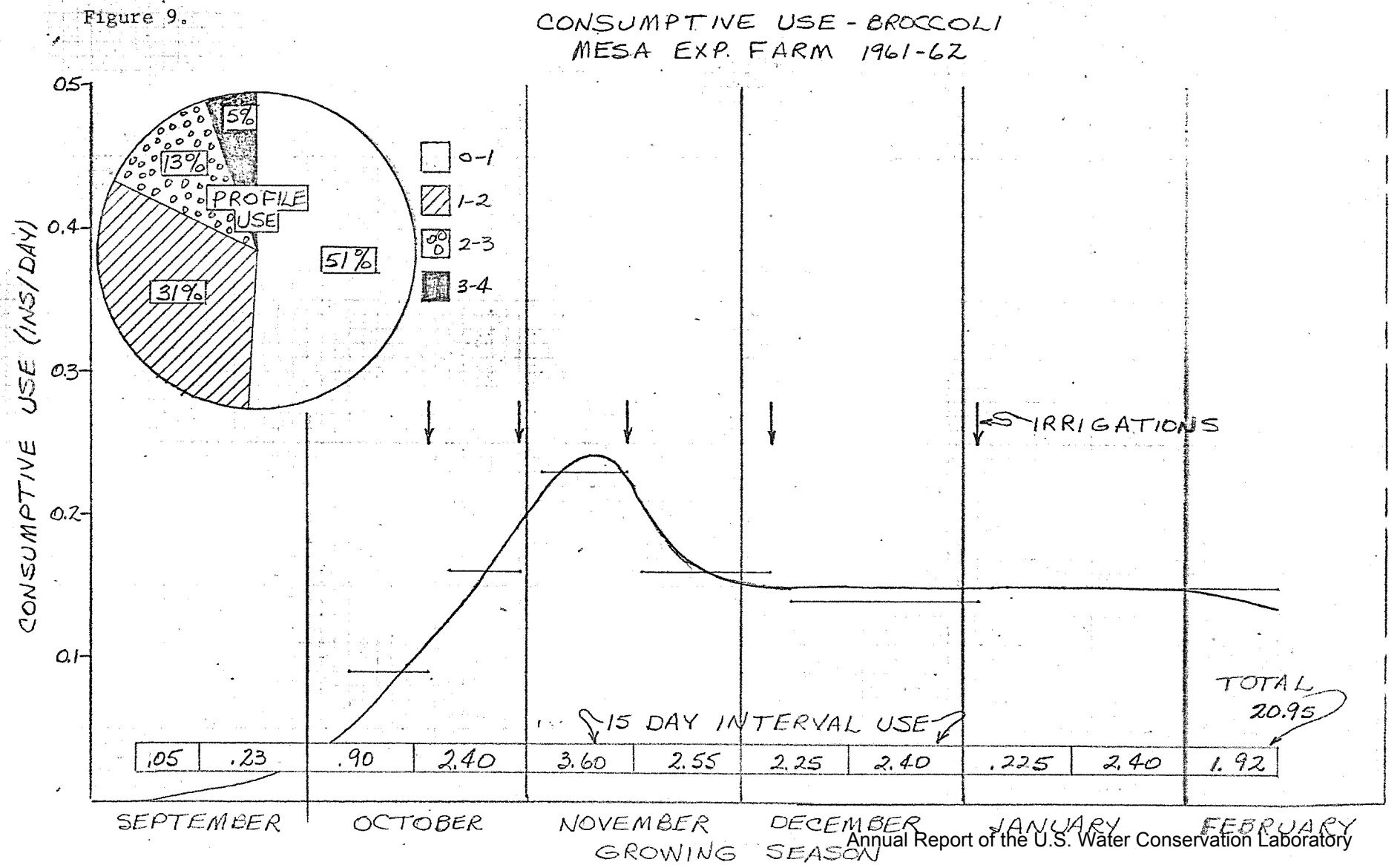
CONSUMPTIVE USE - BROCCOLI
MESA EXP. FARM 1961-62
CONSUMPTIVE USE (INS/DAY)
0.5
0.4
0.3
0.2
0.1
5%
13%
PROFILE USE
51%
31%
0-1
1-2
2-3
3-4
IRRIGATIONS
15 DAY INTERVAL USE
TOTAL 20.95
.105
.23
.90
2.40
3.60
2.55
2.25
2.40
.225
2.40
1.92
SEPTEMBER
OCTOBER
NOVEMBER
DECEMBER
JANUARY
FEBRUARY
GROWING SEASON

Figure 10.

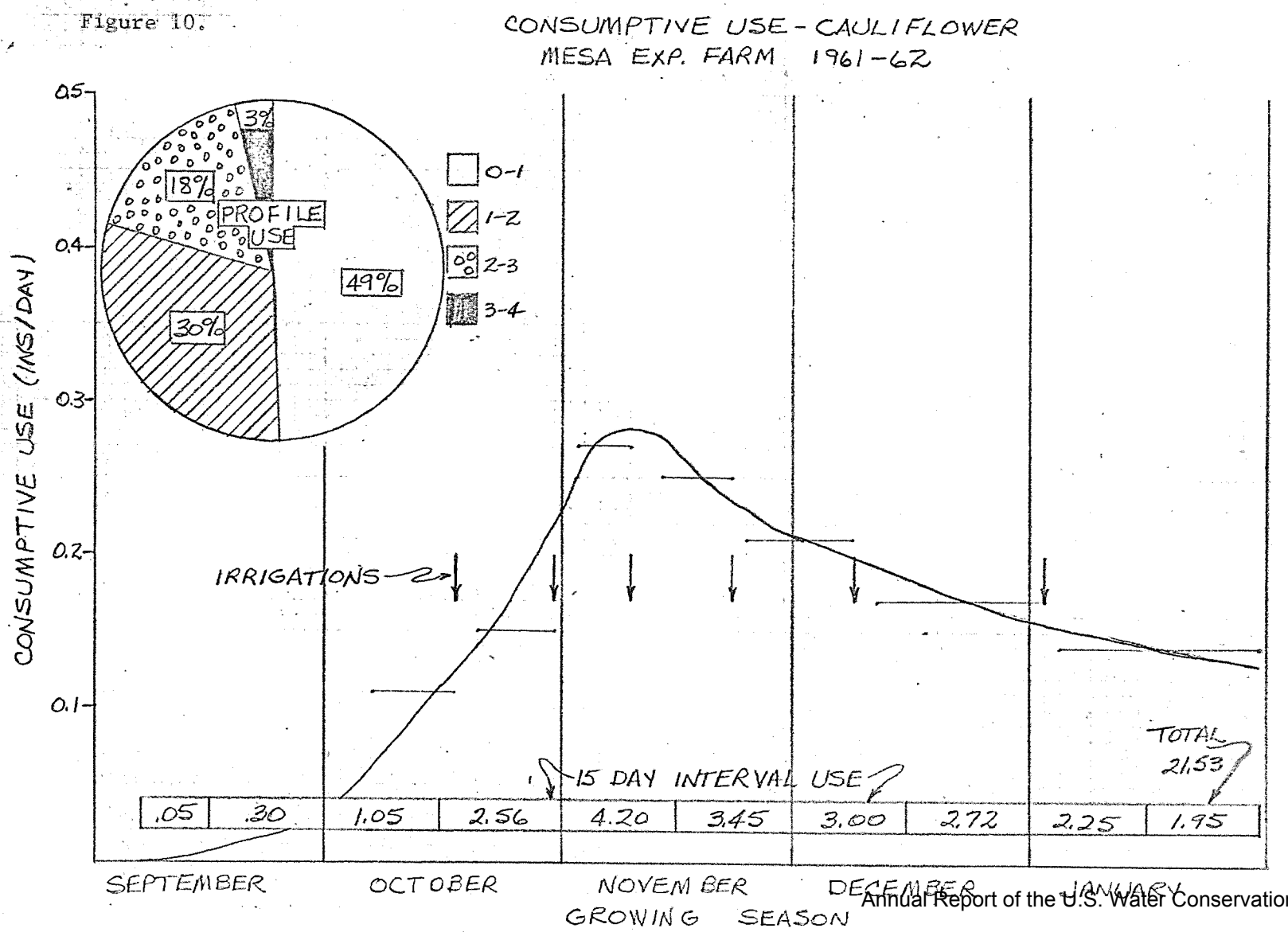

Annual Report of the U.S. Water Conservation Laboratory

Figure 11.

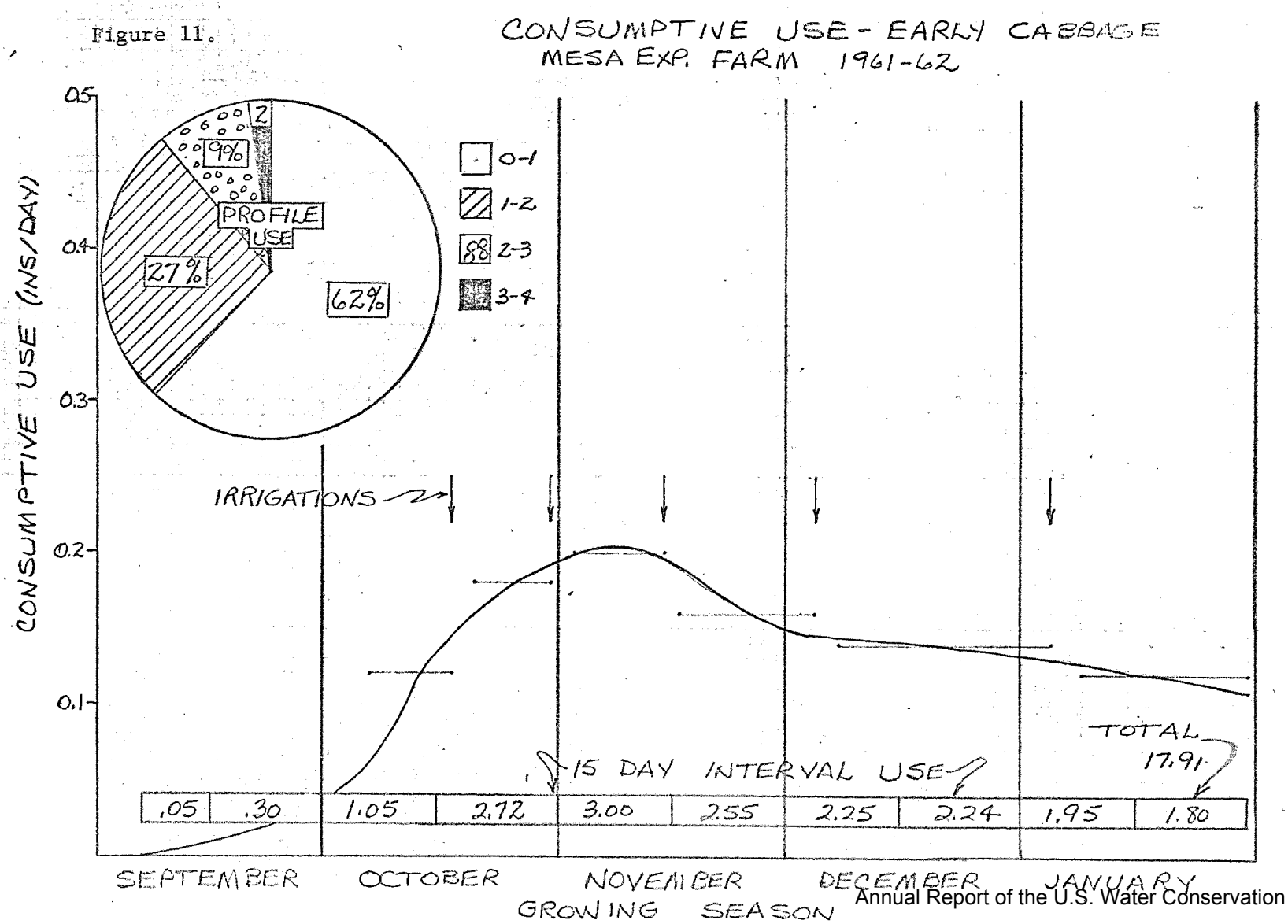
CONSUMPTIVE USE - EARLY CABBAGE
MESA EXP. FARM 1961-62
CONSUMPTIVE USE (INS/DAY)
0.5
0.4
0.3
0.2
0.1
2
9%
PROFILE USE
27%
62%
0-1
1-2
2-3
3-4
IRRIGATIONS
15 DAY INTERVAL USE
TOTAL 17.91
.05
.30
1.05
2.72
3.00
2.55
2.25
2.24
1.95
1.80
SEPTEMBER
OCTOBER
NOVEMBER
DECEMBER
JANUARY
GROWING SEASON

Figure 12.

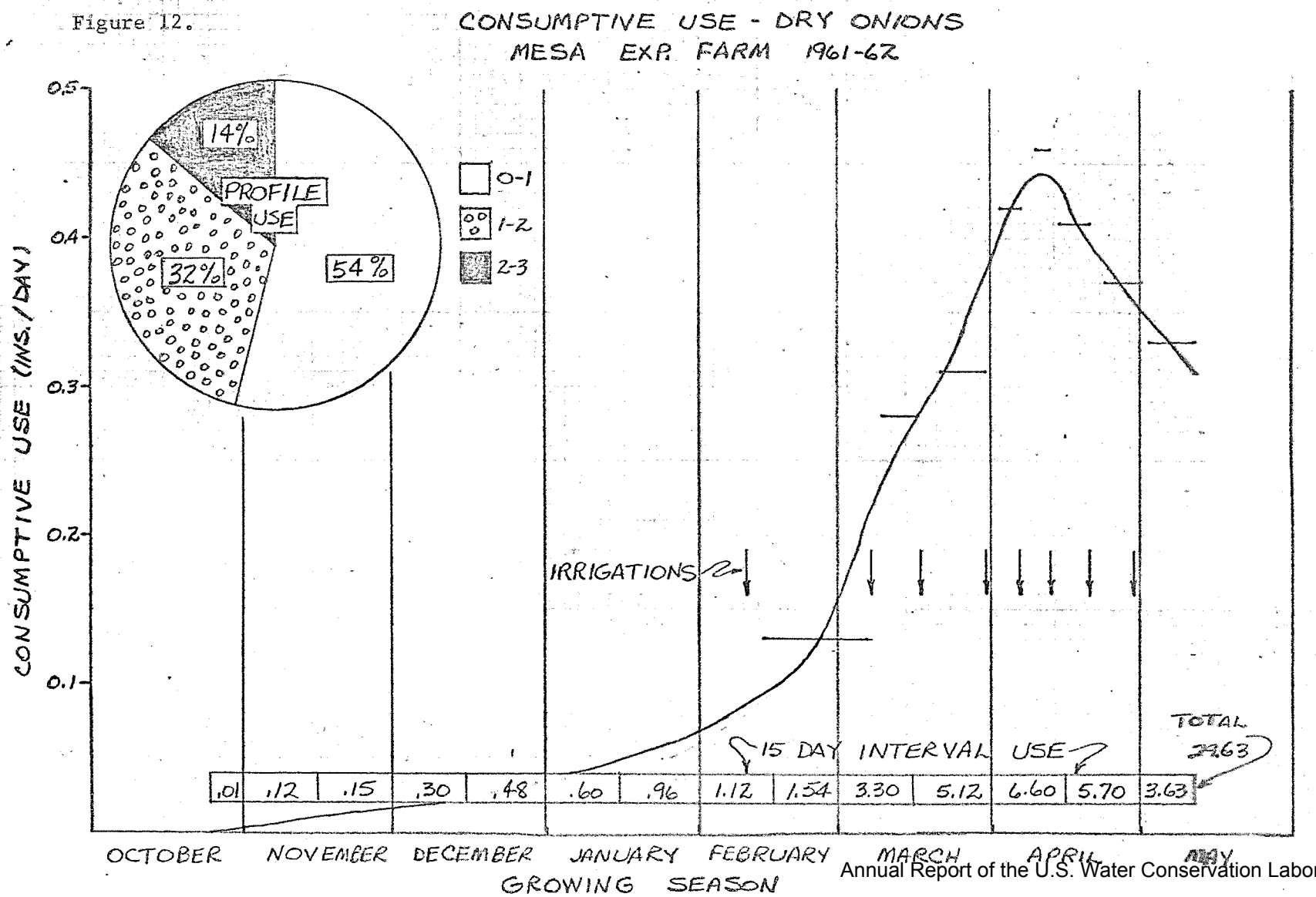
CONSUMPTIVE USE - DRY ONIONS
MESA EXP. FARM 1961-62
CONSUMPTIVE USE (INS./DAY)
0.5
0.4
0.3
0.2
0.1
14%
PROFILE USE
32%
54%
0-1
1-2
2-3
IRRIGATIONS
15 DAY INTERVAL USE
TOTAL 29.63
.01
.12
.15
.30
.48
.60
.96
1.12
1.54
3.30
5.12
6.60
5.70
3.63
OCTOBER
NOVEMBER
DECEMBER
JANUARY
FEBRUARY
MARCH
APRIL
MAY
GROWING SEASON

Figure 13.

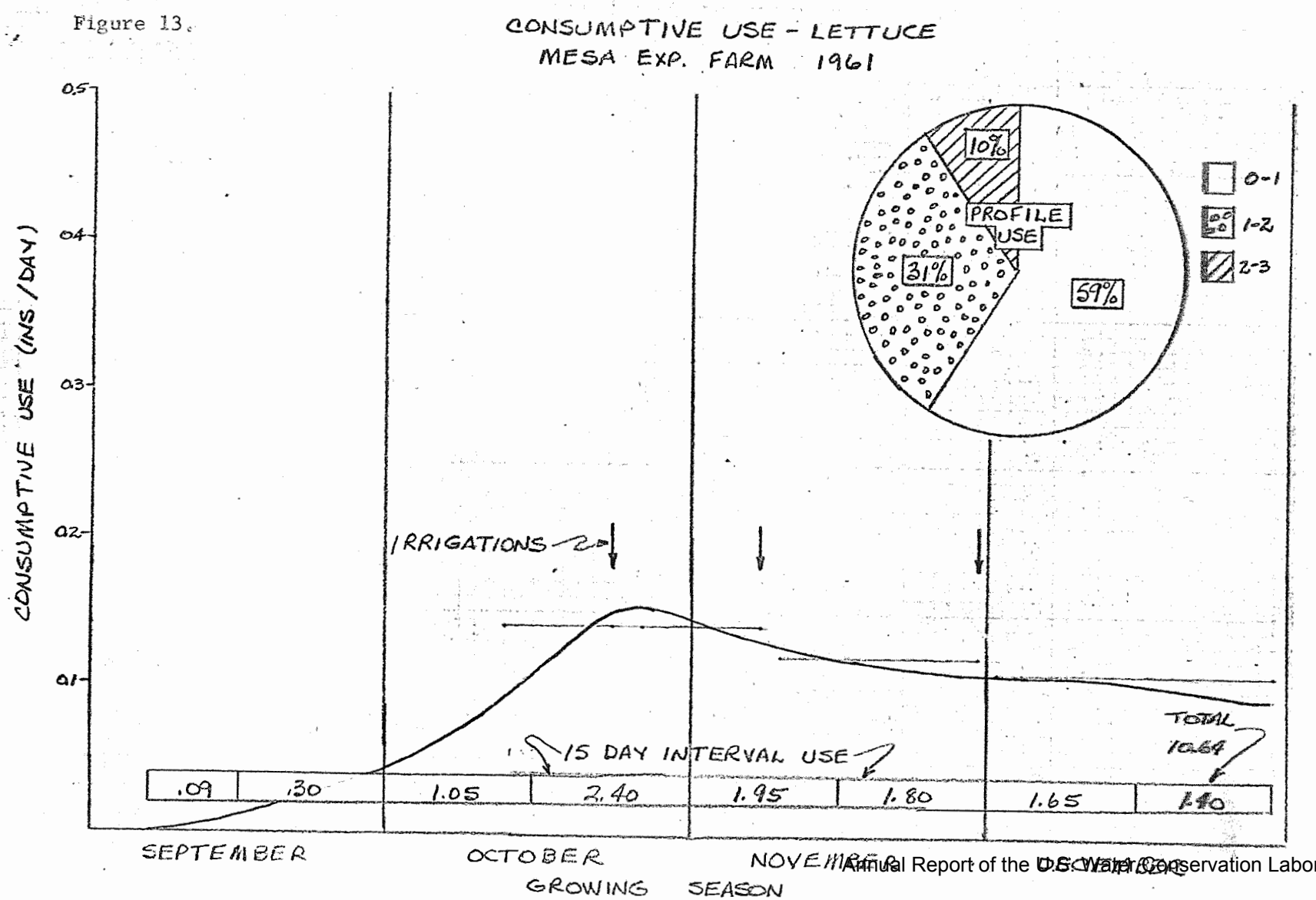
CONSUMPTIVE USE - LETTUCE
MESA EXP. FARM 1961
CONSUMPTIVE USE (INS/DAY)
0.5
0.4
0.3
0.2
0.1
IRRIGATIONS
15 DAY INTERVAL USE
TOTAL
10.64
.09
.30
1.05
2.40
1.95
1.80
1.65
1.40
SEPTEMBER
OCTOBER
NOVEMBER
GROWING SEASON
10%
PROFILE USE
31%
59%
0-1
1-2
2-3

Figure 14.

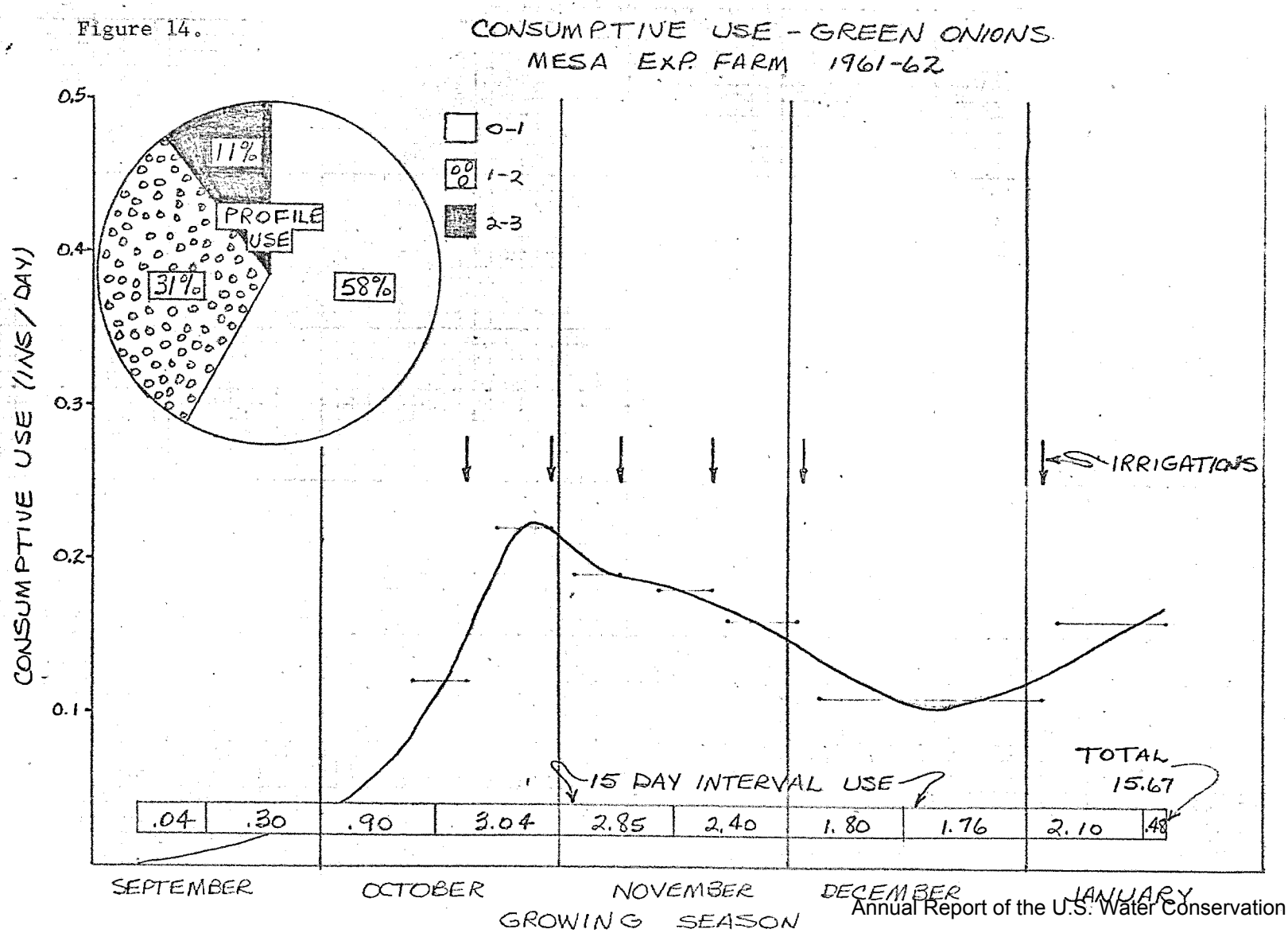
CONSUMPTIVE USE - GREEN ONIONS
MESA EXP. FARM 1961-62
CONSUMPTIVE USE (INS / DAY)
0.5
0.4
0.3
0.2
0.1
0-1
1-2
2-3
11%
PROFILE USE
31%
58%
IRRIGATIONS
15 DAY INTERVAL USE
TOTAL 15.67
.04
.30
.90
3.04
2.85
2.40
1.80
1.76
2.10
.48
SEPTEMBER
OCTOBER
NOVEMBER
DECEMBER
JANUARY
GROWING SEASON

Figure 15.

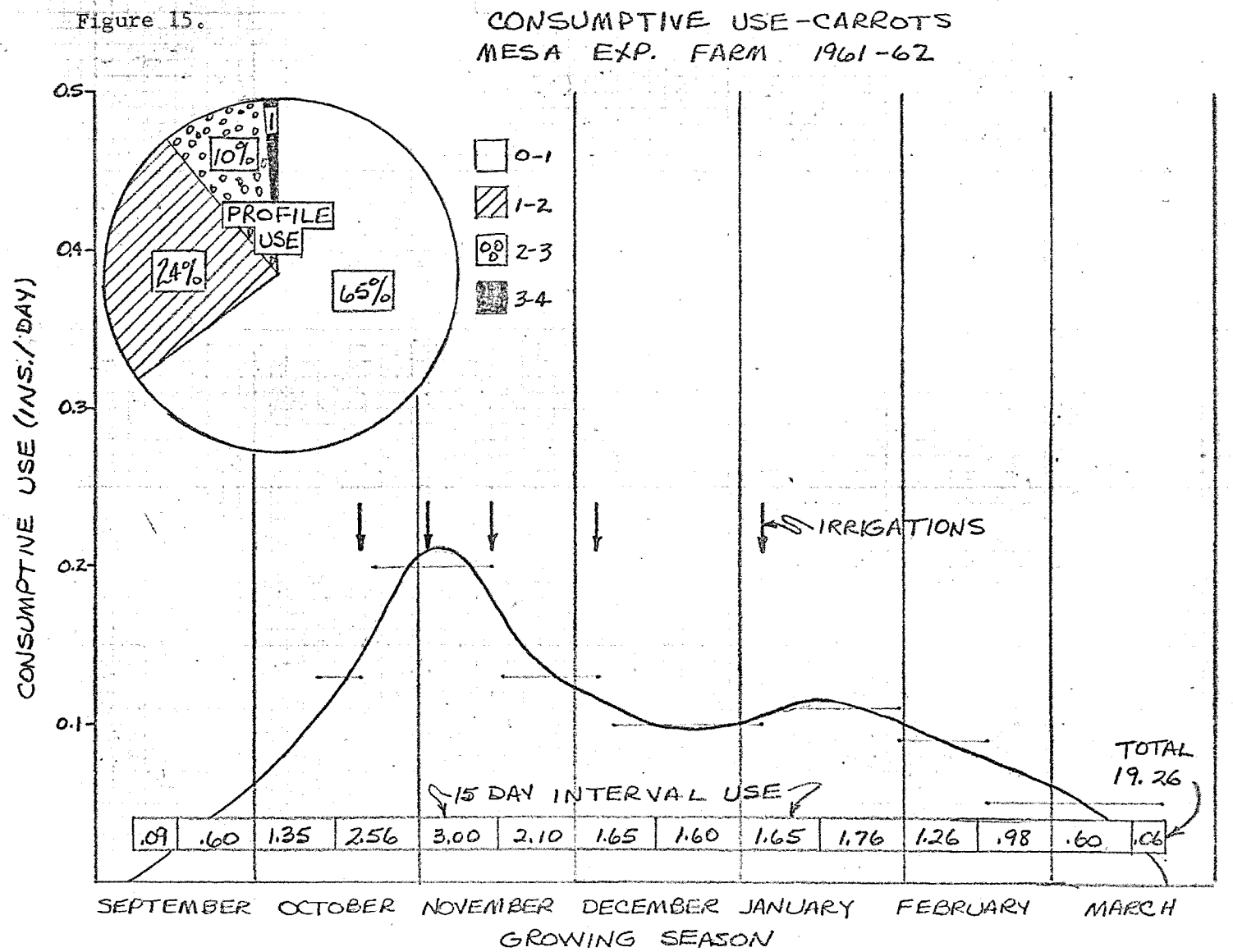
CONSUMPTIVE USE-CARROTS
MESA EXP. FARM 1961-62
CONSUMPTIVE USE (INS./DAY)
0.5
0.4
0.3
0.2
0.1
0-1
1-2
2-3
3-4
10%
PROFILE USE
24%
65%
IRRIGATIONS
15 DAY INTERVAL USE
.09
.60
1.35
2.56
3.00
2.10
1.65
1.60
1.65
1.76
1.26
.98
.60
.06
TOTAL 19.26
SEPTEMBER
OCTOBER
NOVEMBER
DECEMBER
JANUARY
FEBRUARY
MARCH
GROWING SEASON

Figure 16.

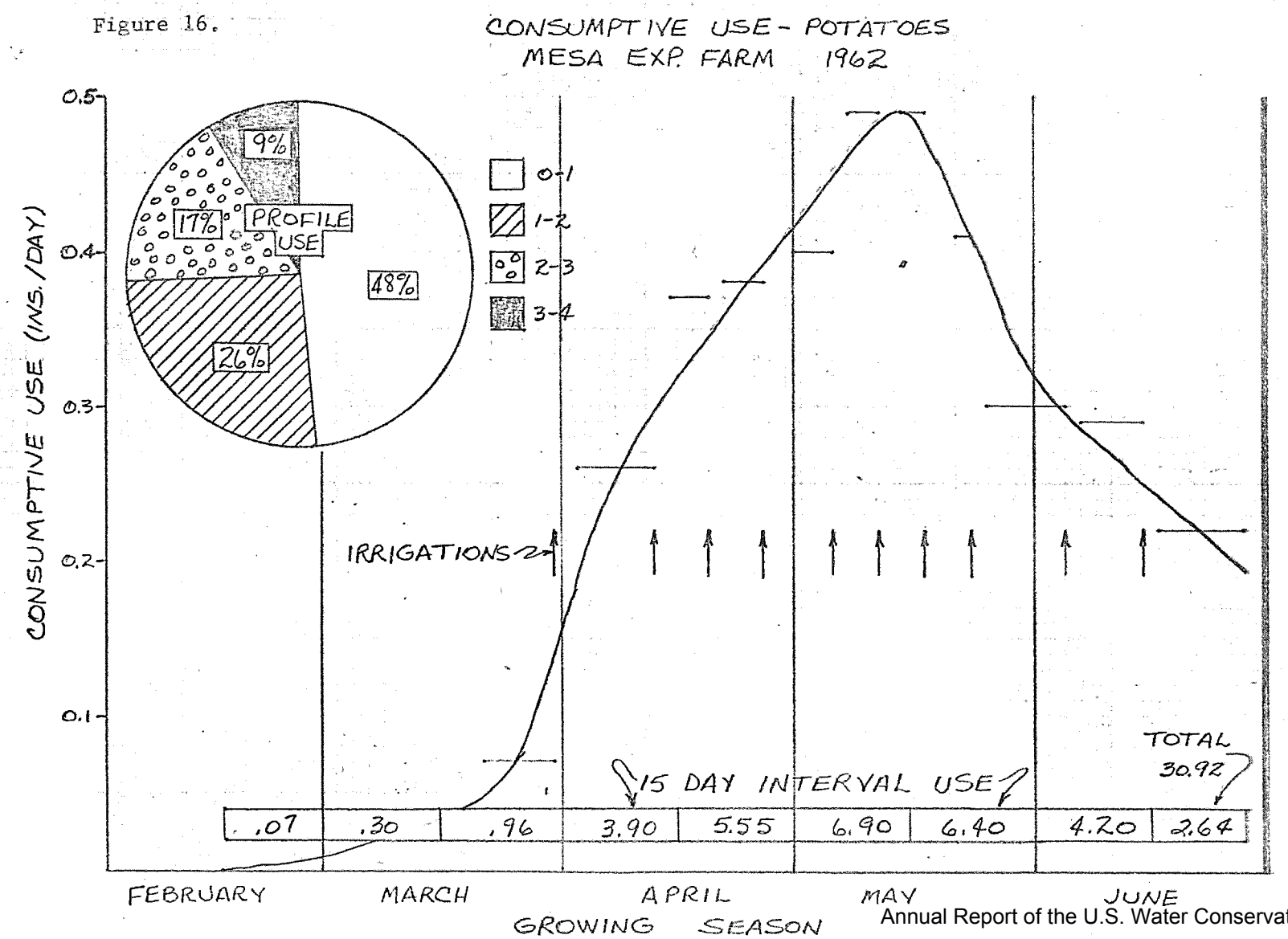
CONSUMPTIVE USE - POTATOES
MESA EXP. FARM 1962
CONSUMPTIVE USE (INS./DAY)
0.5
0.4
0.3
0.2
0.1
9%
17%
PROFILE USE
48%
26%
0-1
1-2
2-3
3-4
IRRIGATIONS
15 DAY INTERVAL USE
TOTAL 30.92
.07
.30
.96
3.90
5.55
6.90
6.40
4.20
2.64
FEBRUARY
MARCH
APRIL
MAY
JUNE
GROWING SEASON

TITLE: ANALYTICAL LABORATORY

PROGRESS:

The work performed by the Analytical Laboratory during 1962 included 598 chemical and physical analyses of 243 soil samples and 355 water samples. A breakdown of the analyses is given in Table 1.

Table 1. Analyses performed by Analytical Laboratory 1962.

Analyses	Number of determinations
Particle size	
a. Hydrometer	142
Moisture characteristics	
a. Pressure cooker	55
b. Pressure membrane	22
pH and saturated conductivity	172
Calcium and Magnesium	376
Sodium and Potassium	178
Carbonate and Bicarbonate	8
Chloride and Sulfate	73
Cation exchange capacity	6
Surface area	15
Nitrate	4
Lithium	12

Techniques for determinations of Lithium in water, and two dyes, Pontacyl Pink and Rhodamine B were investigated using the Beckman Spectrophotometer. Satisfactory results were obtained and measurements of these tracers are now standard laboratory procedures.

PERSONNEL: J. Bennett Miller, F. S. Nakayama, Ray D. Jackson

TITLE: RADIOISOTOPE STORAGE FACILITY.

In July 1962 a radioisotope storage facility was designed and built that would be used to store our sealed radioactive materials, namely, the radium beryllium sources for the neutron probe and the Cs^{137} source for the gamma densitometer probe. This facility is located in Building 2 and is now designated as Room 206.

A 4- × 10- × 2-foot deep volume was excavated in the southeast corner of Room 206. Eleven storage wells were placed in this area and the remaining space was filled with a high density concrete (see Figure 1).

The storage wells (Figure 2) were constructed from 1/4-inch thick cast iron pipe. All welded joints were made moisture-proof. The upper or expanded parts of the wells were also made from 1/4-inch cast iron pipe with moisture-proof welded joints. Lids for the wells were formed from lead to fit snugly in this upper, enlarged portion of the wells. The concrete used to fill in between the wells has a density of 2.5 grams per cubic centimeter. A ceiling to floor partition was installed around the storage area using 2- × 4-inch studs on 16-inch centers with sheet rock on either side. The finished cement floor was coated with a concrete sealer. The door to the storage facility is kept locked at all times.

An exhaust fan with a capacity of approximately 100 cfm was installed in the ceiling. This exhausts the air in the room to the outside of the building. An inlet grill with a fiberglass filter is located in the door; the fan is kept running continuously.

The storage area was monitored with a survey meter when there was a total of 10 millicuries of radium-beryllium sealed sources and 5 millicuries of a Cs^{137} source in four of the storage wells. The highest radiation value obtained was 0.5 milliroentgen per hour when the detector was placed directly on the concrete and on the lead lids. At a distance of 1 foot from the lids, or where the partition is located, the radiation level is less than 0.1 milliroentgen per hour. This value is well below the maximum radiation level permitted in unre stricted areas as stated in the USDA Radiological Safety Handbook of

July 1961. One well is our maximum storage unit and our calculations show that it can store approximately 100 mc without any radiation hazard to people working in the area.

PERSONNEL: R. J. Reginato, F. S. Nakayama, C. H. M. van Bavel.

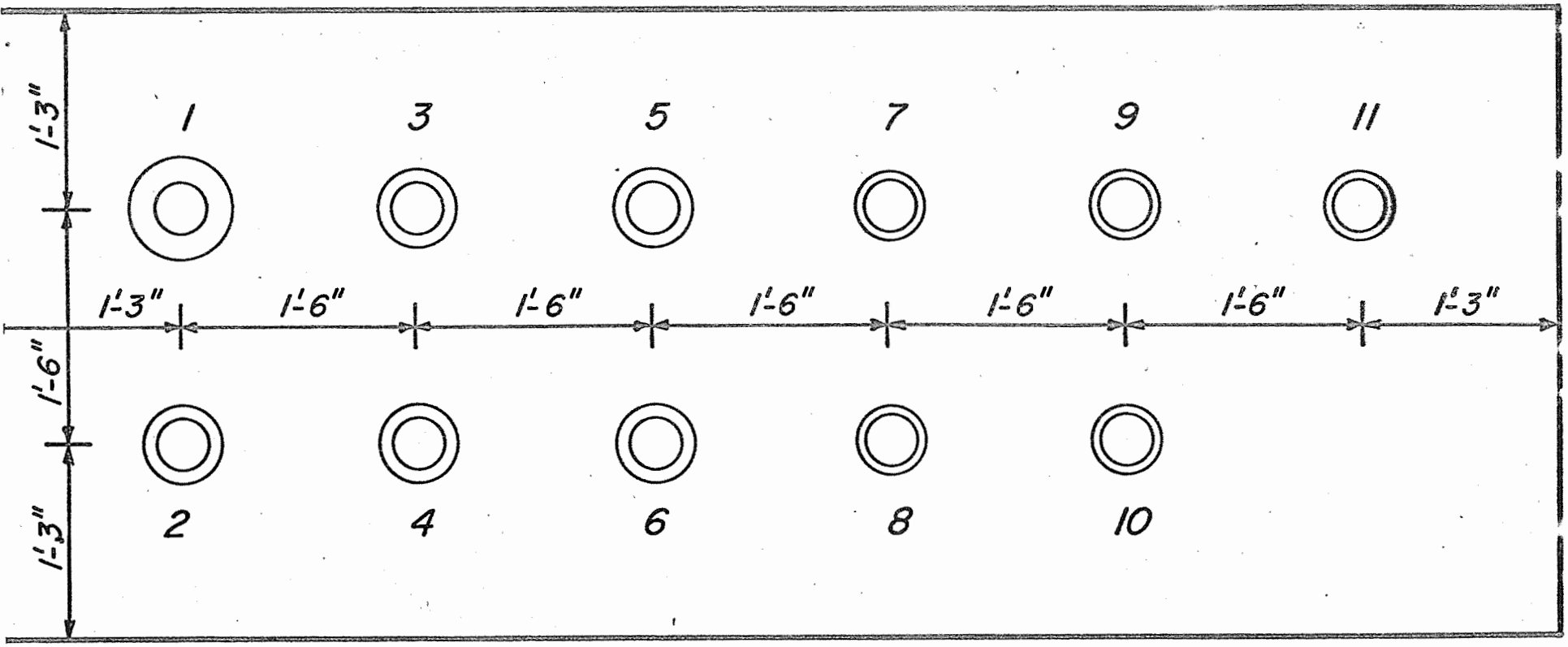

Figure 1. Placement of isotope storage wells in excavated area.

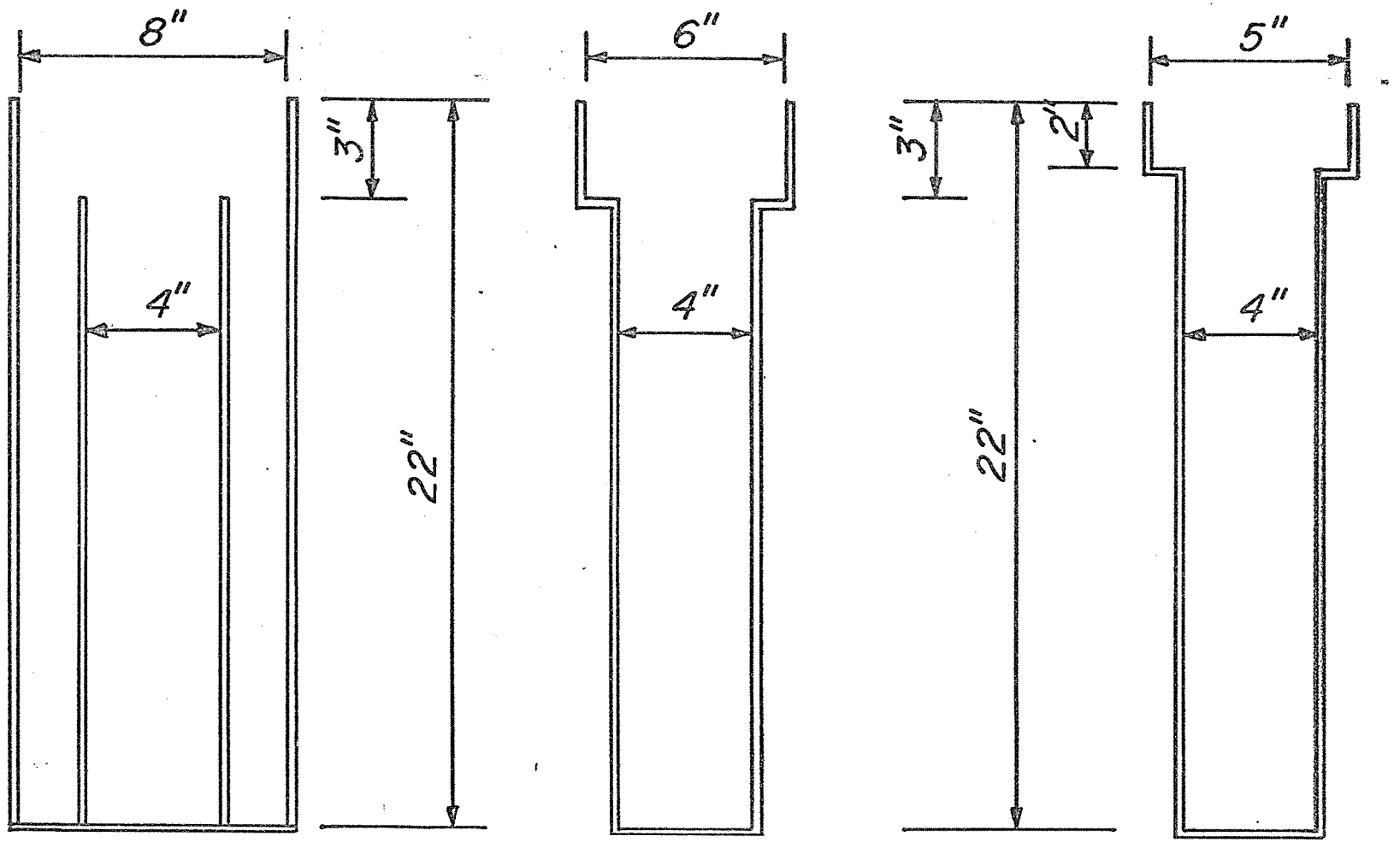

Figure 2. Cross sections of isotope storage wells.

PAPERS PREPARED OR PUBLISHED DURING 1962

	MS. No.
Bouwer, Herman. Analyzing ground-water mounds by resistance network. Jour. Irrig. and Drain. Div., Proc. Amer. Soc. Civ. Engins. 88(IR3):15-36.	42
Bouwer, Herman. Closure for "A variable head technique for seepage meters." Jour. Irrig. and Drain. Div., Proc. Amer. Soc. Civ. Engins. 88(IR2):91-94.	60
Bouwer, Herman, Myers, L. E., and Rice, R. C. Effect of velocity on seepage and its measurement. Jour. Irrig. and Drain. Div., Proc. Amer. Soc. Civ. Engins. 88(IR3): 1-14.	57
Bouwer, Herman. Field determination of hydraulic conductivity above a water table with the double-tube method. Soil Sci. Soc. Amer. Proc. 26(4):330-335.	41
Bouwer, Herman. The flow system below a water spreading basin. Proc. 5th Cong. of Internat. Comm. of Irrig. and Drain., Tokyo, Japan. (Sub. for Pub.).	73
Bouwer, Herman. In-place measurement of soil hydraulic conductivity in the absence of a water table. To be published in Proc. Internat. Soc. Soil Mechs. and Found. Engin., 2nd Asian Region. Conf., Tokyo, Japan.	85
Bouwer, Herman. Measuring soil permeability above a water table and analyzing groundwater mound behavior with a resistance network analog. Proc. 1961 Biennial Conf. on Groundwater Recharge, Berkeley, California.	43
Bouwer, Herman, and Rice, R. C. Seepage meters in seepage and recharge studies. Jour. of Irrig. and Drain. Div., Proc. Amer. Soc. Civ. Engins. (In press).	82
Bouwer, Herman, and van Schilfgaarde, J. Simplified prediction method for the fall of the water table in drained land. Agr. Engin. (Sub. for Pub.).	87
Bouwer, Herman. A variable head technique for seepage meters, with discussion and closure. Trans. Amer. Soc. Civ. Engins. 127(Part III):434-451.	17, 60
Clark, Francis E., Jackson, Ray D., and Gardner, Herbert R., Measurement of microbial thermogenesis in soil. Soil Sci. Soc. Amer. Proc. 26(2):155-160.	38

MS. No.

Denmead, O. T., Fritschen, L. J., and Shaw, R. H. Spatial distribution of net radiation in a corn field. Agron. Jour. 54(6):505-510. 37

Ehrler, William L. Transpiration of alfalfa as affected by low root temperature and other factors of a controlled environment. Agron. Jour. (Sub. for Pub.). 80

Erie, Leonard J. Evaluation of infiltration measurements. Trans. Amer. Soc. Agr. Engins. 5(1):11-13. 20

Erie, Leonard J. Irrigation management for optimum cotton production. To be published in Proc. Beltwide Cotton Proc.-Mech. Conf., Dallas, Texas. 89

Erie, Leonard J., and French, Orrin F. Safflower -- water intelligently! Arizona Farmer-Ranchman 41(7):6. 62

Erie, Leonard J. To make irrigation count, keep your eye on the plant. California Farmer, p. 41. April 7, 1962. 70

Erie, Leonard J., French, Orrin F., and Patterson, Lloyd L. Water management on DPL. Arizona Farmer-Ranchman. 41(11):12-13. 69

Fritschen, Leo J. Condensation on shielded net radiometers. Jour. of Appl. Met. (In press). 75

Fritschen, Leo J. Construction and evaluation of a miniature net radiometer. Jour. of Appl. Met. (In press). 50

Fritschen, Leo J., and Van Bavel, C. H. M. Energy balance components of evaporating surfaces in arid lands. Jour. of Geophysical Res. 67(13):5179-5185. 68

Fritschen, Leo J., and Van Bavel, C. H. M. Evaporation from irrigated land and related atmospheric processes. To be published in Proc. Internat. Union of Geodesy and Geophysics Gen. Assembly, Berkeley, California. 90

Fritschen, Leo J., and Van Bavel, C. H. M. Evaporation from shallow water and related micrometeorological parameters. Jour. of Appl. Met. (In press). 63

Fritschen, Leo J., and Van Bavel, C. H. M. Micrometeorological data handling system. Jour. of Appl. Met. (In press). 67

MS. No.

Jackson, R. D., Van Bavel, C. H. M., and Reginato, R. J. Examination of the pressure plate outflow method for measuring capillary conductivity. Soil Sci. (In press). 86

Jackson, R. D., Reginato, R. J., and Reeves, W. E. A mechanized device for packing soil columns. USDA-ARS 41-52. 54

Jackson, R. D., Nielsen, D. R., Van Bavel, C. H. M., and Nakayama, F. S. On Fick's law for diffusion applied to porous media. Soil Sci. (Sub. for Pub.). 91

Jackson, R. D. Porosity and soil-water diffusivity relations. Soil Sci. Soc. Amer. Proc. (In press). 64

Jackson, R. D. Temperature and soil-water diffusivity relations. Soil Sci. Soc. Amer. Proc. (In press). 77

Myers, Lloyd E. The conservation and beneficial use of water. Proc. 7th Annu. New Mexico Water Conf., Las Cruces, New Mexico. 88

Myers, L. E., and Van Bavel, C. H. M. Measurement and evaluation of water table elevations. Proc. 5th Cong. of Internat. Comn. of Irrig. and Drain., Tokyo, Japan. (Sub. for Pub.). 74

Myers, Lloyd E. Precipitation harvesting. To be published in Proc. Internat. Union of Geodesy and Geophysics Gen. Assembly, Berkeley, California. 84

Myers, Lloyd E. Water conservation - a research challenge. Jour. of Soil and Water Conserv. (Sub. for Pub.). 78

Myers, Lloyd E. Water harvesting. Proc. 16th Annu. Nevada Water Conf., Carson City, Nevada. (Sub. for Pub.). 83

Nakayama, F. S., and Jackson, R. D. Diffusion of tritiated water ($H^3H^1O^{16}$) in Agar Gel and water. Jour. of Phys. Chem. (In press). 81

Nakayama F. S., and Jackson, R. D. Diffusion of tritiated water in soils. Soil Sci. Soc. Amer. Proc. (In press). 72

Nakayama, F. S. and Scott, A. D. Gas sorption by soils and clay minerals: I. Solubility of oxygen in moist materials. Soil Sci. 94(2):106-110. 44

MS. No.

Nakayama, F. S. and Scott, A. D. Gas sorption by soils and clay minerals: II. Capillary effects. Soil Sci. 94(5):292-296. 45

Nakayama, F. S. A punched-card method for systematizing literature references in agronomic research. Agron. Jour. (Notes) 54(4):362. 51

Nakayama, F. S., and Van Bavel, C. H. M. Soil moisture conditions and root activity distribution patterns of sorghum. Agron. Jour. (Sub. for Pub.). 79

Olsen, S. R., Kemper, W. D., and Jackson, R. D. Phosphate diffusion to plant roots. Soil Sci. Soc. Amer. Proc. 26(3):222-227. 39

Van Bavel, C. H. M. Accuracy and source strength in soil moisture neutron probes. Soil Sci. Soc. Amer. Proc. 26(4):405. 56

Van Bavel, C. H. M., and Myers, L. E. An automatic weighing lysimeter. Agr. Engin. 43(10):580-583, 586-588. 58

Van Bavel, C. H. M., and Fritschen, Leo J. Energy balance of bare surfaces in an arid climate. Proc. Symp. on Methodology of Plant Eco-Physiology, Montpellier, France. (In press). 66

Van Bavel, C. H. M. Light-weight rate meter for neutron soil moisture measurement. Soil Sci. 94(6):418-419. 76

Van Bavel, C. H. M., and Reginato, R. J. Precision lysimetry for direct measurement of evaporative flux. Proc. Symp. on Methodology of Plant Eco-Physiology, Montpellier, France. (In press). 65

Van Bavel, C. H. M., Nixon, P. R., and Hauser, V. L. Soil moisture measurement with the neutron method. USDA-ARS 41 Series. (In press). 71